SEX DIFFERENCES IN HYPERTENSION AND THE ROLE OF ENDOTHELIAL TRPV4 CHANNELS IN CEREBROVASCULAR AND COGNITIVE FUNCTION

By

Laura Christine Chambers

A DISSERTATION

Submitted to
Michigan State University
in partial fulfillment of the requirements
for the degree of

Pharmacology and Toxicology – Doctor of Philosophy

2022

ABSTRACT

Vascular cognitive impairment and dementia (VCID) describes a spectrum of cognitive disorders that have a cerebrovascular origin. VCID can range from mild cognitive impairment to frank vascular dementia. The mechanisms behind VCID development are not fully understood and there are no effective treatments available. VCID arises from functional impairment in the small arteries and arterioles in the brain. Hypertension, which affects nearly half of all American adults, is the leading modifiable risk factor for VCID. Hypertension impairs cerebrovascular function that can starve neurons of necessary nutrients, increasing risk of cognitive impairment. My studies focus on cerebral parenchymal arterioles (PAs), which direct blood flow from the pial circulation to the capillaries. Because they lack collateral connections, PAs are considered the weak link in the cerebral perfusion. The occlusion of a single PA creates a discrete column of ischemic tissue that can produce cognitive impairment. PAs are dependent on TRPV4 channels for endothelium-dependent dilation, and there is a strong link between TRPV4 and cognitive function. Previous studies in male rodents showed that hypertension impairs TRPV4-mediated dilation in PAs, and this was associated with memory impairments. When mineralocorticoid receptor (MR) antagonists are administered alongside developing hypertension, these impairments are prevented. However, it is thus far unknown whether MR antagonist treatment can reverse cerebrovascular and cognitive impairments after they have developed. My first aim tests the hypothesis that rats with established hypertension will have impaired TRPV4 function in PAs that is associated with cognitive impairment, and that treatment with the MR antagonist eplerenone can reverse this damage after its development. My second aim focuses on sex differences in

hypertension, as this is a major gap in the literature. Thus far, all studies linking TRPV4 function to cognition have been conducted in male mice. Given that estrogen is vasoprotective in other vascular beds, I hypothesize that hypertensive female mice would be protected against impaired TRPV4 function in PAs, and from the associated cognitive deficits observed in male mice. Lastly, my third aim addresses the importance of TRPV4 channels specifically in the endothelium. There is a consistent link between TRPV4 impairment and cognitive dysfunction, but due to the channel's ubiquitous expression, its role in endothelial cells is unknown. Here, I test the hypothesis that male and female mice with endothelial TRPV4 channel deletion will have cognitive impairment. My studies show that MR antagonism reverses cerebrovascular and cognitive damage in hypertension, and that female sex protects against the development of these impairments. Further, I show that endothelial TRPV4 channel deletion results in cognitive dysfunction and increased inflammation in both male and female mice. My studies show for the first time that young female mice have preserved TRPV4 channel function in PAs that is associated with preserved cognitive function. Further, my data suggest the MR is a promising therapeutic target in hypertensive patients because it not only protects against neurovascular damage but can reverse it after it has developed.

ACKNOWLEDGEMENTS

I am fortunate to have had the guidance and support of many people throughout earning my PhD. I would not be here without all of you.

First and foremost, thank you to my mentor, Dr. Anne Dorrance. I quite literally would not have been able to achieve this milestone without you. Though the way I joined your lab was unconventional, I can't imagine being anywhere else. It's hard to put my gratitude into words. You are just as much a brilliant scientist as you are a compassionate, empathetic mentor, and I am beyond lucky to have been your student. You knew when to push me and when to let me figure things out on my own, and you always made me feel supported. Thank you for your invaluable guidance and patience, and your hilarious wit. And thank you for all the Tablet. You have created a monster.

To Dr. Bill Jackson, thank you challenging me to think critically about my science, and for always encouraging me to try again. You were always there to answer my million and one questions, ranging from hypotheses and experimental observations, to questioning whether time is linear and if extraterrestrials are among us (it's not and they are). Your willingness to have those goofy conversations with me cheered me up on difficult days more than you realize.

Thank you to my committee members Drs. Michelle Mazei-Robison and Nathan Tykocki, for your advice and guidance, and for challenging me to look at my science from different angles.

Thank you to every member of the lab, past and present. To Jessica and Martina Yen, thank you for your massive amounts of help and encouragement. Thank you to Drs. Janice Diaz-Otero and Paulo Pires, for your support no matter the distance. And, of

course, a massive thank you to Dr. Teri Lansdell. I've been lucky to have you by my side every stage of my PhD and I can't begin to tell you how grateful I am for that. Thank you for helping me become a better scientist and thank you for making me laugh so hard I cried at least once a week. You made coming into work fun.

I want to thank my family and friends for their endless support. To my mom and my parents-in-law, thank you for all your encouragement over the years. And to my best friends Jen, Kara, Tara, Kristin, Ryan, Dan, and Ben, thank you for always believing in me. You are family to me, and I credit you all for the maintenance of my sanity. Occasionally for its breakdown, but mostly for its maintenance.

Last, but definitely not least, thank you to my husband, Matthew. I could not have done this without you. You are my safe harbor, and I am forever grateful for you.

TABLE OF CONTENTS

LIST OF ABBREVIATIONS

4α- PDD	4-α-phorbol 12,13-didecanoate
4-HNE	4-Hydroxynonenal
AA	Arachidonic Acid
ACE	Angiotensin-Converting Enzyme
ACE2	Angiotensin-Converting Enzyme 2
aCSF	Artificial Cerebral Spinal Fluid
AITC	Allyl Isothiocyanate
AKAP150	A-Kinase Anchoring Protein 150
AngII	Angiotensin II
AT1R	Type 1 Angiotensin II Receptor
AT2R	Type 2 Angiotensin II Receptor
BH_4	Tetrahydrobiopterin
BCAS	Bilateral Common Carotid Artery Stenosis
BCAO	Bilateral Common Carotid Artery Occlusion
BK_{Ca}	Large Conductance Potassium Channel
BPH	Blood Pressure High
BPL	Blood Pressure Low
BPN	Blood Pressure Normal
CADASIL	Cerebral Autosomal Dominant Arteriopathy with Subcortical Infarcts and Leukoencephalopathy
cAMP	Cyclic Adenosine Monophosphate
Cch	Carbachol
cGMP	Guanosine-3',5'-cyclic monophosphate

COX	Cyclooxygenase
CSVD	Cerebral Small Vessel Disease
E2	Estrogen
EC-MR	Endothelial Cell Mineralocorticoid Receptor
EDH	Endothelium-Derived Hyperpolarization
EDHF	Endothelium-Derived Hyperpolarizing Factor
EETs	Epoxyeicosatrienoic acids
EGTA	Ethylene glycol-bis (β-aminoethyl ether)-N,N,N',N'-Tetraacetic Acid
ENaC	Epithelial Sodium Channels
eNOS	Endothelial Nitric Oxide Synthase
EPL	Eplerenone
ER	Estrogen Receptor
GFAP	Glial Fibrillary Acidic Protein
GPER1	G Protein-Coupled Estrogen Receptor 1
GPCR	G Protein-Coupled Receptor
H_2O_2	Hydrogen Peroxide
Iba-1	Ionized Calcium-Binding Adapter Molecule-1
IK_{Ca}	Intermediate Conductance Potassium Channel
iNOS	Inducible Nitric Oxide Synthase
IL	Interleukin
IP_3	Inositol-1,4,5-triphosphate
IP_3R	Inositol-1,4,5-triphosphate Receptors
K_{IR}	Inward Rectifying Potassium Channels

L-NAME	L-N^G-Nitro Arginine Methyl Ester
L-NNA	L-N^G-Nitro-L-Arginine
MasR	Mas Receptors
MCA	Middle Cerebral Artery
MEJs	Myoendothelial Junctions
MEPs	Myoendothelial Projections
MR	Mineralocorticoid Receptor
MRI	Magnetic Resonance Imaging
NADPH	Nicotinamide Adenine Dinucleotide Phosphate
nNOS	Neuronal Nitric Oxide Synthase
NO	Nitric Oxide
NOS	Nitric Oxide Synthase
NOX2	Nicotinamide Adenine Dinucleotide Phosphate Oxidase 2
NVC	Neurovascular Coupling
NVU	Neurovascular Unit
PA	Parenchymal Arterioles
PCA	Posterior cerebral artery
PIP_2	Phosphatidylinositol 4,5-bisphosphate
PKA	Protein Kinase A
PKC	Protein Kinase C
PLC	Phospholipase C
PSS	Physiological Salt Solution
RAAS	Renin-Angiotensin-Aldosterone System

ROS	Reactive Oxygen Species
RyR	Ryanodine Receptors
sEH	Soluble Epoxide Hydrolase
SHR	Spontaneously Hypertensive Rat
SHRSP	Spontaneously Hypertensive Stroke-Prone Rat
SK_{Ca}	Small Conductance Potassium Channel
SMC	Smooth Muscle Cell
SNP	Sodium Nitroprusside
SYP	Synaptophysin
TNF-α	Tumor Necrosis Factor Alpha
TNFR1	Tumor Necrosis Factor Receptor 1
TRP	Transient Receptor Potential
TRPA	Transient Receptor Potential Ankyrin
TRPA1	Transient Receptor Potential Ankyrin 1
TRPC	Transient Receptor Potential Canonical
TRPC3	Transient Receptor Potential Canonical 3
TRPC6	Transient Receptor Potential Canonical 6
TRPM	Transient Receptor Potential Melastatin
TRPM4	Transient Receptor Potential Melastatin 4
TRPML	Transient Receptor Potential Mucolipin
TRPN	Transient Receptor Potential No Mechanoreceptor Potential
TRPP	Transient Receptor Potential Polycystin
TRPV	Transient Receptor Potential Vanilloid

TRPV4	Transient Receptor Potential Vanilloid 4
$TRPV4_{EC^{-/-}}$	Endothelial Specific Transient Receptor Potential Vanilloid 4 Knockout
TRPY	Transient Receptor Potential Yeast
TXA_2	Thromboxane A_2
UCAO	Unilateral Common Carotid Artery Occlusion
VaD	Vascular Dementia
VCID	Vascular Contributions to Cognitive Impairment and Dementia
VSMC	Vascular Smooth Muscle Cell

Chapter 1:

Sex Differences in Hypertension and the Role of Endothelial TRPV4 Channels in Cerebrovascular and Cognitive Function

1. – Overview

The brain is the most energy-intensive organ in the body, it only accounts for 2% of body weight, yet it uses up to 50% of the available glucose (98). Because the brain lacks its own energy stores, it is critical that cerebral blood flow is spatially and temporally regulated to provide sufficient perfusion to areas with increased neuronal activity. Inadequate cerebral perfusion results in hypoperfusion that, if persistent, can lead to neuronal death.

Though cerebral arteries have some structural similarities with peripheral arteries, including the presence of endothelial and vascular smooth muscle cells (VSMCs), this vascular bed is anatomically and physiologically unique. It therefore needs to be studied as a distinct entity (92). The endothelial cells of the cerebral vasculature are not fenestrated and are instead coupled to one another by tight junctions. This creates a tight seal to form the blood-brain barrier, which, alongside the high selectivity of molecular transport, protects the brain parenchyma from circulating factors (152, 299). The cerebral microvasculature also closely interacts with astrocytes and pericytes in the brain parenchyma to relay appropriate dilatory and contractile signals to alter blood flow (153).

Both the structure and the function of the cerebral circulation is highly susceptible to injury from cardiovascular risk factors such as hypertension. Vascular damage from hypertension increases the risk of vascular dementia (VaD) development. Though epidemiological evidence suggests a sexual dimorphism in the relationship between hypertension and VaD development, little is understood about the mechanisms involved. In this chapter, I will discuss the anatomy and physiology of the cerebral vasculature. I will describe how hypertension and mineralocorticoid receptor (MR) activation affects

cerebrovascular structure and function. This chapter will focus on the role of transient receptor potential (TRP) channels in artery and arteriolar function. Additionally, I will pay special attention to known sex differences throughout each discussed topic.

1.1 – Anatomy of the cerebral circulation

1.1.1 – Extracranial arteries

To perfuse the brain, blood flows through two pairs of large extracranial arteries: the right and left internal carotid arteries and the right and left vertebral arteries (4). The internal carotid arteries arise as bifurcations of the common carotid arteries and continue to branch into the anterior and middle cerebral arteries, supplying 80% of the total cerebral perfusion (4, 38). The remaining 20% is supplied by the vertebral arteries, which arise from the subclavian arteries. The vertebral arteries run along the spinal cord and converge at the brainstem to give rise to the basilar artery; vertebral arteries are therefore a critical source of brain stem and posterior brain perfusion. At the base of the brain, the basilar artery fuses with the circle of Willis, which is a complete anastomotic ring comprised of the anterior communicating artery, anterior cerebral arteries, internal carotid arteries, posterior communicating arteries, and posterior cerebral arteries (PCAs) (291).

1.1.2 – Circle of Willis and intracranial arteries

The first published description of circle of Willis in 1664 by Sir Thomas Willis marked the evolution between medieval to modern understanding of brain anatomy (79). Unique to the cerebral vasculature, this structure is a large anastomotic ring at the base of the brain that allows blood flow regulation across both hemispheres and the anterior and posterior regions (174). In the event of an occlusion, the complex connections throughout the circle of Willis allow for retrograde perfusion to ensure consistent blood

flow. Branching off the circle of Willis are three pairs of large arteries to perfuse each hemisphere: the anterior cerebral artery, posterior cerebral artery (PCA), and the middle cerebral artery (MCA). Each of these arteries branches further to form the pial or leptomeningeal arteries. The pial arteries cover the brain's surface and are rich with anastomotic connections that protect the brain from ischemia. These anastomoses provide alternative routes for blood flow in the event of an arterial occlusion, thereby protecting regional neuronal function (304). The anatomy of the major cerebral arteries is shown in Figure 1.1. The large pial arteries and arterioles contain several layers of VSMCs. The VSMCs are separated from endothelial cells by the internal elastic lamina, an acellular layer consisting primarily of elastin and collagen (171, 306). The internal elastic lamina has perforations, where myoendothelial projections (MEPs) on endothelial cells can contact VSMCs (14). MEPs allow for communication between endothelial cells and VSMCs and exist throughout all segments of the cerebral vasculature (216). MEPs will be discussed in more detail in section 1.2.2.1.

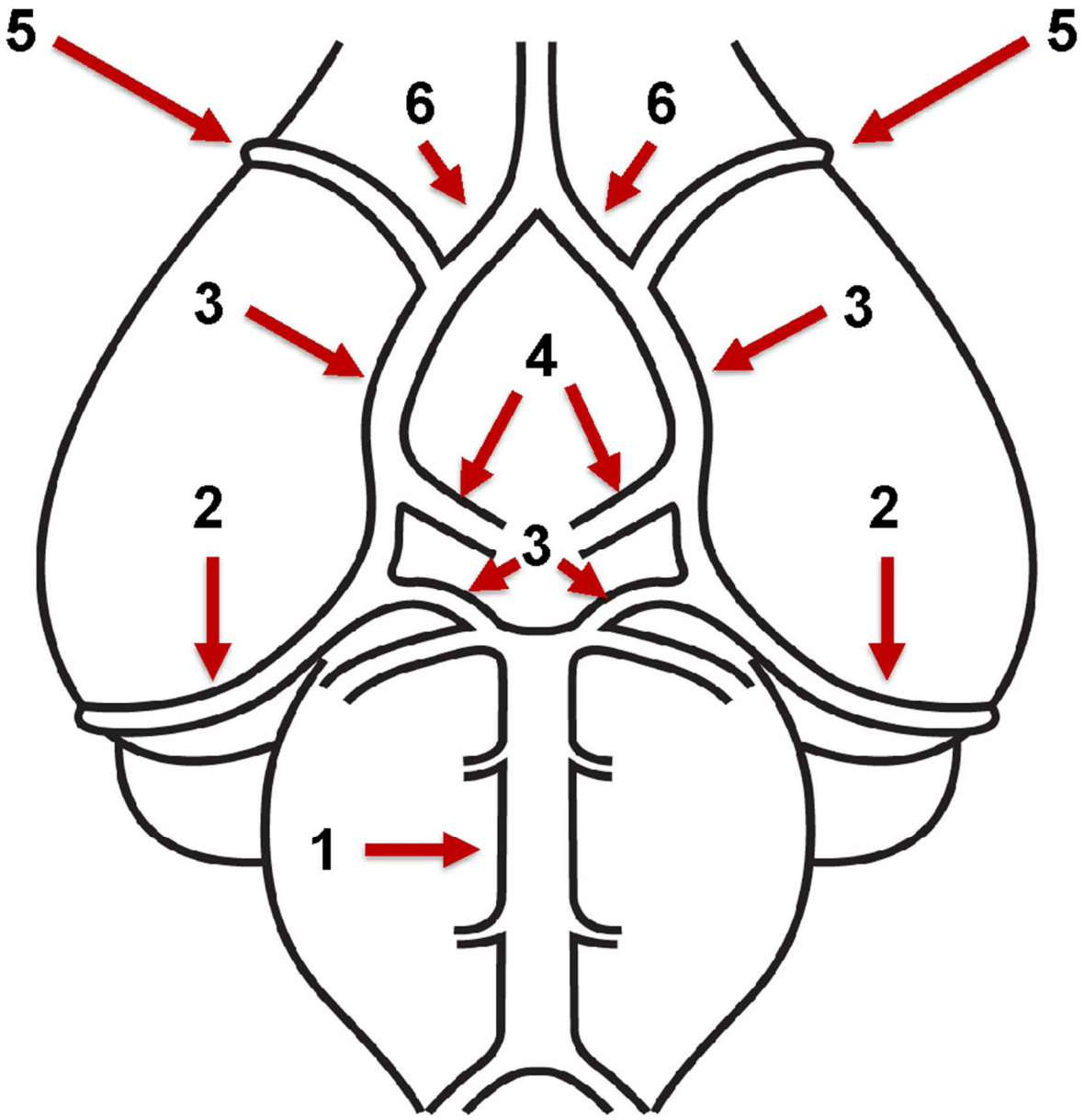

Figure 1.1: Circle of Willis in the rodent cerebral circulation. 1. Basilar artery; 2. Posterior cerebral arteries; 3: Posterior communicating arteries; 4: Internal carotid arteries; 5. Middle cerebral arteries; 6. Anterior cerebral arteries. Figure courtesy of Daniel Bollman.

1.1.3 – Penetrating and parenchymal arterioles

The penetrating arterioles branch nearly perpendicularly from pial arteries into the Virchow-Robin space, a perivascular channel filled with cerebrospinal fluid. Penetrating arterioles give rise to parenchymal arterioles (PAs), which are largely responsible for perfusing the white matter (253, 264). Unlike pial arteries, PAs have only a single layer of VSMCs, which are in direct contact with astrocytic endfeet. PAs ultimately give rise to the capillaries, which are the site of gas and nutrient exchange with neurons. Importantly, PAs have very few collateral connections and therefore function as a distinct vascular unit with their associated capillaries (22, 23). This unique anatomical feature makes PAs and the regions they perfuse particularly vulnerable to ischemia, as there are no routes to redirect blood flow in the event of a blockage. Additionally, relative to other cerebral arterioles, PAs generate a large amount of myogenic tone, which is the property of arteries and arterioles to constrict in response to increases in intralumenal pressure. PAs contribute 30-40% of the total cerebrovascular resistance (45, 47, 48). Because of these qualities, the PAs are considered the weak link in cerebral perfusion. This dissertation will be focused on how hypertension affects the physiology of PAs and aims to identify sex differences in response to hypertension.

1.1.4 – Capillaries

Capillaries are the most abundant vessel type in the brain and account for more than 90% of the cerebral vascular volume. In fact, the human brain is estimated to have 400 miles of capillaries (19). Instead of VSMCs, the capillary endothelial cells are associated with pericytes. Pericytes exist in greater abundance in the brain than in any other vascular bed, with a 1:1-3:1 ratio of endothelial cells to pericytes (13, 221). The role

of cerebral pericytes is controversial. While some have reported that pericytes have a contractile phenotype and can regulate capillary blood flow (119, 129), others argue that these cells lack the smooth muscle actin to do so (142). Capillaries also interact closely with neurons. It is estimated that there is a one-to-one relationship between capillaries and neurons (356) and that neurons are rarely more than 15μm from a capillary (331). From the capillaries, blood is returned to the central sinus through parenchymal venules.

1.1.5 – Veins

After blood flows through the capillaries, it exits the brain through veins and sinuses. The superficial cortical veins in the pia mater are responsible for draining blood from the cerebral cortex and subcortical white matter, while the central veins drain blood from the deep white and gray matter. These veins meet with cortical veins and drain into the superior sagittal sinus (185, 233). The focus of this dissertation is on cerebral arterioles; therefore, discussion of veins and venules will be limited.

1.2 – Cerebrovascular physiology

Because of the brain's high energy demands and lack of energy reserves, it is exceedingly vulnerable to hypoxic injury. It is, therefore, essential that cerebral blood flow is tightly regulated throughout continual fluctuations in intralumenal blood pressure. Maintenance of constant cerebral blood flow is achieved through cerebral autoregulation and the development of myogenic tone. In this section, I will discuss mechanisms that drive these processes and mechanisms of the endothelial regulation of tone.

1.1.6 – Cerebral autoregulation and the myogenic response

Cerebral autoregulation describes the ability of cerebral arteries to maintain a constant blood flow despite continual fluctuations in pressure (48). In healthy adults,

successful autoregulation typically occurs between mean arterial pressures of 60mmHg and 150mmHg. Artery collapse and subsequent ischemia may occur when intraluminal pressure falls below this range. Conversely, when intralumenal pressure rises above this range, force-mediated dilation occurs, and downstream capillaries become vulnerable to injury. Cerebral autoregulation is achieved through the generation of myogenic tone and myogenic reactivity. Cerebral VSMCs have the intrinsic ability to generate myogenic tone, which is a partial constriction that is activated by an increase in intralumenal pressure. Myogenic reactivity describes the ability of arteries to modify their contractile state to accommodate intraluminal pressure fluctuations. Adjustments in arteriolar diameter protect downstream capillaries by preventing intralumenal pressure from getting too high and serve to drive blood flow in the direction of the capillaries when pressures are low. The concept of VSMCs adjusting their contractile state according to changes in blood pressure was first described in 1902 by Bayliss and is, therefore, sometimes referred to as the “Bayliss effect.” The amount of myogenic tone generated is dependent on the segment of the cerebrovascular tree. In the peripheral vasculature, it is primarily smaller arterioles that contribute to vascular resistance. In the brain, however, both large and small cerebral arteries and arterioles play a role in regulating blood flow. The large cerebral arteries contribute about 50% of the cerebrovascular resistance, and the PAs contribute about 40% (45, 91, 141). PAs generate more myogenic tone at lower pressures than larger cerebral arteries, constricting up to 30-40% at 40mmHg in mice (45, 47, 67). The increased resistance is partially due to their smaller diameter, as according to the Hagen-Poiseuille equation, vascular resistance is proportional to the fourth power of the

arterial radius (290). Differences in ion channel expression and activity also likely contribute to these differences and will be discussed in later sections.

The generation of myogenic tone is initiated by an increase in intralumenal pressure, which produces depolarization of VSMCs. VSMC depolarization leads to the activation of L-type voltage-gated Ca^{2+} channels, particularly $Ca_V1.2$. Blockage of these channels prevents myogenic tone generation, demonstrating that calcium is a requirement for the process. The influx of Ca^{2+} through $Ca_V1.2$ channels facilitates myosin light chain kinase phosphorylation and activation of the actin and myosin machinery, producing vasoconstriction. While it is accepted that this is the general mechanism by which myogenic tone generation occurs, the specific ion channels involved in responding to arterial stretch and propagation of this signal are still being identified. Various members of the TRP family of ion channels and epithelial sodium channels (ENaC) likely play a role. A member of the canonical family of TRP channels, TRPC6, is mechanosensitive and is likely involved in sensing arterial stretch. The downregulation of TRPC6 using antisense oligodeoxynucleotides tempered stretch-induced VSMC depolarization and significantly reduced the amount of myogenic tone generated in rat cerebral arteries (338). TRPC6 also contributes to myogenic tone indirectly following GPCR activation, working in concert with a member of the melastatin TRP family, TRPM4. ENaC are also mechanosensitive and Drummond *et al.* found that blockage of these channels with amiloride prevents myogenic tone generation in rat cerebral arteries (73).

The process of myogenic tone generation is complex and features redundant mechanisms to ensure its function. Several studies have identified a key role for phospholipase C (PLC) and diacylglycerol (DAG) in myogenic tone generation (167, 257,

267). A proposed mechanism for stretch-induced depolarization of VSMCs is that the γ1 isoform of PLC is activated by type 1 angiotensin II receptors (AT1R) and Src tyrosine kinase. AT1R type 1b is the primary intralumenal pressure sensor in cerebral arteries (270). PLC activation occurs concomitantly with stretch induced TRPC6 activation, which promotes Ca^{2+} influx through the channel. TRPC6 channels are also activated by DAG generated by PLC (144). PLC activation also leads to inositol triphosphate (IP_3) generation; IP_3 sensitizes its receptors on the sarcoplasmic reticulum to local increases in cytosolic Ca^{2+}. This sensitization facilitates Ca^{2+}-induced Ca^{2+} release of intracellular Ca^{2+} stores and acts synergistically with increased sensitivity to the Ca^{2+} influx from TRPC6 activation, which activates TRPM4. Localized microdomains consisting of these signaling molecules were identified, though it is possible other ion channels and pathways are also involved (120). For example, a role for Ca^{2+}-activated Cl^- channels has been identified (247). Additionally, while tone initiation requires an increase in VSMC Ca^{2+}, myogenic reactivity may also involve increased Ca^{2+} sensitivity (256). The increased Ca^{2+} sensitivity can partially be attributed to RhoA-Rho kinase pathway activation (305). When Rho kinase is inhibited with Y-27632 in rabbit basilar arteries, myogenic tone is inhibited without a change in intracellular Ca^{2+} concentration. Arterial stretch also induces the translocation of RhoA from the cytosol to the cellular membrane, further supporting that this pathway is involved in myogenic tone development (350). A proposed mechanism of myogenic tone development is shown in Figure 1.2.

Negative feedback mechanisms occur alongside myogenic tone to control the amount of vasoconstriction. Large conductance Ca^{2+}-activated potassium channels (BK_{Ca}) are significant contributors to this negative feedback mechanism. The local Ca^{2+}

transients through ryanodine receptors (RyR), known as Ca^{2+} sparks, activate VSMC BK_{Ca} channels. BK_{Ca} activation produces a potassium ion efflux that mitigates depolarization in the cell, thereby promoting vasorelaxation (163). RyR are an essential part of this process, and blocking these receptors prevents the negative feedback mechanism to a similar degree as blocking BK_{Ca} (246). Notably, while VSMCs of PAs express BK_{Ca} channels, they are not active under physiological conditions (54, 55). This lack of negative feedback may contribute to increased myogenic tone in PAs relative to larger cerebral arteries. In rat MCAs, a negative feedback role has been identified for T-type Ca^{2+} channels, as the Ca^{2+} influx through these Ca^{2+} channels activates RyR (131, 132). It is unclear whether this mechanism is active in PAs. Several isoforms of voltage-dependent K^+ channels are expressed in cerebral VSMCs, including $K_V2.1$ (7) and K_V7 channels. These contribute to negative feedback pathways (355).

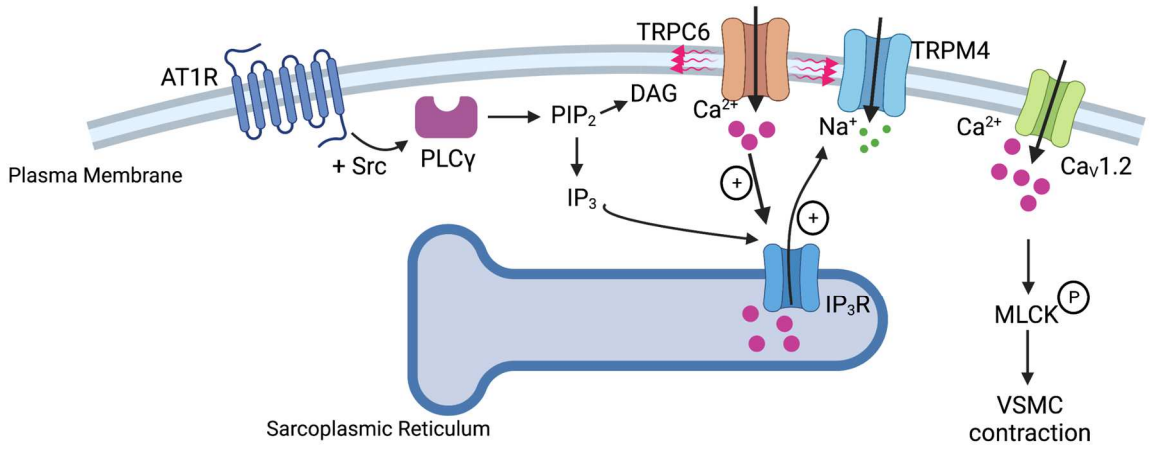

Figure 1.2: Proposed mechanism of myogenic tone development in VSMCs. Activation of AT1R in VSMCs produces PLCγ1 and subsequently IP_3. This occurs concomitantly with stretch induced TRPC6 activation. Activation of IP_3R in the sarcoplasmic reticulum by IP3 increases intracellular Ca^{2+}, which acts synergistically with Ca^{2+} influx through TRPC6 channels to activate TRPM4. Cation influx into the cell depolarizes the plasma membrane and encourages the opening of $Ca_V1.2$, leading to phosphorylation of myosin light chain kinase, and producing vasoconstriction. Figure adapted from (120). Created with BioRender.com

1.1.7 – Endothelial cell regulation of myogenic tone

The amount of myogenic tone generated is modulated by the endothelium. Endothelial cells form the innermost lining of all blood vessels and are oriented in the direction of blood flow. Endothelial cells are the only cell type common to every segment of the cerebrovascular bed, but the mechanisms these cells use to regulate vasodilation differs depending on location (277). A functioning endothelium is necessary for matching cerebral blood flow to neuronal demand, a process known as neurovascular coupling (NVC). NVC will be discussed in detail later. The three signaling mechanisms used by endothelial cells to regulate vasodilation are prostaglandins, nitric oxide (NO), and endothelium-derived hyperpolarization (EDH). The relative contribution of each of these pathways differs based on vessel type. Mechanisms of endothelium-dependent dilation are outlined in Figure 1.3.

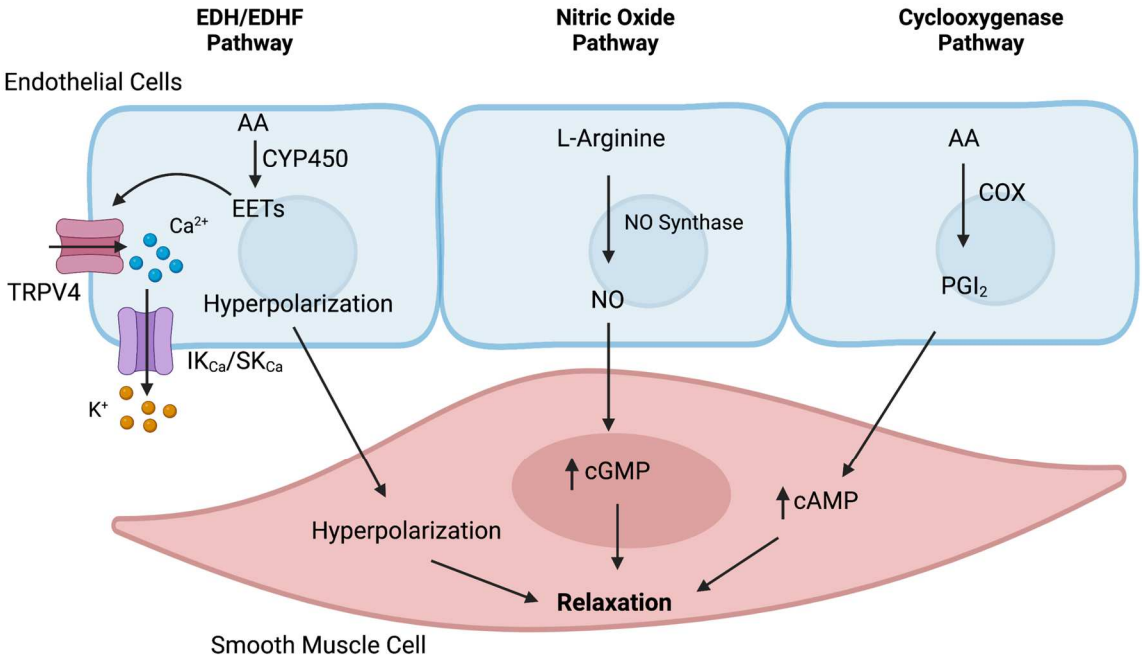

Figure 1.3: Mechanisms of endothelium-dependent dilation. The endothelium contributes to vasodilation through mechanisms involving EDH/EDHF, NO, and COX. Created with BioRender.com.

1.2.2.1 – Myoendothelial projections

Before further discussing the cerebral vasculature and how VSMCs and the endothelium work together to regulate blood flow, it is essential to discuss MEPs, which facilitate communication between these cell types. MEPs provide a means of relaying electrical and chemical signals between endothelial cells and VSMCs. MEPs extend through the internal elastic lamina facilitating direct contact between the two cell types (184). MEPs originate almost exclusively from endothelial cells in mice, but in humans,

about 40% originate from VSMCs (319); the physiological significance of this difference is not yet understood. Gap junctions, which allow for the passage of second messenger molecules between cells, are located in the tip of some MEPs; this subset of MEPs are referred to as myoendothelial junctions (MEJs) (89). Small arterioles tend to have more MEJs than larger vessels. This is likely due to the fact that smaller arterioles rely more heavily on endothelium-derived hyperpolarizing factors (EDHF) for vasodilation (184, 300, 309).

MEJs facilitate the movement of small molecules and charged ions from endothelial cells to VSMCs. Because of this important role, MEJs are required for myoendothelial feedback. Microdomains containing ion channels and receptors involved in EDH-mediated dilation are formed near MEJs. (250). Localization of these key contributors near MEJs is crucial successful intercellular communication. Cellular structures, molecules, and ion channels within these microdomains include the endoplasmic reticulum, caveolae, intermediate conductance Ca^{2+}-activated potassium channels (IK_{Ca}), small conductance Ca^{2+}-activated K^+ channels (SK_{Ca}), and several members of the TRP ion channel family (111, 156, 318). The function of these channels will be discussed in depth in section 1.2.3.

1.2.2.2 – Nitric Oxide

NO, one of the most well-studied vasodilators, was initially referred to as endothelium-dependent relaxing factor. NO is a small molecule that can diffuse through the cellular membranes and thus does not need MEJs to pass to VSMCs. Because NO has a short half-life, it is produced on-demand through three isoforms of nitric oxide synthase (NOS) (154). Neuronal NOS (nNOS) and endothelial NOS (eNOS) are

constitutively expressed, while inducible NOS (iNOS) is expressed under pathological conditions. eNOS is expressed in endothelial cells and is the predominant vascular isoform. eNOS is also expressed in cardiomyocytes, neurons, and platelets. In endothelial cells, NOS signaling is initiated by the activation of G_qPCRs. One such receptor subtype is the muscarinic receptor, which is activated by acetylcholine and its analogues. G_qPCR activation prompts PLC to cleave phosphatidylinositol 4,5-triphosphate into IP_3 and DAG. The activation of IP_3 receptors on the smooth endoplasmic reticulum increases intracellular Ca^{2+} levels, and this activates eNOS (74). Activated NOS catalyzes the oxidation of L-arginine in the presence of cofactor tetrahydrobiopterin (BH_4) to form NO and L-citrulline. This NO diffuses from endothelial cells to VSMCs where it activates soluble guanylyl cyclase. This increases intracellular levels of cyclic guanosine monophosphate (cGMP) that subsequently activates protein kinase G and type 1 cGMP-dependent protein kinase (287). Type 1 cGMP-dependent protein kinase promotes phosphorylation of BK_{Ca} channels and increases the channel's open probability, encouraging vasodilation (196).

In the peripheral vasculature, NO plays an essential role in blood pressure regulation. In the brain, NO is a regulator of cerebral blood flow by contributing to vasodilation and modulating resting tone. It appears that the importance of NO in these roles decreases with decreasing arteriolar lumen diameter and is, therefore, the most important in larger cerebral arteries (140). This reflects observations made in our lab using isolated and pressurized PAs. We showed in PAs that inhibiting cyclooxygenase (COX) and NOS does not change the amount of myogenic tone generated or endothelium-dependent dilation after muscarinic receptor activation (67, 222). This

suggests that EDH is the primary dilatory mechanism in PAs. However, the idea that NO is not an important modulator of myogenic tone or dilation in PAs is controversial, as others have found a role for NO in these processes (44, 46, 63).

1.2.2.3 – Prostaglandins

Prostaglandins are arachidonic acid (AA) metabolites produced by COX. In the cerebral vasculature, all three COX enzymes are expressed, COX-1, COX-2, and COX-3. COX-1 and COX-2 are more well-known and are expressed predominantly in endothelial cells, and to a lesser extent in VSMCs. Each COX enzyme produces prostaglandin H_2 from AA. This product can further be metabolized to prostacyclin (PGI_2), prostaglandin (PGE_2), and thromboxane (TXA_2) (155). While TXA_2 is a vasoconstrictor, both PGI_2 and PGE_2 act as vasodilators. Prostaglandins produce vasodilation by increasing production of cyclic adenosine monophosphate (cAMP), which activates protein kinase A (PKA) in VSMCs (69, 266). PKA production leads to VSMC hyperpolarization in two ways. Firstly, it reduces intracellular Ca^{2+} levels by activating Ca^{2+}-ATPase in the endoplasmic reticulum, leading to the closure of voltage-gated Ca^{2+} channels. Secondly, it opens potassium channels to directly hyperpolarize the cell, resulting in vasodilation. Prostaglandins contribute to the regulation of basal cerebral blood flow in the large pial arteries (183), but appear to have little to no role in endothelium-dependent dilation in PAs (67, 223). Notably, the contribution of prostaglandins, particularly PGI_2, to cerebral blood flow regulation appears to change with age. A study determining differences in vasoreactivity between infants and adults found that infants have greater PGI_2 activity in their vertebral arteries than adults. Conversely, vertebral arteries in adults had greater NO activity than infants (39).

1.2.2.4 – Endothelium-derived hyperpolarization / endothelium-derived hyperpolarization factors

The importance of specific dilatory mechanisms differs throughout the cerebrovascular network, including in the transition between PAs and capillaries (160, 161, 326). To fit within the focus of this dissertation, discussion will be limited to mechanisms important in PAs. EDH-mediated dilation is the dilation that remains after NO and prostaglandin production are blocked and is mediated by endothelial cell hyperpolarization. This dilation mechanism is primarily driven by endothelial Ca^{2+}-activated K^+ channels, which respond to local intracellular increases in Ca^{2+} to produce a K^+ efflux out of the endothelial cell. This loss of positive charge hyperpolarizes the cell. This hyperpolarization is transmitted to VSMCs through MEJs, resulting in VSMC hyperpolarization and subsequent deactivation of voltage-gated Ca^{2+} channels (161). The hyperpolarization initiated by IK_{Ca}/SK_{Ca} channels activates inwardly rectifying K^+ channels (K_{IR}) in both endothelial and VSMCs, which serves to amplify the signal (159, 317). The importance of EDH in arteriolar dilation appears to vary between vascular segments, increasing in significance with decreasing lumen diameter (111, 309). As mentioned previously, BK_{Ca} channels promote vasorelaxation in the larger pial arteries. However, in PAs, EDH mediated dilation requires IK_{Ca} and SK_{Ca} channel activation instead. These channels can be activated through various processes, including IP_3 signaling and TRP channel activation. Because these channels depend on signals instigated by other proteins in the cell, their localization close to other ion channels and MEJs is central to their function. Their proximity to TRP channels is critical, as these Ca^{2+}-permeable channels are crucial players in endothelium-dependent dilation in small cerebral

arterioles. Because of the importance of TRP channels in cerebral vascular dilation, they will be discussed in depth in section 1.2.3.

Though K^+ is regarded as an EDHF, many other molecules act as EDHFs or stimulate EDH-mediated dilation (29). Other EDHFs in the cerebral circulation include hydrogen peroxide (H_2O_2) and epoxyeicosatrienoic acids (EETs). H_2O_2 is a product of oxidative stress and produces robust dilation in cerebral arteries; however, the mechanisms involved in this dilation are species dependent. For example, in piglet pial arterioles, H_2O_2 initially produces constriction which is then followed by dilation (203). In feline cerebral arteries, H_2O_2 produces dilation that is dependent on hydroxyl radicals, a product of H_2O_2 metabolism. However, at higher concentrations, this dilation becomes hydroxyl radical independent (337). In rat cerebral arteries, H_2O_2 can induce bradykinin-mediated dilation (312), though, notably, other groups have identified a role for NO in this dilation instead of H_2O_2 (124).

EETs are formed through the AA metabolism by cytochrome P450 enzymes (25, 354). In cerebral endothelial cells, this process is primarily facilitated by CYP2J2, and partially by CYP2C8 (100, 240). Several EETs isoforms are vasoactive, but 11,12-EET and 14,15-EET are the most important in the cerebral vasculature (351, 352). The formation of these EETs is stimulated by acetylcholine, bradykinin, vascular stretch and shear stress (29, 30). EETs are endogenous agonists of TRPV4 channels (86). EETs are deactivated by soluble epoxide hydrolase (sEH) to form dihydroxyeicosatrienoic acids. Thus, sEH inhibitors are a potential therapeutic strategy in conditions marked by endothelial dysfunction. While this section describes a few known EDHFs, it is important to note that there may be other EDHFs that have yet to be identified.

1.2.2.5 – Sex differences in cerebral blood flow and its regulation

Across species, females reliably have greater resting cerebral blood flow compared to males (1, 6, 127, 211, 288). This trend begins in children, with girls between four and eight years of age having 9-15% higher cerebral blood flow than boys, depending on which artery is measured (329). Both sexes experience a reduction in cerebral blood flow as they enter puberty, but girls have an increase in mid-adolescence (303). Greater cerebral blood flow in females continues through adulthood, averaging an 11% elevation compared to males from 18-72 years of age (288). The brains of females also receive a higher percentage of cardiac output across ages compared to males, though this declines with increasing age in both sexes (339). The impact of the female sex on cerebral blood flow is controlled by female sex hormones; post-menopausal women undergoing hormone replacement therapy experience a global increase in cerebral blood flow (180). This increase in cerebral blood flow is not a function of artery remodeling as the pial arteries of female humans and rodents have smaller diameters than males (206, 308, 335). Myogenic tone development has an inverse relationship with arterial size, with smaller arterioles developing greater myogenic tone, suggesting that arteries from females may develop more myogenic tone than those from males. However, evidence in the literature of this sex difference is mixed. Some studies have measured greater tone development in MCAs of young female compared to male rats (280). However, several studies, including data from our lab, observe no difference in myogenic tone between the sexes at baseline (311), while others observe reduced tone development in females (113). Thus, the elevated cerebral blood flow in females may be explained by greater

flow-mediated dilation in arteries from females (145, 295), which is mediated through NO activity (328).

The effect of estrogen (E2) on NO synthesis is a major driver of observed sex differences in vascular function. E2 upregulates eNOS expression (138, 218, 231), which has implications in flow-mediated dilation and endothelial regulation of tone. Human endothelial cells from females have more eNOS expression and activity than cells from males (35). This effect is mimicked by *in vivo* studies in humans and rodents that show females produce more NO than males (102, 113). This elevated NO production in females is E2 dependent; E2 supplementation in both males and ovariectomized females results in greater NO production, less myogenic tone, and more vasodilation (104, 113, 231, 232, 313). Further demonstrating the importance of E2 in NO production, aromatase inhibition, thereby blocking the conversion of testosterone to E2, decreases endothelium-dependent dilation in cerebral arteries in female, but not male mice (357).

In addition to modulating NO synthesis, E2 also increases the synthesis of prostacyclin in arteries throughout various organ types (166, 173, 244). In ovariectomized female rats, chronic E2 treatment increased prostacyclin production in cerebral blood vessels (258). Studies using ovine uterine artery endothelial cells revealed that E2 affects prostacyclin production by activating estrogen receptor (ER)-α (170). The importance of this E2-mediated effect on brain function is unclear.

Because of the importance of EDH in cerebral PAs, the effect of sex on EDH is of particular interest. Two important studies from Liu *et al.* revealed that mesenteric arteries from ovariectomized female rats have impaired EDH-mediated dilation, which is reversed after E2 treatment (209, 210). Inhibiting gap junctions with 18α-glycyrrhetinic acid

produced a similar reduction in EDH-mediated dilation in ovary-intact female rats. This study presented the possibility that the gap junctions required for EDH-mediated are regulated by E2. Indeed, immunohistochemical analysis revealed that the expression of connexin-43, a critical component of myoendothelial gap junctions, was reduced in ovariectomized rats and this deficit was corrected by E2 treatment (209). These studies suggest E2 regulates the expression of connexins, which influences EDH activity in the vasculature.

1.2.3 – TRP channels in the vasculature

TRP channels are a superfamily of ion channels that are widely expressed throughout various cell types in multicellular organisms. TRP channels are involved in a wide range of processes, including taste, pain, vision, thermosensation, neuronal signaling, and more. There are eight subfamilies of TRP channels and 28 distinct channels. The subfamilies include ankyrin (TRPA), canonical (TRPC), polycystin (TRPP), melastatin (TRPM), vanilloid (TRPV), mucolipin (TRPML), no mechanoreceptor potential (TRPN), and yeast (TRPY); the final two subtypes are not expressed in rodents or humans. I will only discuss TRP channels that are important for cerebrovascular function: TRPA, TRPC, TRPM, and TRPV, paying particular attention to TRPV4 channels.

1.2.3.1 – Vascular TRPA1 channels

TRPA1 is the only member of the TRPA family. This channel subtype has 18 C-terminal ankyrin repeats in its unique structure that provides its namesake. TRPA1 is Ca^{2+}-permeable, non-selective, and comprises four identical subunits (87). Though not expressed in peripheral endothelial cells, TRPA1 is expressed in the cerebral endothelium of both rodents and humans (24, 322). There is a wide range of compounds

that can activate TRPA1, ranging from mustard oil (allyl isothiocyanate; AITC), garlic oil (allicin), and tear gas (acrolein; (86, 177)). Importantly, TRPA1 is also activated by oxidative stress products, including 4-hydroxynonenal (4-HNE). This is reflected by the colocalization of these channels with nicotinamide adenine dinucleotide phosphate (NADPH) oxidase 2 (NOX2), putting them near the source of reactive oxygen species (ROS). Pressure myography was used in the initial studies to determine the role of TRPA1 channels in cerebral arteries. TRPA1 activation was found to produce endothelium-dependent dilation through activation of IK_{Ca}, and these channels colocalized with one another near MEJs (81). Therefore, TRPA1 channels likely contribute to EDH in cerebral arterioles, though their basal function is poorly understood.

1.2.3.2 – Vascular TRPV3 channels

Though most well-known for their role in pain, itch, and wound healing in the skin, TRPV3 channels are also expressed in cerebral VSMCs and endothelial cells. This channel is activated by various dietary compounds, including carvacrol (oregano), eugenol (clove), vanillin (vanilla), and thymol (thyme) (82, 271, 344). Using pressurized PAs and increasing concentrations of carvacrol, a role for TRPV3 channels was identified in EDH-mediated dilation (271). However, to date, no endogenous agonists have been identified, and it is unlikely that dietary TRPV3 activators reach concentrations in the cerebral circulation sufficient to activate the channel.

1.2.3.3 – Vascular TRPC channels

TRPC channels play a key role in store operated Ca^{2+} entry and vasoconstriction. Store operated Ca^{2+} entry is triggered by the emptying of intracellular Ca^{2+} stores in the sarco/endoplasmic reticulum, thereby promoting the replenishment of these stores.

TRPC1, TRPC4, and TRPC5 have each been implicated in this role in VSMCs of cerebral arteries and arterioles of rats and rabbits (126, 207, 345). In vascular endothelial cells, TRPC1 channels form heteromeric channels with TRPV1 to bring Ca^{2+} into the cell (217). TRPC3 and TRPC6 channels have been implicated in vasoconstriction and TRPC6 is important in myogenic tone generation. In both mesenteric and cerebral arteries, membrane-bound TRPC3 channels form a complex with IP3Rs to increase intracellular Ca^{2+} and vasoconstriction (2, 3, 340). VSMC TRPC3 channels are activated by endothelin-1 and AngII, both agonists of GPCRs (208, 296). As mentioned earlier, TRPC6 channels contribute to myogenic tone generation in cerebral arteries. Cerebral arteries from rats with low TRPC6 expression exhibited less pressure-induced depolarization and generated less myogenic tone than control arteries (338). Similar results were observed using isolated MCA segments from $TRPC6^{-/-}$ mice. In this study, TRPC6 knockout completely abolished pressure-induced constriction, demonstrating the importance of these channels in myogenic tone (248). Yet, it is unclear if TRPC6 acts as a mechanosensor, or if it is responding as part of a signaling cascade.

1.2.3.4 – Vascular TRPM channels

TRPM4 channels are not Ca^{2+}-permeable but conduct the flow of monovalent ions, mainly Na^{+}, into the cell. In rat cerebral arteries, TRPM4 channels regulate VSMC pressure- and stretch-induced depolarization and vasoconstriction (85). TRPM4 channels are activated by Ca^{2+} released by the sarcoplasmic reticulum via IP_3Rs, which occurs after mechanical activation of other channels, or direct activation of G_qPCRs, including AT1Rs (118). Depolarization resulting from TRPM4 activation triggers the opening of voltage-

gated Ca^{2+} channels. In PAs, TRPM4 channels are coupled to mechanosensitive purinergic receptors to contribute to development of myogenic tone (212).

1.2.3.5 – Vascular TRPV4 channels

TRPV4 channels are vital for proper cerebrovascular function. While other TRP channels have been implicated in cerebral vascular physiology, TRPV4 channels are the most well-studied and are undoubtedly essential to vascular function. These channels respond to a wide range of stimuli, including temperature, pH, and mechanical stimuli. They can be directly activated by their endogenous agonist, EETs (49, 57, 327), as well as indirectly through activation of G_qPCRs (40). Chemical activators of TRPV4 channels include GSK1016790A and 4-α-phorbol 12,13- didecanoate (4α- PDD) (16, 263, 336).

TRPV4 channels are essential regulators of both PA dilation and cognition. Our lab has demonstrated that in the presence of L-N^G-nitro arginine methyl ester (L-NAME) and indomethacin (to inhibit NO and prostacyclin-mediated dilation, respectively), PA dilation in response to G_qPCR activation with carbachol is unchanged. When PAs are incubated with TRPV4 antagonist GSK2193874, dilation is blocked entirely (67). Further, rats with a global TRPV4 knockout have abolished endothelium-dependent dilation in PAs (66). Importantly, our group has consistently found across models that impaired TRPV4 function in PAs is linked to cognitive impairment (37, 66, 67, 224).

TRPV4 activation produces dilation through a Ca^{2+} influx that activates nearby IK_{Ca}/SK_{Ca} channels, producing EDH. As mentioned previously, K_{IR} channels activate in response to this hyperpolarization to amplify the signal. TRPV4 and K_{IR} channels have an important reciprocal relationship with one another that depends on PIP_2 to determine which channel is active. When PIP_2 levels are elevated, TRPV4 channel activity is

reduced, while K_{IR} channel activity is high. Conversely, K_{IR} channels have low activity when PIP_2 levels are low, and TRPV4 channel activity increases. This allows G_qPCRs, which break down PIP_2, to act as a functional toggle between the two channels (134). When TRPV4 channels are active, the localization of TRPV4 channels and interaction with other proteins in the cell is paramount to fulfill their functional role. TRPV4 channels that contribute to endothelium-dependent dilation are localized to MEJs in a four-channel structure (315). PKA and PKC are both enhancers of TRPV4 activation. These proteins are anchored by a third protein called A-kinase anchoring protein-150 (AKAP150). Therefore, TRPV4 channels must be near AKAP150 to be able to propagate the signal appropriately. Endothelium-dependent dilation is impaired when communication between TRPV4 and AKAP150 is disrupted. The Ca^{2+} influx through TRPV4 is so robust that a maximal dilatory effect is achieved by activating only three channels (315). Figure 1.4 features key components at MEPs involved in TRPV4-mediated dilation. This is discussed further in section 1.3.3.

It is generally accepted that TRPV4 channels respond either directly or indirectly to mechanical stimuli to produce dilation. However, the exact mechanisms involved are a topic of debate. Though a recent study reported that TRPV4 channels are not sensitive to mechanical stretch (251), other studies disagree. For example, rat carotid arteries do not undergo shear stress-induced vasodilation in the presence of ruthenium red, a TRPV4 inhibitor (189). Additionally, carotid arteries from TRPV4 knockout mice have significantly blunted flow-mediated dilation (136). In mouse mesenteric arteries, TRPV4 activation produced dilation through a mechanism involving both eNOS and EDH, and this was linked to shear stress (236). It is well-supported in the literature that TRPV4 channels are

at least indirectly activated by arterial stretch. However, most of these studies were conducted using peripheral arteries, and these mechanisms might not extrapolate to the cerebral vasculature.

In VSMCs, TRPV4 channel activation has been linked to myogenic tone modulation. Similar to endothelial TRPV4 channels, those expressed in arterial myocytes must be near A-kinase anchoring protein 150 (AKAP150) to be effective. In VSMCs, Ca^{2+} sparklets through TRPV4 channels activate RyRs on the sarcoplasmic reticulum, producing a Ca^{2+} spark. These sparks activate BK_{Ca} channels to hyperpolarize the cell, resulting in vasorelaxation (83, 84). In cerebral arteries, this has been linked to AngII signaling; AngII activates G_qPCRs that produce PKC, which increases TRPV4 phosphorylation (237). As mentioned previously, though PAs express BK_{Ca} channels, they are not active under physiological conditions (54). Therefore, the specific mechanism by which TRPV4 channels contribute to tone modulation in PA VSMCs is not well understood. Studies from our lab suggest these channels may not have much of a role in tone regulation under baseline conditions but may increase tone in pathological states like hypertension. This was shown in PAs of AngII-hypertensive mice, where TRPV4 inhibition reduced tone by ~20% (67).

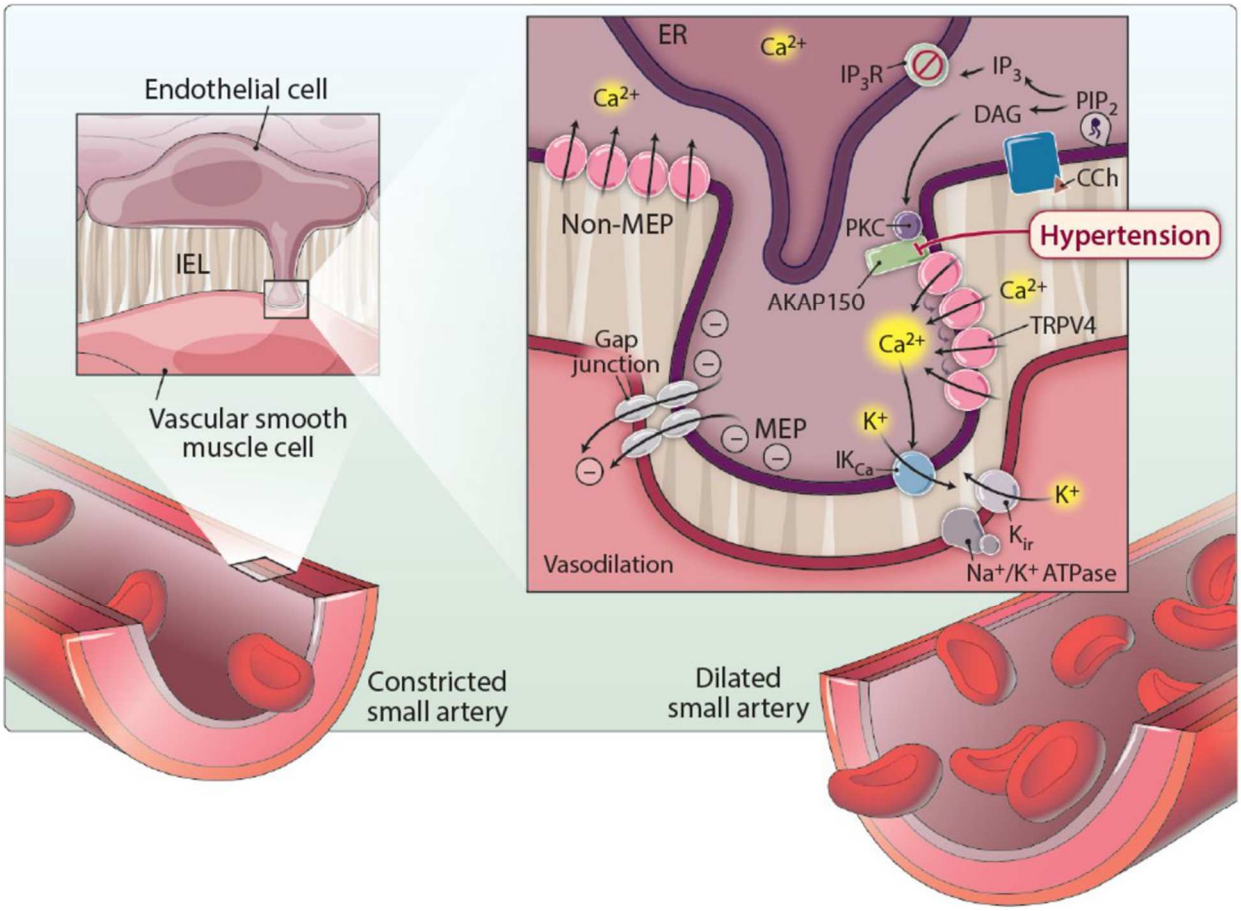

Figure 1.4: TRPV4-mediated dilation at MEPs. At MEPs, diffusible factors can pass from endothelial cells to VSMCs to contribute to the endothelial regulation of myogenic tone. G_qPCR activation via agonists such as carbachol (CCh) cause the breakdown of PIP_2 to DAG and IP_3. DAG goes on to activate PKC, which is anchored to MEPs by AKAP150. TRPV4 activity is enhanced by PKC; when TRPV4 and AKAP150 are close enough to one another, Ca^{2+} sparklets through TRPV4 channels activate nearby IK_{Ca}/SK_{Ca} channels, hyperpolarizing the cell. This hyperpolarization crosses through MEPs to VSMCs to produce vasodilation. Vascular pathologies, such as hypertension, facilitate the uncoupling of TRPV4 from AKAP150, leading to a failure to propagate Ca^{2+} signaling and, therefore, endothelial dysfunction. Reproduced with permission from (15).

1.2.3.6 – Sex differences in TRP channels

While studies investigating sex differences in TRP channel expression and function are limited, there is evidence that sex hormones play a role in regulating these ion channels in some contexts. E2 may regulate the function of members of the TRPV family. For example, TRPV1 appears unimportant for basal uterine mechanosensation, but plays a role in uterine pain sensation in the presence of E2 (349). In the brain, TRPV channel expression varies with fluctuating E2 levels in the estrus cycle of female mice (194). Of particular interest, TRPV4 channels have elevated expression in several brain regions, including the hippocampus, during the proestrus cycle where E2 levels are highest. It is unclear what effect this has on cerebral blood flow regulation, if any.

1.2.4 – The neurovascular unit and neurovascular coupling

Because the brain does not have its own energy stores, cerebral blood flow must be tightly regulated to provide swift increases in flow to areas with high neuronal activity. The increase in blood flow provides the neurons with oxygen and glucose required to function and serves to remove waste products. This crucial process is termed functional hyperemia and is achieved through NVC. NVC relies on seamless communication among VSMCs, endothelial cells, pericytes, astrocytes, and neurons. Together, these cells comprise the neurovascular unit (NVU) (48, 153). The cells in the NVU relay signals to one another to prompt a spatially and temporally appropriate increase in blood flow to meet neuronal demands (176, 243). Disruptions in NVC result in cerebral injury that can range from a mild impact to, in extreme cases, local tissue death. The many processes involved in NVC share similarities, complement, and overlap with one another, acting as

fail-safes to protect against dysfunction. This redundancy reflects the importance of NVC in appropriate brain function and health.

Classically, NVC has been viewed as having neuron-to-vessel directionality, with neuronal activity driving the direction of blood flow. However, recent studies suggest this communication is bidirectional. Vasculo-neuronal coupling was first reported by Kim *et al.* where they demonstrated that PA constriction was associated with reduced neuronal activity. Conversely, PA dilation was related to elevated neuronal activity (186, 187). While the mechanisms involved are not fully known, astrocytic Ca^{2+} transients through TRPV4 channels appear to be involved (274). These novel studies utilized a valuable methodology, taking advantage of whole brain slices that left the NVU intact. This allowed for a unique analysis of intercellular communication during NVC.

Endothelium-dependent dilation mechanisms described in previous sections are important for NVC; to prevent redundancy, this section will focus on mechanisms unique to NVC. Direct interactions of neurotransmitters with the cerebral vasculature likely contribute to NVC. Glutamate, an excitatory neurotransmitter, activates astrocytic $G_{q/11}$ metabotropic glutamate receptors, producing a Ca^{2+} wave. Through this increase in intracellular Ca^{2+}, pathways are stimulated to produce and release EETs, NO, and prostaglandins, which produce vasodilation by interacting with VSMCs in neighboring PAs (99, 150).

There has recently been an increased focus on NVC mechanisms involving capillaries, which do not have VSMCs. For blood flow to be increased in capillaries, there must also be dilation in upstream arteries and arterioles. To this end, there must be a retrograde signal that starts in capillaries and moves upward to PAs to trigger dilation.

Studies to elucidate these mechanisms have pinpointed K_{IR} as a likely component of the retrograde signal. K_{IR} channels are activated by extracellular K^+ and produce a robust and rapid efflux of K^+ to hyperpolarize the cell (216, 298). Mechanisms involving these channels were explored using elegant *ex vivo* preparations of cannulated and pressurized PAs with attached capillaries. Applying a localized pico-spritz of K^+ to the capillaries produced PA dilation. When the microvessel preparations were pretreated with $BaCl_2$ to block the pore of K_{IR} channels, PAs did not dilate after capillary K^+ exposure, confirming the role of K_{IR} in this process. The significance of $K_{IR}2.1$ channels in NVC was further explored using $K_{IR}2.1^{-/-}$ mice and cranial window preparations to better view the microvasculature during laser Doppler flowmetry. Mice lacking these channels had reduced cerebral blood flow response to whisker stimulation compared to control, confirming the proposed mechanism involving $K_{IR}2.1$ channels functions *in vivo* (215). Notably, these channels require the presence of phosphatidylinositol 4,5-bisphosphate (PIP_2) to function. As previously mentioned, $K_{IR}2.1$ and TRPV4 channels act in opposition to one another in endothelial cells, and the presence of PIP_2 acts as a molecular switch to toggle between the two channels' functions (133, 134). These studies suggest that capillary K_{IR} channels are activated either in direct response to extracellular K^+ produced by neurons after firing or indirectly as a result of astrocytic BK_{Ca} activation, which occurs in response to increases in astrocytic intracellular Ca^{2+}.

A role for TRPA1 channels has been identified in the retrograde dilatory signal from capillaries to PAs. Using microvessel preparations like those described earlier, capillary TRPA1 activation stimulated pannexin-1 channel activation in endothelial cells. This caused an efflux of ATP that is proposed to activate P2X receptors on neighboring

endothelial cells. This signal is propagated upward until the junction of the capillary and PA, where the resulting Ca^{2+} increase activates IK_{Ca}/SK_{Ca} to cause PA dilation. This proposed pathway is dependent on K_{IR} and IK_{Ca}/SK_{Ca}; the use of antagonists against these channels reduces capillary TRPA1-induced PA dilation. The use of endothelial $TRPA1^{-/-}$ mice supported the existence of this hypothesized pathway, as these mice exhibited impaired NVC in response to whisker stimulation compared to TRPA1-intact mice (326). Because TRPA1 channels are activated by lipid peroxidation products formed in times of elevated oxidative stress (87, 322), it is thus far unclear how the role of TRPA1 channels in NVC would be impacted during pathological states.

The elucidation of mechanisms involved in NVC is an ongoing effort, and several proposed mechanisms have not been discussed in depth here because the evidence to support them is limited. Of note, there may be a role for astrocytic PGE_2 in NVC (122) and a potential requirement for endothelial caveolae (42). The field is working to discover mechanisms involved in NVC and to determine how the already identified pathways work in concert with one another. A representation of the NVU is shown in Figure 1.5.

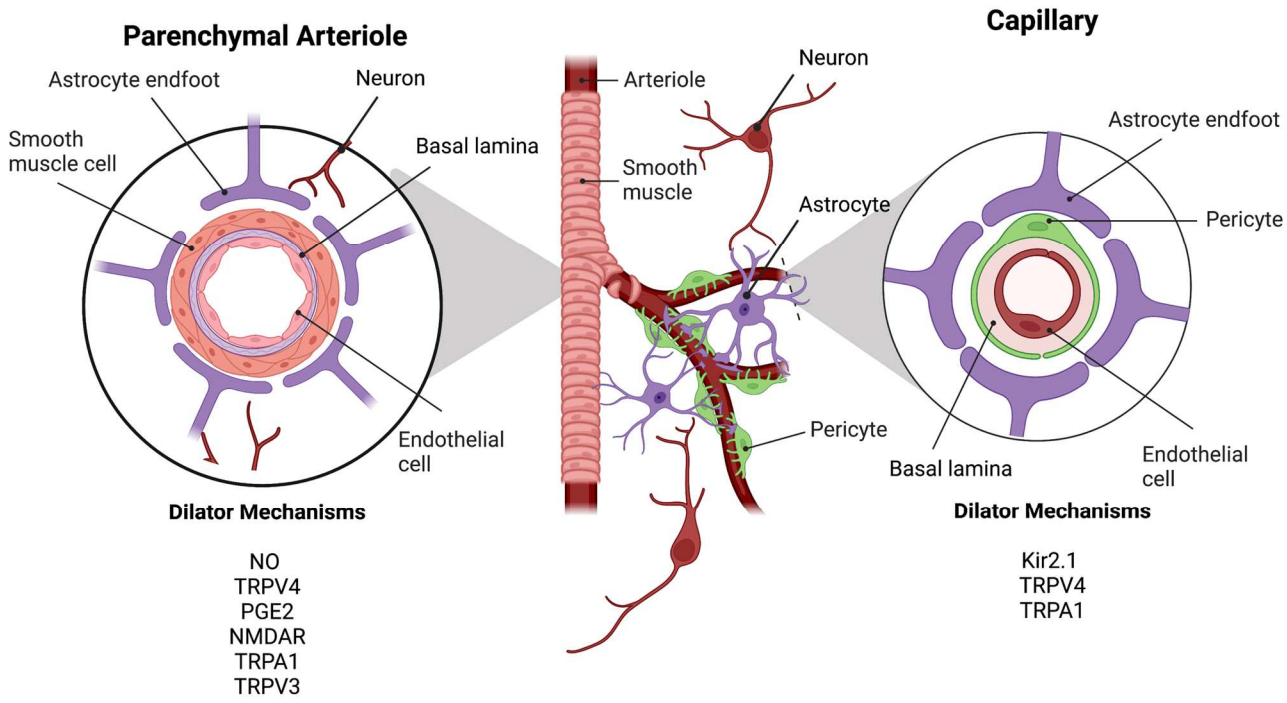

Figure 1.5: The neurovascular unit. At the level of the PA (left), the NVU contains endothelial cells, VSMCs, astrocytes, and neurons. Important dilatory mechanisms to PAs include NO, TRPV4, PGE2, NMDAR, TRPA1, and TRPV3. At the capillary level (right), VSMCs are replaced with pericytes. Important dilatory mechanisms in capillaries include $K_{IR}2.1$, TRPV4, and TRPA1. Created with BioRender.com.

1.3 – The effect of hypertension on the cerebral vasculature

Nearly half of the United States population has hypertension; of these, only a quarter have their blood pressure under control (286). Prolonged blood pressure elevations damage the structure and function of cerebral arteries and arterioles, increasing the risk for various conditions, including VaD. This section will discuss hypertension-induced alterations to the vasculature. While cerebral arteries will be the

focus, significant information obtained from other vascular beds will also be included where appropriate.

1.3.1 – Experimental models of hypertension

Because much of what we know about the impact of hypertension on cerebrovascular health is from rodent models of hypertension, it is important to discuss these models. This section will briefly review a few of the most used models of hypertension, paying particular attention to models relevant to the work in this dissertation. For brevity and relevance, sex differences will only be discussed in AngII-hypertension.

1.3.1.1 – Genetic models of hypertension

Some of the most common methods of studying hypertension involve genetic rodent models that exhibit increased sympathetic nervous system activity observed in hypertensive patients (90). Spontaneously hypertensive rats (SHR) develop hypertension that coincides with an increase in sympathetic activity when compared to normotensive Wistar-Kyoto (WKY) control rats (172). Over the first eight weeks of life, hypertension can be prevented by sympathectomy alongside treatment with the α-adrenoceptor antagonist prazosin, demonstrating the dependence of the rats' hypertension development on sympathetic nervous system activation (191). SHR, and their more stroke-prone cousin, the spontaneously hypertensive stroke-prone rat (SHRSP), are often used because of the multifactorial nature of their hypertension that mimics the human condition. Around the time the SHR was being developed, Lewis Dahl developed the Dahl salt-sensitive rat strain, which becomes hypertensive when given a normal salt diet (56). In mice, a genetically hypertensive strain was developed alongside related controls, termed the blood pressure high (BPH), blood pressure low (BPL), and blood pressure normal (BPN)

strains (158). These mice, similar to the SHR, have multifactorial hypertension, and the mechanisms behind its development have not been fully elucidated. While these models of hypertension are useful in their own right, a major drawback lies in the early age at which hypertension develops, often in the first several weeks of life. This complicates comparisons to humans, and these models are not ideal for studying diseases of the elderly.

1.3.1.2 – Inducible models of hypertension

Several popular models use pharmacological and dietary agents to induce hypertension. In Spague Dawley (SD) and Wistar rats and C57BL/6J mice, hypertension can be induced using implantation of deoxycorticosterone (DOCA)- salt pellets alongside administration of 0.9-1.7% NaCl in drinking water and uninephrectomy. Control rodents are given a placebo pellet instead of DOCA, with other treatments remaining the same. These are low-renin models of hypertension, so the animals require concomitant treatment with a low dose of K^+ to prevent hypokalemia. Hypertension can also be induced by preventing NO production with L-NAME or L-N^G-nitro-L-arginine (L-NNA) administration, often in the drinking water (165). Because this is not a particularly physiologically relevant model of hypertension, it is of limited utility.

1.3.1.3 – Angiotensin II-hypertension

One of the most common experimental models of hypertension is AngII-dependent hypertension. AngII-hypertension classifies as an inducible model of hypertension, but due to its relevance in this dissertation it will be discussed in detail. AngII exerts detrimental effects on the vasculature primarily through activation of AT1R. Two of the most common and most effective antihypertensive treatments are ACE inhibitors and

angiotensin receptor blockers, which directly act to prevent AngII synthesis and prevent receptor activation, respectively. Because of this, AngII-hypertension models are clinically relevant. A particular strength of the AngII-hypertension model is the ability to induce hypertension at any age, thereby having more control over the study design. Further, combining this model with knockout mice is useful in elucidating effects of single genes on blood pressure development. AngII is often infused via osmotic minipumps, which requires a minor surgery and has a healing time of just a few days. The experimenter can choose the dose of AngII infused, which often ranges from 50ng/kg/min to 1000 ng/kg/min and beyond. Lower doses are referred to as slow-pressor doses, speaking to the slow development of hypertension. Higher doses are considered pressor doses. Because of price considerations in the dosage, this model is most often used in mice and is used infrequently in rats. AngII infusion can be used alongside increased sodium intake, exacerbating effects (165, 205).

AngII-hypertension induces alterations in vascular structure, endothelial dysfunction, and impairments in NVC (65, 67, 182). The mechanisms involved in these processes are discussed in appropriate sections throughout this chapter. An emphasis should be placed on the concept that the negative consequences of AngII signaling extend beyond vasoconstriction. Specifically, AngII increases NADPH oxidase activity in vascular cells, contributing to increased oxidative stress. Further, AngII increases aldosterone production, which also contributes to NOX production (239, 293). Elevations in NOX-derived superoxide production and associated endothelial dysfunction can be prevented in AngII-hypertensive rats treated with the AT1R antagonist losartan (265, 278). Endogenous NOX-derived ROS are involved in a positive-feedback cycle that

increases AT1R expression, continually adding to the amount of ROS in the system and contributing to increased blood pressure (252).

Studies from our lab have shown that AngII-hypertension causes inward hypotrophic remodeling of PAs and endothelial dysfunction characterized by impaired TRPV4 function. These observations are associated with reductions in cerebral blood flow and cognitive impairment. Additionally, due to its role in the renin-angiotensin-aldosterone system (RAAS), AngII-hypertension leads to elevated aldosterone production and, subsequently, more MR activation. When AngII-hypertensive mice are treated with an MR antagonist, the vascular and cognitive consequences of AngII infusion are prevented. This presents the possibility that many vascular effects previously attributed to AngII may actually be mediated by MR activation. The consequences of increased MR activation are described in section 1.4.

1.3.1.4 – Sex differences in angiotensin II-hypertension

Studies have reliably found that young female mice are largely protected from the detrimental impacts of AngII-hypertension. Male mice infused with 800ng/kg/min AngII become hypertensive, while female mice do not (341, 342). To test the role of sex hormones, a separate study used castrated male and ovariectomized female mice and compared them to their intact counterparts. Castrated male mice had lower mean arterial pressure after AngII infusion than control, while ovariectomized female mice became hypertensive. The resistance of female mice to AngII-hypertension was mediated by ER-α (343). In male mice, AngII-hypertension is associated with increased ROS production; this is not the case in female mice (220). The superoxide dismutase mimetic tempol dampens the AngII-hypertensive response in male but not female mice (341),

demonstrating the detrimental impact of ROS on AngII-hypertension and its sex dependence. A common flaw of studies examining sex differences is that they rarely assess the sexes side-by-side and instead rely upon comparisons from previous studies. This complicates findings as the mice are no longer experimented upon under the exact same conditions, and the studies are often conducted by different experimenters. Studies within this dissertation will examine the sexes side-by-side to limit interexperimental variability.

1.3.2 – The renin-angiotensin-aldosterone system

Before discussing how hypertension impacts the cerebrovascular system, it is important to describe the RAAS. The RAAS is an essential regulator of blood pressure. Renin is secreted from renal juxtaglomerular cells in response to decreases in blood pressure or Na^+ load. Renin cleaves angiotensinogen, which circulates in the plasma after being released from the liver. This forms angiotensin I, a physiologically inactive molecule. Angiotensin I is converted to AngII in endothelial cells by angiotensin-converting enzyme (ACE). AngII activates AT1R and type 2 AngII receptors (AT2R), which are GPCRs with opposing vascular effects. In the plasma, AngII is further degraded to angiotensin III, which has similar vascular effects as AngII through activation of both AT1R and AT2R (255). Angiotensin III can also be converted to angiotensin IV, which positively affects vascular function and cognition after activating the angiotensin IV receptor, though the mechanisms behind this are unclear (292). In addition to being a precursor to AngII, angiotensin I can be converted into angiotensin-(1-7) that activates Mas receptors (MasR) (103). Importantly, AngII plays an essential role in stimulating

aldosterone synthesis in the zona glomerulosa of the adrenal cortex (254). Aldosterone acts as an agonist on the MR, which will be discussed in detail in section 1.4.

AT1R activation is responsible for the majority of AngII's effects, including vasoconstriction and increased Na^+ retention, through its ability to simulate aldosterone production. Beyond its effects on blood pressure, AT1R activation increases ROS generation, oxidative stress, fibrosis, and cellular proliferation and migration (62, 179). In VSMCs, AT1R-induced cellular proliferation contributes to vascular remodeling. Blockade of AT1R reverses the inward remodeling of cerebral arteries in SHR, demonstrating the importance of this pathway in remodeling associated with hypertension (80). The increased oxidative stress that occurs after AT1R activation is associated with reduced eNOS expression and phosphorylation and uncoupling of the enzyme (36, 68). AT1R blockade in SHR restores eNOS expression and improves NO bioavailability (347). Importantly, while humans only express one version of AT1R, rodents express two similar subtypes: $AT1R_a$ and $AT1R_b$. In VSMCs of cerebral pial arteries, $AT1R_b$ is much more highly expressed than $AT1R_a$. In VSMCs of PAs, these receptor subtypes are expressed in relatively equal amounts, though there is a lower overall expression of both isoforms in PAs (348). In both pial arteries and PAs, $AT1R_b$ are important for the initiation of myogenic tone, but not for its maintenance. $AT1R_a$ is important for myogenic tone generation in PAs but not pial arteries, highlighting differentiation of receptor expression and function throughout the vascular network (270, 348). Because AT1R antagonists like losartan bind similarly to both receptor subtypes, studies investigating their differential roles typically combine AT1R antagonist treatment with a genetic knockout of one of the subtypes (348). While these studies shed light on the differing roles of AT1R subtypes in rodents, the

physiological relevance of the receptor subtype expression in rodents versus humans is not yet clear.

To balance the vasoconstrictor and inflammatory effects of AngII, AT2R acts in opposition to AT1R to promote vasodilation, antiproliferation, and anti-inflammatory responses (157, 204). Because of these functions, AT2R are considered the protective arm of the RAAS. The vasodilatory effect of AT2R was first demonstrated in a study that selectively overexpressed AT2R in aortic VSMCs of transgenic mice. When infused with AngII, these mice did not develop hypertension (332). The dilatory effects of AT2R activation have been attributed to increased baroreflex sensitivity, bradykinin-mediated NO production, and Na^+ excretion, though the specific mechanisms are still incompletely understood (130, 235).

In addition to AT2R, activation of MasR by angiotensin-(1-7) is also associated with vasoprotection. Angiotensin-(1-7) is produced by elevated angiotensin-converting enzyme 2 (ACE2) activity. Increased MasR activation improves baroreflex sensitivity and increases NO release, which contributes to vasodilation. This receptor also has antifibrotic, antihypertrophic, and antithrombotic properties that counteract AT1R signaling (234, 301). In summary, the AngII-ACE-AT1R axis is associated with increased blood pressure, cellular proliferation and migration, oxidative stress, and increased inflammation, while the angiotensin-(1-7)-ACE2-MasR/AT2R axis acts in opposition to those effects.

1.3.2.1 – Sex differences in RAAS

There are sex differences in RAAS that are important to discuss when considering sex dependent responses to hypertension. Premenopausal women are less likely to

develop hypertension than men of the same age, but this protection disappears after menopause (50). Cardiovascular protection in women is partially because of sex hormones' impact on RAAS activation. Female rodents express a higher ratio of AT2R to AT1R compared to males as well as greater ACE2 expression, leading to more angiotensin-(1-7)/MasR activity (297, 310). This shifts the balance of RAAS to favor cardiovascular protection. These effects are estrogen dependent and reflect observations in humans (321). For example, in heart tissue samples from elderly men, treatment with E2 upregulated ACE2, AT2R, and MasR expression and these changes were associated with reduced inflammation and oxidative stress (26). Conversely, testosterone increased ACE activity and AT1R expression, favoring the vasoconstrictive and inflammatory arm of RAAS (41, 105). Further demonstrating the sex dependence of RAAS receptor expression, castrated male rats had a reduced AT1R to AT2R ratio in the vasculature, which was reversible by testosterone replenishment (238). A summary of sex differences in RAAS balance are featured in Figure 1.6. The sex differences in hypertension that are discussed in the following sections may at least in part be attributed to the differing emphases in RAAS pathways.

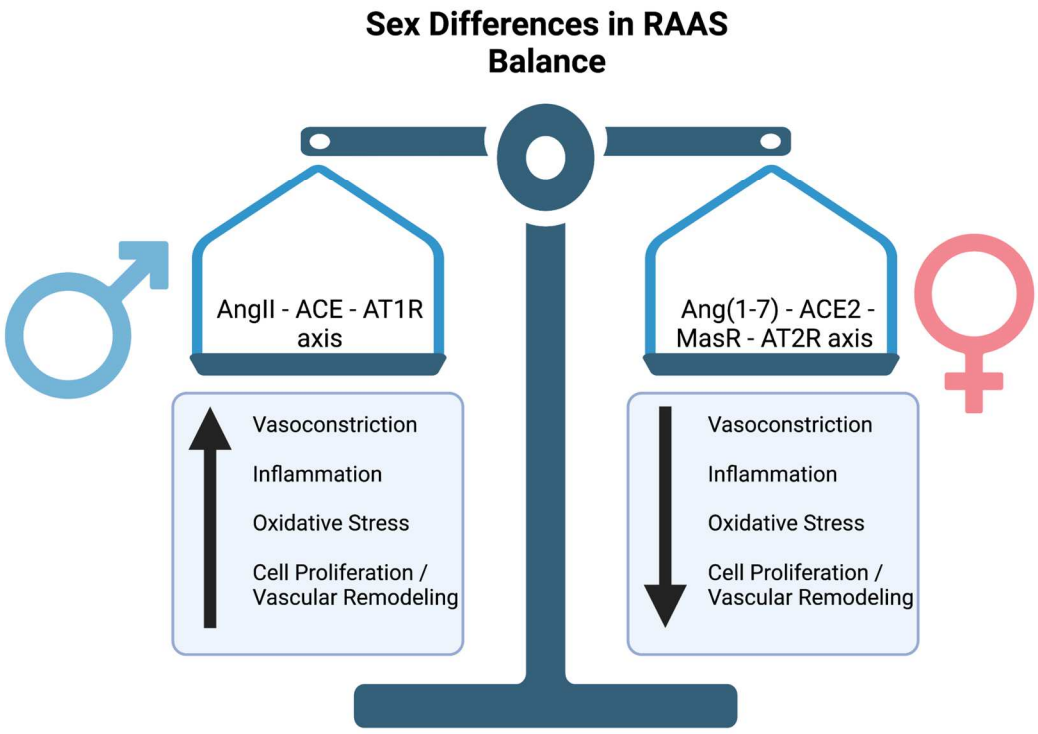

Figure 1.6. Sex differences in RAAS balance. Both males and females experience the consequences of the activation of both arms of the RAAS. However, male sex contributes to a greater weight placed on the AngII-ACE-AT1R axis of RAAS, leading to more vasoconstriction, inflammation, oxidative stress, and vascular remodeling. Female sex contributes to a favoring of the angiotensin (1-7)-ACE2-MasR-AT2R axis of RAAS, which protects against the effects of the opposing axis and exerts cardioprotective effects. Created with BioRender.com.

1.3.3 – Hypertension and cerebrovascular structure and rarefaction

Hypertension is associated with artery remodeling in both the peripheral and the cerebral vasculature. Artery remodeling describes changes in arterial structure regarding the lumen diameter and wall thickness. These changes are most accurately assessed in

fully dilated or blood vessels in Ca^{2+}-free buffer. Inward and outward remodeling describe reductions and increases in lumen diameter, while hypotrophic and hypertrophic describe reductions and increases in wall thickness, respectively. Eutrophic remodeling indicates changes in lumen diameter and/or wall thickness without a change in the overall wall cross-sectional area (242). Artery remodeling is initiated as a protective measure to normalize the increase in wall stress resulting from elevated blood pressure. In fact, if cerebral arteries fail to remodel during hypertension, the risk increases for blood-brain barrier breakdown and vasogenic edema (148). However, if hypertension is sustained, the changes in vascular structure can impede appropriate blood flow regulation and become pathogenic. In large cerebral arteries, hypertension leads to inward hypertrophic remodeling (71, 268, 284). In PAs, however, hypertension induces inward hypertrophic remodeling in SHRSP (269), but inward hypotrophic remodeling in AngII-hypertensive mice (65). The cause for a reduction in PA wall thickness after AngII infusion is unclear. PAs have only a single layer of VSMCs, indicating this must result from a change in the structure of single VSMCs. Though hypertension-induced arterial remodeling has been characterized in the cerebral arteries and arterioles of rodents, data from cerebral arteries of humans is lacking. A recently published study using post-mortem tissue identified no statistically significant differences in wall thickness or wall area of major cerebral arteries between hypertensive and normotensive patients. Analyzing tissue from males and females separately did not change the outcome, though the study may have been underpowered when further separated into these groups. A significant limitation of this study is that results were not stratified based on the severity of hypertension, and normal anatomical variation may have complicated comparisons (334). Moreover, the treatment

status of these patients was unknown, which likely adds variability and complicates data interpretation. Nonetheless, these data emphasize the need for studies using human tissue and urge caution in the extrapolation of rodent data to humans.

Beyond alterations in arterial structure, hypertension can also contribute to vascular rarefaction, which is a reduction in the number of perfused arterioles and capillaries. Rarefaction of cerebral arterioles has been observed across various models of hypertension (262, 314). A reduction in perfused arterioles and capillaries reduces the amount of blood capable of reaching neurons, which increases cognitive decline risk (53). In our lab, AngII-hypertensive mice did not exhibit rarefaction, despite having cerebral hypoperfusion (65).

1.3.3.1 – Sex differences in hypertension-associated vascular remodeling

There is minimal data on sex differences in cerebrovascular remodeling in hypertension. Our lab has reported that both male and female SHRSP undergo inward eutrophic remodeling of MCAs (282, 285). In heart tissue, however, female rats underwent less hypertrophic remodeling than males after volume overload and myocardial infarction, reflecting human observations (61, 78). Female SHR exhibited delayed myocardial remodeling with age compared to their male counterparts, which was associated with increased AT2R and MasR expression in females (5). A major strength of this study is the parallel analysis of the sexes across a range of ages. Studying both males and females alongside one another in the same set of experiments limits variability that can occur when groups are studied in separate sets of experiments. However, heart tissue and vascular tissue experience very different physical forces *in vivo*, so it is unclear how well these data can be extrapolated to the vasculature.

1.3.4 – Hypertension and endothelial dysfunction

Hypertension leads to endothelial dysfunction, characterized by the endothelium's failure to send vasodilatory signals to the VSMCs (128). In hypertension, eNOS can uncouple from its cofactor BH_4, causing the preferential production of superoxide over NO. Additionally, superoxide interacts with NO to form peroxynitrite, limiting the amount of available NO (101, 178). Early studies using intravital microscopy in pial arteries compared SHRSP and WKY rats. These studies showed that SHRSP have intact endothelium-independent vasodilatory function, but endothelium-dependent dilation induced by acetylcholine is severely blunted (225). A significant component of this endothelial impairment results from dysfunctional NO signaling; this finding is consistent throughout hypertensive models and vessel types. In both SHR and SHRSP, eNOS mRNA expression was reduced in the cerebral frontal cortex compared to WKY. This was accompanied by reduced eNOS protein expression and phosphorylation, suggesting that the effects of reduced eNOS expression are compounded by reduced activation (169). In Dahl salt-sensitive hypertensive rats, mesenteric arteries exhibit endothelial dysfunction (325) that was associated with reduced eNOS mRNA expression (109), and NO-mediated dilation was also impaired in cerebral arterioles of AngII-hypertensive rats (114). Importantly, AT1R antagonism in SHR normalized eNOS mRNA and protein expression, suggesting the impaired NO signaling occurs at least partially as a result of AT1R activation (9, 347).

Hypertension also impairs EDH-mediated dilation in peripheral and cerebral arteries. For example, in SHR, EDH-mediated dilation in mesenteric arteries was impaired relative to WKY rats (107). Other studies measuring EDH-mediated dilation in very young

SHR that had not yet developed hypertension did not observe impairment, suggesting the dysfunction occurs secondary to hypertension (106). It is important to note, however, that in genetic models of hypertension, blood pressure elevates with age, which complicates the conclusion that impaired endothelial function is a result of hypertension versus a result of aging in these models. Further, in these models it is difficult to tease out the order of events; it is possible that hypertension develops as a result of endothelial dysfunction, rather than hypertension leading to endothelial dysfunction.

Studies from our lab and others have pinpointed disrupted signaling though TRPV4 channels and reduced TRPV4 mRNA expression as key components of the impaired EDH-mediated dilation. Mesenteric arteries from SHRSP exhibit impaired TRPV4-mediated dilation that is associated with reduced TRPV4 and SK_{Ca} mRNA expression (307). Our lab showed that in AngII-hypertensive male mice, TRPV4-mediated dilation in PAs is impaired and TRPV4 and IK_{Ca} mRNA expression is reduced in cerebral arteries. These findings were associated with cognitive dysfunction, suggesting TRPV4 is a potential mechanistic link between hypertension and VaD (67). A critical study by Sonkusare *et al.* proposed a mechanism beyond reduced ion channel expression. In this study, impaired TRPV4-mediated dilation in mesenteric arteries of AngII-hypertensive mice was associated with reduced localization of AKAP150 to MEPs (316), further highlighting the importance of TRPV4 and AKAP150 interaction. Disrupted localization of these proteins is also associated with obesity-induced hypertension and worsened by peroxynitrite (260), suggesting oxidative stress is a driver of TRPV4-AKAP150 disruption.

1.3.4.1 – Sex differences in hypertension-associated endothelial dysfunction

The majority of studies assessing the impact of biological sex on hypertension-induced endothelial dysfunction have focused on NO. In AngII-hypertensive mice, acetylcholine-induced dilation in cerebral arteries was impaired in males but not females. This endothelial dysfunction was associated with oxidative stress in male mice and was reversible after treatment with superoxide dismutase (43). Similar results were observed when comparing male and female WKY and SHRSP. In both strains, aortas from female rats had greater NO bioavailability than males (230). The ability of E2 to attenuate oxidative stress likely contributes to the resistance of females to NO dysfunction in hypertension (10). It is unclear if sex differences in EDH-mediated dilation occur during hypertension, and this is a major focus of this dissertation.

1.3.5 – Hypertension and impairments in NVC

It has been well-established that hypertension disrupts NVC (149, 168). Because the cerebral endothelium is an essential component of the NVU, hypertension-induced impairments in dilatory pathways mentioned previously also lead to impairments in NVC; to avoid redundancy, they will not be repeated here.

Experimentally, NVC is assessed by measuring cerebral blood flow before and during a physical stimulus, such as whisker or paw stimulation. In rodent studies, AngII has been identified as a disruptor of NVC. However, it is still unclear how much of this impairment can be attributed to blood pressure elevation versus the direct effects of AngII on vasoconstriction. In studies using a slow-pressor dose of AngII (600ng/kg/min), impairments in NVC occurred before the onset of hypertension (32), suggesting direct AngII effects are to blame. This concept was shown in a separate study that used topical

administration of AngII to show the cerebrovascular effects are similar to those after systemic AngII infusion (117). Further, another study compared NVC in AngII-treated mice with mice given phenylephrine to increase blood pressure to the same magnitude. AngII-treated mice had impaired NVC, while phenylephrine-treated mice did not (182). A separate study used a topical application of superoxide dismutase on the brains of AngII-infused mice during whisker stimulation. Mice with superoxide dismutase treatment do not have impaired NVC relative to controls. Further, mice with reduced NADPH oxidase activity through gp91 deletion are also protected from impaired NVC after AngII infusion. These studies demonstrate that AngII impairs functional hyperemia via increased NADPH oxidase activity and subsequent NVU disruption, not through its effect on blood pressure (181). These studies were vital in showing that AngII has direct detrimental effects on the vasculature that impairs NVC.

The effect of hypertension on NVC has also been observed in genetic rat models of hypertension. In 20- and 40-week-old SHR, the blood flow response to whisker stimulation was attenuated as blood pressure increased. When these rats were treated with verapamil or losartan for two weeks to reduce blood pressure, NVC remained impaired, providing more evidence that hypertension-induced impairments in NVC extend beyond blood pressure elevation (27). It is possible in this model that neurons and arterioles had been damaged enough at that point that signals for increased blood flow could not be sent or received successfully.

As previously mentioned, increased oxidative stress has been implicated in hypertension-associated cerebrovascular dysfunction. The role of oxidative stress in NVC impairment was measured in 24-month-old mice. These mice did not have increased

blood pressure relative to young controls but had impaired NVC that was reversed after treatment with resveratrol, a polyphenolic compound that reduces ROS (330). This suggests increases in oxidative stress observed in hypertension are an essential mediator of impairments in functional hyperemia.

1.3.5.1 – Impact of sex on NVC in hypertension

Randomly cycling AngII-infused female mice are protected against the impaired NVC observed in AngII-infused male mice (116). However, the impact of AngII infusion on cerebrovascular function in female mice differs across the estrus cycle. Cerebral blood flow response in female mice following whisker stimulation is impaired to a similar degree as male mice during the diestrus phase of the cycle where E2 is low. Similarly, ROS production was elevated during diestrus, corresponding with impaired NVC. Conversely, NVC remains intact during the proestrus and estrus phases of the cycle, which are characterized by elevated E2 levels. The protective effect of high E2 in the proestrus phase was negated by topical treatment of the ER inhibitor ICI182,780 (31). The concept that E2 is essential for appropriate neurovascular function was recently addressed in a study that used 4-vinylcyclohexene diepoxide (VCD) to induce menopause in young female mice. This model uses a series of injections to cause gradual ovarian failure that mimics menopause. This study revealed that menopausal mice have impaired NVC compared to ovary-intact controls (21). Together, these data raise the possibility that in humans, the female brain is more susceptible to damage in phases of the menstrual cycle where E2 is low. This coincides with data demonstrating that myocardial ischemia is more likely to occur in women during low E2 times in the menstrual cycle (213). Cerebral autoregulation, however, appears to be unaffected by phases of the menstrual cycle,

suggesting the impact of E2 on vascular function may be species and context-dependent (97). It is important to note that both human studies had very low sample sizes (n=9 and n=13 women, respectively), so further study is necessary to draw confident conclusions.

1.4 – Mineralocorticoid receptors

The mineralocorticoid receptor (MR) is classically described as a regulator of fluid homeostasis in the kidneys, subsequently regulating blood pressure through Na^+ and K^+ transport. However, the MR is also expressed in cardiomyocytes, macrophages, VSMCs, and endothelial cells, as well as some brain regions including the hippocampus, and its activation has direct cardiovascular effects (58, 125, 227, 323). The MR is a nuclear receptor that functions as a transcription factor to regulate gene expression. The MR is the primary target of aldosterone but can also be activated by other endogenous ligands, including cortisol (humans), corticosterone (rodents), and progesterone. Cortisol functions as an MR antagonist until tissue injury or increases in oxidative stress occur, at which point it will function as an agonist. Cortisol is present in the plasma at much greater concentrations than aldosterone, giving this hormone more potential to activate the MR than aldosterone (190). The amount of cortisol-mediated MR activation depends on the local expression of the 11β-hydroxysteroid dehydrogenase-type 2 (11βHSD2), which converts cortisol to its inactive metabolite cortisone. It is because of this enzyme that aldosterone activates the MR more frequently than cortisol or corticosterone (17). MR activation plays an important role in signaling cascades outside of blood pressure regulation, and excess activation is associated with adverse cardiac events, inflammation, endothelial dysfunction, and stroke (76, 95). This section will focus on the function of MR signaling in the vasculature.

1.4.1 – Vascular mineralocorticoid receptors

Because 11βHSD2 is highly expressed in VSMCs and endothelial cells, the primary MR agonist in the vasculature is aldosterone. Beyond aldosterone, MR in VSMCs can be activated after AT1R stimulation by AngII, amplifying the impacts of excess RAAS activation on the vasculature (162). MR expression increases with age in both rat aortic smooth muscle cells (SMCs) (193) and in resistance arteries (77), and its expression in SMCs is associated with vascular remodeling and fibrosis (110). Using SMC-MR knockout mice, a role for this receptor was identified in age-associated processes, including the development of hypertension, increases in oxidative stress, and increases in cardiac and vascular stiffness and fibrosis (188, 228). Resistance arteries from young mice with SMC-MR knockout generate less myogenic tone and have reduced L-type Ca^{2+} channel expression and activity. These arteries also exhibit less vasoconstriction in response to phenylephrine administration or AngII infusion (228). That SMC-MR knockout prevents vasoconstriction after phenylephrine administration shows that this receptor influences contractile state even in the absence of excess MR activation. Together, these data demonstrate the importance of SMC-MR in contractile capabilities of the vasculature. It is important to note that most MR studies were conducted in the peripheral vasculature, and it is not clear if the results directly translate to the cerebral vasculature.

Unlike the SMC-MR, the MR expressed in endothelial cells at physiological levels (EC-MR) does not appear to play an important role in determining basal blood pressure (281). The endothelial MR also does not impact the hypertensive response to AngII infusion, AngII with L-NAME, or high salt intake (65, 241). However, over-expression of the EC-MR leads to significant detrimental effects. Mice overexpressing the EC-MR, have

elevated blood pressure compared to control and vasoconstriction in mesenteric arteries exposed to phenylephrine, the thromboxane A_2 analog U46619, AngII, and endothelin-1 is enhanced. This increased vasoconstriction was not associated with endothelial dysfunction or elevated aldosterone or corticosterone levels, so the amount of excess EC-MR activation was likely subtle (249). These results are at odds with those demonstrating that excess EC-MR activation leads to endothelial dysfunction, suggesting the possibility that increased vasoconstriction occurs before the onset of endothelial dysfunction. Additionally, SHR have increased EC-MR expression in the mesenteric microcirculation, this might contributes to their hypertensive phenotype and impaired vascular reactivity (64). Though EC-MR activation is not associated with adverse physiological consequences at baseline, in situations of cardiovascular stress such as hypertension, EC-MR activation is related to endothelial dysfunction. In AngII-hypertensive mice, EC-MR knockout prevented endothelial dysfunction in mesenteric arteries. Endothelial function in coronary arteries was not improved, suggesting the role of EC-MR during hypertension is dependent on the vascular bed (241). Our lab demonstrated that in cerebral PAs, AngII-hypertension induces inward hypotrophic remodeling and endothelial dysfunction that is prevented by EC-MR deletion, suggesting an essential role of EC-MR activation in hypertension-associated cerebrovascular damage (65, 67). The impact of EC-MR activity on vascular remodeling and endothelial dysfunction may be partly mediated by ENaC. EC-MR activation increases endothelial ENaC expression, and its activation is associated with reduced NO production and increased vascular stiffness. These effects can be mitigated by spironolactone, indicating the resulting vascular damage from ENaC signaling is linked to MR (195).

Beyond its impact on vascular function, the EC-MR has been implicated in inflammation and thrombosis (164). Stimulation of EC-MR by aldosterone in human coronary arteries induces the transcription of intercellular adhesion molecule 1 (ICAM1), a molecule that promotes the adhesion and migration of leukocytes, thereby increasing inflammation (33). In control mice, EC-MR activation by aldosterone promotes thrombosis, but this process is impaired in EC-MR overexpressing mice, suggesting the role of EC-MR can change in pathological conditions (198).

1.4.2 – Mineralocorticoid receptor antagonists

Given that around 10% of hypertensive patients have hyperaldosteronism, using MR antagonists to treat hypertension is a promising therapeutic strategy (28). The use of MR antagonists has been proven useful regardless of the agonist activating the receptor (273). Spironolactone and eplerenone (EPL) are two of the three FDA-approved MR antagonists available. A third FDA-approved MR antagonist, finerenone, is approved only in the context of chronic kidney disease, and unlike the other MR antagonists, finerenone is non-steroidal (279). Spironolactone, a K^+-sparing diuretic, was first generated as an antihypertensive drug. Spironolactone is a potent competitive MR antagonist, but because it is not specific, it has undesirable off-target effects. This drug also activates progesterone receptors and blocks androgen receptors, which affects menstrual regularity in women and can cause sexual dysfunction in men, respectively. Because of these effects, EPL was generated as a more selective MR antagonist, though it is not as potent (199). These two drugs also differ in how they are metabolized. Spironolactone is a pharmacologically active prodrug; while the parent compound has biological effects, the primary action comes from its metabolites. The most notable metabolite is canrenone,

which is often used in laboratory animal studies because it has fewer off-target effects than spironolactone and can easily be administered in drinking water (11, 12). EPL has no pharmacologically active metabolites (51).

Several studies have noted the beneficial effects of MR antagonism on the cerebral circulation during hypertension. After the development of hypertension, MR antagonism reverses the remodeling of the MCA (284, 285) and PAs in SHRSP (269). In PAs and PCAs of AngII-hypertensive mice, MR antagonism prevents remodeling from occurring (65). MR antagonism also improves pial artery and PA endothelial function during hypertension (67, 226). Importantly, these effects are blood pressure independent, as these effects occurred in the absence of blood pressure alterations.

MR antagonism also has a beneficial impact on the vasculature in the context of stroke. MR activation in SHRSP exacerbates cerebrovascular damage after stroke (72), and treatment with spironolactone reduces cerebral infarct size, which was linked to improvements in artery structure (70). One of the mechanisms involved in MR-associated cerebrovascular damage is the receptor's effect on inflammation and ROS generation. NOX1 expression is elevated in SHRSP compared to WKY rats, and this is prevented with treatment with the active metabolite of spironolactone, canrenoic acid. Reductions in NOX1 expression are associated with improved endothelial function in mesenteric arteries. This is associated with reduced collagen I mRNA expression and reduced expression of profibrotic signaling molecules p66Shc and p38MAPK. Additionally, NOX1 knockout mice infused with aldosterone did not exhibit increases in markers of vascular fibrosis observed in control mice (137).

Notably, MR-associated endothelial dysfunction is associated with cognitive decline (67). The relationship between MR antagonism and cognitive function in human studies is complicated and appears context and age dependent. In healthy young men, spironolactone treatment worsens cognitive performance (259), while MR stimulation improves cognition in both young and elderly healthy patients (143). In contexts where the MR is already overstimulated, however, MR antagonism is beneficial. Recent studies in human patients with essential hypertension have revealed that plasma aldosterone levels are negatively correlated with cognitive performance, and early intervention with EPL treatment improves cognition (346). Because the MR is also expressed in neurons, it is difficult to determine how much of these effects are attributable to MR antagonism in the vasculature versus in the neurons themselves (283). Further, it is unclear whether cognitive dysfunction can be reversed with MR antagonism or merely prevented. In my dissertation, I aim to determine whether an improvement in cognition is possible with MR blockade alongside a reversal of endothelial dysfunction after their development in hypertension.

1.4.3 – Sex differences and the mineralocorticoid receptor

It is becoming clear that female sex hormones play a role in MR signaling, which likely influences sex differences observed in cardiovascular disease. Recent reports have suggested that in both humans and mice, females express more EC-MR than males at baseline (96). Further, sex hormone ablation in female mice followed by progesterone supplementation and estrus cycle monitoring, revealed that the elevated EC-MR expression is progesterone dependent, and expression levels change throughout the estrus cycle in response to progesterone concentration (96). Increased MR expression

may be a compensatory mechanism, as progesterone is an MR antagonist. In human adrenocortical tissue, E2 was found to regulate aldosterone production. E2 activation of the ER-β inhibits aldosterone synthesis, when this receptor is blocked, aldosterone synthase expression and aldosterone production increase. Conversely, activation of the non-genomic ER, G protein-coupled estrogen receptor 1 (GPER1), increased aldosterone production, suggesting E2 regulates aldosterone production through a balance of ER activation (34). It is important to note that these studies were conducted in tissues from patients with aldosterone-producing adenoma. Therefore, whether the same findings would hold true under healthy conditions is unclear. In human embryonic kidney-293 cells, E2-activated ER-α appears to form a complex with the MR in the nucleus, preventing the MR from acting as a transcription factor. This suggests E2 signaling potentially acts as a protective mechanism against excess MR activation (18). It is evident that female sex hormones interact with the MR and its activators to influence cell signaling, but how these processes work in concert with one another is not yet fully clear.

The data concerning sex differences in MR antagonism are complicated. For example, in a model of myocardial infarction, cardiac remodeling is more attenuated in the hearts of female rats than male rats after EPL treatment (175), suggesting that the MR is an important therapeutic target for women with myocardial infarction. In a stroke study, however, spironolactone treatment did not improve infarct size in female SHRSP after stroke, despite having beneficial effects in male SHRSP (282). The most consistent data concerning sex and treatment with MR antagonists are in the context of obesity. Both clinical and experimental reports suggest females are more prone to obesity-induced endothelial dysfunction than males (146, 320), and plasma aldosterone levels are

increased to a greater degree in obese women (121). In mice, obesity induces endothelial dysfunction of mesenteric resistance arteries in female, but not male mice (59, 146), a finding that may result from a sexually dimorphic response to increased leptin production (94). Obesity-induced endothelial dysfunction in female mice is prevented by MR antagonism or EC-MR deletion by increasing NO bioavailability. A recent study by Biwer *et al* studied the potential interaction between the MR and ER-α in endothelial cells, revealing that EC-MR deletion improved endothelial function by increasing NO-mediated dilation, which is prevented by simultaneous deletion of ER-α. The proposed mechanism is that EC-MR and ER-α compete for a binding site on striatin to exert their effects on the vasculature (20). Understanding how E2 and the MR interact is critical to identify populations that would benefit from MR inhibition.

1.5 – Vascular contributions to cognitive impairment and dementia

Vascular contributions to cognitive impairment and dementia (VCID) describe a group of disorders characterized by cognitive dysfunction that arises from a cerebrovascular origin. VCID can range from mild cognitive impairment to full-blown VaD. VaD is the second most common subtype of dementia following Alzheimer's disease, in its pure form, it is responsible for 20-30% of all dementia cases, and its prevalence doubles every 5.3 years (123). Notably, at autopsy, nearly half of Alzheimer's patients are found to have a cerebrovascular component to their disease, thereby exacerbating disease progression. Symptoms of VCID vary but can include mental fogginess, personality changes, memory impairments, and executive dysfunction that impacts daily living. Though cognitive testing can help physicians identify VCID, official diagnoses often must be accompanied by neuroimaging. Magnetic resonance imaging (MRI) is useful in

identifying cerebrovascular abnormalities characteristic of VCID, including infarcts and microinfarcts, cerebral microbleeds, white matter lesions, and arteriosclerosis or amyloid angiopathy. These are typical manifestations of cerebral small vessel disease (CSVD(123)). White matter lesions are a particularly common correlate of cognitive impairment. They can occur in conditions such as hypertension or genetic disorders like Cerebral Autosomal Dominant Arteriopathy with Subcortical Infarcts and Leukoencephalopathy (CADASIL) (219, 276). In the absence of obvious clinical issues such as a stroke, brain imaging scans are not routinely performed. VCID is difficult to diagnose in the living and, unfortunately, has no effective therapies. Existing treatments cannot specifically target VCID pathology and instead focus on treating risk factors. The leading risk factor for VCID is aging, but modifiable risk factors include obesity, sedentary lifestyle, preeclampsia, diabetes, heart disease, stroke, and, importantly for this dissertation, hypertension.

1.5.1 – Hypertension as a risk factor for VCID

Major risk factors for VCID include conditions that disrupt NVC or otherwise interrupt cerebral perfusion. As mentioned previously, cerebral hypoperfusion results in inadequate delivery of oxygen and glucose to neurons, thereby contributing to neuronal dysfunction observed in cognitive decline. Because of its detrimental effect on the vasculature, hypertension is the leading modifiable risk factor for VCID (151). Untreated hypertensive patients exhibit a blunted cerebral blood flow response during memory tasks compared to normotensive control patients (168). Medicated hypertensive patients that have their blood pressure controlled, however, do not exhibit impairments in NVC compared to normotensive controls (202). In epidemiological studies, a link between

uncontrolled hypertension and cognitive decline has been consistently reported (88, 112, 201). The increased VCID risk in hypertensive patients is particularly strong in those that have hypertension at midlife. A recent systematic review and meta-analysis reviewing 209 prospective studies found that having a systolic blood pressure of 140mmHg or greater in midlife increased one's risk of late-life dementia development by 37-52%. Even a systolic blood pressure of 130mmHg corresponded to an excess dementia risk of more than 34% (261). This study is one of the most comprehensive meta-analyses available and provides valuable insight regarding VCID risk. A separate longitudinal study that followed a group of 2,268 men over 40 years showed similar results, with a consistent link between elevated systolic blood pressure and future VaD development (289). Importantly, the relationship between hypertension and dementia risk does not appear to exist in those that become hypertensive later in life, unless mild cognitive impairment already exists (261). These studies highlight the importance of controlling blood pressure in midlife, and some have found that mid-life antihypertensive treatment reduces the risk of cognitive decline (147). However, steep reductions in blood pressure in prehypertensive older adults have also been linked to dementia, suggesting age should be considered when prescribing antihypertensive therapy (229).

1.5.2 – Sex differences in VCID risk

Data concerning sex differences in dementia development are inconsistent. When investigating overall dementia prevalence, more women are diagnosed than men, though this is likely due to Alzheimer's risk being greater in women (8). When investigating VaD prevalence specifically, several studies have identified an insignificant trend toward greater risk in men (52, 108), or have not identified a sex difference at all (8). Studies that

controlled for age have identified a greater VaD risk in men until age 85-90, at which point risk is more significant in women (214, 294). These results may be influenced by the survival bias of women, so care should be taken in their interpretation.

Inconsistencies reported in the influence of sex on VaD development can largely be attributed to a failure of these studies to appropriately assess sex differences within the study design. Studies that included women and assessed their risk separately from the men in the study found that hypertension increases VaD risk in women only (115, 139). Further, hypertension, specifically during midlife, is associated with a 65% increased VaD risk in women but not men (115). Whether the efficacy of antihypertensive therapy affects the sexes differently is yet to be established.

1.5.3 – Experimental models of VCID

A major hurdle in identifying therapeutic targets for VCID has been the lack of appropriate animal models. The most widely accepted models induce chronic cerebral hypoperfusion by reducing blood flow through the common carotid arteries. There are several different ways this can be achieved. Bilateral common carotid artery stenosis (BCAS) uses micro coils or sutures around the artery to reduce blood flow to the brain. Instead of stenosing the arteries, unilateral common carotid artery occlusion (UCAO) and bilateral common carotid artery occlusion (BCAO) completely tie off one or both arteries to reduce cerebral blood flow. Complete occlusion of the arteries is associated with high mortality rates. To circumvent this, some studies only occlude for a designated period of time, often less than 20 minutes (353). The benefit of these models is the ability to study reduced cerebral perfusion without interference from other VCID risk factors. A major limitation is that the reduced cerebral perfusion in these models is quite sudden. In

recognition of this limitation, a separate model was developed that utilizes ameroid constrictors placed around the carotid arteries that absorbs extracellular matrix fluid over time. This produces a gradual reduction of arterial diameter, producing a reduction in cerebral blood flow that worsens over time (75). Aside from models that focus on reduced cerebral blood flow, hypertensive models are also widely used to assess cognitive decline in rodents. BPH mice have cognitive impairment that is associated with reduced cerebral blood flow (93, 135). We have reported similar findings in AngII-hypertensive mice (65, 67). In rats, the SHRSP exhibits characteristics of CSVD and cognitive decline. The white matter damage observed in SHRSP during MRI is similar to that observed in human patients with VCID (333). There is also a mouse model termed the CADASIL mouse, which features a Notch3 mutation observed in human CADASIL patients (275). These mice exhibit impairments in cerebrovascular reactivity in old age (197).

Many behavioral assessments can be used to test cognitive function in rodents. For brevity, I will focus on tests I used that will be discussed in future chapters. Ahead of all memory tasks discussed, mice and rats were acclimated to handling, as well as to the room where the testing occurred, over the course of three days. To assess spatial working and spatial reference memory, I used the Y-maze. The Y-maze consists of three equally sized arms placed at 120° angles from each other. Spontaneous alternation behavior was measured to assess spatial working memory (192). To this end, the rodent is placed at the end of one arm of the maze and allowed to freely explore for 3 minutes. A total of 8 arm entries are required to be included in the analysis. A rodent with a functional memory will remember where it has already been in the maze and will preferentially enter the arm it has visited least recently. A correct alternation occurs when the rodent consecutively

enters all three arms of the maze. A high percentage of spontaneous alternation behavior indicates intact spatial working memory.

Appropriate spatial working memory requires successful communication between the hippocampus and the prefrontal cortex (302, 324). The Y-maze can be used again to assess spatial reference memory. This test must take place at least a week apart from the spontaneous alternation task to allow mice time to forget the maze. To assess spatial reference memory, the rodent is placed in the maze with one of the arms blocked off. After exploring the two arms of the maze for 5 minutes, the rodent is placed back in its home cage for a retention period of 60 minutes. After the retention period, the rodent is placed back into the maze with all three arms available for exploration. The percentage of time the rodent spends in the novel arm over 2 minutes is measured. Because rodents prefer novel places, a rodent with intact spatial reference memory will preferentially explore the arm that was previously closed off, while a rodent that has impaired spatial reference memory will spend 33% of its time in each arm (192).

Spatial memory can also be assessed using the Barnes maze. The Barnes maze is a hippocampus-dependent task where rodents use visual cues in their surrounding environment to learn the location of an escape hole (272). The testing apparatus is a circular table with holes lining the perimeter. All holes except the escape hole are covered, and rodents undergo 3 training trials per day for 4 days to learn its location. A weak aversive stimulus is applied during the training period to motivate the animals to find the escape hole, at which point the aversive stimulus is removed. The aversive stimulus used in our protocol is a 4000Hz static sound, though a buzzer or a light can also be used. On the fifth day, the mice are tested on their ability to remember the location of the escape

hole. To this end, the escape hole is kept in the same place but is covered, and the rodents are tracked as they move around the maze. A rodent with cognitive impairment will take longer to locate the escape hole and spend less time around the escape hole location compared to a rodent with intact cognition. The Barnes maze is a useful tool to assess cognition in mice and rats, and has been used in multiple studies linking hypertension to cognitive decline (67, 93, 200).

Nest building is essential for mice. Quality nests protect against body heat loss, provide shelter from predators, and are important for reproduction. Because nesting is not purely for reproductive purposes, both male and female mice make nests. A hallmark of dementia is the impairment in activities of daily living. Because nest building is a critical component of daily living in mice, assessing nest building is growing in popularity as a measure of their cognitive well-being (245). This is an easily measured assessment, as it requires no special equipment or training of the mice and can be conducted in their home cages. To assess nest quality, new cages with fresh nesting material are given to the mice one hour before the start of their dark cycle. After 24 hours, the new nests are measured on a scale of 0-5, with 0 being the worst and 5 being the best. A quantitative nesting test can also be administered. For this task, mice are given a pre-weighed cotton square nestlet and are allowed one hour to shred it and incorporate it into their nests. The nestlet is weighed again, and the percentage of the nestlet shredded is calculated (60). The behavioral tests mentioned here are featured in Figure 1.7.

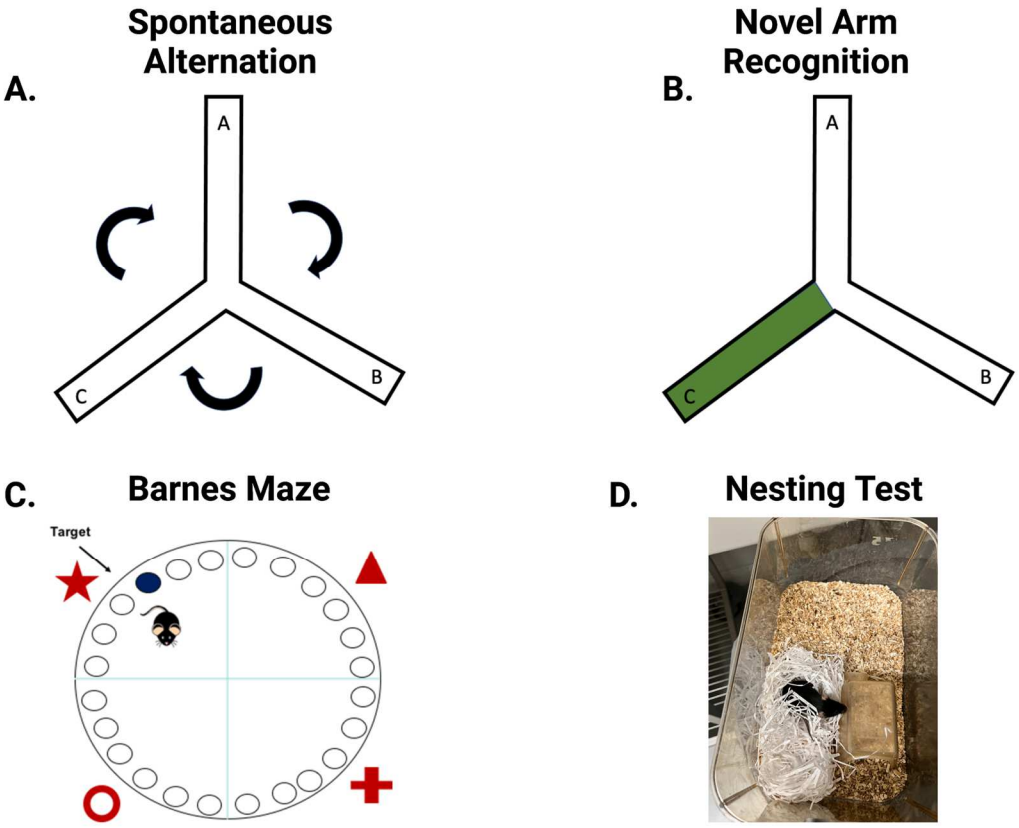

Figure 1.7. Behavior assessments used. A) The spontaneous alternation task in the Y-maze was used to assess spatial working memory. B) The novel arm Y-maze test was used to assess spatial reference memory and C) Barnes maze was used to test spatial learning memory. D) Nesting ability was assessed as an indicator of carrying out tasks of daily living.

1.6 – Scope of this project

Given the background information and the knowledge gaps in the literature highlighted throughout this chapter, the central hypothesis for this project is that

endothelial TRPV4 channel function is essential for PA function and cognition, and its dysfunction or absence is associated with cerebrovascular and cognitive impairment. Additionally, I hypothesized that female mice would be protected from impaired TRPV4 signaling and cognitive dysfunction in hypertension. The hypotheses of this dissertation are shown in Figure 1.8. These hypotheses were tested with the following experimental aims:

1.6.1 – MR antagonism after the development of cerebrovascular and cognitive dysfunction

In both mouse and rat models of hypertension, MR antagonism is protective against cerebrovascular damage and cognitive decline. However, because treatment in these studies began alongside the development of hypertension, it is unknown whether MR antagonism in midlife can reverse the damage done by hypertension or whether it is merely preventative. These studies used aged SHRSP and a novel treatment paradigm that began after the development of hypertension to test the hypothesis that MR antagonism can reverse impairments in PA dilation and cognition.

1.6.2 – Sex differences in AngII-hypertension

As mentioned previously, there is a wide knowledge gap in the literature regarding the influence of biological sex in cerebrovascular and cognitive dysfunction in hypertension. Our lab previously demonstrated that AngII-hypertension in young male mice results in impaired TRPV4-mediated dilation in PAs and induced cognitive decline. With the understanding that E2 protects against neuroinflammation, a significant contributor to vascular and cognitive impairment, I hypothesized that age-matched female

mice would be protected against impaired TRPV4-mediated dilation in PAs and protected against cognitive dysfunction.

1.6.3 – Endothelial TRPV4 deletion

TRPV4 channels are well-established contributors to appropriate neurovascular function. Because of the ubiquitous expression of TRPV4 in cells in the neurovascular unit, it has thus far been impossible to determine cell-specific contributions of the channel. This study used endothelial-specific TRPV4 knockout mice to test the hypothesis that endothelial TRPV4 channels are essential for PA and cognitive function.

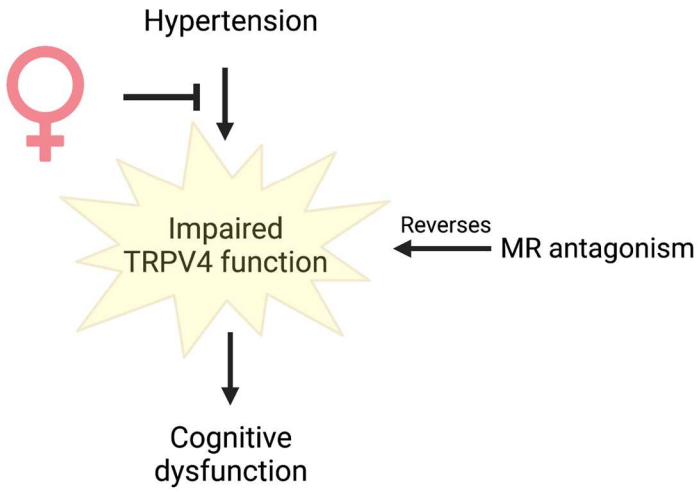

Figure 1.8: Schematic of the overarching hypotheses of this project. Female sex protects against impaired TRPV4 function and subsequent cognitive decline in hypertension. After the development impaired TRPV4 function and cognitive decline in hypertension, MR antagonism will reverse the damage. TRPV4 function is central to cerebrovascular and cognitive wellbeing and its dysfunction, or deletion, will result in cognitive decline.

REFERENCES

1. **Aanerud J**, **Borghammer P**, **Rodell A**, **Jónsdottir KY**, **Gjedde A**. Sex differences of human cortical blood flow and energy metabolism. *J Cereb Blood Flow Metab* 37: 2433–2440, 2017. doi: 10.1177/0271678X16668536.

2. **Adebiyi A**, **Thomas-Gatewood CM**, **Leo MD**, **Kidd MW**, **Neeb ZP**, **Jaggar JH**. An elevation in physical coupling of type 1 inositol 1,4,5-trisphosphate (IP3) receptors to transient receptor potential 3 (TRPC3) channels constricts mesenteric arteries in genetic hypertension. *Hypertension* 60: 1213–1219, 2012. doi: 10.1161/HYPERTENSIONAHA.112.198820.

3. **Adebiyi A**, **Zhao G**, **Narayanan D**, **Thomas-Gatewood CM**, **Bannister JP**, **Jaggar JH**. Isoform-selective physical coupling of TRPC3 channels to IP3 receptors in smooth muscle cells regulates arterial contractility. *Circ Res* 106: 1603–1612, 2010. doi: 10.1161/CIRCRESAHA.110.216804.

4. **Agarwal N**, **Carare RO**. Cerebral vessels: an overview of anatomy, physiology, and role in the drainage of fluids and solutes. *Front Neurol* 11: 611485, 2020. doi: 10.3389/fneur.2020.611485.

5. **Al-Gburi S**, **Deussen AJ**, **Galli R**, **Muders MH**, **Zatschler B**, **Neisser A**, **Müller B**, **Kopaliani I**. Sex-specific differences in age-dependent progression of aortic dysfunction and related cardiac remodeling in spontaneously hypertensive rats. *Am J Physiol Regul Integr Comp Physiol* 312: R835–R849, 2017. doi: 10.1152/ajpregu.00231.2016.

6. **Alisch JSR**, **Khattar N**, **Kim RW**, **Cortina LE**, **Rejimon AC**, **Qian W**, **Ferrucci L**, **Resnick SM**, **Spencer RG**, **Bouhrara M**. Sex and age-related differences in cerebral blood flow investigated using pseudo-continuous arterial spin labeling magnetic resonance imaging. *Aging (Albany NY)* 13: 4911–4925, 2021. doi: 10.18632/aging.202673.

7. **Amberg GC**, **Santana LF**. Kv2 channels oppose myogenic constriction of rat cerebral arteries. *Am J Physiol, Cell Physiol* 291: C348-56, 2006. doi: 10.1152/ajpcell.00086.2006.

8. **Andersen K**, **Launer LJ**, **Dewey ME**, **Letenneur L**, **Ott A**, **Copeland JR**, **Dartigues JF**, **Kragh-Sorensen P**, **Baldereschi M**, **Brayne C**, **Lobo A**, **Martinez-Lage JM**, **Stijnen T**, **Hofman A**. Gender differences in the incidence of AD and vascular dementia: The EURODEM Studies. EURODEM Incidence Research Group. *Neurology* 53: 1992–1997, 1999. doi: 10.1212/wnl.53.9.1992.

9. **Ando H**, **Zhou J**, **Macova M**, **Imboden H**, **Saavedra JM**. Angiotensin II AT1 receptor blockade reverses pathological hypertrophy and inflammation in brain

microvessels of spontaneously hypertensive rats. *Stroke* 35: 1726–1731, 2004. doi: 10.1161/01.STR.0000129788.26346.18.

10. **Arias-Loza P-A**, **Muehlfelder M**, **Pelzer T**. Estrogen and estrogen receptors in cardiovascular oxidative stress. *Pflugers Arch* 465: 739–746, 2013. doi: 10.1007/s00424-013-1247-7.

11. **Armanini D**, **Karbowiak I**, **Goi A**, **Mantero F**, **Funder JW**. In-vivo metabolites of spironolactone and potassium canrenoate: determination of potential anti-androgenic activity by a mouse kidney cytosol receptor assay. *Clin Endocrinol (Oxf)* 23: 341–347, 1985.

12. **Armanini D**, **Sabbadin C**, **Donà G**, **Clari G**, **Bordin L**. Aldosterone receptor blockers spironolactone and canrenone: two multivalent drugs. *Expert Opin Pharmacother* 15: 909–912, 2014. doi: 10.1517/14656566.2014.896901.

13. **Armulik A**, **Genové G**, **Betsholtz C**. Pericytes: developmental, physiological, and pathological perspectives, problems, and promises. *Dev Cell* 21: 193–215, 2011. doi: 10.1016/j.devcel.2011.07.001.

14. **Aydin F**, **Rosenblum WI**, **Povlishock JT**. Myoendothelial junctions in human brain arterioles. *Stroke* 22: 1592–1597, 1991. doi: 10.1161/01.str.22.12.1592.

15. **Bagher P**, **Garland CJ**. Scaffolding builds to reduce blood pressure. *Sci Signal* 7: pe16, 2014. doi: 10.1126/scisignal.2005527.

16. **Baratchi S**, **Keov P**, **Darby WG**, **Lai A**, **Khoshmanesh K**, **Thurgood P**, **Vahidi P**, **Ejendal K**, **McIntyre P**. The TRPV4 agonist GSK1016790A regulates the membrane expression of TRPV4 channels. *Front Pharmacol* 10: 6, 2019. doi: 10.3389/fphar.2019.00006.

17. **Barrera-Chimal J**, **Jaisser F**. Vascular mineralocorticoid receptor activation and disease. *Exp Eye Res* 188: 107796, 2019. doi: 10.1016/j.exer.2019.107796.

18. **Barrett Mueller K**, **Lu Q**, **Mohammad NN**, **Luu V**, **McCurley A**, **Williams GH**, **Adler GK**, **Karas RH**, **Jaffe IZ**. Estrogen receptor inhibits mineralocorticoid receptor transcriptional regulatory function. *Endocrinology* 155: 4461–4472, 2014. doi: 10.1210/en.2014-1270.

19. **Begley DJ**, **Brightman MW**. Structural and functional aspects of the blood-brain barrier. *Prog Drug Res* 61: 39–78, 2003. doi: 10.1007/978-3-0348-8049-7_2.

20. **Biwer LA**, **Carvajal BV**, **Lu Q**, **Man JJ**, **Jaffe IZ**. Mineralocorticoid and estrogen receptors in endothelial cells coordinately regulate microvascular function in obese female mice. *Hypertension* 77: 2117–2126, 2021. doi: 10.1161/HYPERTENSIONAHA.120.16911.

21. **Blackwell JA**, **Silva JF**, **Louis EM**, **Savu A**, **Largent-Milnes TM**, **Brooks HL**, **Pires PW**. Cerebral arteriolar and neurovascular dysfunction after chemically-induced menopause in mice. .

22. **Blinder P**, **Shih AY**, **Rafie C**, **Kleinfeld D**. Topological basis for the robust distribution of blood to rodent neocortex. *Proc Natl Acad Sci USA* 107: 12670–12675, 2010. doi: 10.1073/pnas.1007239107.

23. **Blinder P**, **Tsai PS**, **Kaufhold JP**, **Knutsen PM**, **Suhl H**, **Kleinfeld D**. The cortical angiome: an interconnected vascular network with noncolumnar patterns of blood flow. *Nat Neurosci* 16: 889–897, 2013. doi: 10.1038/nn.3426.

24. **Bodkin JV**, **Thakore P**, **Aubdool AA**, **Liang L**, **Fernandes ES**, **Nandi M**, **Spina D**, **Clark JE**, **Aaronson PI**, **Shattock MJ**, **Brain SD**. Investigating the potential role of TRPA1 in locomotion and cardiovascular control during hypertension. *Pharmacol Res Perspect* 2: e00052, 2014. doi: 10.1002/prp2.52.

25. **Bogatcheva NV**, **Sergeeva MG**, **Dudek SM**, **Verin AD**. Arachidonic acid cascade in endothelial pathobiology. *Microvasc Res* 69: 107–127, 2005. doi: 10.1016/j.mvr.2005.01.007.

26. **Bukowska A**, **Spiller L**, **Wolke C**, **Lendeckel U**, **Weinert S**, **Hoffmann J**, **Bornfleth P**, **Kutschka I**, **Gardemann A**, **Isermann B**, **Goette A**. Protective regulation of the ACE2/ACE gene expression by estrogen in human atrial tissue from elderly men. *Exp Biol Med (Maywood)* 242: 1412–1423, 2017. doi: 10.1177/1535370217718808.

27. **Calcinaghi N**, **Wyss MT**, **Jolivet R**, **Singh A**, **Keller AL**, **Winnik S**, **Fritschy J-M**, **Buck A**, **Matter CM**, **Weber B**. Multimodal imaging in rats reveals impaired neurovascular coupling in sustained hypertension. *Stroke* 44: 1957–1964, 2013. doi: 10.1161/STROKEAHA.111.000185.

28. **Calhoun DA**. Hyperaldosteronism as a common cause of resistant hypertension. *Annu Rev Med* 64: 233–247, 2013. doi: 10.1146/annurev-med-042711-135929.

29. **Campbell WB**, **Fleming I**. Epoxyeicosatrienoic acids and endothelium-dependent responses. *Pflugers Arch* 459: 881–895, 2010. doi: 10.1007/s00424-010-0804-6.

30. **Campbell WB**, **Gebremedhin D**, **Pratt PF**, **Harder DR**. Identification of epoxyeicosatrienoic acids as endothelium-derived hyperpolarizing factors. *Circ Res* 78: 415–423, 1996. doi: 10.1161/01.res.78.3.415.

31. **Capone C**, **Anrather J**, **Milner TA**, **Iadecola C**. Estrous cycle-dependent neurovascular dysfunction induced by angiotensin II in the mouse neocortex. *Hypertension* 54: 302–307, 2009. doi: 10.1161/HYPERTENSIONAHA.109.133249.

32. **Capone C**, **Faraco G**, **Park L**, **Cao X**, **Davisson RL**, **Iadecola C**. The cerebrovascular dysfunction induced by slow pressor doses of angiotensin II precedes the development of hypertension. *Am J Physiol Heart Circ Physiol* 300: H397-407, 2011. doi: 10.1152/ajpheart.00679.2010.

33. **Caprio M**, **Newfell BG**, **Ia Sala A**, **Baur W**, **Fabbri A**, **Rosano G**, **Mendelsohn ME**, **Jaffe IZ**. Functional mineralocorticoid receptors in human vascular endothelial cells regulate intercellular adhesion molecule-1 expression and promote leukocyte adhesion. *Circ Res* 102: 1359–1367, 2008. doi: 10.1161/CIRCRESAHA.108.174235.

34. **Caroccia B**, **Seccia TM**, **Campos AG**, **Gioco F**, **Kuppusamy M**, **Ceolotto G**, **Guerzoni E**, **Simonato F**, **Mareso S**, **Lenzini L**, **Fassina A**, **Rossi GP**. GPER-1 and estrogen receptor-β ligands modulate aldosterone synthesis. *Endocrinology* 155: 4296–4304, 2014. doi: 10.1210/en.2014-1416.

35. **Cattaneo MG**, **Vanetti C**, **Decimo I**, **Di Chio M**, **Martano G**, **Garrone G**, **Bifari F**, **Vicentini LM**. Sex-specific eNOS activity and function in human endothelial cells. *Sci Rep* 7: 9612, 2017. doi: 10.1038/s41598-017-10139-x.

36. **Chalupsky K**, **Cai H**. Endothelial dihydrofolate reductase: critical for nitric oxide bioavailability and role in angiotensin II uncoupling of endothelial nitric oxide synthase. *Proc Natl Acad Sci USA* 102: 9056–9061, 2005. doi: 10.1073/pnas.0409594102.

37. **Chambers LC**, **Diaz-Otero JM**, **Fisher CL**, **Jackson WF**, **Dorrance AM**. Mineralocorticoid receptor antagonism improves transient receptor potential vanilloid 4-dependent dilation of cerebral parenchymal arterioles and cognition in a genetic model of hypertension. *J Hypertens* 40: 1722–1734, 2022. doi: 10.1097/HJH.0000000000003208.

38. **Charlick M**, **M Das J**. Anatomy, head and neck, internal carotid arteries. In: *StatPearls*. Treasure Island (FL): StatPearls Publishing, 2022.

39. **Charpie JR**, **Schreur KD**, **Papadopoulos SM**, **Webb RC**. Endothelium dependency of contractile activity differs in infant and adult vertebral arteries. *J Clin Invest* 93: 1339–1343, 1994. doi: 10.1172/JCI117093.

40. **Chen Y-L**, **Sonkusare SK**. Endothelial TRPV4 channels and vasodilator reactivity. *Curr Top Membr* 85: 89–117, 2020. doi: 10.1016/bs.ctm.2020.01.007.

41. **Chinnathambi V**, **More AS**, **Hankins GD**, **Yallampalli C**, **Sathishkumar K**. Gestational exposure to elevated testosterone levels induces hypertension via heightened vascular angiotensin II type 1 receptor signaling in rats. *Biol Reprod* 91: 6, 2014. doi: 10.1095/biolreprod.114.118968.

42. **Chow BW**, **Nuñez V**, **Kaplan L**, **Granger AJ**, **Bistrong K**, **Zucker HL**, **Kumar P**, **Sabatini BL**, **Gu C**. Caveolae in CNS arterioles mediate neurovascular coupling. *Nature* 579: 106–110, 2020. doi: 10.1038/s41586-020-2026-1.

43. **Chrissobolis S**, **Faraci FM**. Sex differences in protection against angiotensin II-induced endothelial dysfunction by manganese superoxide dismutase in the cerebral circulation. *Hypertension* 55: 905–910, 2010. doi: 10.1161/HYPERTENSIONAHA.109.147041.

44. **Cipolla MJ**, **Bullinger LV**. Reactivity of brain parenchymal arterioles after ischemia and reperfusion. *Microcirculation* 15: 495–501, 2008. doi: 10.1080/10739680801986742.

45. **Cipolla MJ**, **Li R**, **Vitullo L**. Perivascular innervation of penetrating brain parenchymal arterioles. *J Cardiovasc Pharmacol* 44: 1–8, 2004. doi: 10.1097/00005344-200407000-00001.

46. **Cipolla MJ**, **Smith J**, **Kohlmeyer MM**, **Godfrey JA**. SKCa and IKCa Channels, myogenic tone, and vasodilator responses in middle cerebral arteries and parenchymal arterioles: effect of ischemia and reperfusion. *Stroke* 40: 1451–1457, 2009. doi: 10.1161/STROKEAHA.108.535435.

47. **Cipolla MJ**, **Sweet J**, **Chan S-L**, **Tavares MJ**, **Gokina N**, **Brayden JE**. Increased pressure-induced tone in rat parenchymal arterioles vs. middle cerebral arteries: role of ion channels and calcium sensitivity. *J Appl Physiol* 117: 53–59, 2014. doi: 10.1152/japplphysiol.00253.2014.

48. **Cipolla MJ**. *The Cerebral Circulation*. San Rafael (CA): Morgan & Claypool Life Sciences, 2009.

49. **Clapham DE**. TRP channels as cellular sensors. *Nature* 426: 517–524, 2003. doi: 10.1038/nature02196.

50. **Colafella KMM**, **Denton KM**. Sex-specific differences in hypertension and associated cardiovascular disease. *Nat Rev Nephrol* 14: 185–201, 2018. doi: 10.1038/nrneph.2017.189.

51. **Cook CS**, **Berry LM**, **Bible RH**, **Hribar JD**, **Hajdu E**, **Liu NW**. Pharmacokinetics and metabolism of [14C]eplerenone after oral administration to humans. *Drug Metab Dispos* 31: 1448–1455, 2003. doi: 10.1124/dmd.31.11.1448.

52. **Copeland JR**, **McCracken CF**, **Dewey ME**, **Wilson KC**, **Doran M**, **Gilmore C**, **Scott A**, **Larkin BA**. Undifferentiated dementia, Alzheimer's disease and vascular dementia: age- and gender-related incidence in Liverpool. The MRC-ALPHA Study. *Br J Psychiatry* 175: 433–438, 1999. doi: 10.1192/bjp.175.5.433.

53. **Csiszar A**, **Tarantini S**, **Fülöp GA**, **Kiss T**, **Valcarcel-Ares MN**, **Galvan V**, **Ungvari Z**, **Yabluchanskiy A**. Hypertension impairs neurovascular coupling and promotes microvascular injury: role in exacerbation of Alzheimer's disease. *Geroscience* 39: 359–372, 2017. doi: 10.1007/s11357-017-9991-9.

54. **Dabertrand F**, **Nelson MT**, **Brayden JE**. Acidosis dilates brain parenchymal arterioles by conversion of calcium waves to sparks to activate BK channels. *Circ Res* 110: 285–294, 2012. doi: 10.1161/CIRCRESAHA.111.258145.

55. **Dabertrand F**, **Nelson MT**, **Brayden JE**. Ryanodine receptors, calcium signaling, and regulation of vascular tone in the cerebral parenchymal microcirculation. *Microcirculation* 20: 307–316, 2013. doi: 10.1111/micc.12027.

56. **Dahl LK**, **Heine M**, **Tassinari L**. Role of genetic factors in susceptibility to experimental hypertension due to chronic excess salt ingestion. *Nature* 194: 480–482, 1962. doi: 10.1038/194480b0.

57. **Darby WG**, **Grace MS**, **Baratchi S**, **McIntyre P**. Modulation of TRPV4 by diverse mechanisms. *Int J Biochem Cell Biol* 78: 217–228, 2016. doi: 10.1016/j.biocel.2016.07.012.

58. **Davel AP**, **Anwar IJ**, **Jaffe IZ**. The endothelial mineralocorticoid receptor: mediator of the switch from vascular health to disease. *Curr Opin Nephrol Hypertens* 26: 97–104, 2017. doi: 10.1097/MNH.0000000000000306.

59. **Davel AP**, **Lu Q**, **Moss ME**, **Rao S**, **Anwar IJ**, **DuPont JJ**, **Jaffe IZ**. Sex-Specific Mechanisms of Resistance Vessel Endothelial Dysfunction Induced by Cardiometabolic Risk Factors. *J Am Heart Assoc* 7, 2018. doi: 10.1161/JAHA.117.007675.

60. **Deacon RMJ**. Assessing nest building in mice. *Nat Protoc* 1: 1117–1119, 2006. doi: 10.1038/nprot.2006.170.

61. **Deschepper CF**, **Llamas B**. Hypertensive cardiac remodeling in males and females: from the bench to the bedside. *Hypertension* 49: 401–407, 2007. doi: 10.1161/01.HYP.0000256279.49882.d8.

62. **De Silva TM**, **Faraci FM**. Effects of angiotensin II on the cerebral circulation: role of oxidative stress. *Front Physiol* 3: 484, 2012. doi: 10.3389/fphys.2012.00484.

63. **De Silva TM**, **Modrick ML**, **Dabertrand F**, **Faraci FM**. Changes in cerebral arteries and parenchymal arterioles with aging: role of rho kinase 2 and impact of genetic background. *Hypertension* 71: 921–927, 2018. doi: 10.1161/HYPERTENSIONAHA.118.10865.

64. **DeLano FA**, **Schmid-Schönbein GW**. Enhancement of glucocorticoid and mineralocorticoid receptor density in the microcirculation of the spontaneously hypertensive rat. *Microcirculation* 11: 69–78, 2004. doi: 10.1080/10739680490266207.

65. **Diaz-Otero JM**, **Fisher C**, **Downs K**, **Moss EM**, **Jaffe IZ**, **Jackson WF**, **Dorrance AM**. Endothelial Mineralocorticoid Receptor Mediates Parenchymal Arteriole and Posterior Cerebral Artery Remodeling During Angiotensin II–Induced Hypertension. .

66. **Diaz-Otero JM**, **Yen T-C**, **Ahmad A**, **Laimon-Thomson E**, **Abolibdeh B**, **Kelly K**, **Lewis MT**, **Wiseman RW**, **Jackson WF**, **Dorrance AM**. Transient receptor potential vanilloid 4 channels are important regulators of parenchymal arteriole dilation and cognitive function. *Microcirculation* 26: e12535, 2019. doi: 10.1111/micc.12535.

67. **Diaz-Otero JM**, **Yen T-C**, **Fisher C**, **Bota D**, **Jackson WF**, **Dorrance AM**. Mineralocorticoid receptor antagonism improves parenchymal arteriole dilation via a TRPV4-dependent mechanism and prevents cognitive dysfunction in hypertension. *Am J Physiol Heart Circ Physiol* 315: H1304–H1315, 2018. doi: 10.1152/ajpheart.00207.2018.

68. **Ding J**, **Yu M**, **Jiang J**, **Luo Y**, **Zhang Q**, **Wang S**, **Yang F**, **Wang A**, **Wang L**, **Zhuang M**, **Wu S**, **Zhang Q**, **Xia Y**, **Lu D**. Angiotensin II decreases endothelial nitric oxide synthase phosphorylation via AT1R nox/ros/pp2a pathway. *Front Physiol* 11: 566410, 2020. doi: 10.3389/fphys.2020.566410.

69. **Dong H**, **Waldron GJ**, **Cole WC**, **Triggle CR**. Roles of calcium-activated and voltage-gated delayed rectifier potassium channels in endothelium-dependent vasorelaxation of the rabbit middle cerebral artery. *Br J Pharmacol* 123: 821–832, 1998. doi: 10.1038/sj.bjp.0701680.

70. **Dorrance AM**, **Osborn HL**, **Grekin R**, **Webb RC**. Spironolactone reduces cerebral infarct size and EGF-receptor mRNA in stroke-prone rats. *Am J Physiol Regul Integr Comp Physiol* 281: R944-50, 2001. doi: 10.1152/ajpregu.2001.281.3.R944.

71. **Dorrance AM**, **Pollock DM**, **Romanko OP**, **Stepp DW**. A high-potassium diet reduces infarct size and improves vascular structure in hypertensive rats. *Am J Physiol Regul Integr Comp Physiol* 292: R415-22, 2007. doi: 10.1152/ajpregu.00438.2005.

72. **Dorrance AM**, **Rupp NC**, **Nogueira EF**. Mineralocorticoid receptor activation causes cerebral vessel remodeling and exacerbates the damage caused by cerebral ischemia. *Hypertension* 47: 590–595, 2006. doi: 10.1161/01.HYP.0000196945.73586.0d.

73. **Drummond HA**, **Gebremedhin D**, **Harder DR**. Degenerin/epithelial Na+ channel proteins: components of a vascular mechanosensor. *Hypertension* 44: 643–648, 2004. doi: 10.1161/01.HYP.0000144465.56360.ad.

74. **Dudzinski DM**, **Igarashi J**, **Greif D**, **Michel T**. The regulation and pharmacology of endothelial nitric oxide synthase. *Annu Rev Pharmacol Toxicol* 46: 235–276, 2006. doi: 10.1146/annurev.pharmtox.44.101802.121844.

75. **Duncombe J**, **Kitamura A**, **Hase Y**, **Ihara M**, **Kalaria RN**, **Horsburgh K**. Chronic cerebral hypoperfusion: a key mechanism leading to vascular cognitive impairment and dementia. Closing the translational gap between rodent models and human vascular cognitive impairment and dementia. *Clin Sci* 131: 2451–2468, 2017. doi: 10.1042/CS20160727.

76. **DuPont JJ**, **Jaffe IZ**. 30 YEARS OF THE MINERALOCORTICOID RECEPTOR: The role of the mineralocorticoid receptor in the vasculature. *J Endocrinol* 234: T67–T82, 2017. doi: 10.1530/JOE-17-0009.

77. **DuPont JJ**, **McCurley A**, **Davel AP**, **McCarthy J**, **Bender SB**, **Hong K**, **Yang Y**, **Yoo J-K**, **Aronovitz M**, **Baur WE**, **Christou DD**, **Hill MA**, **Jaffe IZ**. Vascular mineralocorticoid receptor regulates microRNA-155 to promote vasoconstriction and rising blood pressure with aging. *JCI Insight* 1: e88942, 2016. doi: 10.1172/jci.insight.88942.

78. **Du X-J**, **Fang L**, **Kiriazis H**. Sex dimorphism in cardiac pathophysiology: experimental findings, hormonal mechanisms, and molecular mechanisms. *Pharmacol Ther* 111: 434–475, 2006. doi: 10.1016/j.pharmthera.2005.10.016.

79. **Dumitrescu AM**, **Costea CF**, **Cucu AI**, **Dumitrescu GF**, **Turliuc MD**, **Scripcariu DV**, **Ciocoiu M**, **Tănase DM**, **Turliuc Ş**, **Bogdănici CM**, **Nicoară SD**, **Cărăuleanu A**, **Schmitzer S**, **Sava A**. The discovery of the circle of Willis as a result of using the scientific method in anatomical dissection. *Rom J Morphol Embryol* 61: 959–965, 2020. doi: 10.47162/RJME.61.3.38.

80. **Dupuis F**, **Atkinson J**, **Limiñana P**, **Chillon J-M**. Comparative effects of the angiotensin II receptor blocker, telmisartan, and the angiotensin-converting enzyme inhibitor, ramipril, on cerebrovascular structure in spontaneously hypertensive rats. *J Hypertens* 23: 1061–1066, 2005. doi: 10.1097/01.hjh.0000166848.95592.a5.

81. **Earley S**, **Gonzales AL**, **Crnich R**. Endothelium-dependent cerebral artery dilation mediated by TRPA1 and Ca2+-Activated K+ channels. *Circ Res* 104: 987–994, 2009. doi: 10.1161/CIRCRESAHA.108.189530.

82. **Earley S**, **Gonzales AL**, **Garcia ZI**. A dietary agonist of transient receptor potential cation channel V3 elicits endothelium-dependent vasodilation. *Mol Pharmacol* 77: 612–620, 2010. doi: 10.1124/mol.109.060715.

83. **Earley S**, **Heppner TJ**, **Nelson MT**, **Brayden JE**. TRPV4 forms a novel Ca2+ signaling complex with ryanodine receptors and BKCa channels. *Circ Res* 97: 1270–1279, 2005. doi: 10.1161/01.RES.0000194321.60300.d6.

84. **Earley S**, **Pauyo T**, **Drapp R**, **Tavares MJ**, **Liedtke W**, **Brayden JE**. TRPV4-dependent dilation of peripheral resistance arteries influences arterial pressure. *Am J Physiol Heart Circ Physiol* 297: H1096-102, 2009. doi: 10.1152/ajpheart.00241.2009.

85. **Earley S**, **Waldron BJ**, **Brayden JE**. Critical role for transient receptor potential channel TRPM4 in myogenic constriction of cerebral arteries. *Circ Res* 95: 922–929, 2004. doi: 10.1161/01.RES.0000147311.54833.03.

86. **Earley S**. Endothelium-dependent cerebral artery dilation mediated by transient receptor potential and Ca2+-activated K+ channels. *J Cardiovasc Pharmacol* 57: 148–153, 2011. doi: 10.1097/FJC.0b013e3181f580d9.

87. **Earley S**. TRPA1 channels in the vasculature. *Br J Pharmacol* 167: 13–22, 2012. doi: 10.1111/j.1476-5381.2012.02018.x.

88. **Elias MF**, **Wolf PA**, **D'Agostino RB**, **Cobb J**, **White LR**. Untreated blood pressure level is inversely related to cognitive functioning: the Framingham Study. *Am J Epidemiol* 138: 353–364, 1993. doi: 10.1093/oxfordjournals.aje.a116868.

89. **Ellinsworth DC**, **Earley S**, **Murphy TV**, **Sandow SL**. Endothelial control of vasodilation: integration of myoendothelial microdomain signalling and modulation by epoxyeicosatrienoic acids. *Pflugers Arch* 466: 389–405, 2014. doi: 10.1007/s00424-013-1303-3.

90. **Esler M**. The sympathetic system and hypertension. *Am J Hypertens* 13: 99S-105S, 2000.

91. **Faraci FM**, **Heistad DD**. Regulation of large cerebral arteries and cerebral microvascular pressure. *Circ Res* 66: 8–17, 1990. doi: 10.1161/01.res.66.1.8.

92. **Faraci FM**. Protecting against vascular disease in brain. *Am J Physiol Heart Circ Physiol* 300: H1566-82, 2011. doi: 10.1152/ajpheart.01310.2010.

93. **Faraco G**, **Sugiyama Y**, **Lane D**, **Garcia-Bonilla L**, **Chang H**, **Santisteban MM**, **Racchumi G**, **Murphy M**, **Van Rooijen N**, **Anrather J**, **Iadecola C**. Perivascular macrophages mediate the neurovascular and cognitive dysfunction associated with hypertension. *J Clin Invest* 126: 4674–4689, 2016. doi: 10.1172/JCI86950.

94. **Faulkner JL**, **Belin de Chantemèle EJ**. Sex differences in mechanisms of hypertension associated with obesity. *Hypertension* 71: 15–21, 2018. doi: 10.1161/HYPERTENSIONAHA.117.09980.

95. **Faulkner JL**, **Belin de Chantemèle EJ**. Mineralocorticoid receptor and endothelial dysfunction in hypertension. *Curr Hypertens Rep* 21: 78, 2019. doi: 10.1007/s11906-019-0981-4.

96. **Faulkner JL**, **Kennard S**, **Huby A-C**, **Antonova G**, **Lu Q**, **Jaffe IZ**, **Patel VS**, **Fulton DJR**, **Belin de Chantemèle EJ**. Progesterone Predisposes Females to Obesity-Associated Leptin-Mediated Endothelial Dysfunction via Upregulating Endothelial MR (Mineralocorticoid Receptor) Expression. *Hypertension* 74: 678–686, 2019. doi: 10.1161/HYPERTENSIONAHA.119.12802.

97. **Favre ME**, **Serrador JM**. Sex differences in cerebral autoregulation are unaffected by menstrual cycle phase in young, healthy women. *Am J Physiol Heart Circ Physiol* 316: H920–H933, 2019. doi: 10.1152/ajpheart.00474.2018.

98. **Fehm HL**, **Kern W**, **Peters A**. The selfish brain: competition for energy resources. In: *Hypothalamic Integration of Energy Metabolism, Proceedings of the 24th International Summer School of Brain Research, held at the Royal Netherlands Academy of Arts and Sciences*. Elsevier, 2006, p. 129–140.

99. **Filosa JA**, **Blanco VM**. Neurovascular coupling in the mammalian brain. *Exp Physiol* 92: 641–646, 2007. doi: 10.1113/expphysiol.2006.036368.

100. **Fleming I**. Epoxyeicosatrienoic acids, cell signaling and angiogenesis. *Prostaglandins Other Lipid Mediat* 82: 60–67, 2007. doi: 10.1016/j.prostaglandins.2006.05.003.

101. **Förstermann U**, **Münzel T**. Endothelial nitric oxide synthase in vascular disease: from marvel to menace. *Circulation* 113: 1708–1714, 2006. doi: 10.1161/CIRCULATIONAHA.105.602532.

102. **Forte P**, **Kneale BJ**, **Milne E**, **Chowienczyk PJ**, **Johnston A**, **Benjamin N**, **Ritter JM**. Evidence for a difference in nitric oxide biosynthesis between healthy women and men. *Hypertension* 32: 730–734, 1998. doi: 10.1161/01.hyp.32.4.730.

103. **Fountain JH**, **Lappin SL**. Physiology, renin angiotensin system. In: *StatPearls*. Treasure Island (FL): StatPearls Publishing, 2022.

104. **Fredette NC**, **Meyer MR**, **Prossnitz ER**. Role of GPER in estrogen-dependent nitric oxide formation and vasodilation. *J Steroid Biochem Mol Biol* 176: 65–72, 2018. doi: 10.1016/j.jsbmb.2017.05.006.

105. **Freshour JR**, **Chase SE**, **Vikstrom KL**. Gender differences in cardiac ACE expression are normalized in androgen-deprived male mice. *Am J Physiol Heart Circ Physiol* 283: H1997-2003, 2002. doi: 10.1152/ajpheart.01054.2001.

106. **Fujii K**, **Ohmori S**, **Tominaga M**, **Abe I**, **Takata Y**, **Ohya Y**, **Kobayashi K**, **Fujishima M**. Age-related changes in endothelium-dependent hyperpolarization in the rat mesenteric artery. *Am J Physiol* 265: H509-16, 1993. doi: 10.1152/ajpheart.1993.265.2.H509.

107. **Fujii K**, **Tominaga M**, **Ohmori S**, **Kobayashi K**, **Koga T**, **Takata Y**, **Fujishima M**. Decreased endothelium-dependent hyperpolarization to acetylcholine in smooth muscle of the mesenteric artery of spontaneously hypertensive rats. *Circ Res* 70: 660–669, 1992. doi: 10.1161/01.res.70.4.660.

108. **Fujishima M**, **Kiyohara Y**. Incidence and risk factors of dementia in a defined elderly Japanese population: the Hisayama study. *Ann N Y Acad Sci* 977: 1–8, 2002. doi: 10.1111/j.1749-6632.2002.tb04793.x.

109. **Gadkari TV**, **Cortes N**, **Madrasi K**, **Tsoukias NM**, **Joshi MS**. Agmatine induced NO dependent rat mesenteric artery relaxation and its impairment in salt-sensitive hypertension. *Nitric Oxide* 35: 65–71, 2013. doi: 10.1016/j.niox.2013.08.005.

110. **Galmiche G**, **Pizard A**, **Gueret A**, **El Moghrabi S**, **Ouvrard-Pascaud A**, **Berger S**, **Challande P**, **Jaffe IZ**, **Labat C**, **Lacolley P**, **Jaisser F**. Smooth muscle cell mineralocorticoid receptors are mandatory for aldosterone-salt to induce vascular stiffness. *Hypertension* 63: 520–526, 2014. doi: 10.1161/HYPERTENSIONAHA.113.01967.

111. **Garland CJ**, **Dora KA**. EDH: endothelium-dependent hyperpolarization and microvascular signalling. *Acta Physiol (Oxf)* 219: 152–161, 2017. doi: 10.1111/apha.12649.

112. **Gąsecki D**, **Kwarciany M**, **Nyka W**, **Narkiewicz K**. Hypertension, brain damage and cognitive decline. *Curr Hypertens Rep* 15: 547–558, 2013. doi: 10.1007/s11906-013-0398-4.

113. **Geary GG**, **Krause DN**, **Duckles SP**. Estrogen reduces myogenic tone through a nitric oxide-dependent mechanism in rat cerebral arteries. *Am J Physiol Heart Circ Physiol* 275: H292–H300, 1998. doi: 10.1152/ajpheart.1998.275.1.H292.

114. **Gerzanich V**, **Ivanova S**, **Zhou H**, **Simard JM**. Mislocalization of eNOS and upregulation of cerebral vascular Ca2+ channel activity in angiotensin-hypertension. *Hypertension* 41: 1124–1130, 2003. doi: 10.1161/01.HYP.0000066288.20169.21.

115. **Gilsanz P**, **Mayeda ER**, **Glymour MM**, **Quesenberry CP**, **Mungas DM**, **DeCarli C**, **Dean A**, **Whitmer RA**. Female sex, early-onset hypertension, and risk of dementia. *Neurology* 89: 1886–1893, 2017. doi: 10.1212/WNL.0000000000004602.

116. **Girouard H**, **Lessard A**, **Capone C**, **Milner TA**, **Iadecola C**. The neurovascular dysfunction induced by angiotensin II in the mouse neocortex is sexually dimorphic. *Am J Physiol Heart Circ Physiol* 294: H156-63, 2008. doi: 10.1152/ajpheart.01137.2007.

117. **Girouard H**, **Park L**, **Anrather J**, **Zhou P**, **Iadecola C**. Angiotensin II attenuates endothelium-dependent responses in the cerebral microcirculation through nox-2-derived radicals. *Arterioscler Thromb Vasc Biol* 26: 826–832, 2006. doi: 10.1161/01.ATV.0000205849.22807.6e.

118. **Gonzales AL**, **Amberg GC**, **Earley S**. Ca2+ release from the sarcoplasmic reticulum is required for sustained TRPM4 activity in cerebral artery smooth muscle cells. *Am J Physiol, Cell Physiol* 299: C279-88, 2010. doi: 10.1152/ajpcell.00550.2009.

119. **Gonzales AL**, **Klug NR**, **Moshkforoush A**, **Lee JC**, **Lee FK**, **Shui B**, **Tsoukias NM**, **Kotlikoff MI**, **Hill-Eubanks D**, **Nelson MT**. Contractile pericytes determine the direction of blood flow at capillary junctions. *Proc Natl Acad Sci USA* 117: 27022–27033, 2020. doi: 10.1073/pnas.1922755117.

120. **Gonzales AL**, **Yang Y**, **Sullivan MN**, **Sanders L**, **Dabertrand F**, **Hill-Eubanks DC**, **Nelson MT**, **Earley S**. A PLCγ1-dependent, force-sensitive signaling network in the myogenic constriction of cerebral arteries. *Sci Signal* 7: ra49, 2014. doi: 10.1126/scisignal.2004732.

121. **Goodfriend TL**, **Kelley DE**, **Goodpaster BH**, **Winters SJ**. Visceral obesity and insulin resistance are associated with plasma aldosterone levels in women. *Obes Res* 7: 355–362, 1999. doi: 10.1002/j.1550-8528.1999.tb00418.x.

122. **Gordon GRJ**, **Choi HB**, **Rungta RL**, **Ellis-Davies GCR**, **MacVicar BA**. Brain metabolism dictates the polarity of astrocyte control over arterioles. *Nature* 456: 745–749, 2008. doi: 10.1038/nature07525.

123. **Gorelick PB**, **Scuteri A**, **Black SE**, **DeCarli C**, **Greenberg SM**, **Iadecola C**, **Launer LJ**, **Laurent S**, **Lopez OL**, **Nyenhuis D**, **Petersen RC**, **Schneider JA**, **Tzourio C**, **Arnett DK**, **Bennett DA**, **Chui HC**, **Higashida RT**, **Lindquist R**, **Nilsson PM**, **Roman GC**, **Sellke FW**, **Seshadri S**. Vascular contributions to cognitive impairment and dementia. *Stroke* 42: 2672–2713, 2011. doi: 10.1161/STR.0b013e3182299496.

124. **Görlach C**, **Wahl M**. Bradykinin dilates rat middle cerebral artery and its large branches via endothelial B2 receptors and release of nitric oxide. *Peptides* 17: 1373–1378, 1996.

125. **Gueret A**, **Harouki N**, **Favre J**, **Galmiche G**, **Nicol L**, **Henry J-P**, **Besnier M**, **Thuillez C**, **Richard V**, **Kolkhof P**, **Mulder P**, **Jaisser F**, **Ouvrard-Pascaud A**. Vascular smooth muscle mineralocorticoid receptor contributes to coronary and left ventricular dysfunction after myocardial infarction. *Hypertension* 67: 717–723, 2016. doi: 10.1161/HYPERTENSIONAHA.115.06709.

126. **Guibert C**, **Beech DJ**. Positive and negative coupling of the endothelin ETA receptor to Ca2+-permeable channels in rabbit cerebral cortex arterioles. *J Physiol (Lond)* 514 (Pt 3): 843–856, 1999. doi: 10.1111/j.1469-7793.1999.843ad.x.

127. **Gur RC**, **Gur RE**, **Obrist WD**, **Hungerbuhler JP**, **Younkin D**, **Rosen AD**, **Skolnick BE**, **Reivich M**. Sex and handedness differences in cerebral blood flow during rest and cognitive activity. *Science* 217: 659–661, 1982. doi: 10.1126/science.7089587.

128. **Hadi HAR**, **Carr CS**, **Al Suwaidi J**. Endothelial dysfunction: cardiovascular risk factors, therapy, and outcome. *Vasc Health Risk Manag* 1: 183–198, 2005.

129. **Hall CN**, **Reynell C**, **Gesslein B**, **Hamilton NB**, **Mishra A**, **Sutherland BA**, **O'Farrell FM**, **Buchan AM**, **Lauritzen M**, **Attwell D**. Capillary pericytes regulate cerebral blood flow in health and disease. *Nature* 508: 55–60, 2014. doi: 10.1038/nature13165.

130. **Hannan RE**, **Davis EA**, **Widdop RE**. Functional role of angiotensin II AT2 receptor in modulation of AT1 receptor-mediated contraction in rat uterine artery: involvement of bradykinin and nitric oxide. *Br J Pharmacol* 140: 987–995, 2003. doi: 10.1038/sj.bjp.0705484.

131. **Harraz OF**, **Abd El-Rahman RR**, **Bigdely-Shamloo K**, **Wilson SM**, **Brett SE**, **Romero M**, **Gonzales AL**, **Earley S**, **Vigmond EJ**, **Nygren A**, **Menon BK**, **Mufti RE**, **Watson T**, **Starreveld Y**, **Furstenhaupt T**, **Muellerleile PR**, **Kurjiaka DT**, **Kyle BD**, **Braun AP**, **Welsh DG**. Ca(V)3.2 channels and the induction of negative feedback in cerebral arteries. *Circ Res* 115: 650–661, 2014. doi: 10.1161/CIRCRESAHA.114.304056.

132. **Harraz OF**, **Brett SE**, **Zechariah A**, **Romero M**, **Puglisi JL**, **Wilson SM**, **Welsh DG**. Genetic ablation of CaV3.2 channels enhances the arterial myogenic response by modulating the RyR-BKCa axis. *Arterioscler Thromb Vasc Biol* 35: 1843–1851, 2015. doi: 10.1161/ATVBAHA.115.305736.

133. **Harraz OF**, **Longden TA**, **Dabertrand F**, **Hill-Eubanks D**, **Nelson MT**. Endothelial GqPCR activity controls capillary electrical signaling and brain blood

flow through PIP2 depletion. *Proc Natl Acad Sci USA* 115: E3569–E3577, 2018. doi: 10.1073/pnas.1800201115.

134. **Harraz OF**, **Longden TA**, **Hill-Eubanks D**, **Nelson MT**. PIP2 depletion promotes TRPV4 channel activity in mouse brain capillary endothelial cells. *eLife* 7: e38689, 2018. doi: 10.7554/eLife.38689.

135. **Hartman RE**, **Kamper JE**, **Goyal R**, **Stewart JM**, **Longo LD**. Motor and cognitive deficits in mice bred to have low or high blood pressure. *Physiol Behav* 105: 1092–1097, 2012. doi: 10.1016/j.physbeh.2011.11.022.

136. **Hartmannsgruber V**, **Heyken W-T**, **Kacik M**, **Kaistha A**, **Grgic I**, **Harteneck C**, **Liedtke W**, **Hoyer J**, **Köhler R**. Arterial response to shear stress critically depends on endothelial TRPV4 expression. *PLoS ONE* 2: e827, 2007. doi: 10.1371/journal.pone.0000827.

137. **Harvey AP**, **Montezano AC**, **Hood KY**, **Lopes RA**, **Rios F**, **Ceravolo G**, **Graham D**, **Touyz RM**. Vascular dysfunction and fibrosis in stroke-prone spontaneously hypertensive rats: The aldosterone-mineralocorticoid receptor-Nox1 axis. *Life Sci* 179: 110–119, 2017. doi: 10.1016/j.lfs.2017.05.002.

138. **Hayashi T**, **Yamada K**, **Esaki T**, **Kuzuya M**, **Satake S**, **Ishikawa T**, **Hidaka H**, **Iguchi A**. Estrogen increases endothelial nitric oxide by a receptor-mediated system. *Biochem Biophys Res Commun* 214: 847–855, 1995. doi: 10.1006/bbrc.1995.2364.

139. **Hébert R**, **Lindsay J**, **Verreault R**, **Rockwood K**, **Hill G**, **Dubois MF**. Vascular dementia : incidence and risk factors in the Canadian study of health and aging. *Stroke* 31: 1487–1493, 2000. doi: 10.1161/01.str.31.7.1487.

140. **Heiss C**, **Rodriguez-Mateos A**, **Kelm M**. Central role of eNOS in the maintenance of endothelial homeostasis. *Antioxid Redox Signal* 22: 1230–1242, 2015. doi: 10.1089/ars.2014.6158.

141. **Heistad DD**, **Marcus ML**, **Abboud FM**. Role of large arteries in regulation of cerebral blood flow in dogs. *J Clin Invest* 62: 761–768, 1978. doi: 10.1172/JCI109187.

142. **Hill RA**, **Tong L**, **Yuan P**, **Murikinati S**, **Gupta S**, **Grutzendler J**. Regional blood flow in the normal and ischemic brain is controlled by arteriolar smooth muscle cell contractility and not by capillary pericytes. *Neuron* 87: 95–110, 2015. doi: 10.1016/j.neuron.2015.06.001.

143. **Hinkelmann K**, **Wingenfeld K**, **Kuehl LK**, **Fleischer J**, **Heuser I**, **Wiedemann K**, **Otte C**. Stimulation of the mineralocorticoid receptor improves memory in young

and elderly healthy individuals. *Neurobiol Aging* 36: 919–924, 2015. doi: 10.1016/j.neurobiolaging.2014.09.008.

144. **Hofmann T**, **Obukhov AG**, **Schaefer M**, **Harteneck C**, **Gudermann T**, **Schultz G**. Direct activation of human TRPC6 and TRPC3 channels by diacylglycerol. *Nature* 397: 259–263, 1999. doi: 10.1038/16711.

145. **Hopkins ND**, **Dengel DR**, **Stratton G**, **Kelly AS**, **Steinberger J**, **Zavala H**, **Marlatt K**, **Perry D**, **Naylor LH**, **Green DJ**. Age and sex relationship with flow-mediated dilation in healthy children and adolescents. *J Appl Physiol* 119: 926–933, 2015. doi: 10.1152/japplphysiol.01113.2014.

146. **Huby A-C**, **Otvos L**, **Belin de Chantemèle EJ**. Leptin Induces Hypertension and Endothelial Dysfunction via Aldosterone-Dependent Mechanisms in Obese Female Mice. *Hypertension* 67: 1020–1028, 2016. doi: 10.1161/HYPERTENSIONAHA.115.06642.

147. **Hughes D**, **Judge C**, **Murphy R**, **Loughlin E**, **Costello M**, **Whiteley W**, **Bosch J**, **O'Donnell MJ**, **Canavan M**. Association of Blood Pressure Lowering With Incident Dementia or Cognitive Impairment: A Systematic Review and Meta-analysis. *JAMA* 323: 1934–1944, 2020. doi: 10.1001/jama.2020.4249.

148. **Iadecola C**, **Davisson RL**. Hypertension and cerebrovascular dysfunction. *Cell Metab* 7: 476–484, 2008. doi: 10.1016/j.cmet.2008.03.010.

149. **Iadecola C**, **Gottesman RF**. Neurovascular and cognitive dysfunction in hypertension. *Circ Res* 124: 1025–1044, 2019. doi: 10.1161/CIRCRESAHA.118.313260.

150. **Iadecola C**, **Nedergaard M**. Glial regulation of the cerebral microvasculature. *Nat Neurosci* 10: 1369–1376, 2007. doi: 10.1038/nn2003.

151. **Iadecola C**, **Yaffe K**, **Biller J**, **Bratzke LC**, **Faraci FM**, **Gorelick PB**, **Gulati M**, **Kamel H**, **Knopman DS**, **Launer LJ**, **Saczynski JS**, **Seshadri S**, **Zeki Al Hazzouri A**, **American Heart Association Council on Hypertension; Council on Clinical Cardiology; Council on Cardiovascular Disease in the Young; Council on Cardiovascular and Stroke Nursing; Council on Quality of Care and Outcomes Research; and Stroke Council**. Impact of hypertension on cognitive function: A scientific statement from the american heart association. *Hypertension* 68: e67–e94, 2016. doi: 10.1161/HYP.0000000000000053.

152. **Iadecola C**. Neurovascular regulation in the normal brain and in Alzheimer's disease. *Nat Rev Neurosci* 5: 347–360, 2004. doi: 10.1038/nrn1387.

153. **Iadecola C**. The Neurovascular Unit Coming of Age: A Journey through Neurovascular Coupling in Health and Disease. *Neuron* 96: 17–42, 2017. doi: 10.1016/j.neuron.2017.07.030.

154. **Ignarro LJ**, **Fukuto JM**, **Griscavage JM**, **Rogers NE**, **Byrns RE**. Oxidation of nitric oxide in aqueous solution to nitrite but not nitrate: comparison with enzymatically formed nitric oxide from L-arginine. *Proc Natl Acad Sci USA* 90: 8103–8107, 1993. doi: 10.1073/pnas.90.17.8103.

155. **Imig JD**. Eicosanoid blood vessel regulation in physiological and pathological states. *Clin Sci* 134: 2707–2727, 2020. doi: 10.1042/CS20191209.

156. **Isakson BE**, **Ramos SI**, **Duling BR**. Ca2+ and inositol 1,4,5-trisphosphate-mediated signaling across the myoendothelial junction. *Circ Res* 100: 246–254, 2007. doi: 10.1161/01.RES.0000257744.23795.93.

157. **Ismael S**, **Ishrat T**. Compound 21, a Direct AT2R Agonist, Induces IL-10 and Inhibits Inflammation in Mice Following Traumatic Brain Injury. *Neuromolecular Med* 24: 274–278, 2022. doi: 10.1007/s12017-021-08687-7.

158. **Jackson KL**, **Head GA**, **Gueguen C**, **Stevenson ER**, **Lim K**, **Marques FZ**. Mechanisms responsible for genetic hypertension in schlager BPH/2 mice. *Front Physiol* 10: 1311, 2019. doi: 10.3389/fphys.2019.01311.

159. **Jackson WF**. Boosting the signal: Endothelial inward rectifier K+ channels. *Microcirculation* 24, 2017. doi: 10.1111/micc.12319.

160. **Jackson WF**. Introduction to ion channels and calcium signaling in the microcirculation. *Curr Top Membr* 85: 1–18, 2020. doi: 10.1016/bs.ctm.2020.01.001.

161. **Jackson WF**. Endothelial Ion Channels and Cell-Cell Communication in the Microcirculation. *Front Physiol* 13: 805149, 2022. doi: 10.3389/fphys.2022.805149.

162. **Jaffe IZ**, **Mendelsohn ME**. Angiotensin II and aldosterone regulate gene transcription via functional mineralocortocoid receptors in human coronary artery smooth muscle cells. *Circ Res* 96: 643–650, 2005. doi: 10.1161/01.RES.0000159937.05502.d1.

163. **Jaggar JH**, **Porter VA**, **Lederer WJ**, **Nelson MT**. Calcium sparks in smooth muscle. *Am J Physiol, Cell Physiol* 278: C235-56, 2000. doi: 10.1152/ajpcell.2000.278.2.C235.

164. **Jaisser F**, **Farman N**. Emerging roles of the mineralocorticoid receptor in pathology: toward new paradigms in clinical pharmacology. *Pharmacol Rev* 68: 49–75, 2016. doi: 10.1124/pr.115.011106.

165. **Jama HA**, **Muralitharan RR**, **Xu C**, **O'Donnell JA**, **Bertagnolli M**, **Broughton BRS**, **Head GA**, **Marques FZ**. Rodent models of hypertension. *Br J Pharmacol* 179: 918–937, 2022. doi: 10.1111/bph.15650.

166. **Janowiak MA**, **Magness RR**, **Habermehl DA**, **Bird IM**. Pregnancy increases ovine uterine artery endothelial cyclooxygenase-1 expression. *Endocrinology* 139: 765–771, 1998. doi: 10.1210/endo.139.2.5739.

167. **Jarajapu YPR**, **Knot HJ**. Role of phospholipase C in development of myogenic tone in rat posterior cerebral arteries. *Am J Physiol Heart Circ Physiol* 283: H2234-8, 2002. doi: 10.1152/ajpheart.00624.2002.

168. **Jennings JR**, **Muldoon MF**, **Ryan C**, **Price JC**, **Greer P**, **Sutton-Tyrrell K**, **van der Veen FM**, **Meltzer CC**. Reduced cerebral blood flow response and compensation among patients with untreated hypertension. *Neurology* 64: 1358–1365, 2005. doi: 10.1212/01.WNL.0000158283.28251.3C.

169. **Jesmin S**, **Togashi H**, **Mowa CN**, **Ueno K**, **Yamaguchi T**, **Shibayama A**, **Miyauchi T**, **Sakuma I**, **Yoshioka M**. Characterization of regional cerebral blood flow and expression of angiogenic growth factors in the frontal cortex of juvenile male SHRSP and SHR. *Brain Res* 1030: 172–182, 2004. doi: 10.1016/j.brainres.2004.10.004.

170. **Jobe SO**, **Ramadoss J**, **Wargin AJ**, **Magness RR**. Estradiol-17β and its cytochrome P450- and catechol-O-methyltransferase-derived metabolites selectively stimulate production of prostacyclin in uterine artery endothelial cells: role of estrogen receptor-α versus estrogen receptor-β. *Hypertension* 61: 509–518, 2013. doi: 10.1161/HYPERTENSIONAHA.112.200717.

171. **Jones PA**, **Scott-Burden T**, **Gevers W**. Glycoprotein, elastin, and collagen secretion by rat smooth muscle cells. *Proc Natl Acad Sci USA* 76: 353–357, 1979. doi: 10.1073/pnas.76.1.353.

172. **Judy WV**, **Watanabe AM**, **Henry DP**, **Besch HR**, **Murphy WR**, **Hockel GM**. Sympathetic nerve activity: role in regulation of blood pressure in the spontaenously hypertensive rat. *Circ Res* 38: 21–29, 1976. doi: 10.1161/01.res.38.6.21.

173. **Jun SS**, **Chen Z**, **Pace MC**, **Shaul PW**. Estrogen upregulates cyclooxygenase-1 gene expression in ovine fetal pulmonary artery endothelium. *J Clin Invest* 102: 176–183, 1998. doi: 10.1172/JCI2034.

174. **Kalsoum E**, **Leclerc X**, **Drizenko A**, **Pruvo JP**. Circle of Willis. In: *Encyclopedia of the neurological sciences*. Elsevier, 2014, p. 803–805.

175. **Kanashiro-Takeuchi RM**, **Heidecker B**, **Lamirault G**, **Dharamsi JW**, **Hare JM**. Sex-specific impact of aldosterone receptor antagonism on ventricular remodeling and gene expression after myocardial infarction. *Clin Transl Sci* 2: 134–142, 2009. doi: 10.1111/j.1752-8062.2009.00094.x.

176. **Kaplan L**, **Chow BW**, **Gu C**. Neuronal regulation of the blood-brain barrier and neurovascular coupling. *Nat Rev Neurosci* 21: 416–432, 2020. doi: 10.1038/s41583-020-0322-2.

177. **Karashima Y**, **Prenen J**, **Talavera K**, **Janssens A**, **Voets T**, **Nilius B**. Agonist-induced changes in Ca(2+) permeation through the nociceptor cation channel TRPA1. *Biophys J* 98: 773–783, 2010. doi: 10.1016/j.bpj.2009.11.007.

178. **Katusic ZS**. Vascular endothelial dysfunction: does tetrahydrobiopterin play a role? *Am J Physiol Heart Circ Physiol* 281: H981-6, 2001. doi: 10.1152/ajpheart.2001.281.3.H981.

179. **Kawai T**, **Forrester SJ**, **O'Brien S**, **Baggett A**, **Rizzo V**, **Eguchi S**. AT1 receptor signaling pathways in the cardiovascular system. *Pharmacol Res* 125: 4–13, 2017. doi: 10.1016/j.phrs.2017.05.008.

180. **Kaya E**, **Sahin FK**, **Köken G**, **Köse M**, **Cevrioglu AS**. Acute effect of intranasal estrogen on cerebral and cerebellar perfusion in postmenopausal women. *Maturitas* 59: 72–82, 2008. doi: 10.1016/j.maturitas.2007.10.004.

181. **Kazama K**, **Anrather J**, **Zhou P**, **Girouard H**, **Frys K**, **Milner TA**, **Iadecola C**. Angiotensin II impairs neurovascular coupling in neocortex through NADPH oxidase-derived radicals. *Circ Res* 95: 1019–1026, 2004. doi: 10.1161/01.RES.0000148637.85595.c5.

182. **Kazama K**, **Wang G**, **Frys K**, **Anrather J**, **Iadecola C**. Angiotensin II attenuates functional hyperemia in the mouse somatosensory cortex. *Am J Physiol Heart Circ Physiol* 285: H1890-9, 2003. doi: 10.1152/ajpheart.00464.2003.

183. **Kellawan JM**, **Peltonen GL**, **Harrell JW**, **Roldan-Alzate A**, **Wieben O**, **Schrage WG**. Differential contribution of cyclooxygenase to basal cerebral blood flow and hypoxic cerebral vasodilation. *Am J Physiol Regul Integr Comp Physiol* 318: R468–R479, 2020. doi: 10.1152/ajpregu.00132.2019.

184. **Kerr PM**, **Tam R**, **Ondrusova K**, **Mittal R**, **Narang D**, **Tran CHT**, **Welsh DG**, **Plane F**. Endothelial feedback and the myoendothelial projection. *Microcirculation* 19: 416–422, 2012. doi: 10.1111/j.1549-8719.2012.00187.x.

185. **Kiliç T**, **Akakin A**. Anatomy of cerebral veins and sinuses. *Front Neurol Neurosci* 23: 4–15, 2008. doi: 10.1159/000111256.

186. **Kim KJ**, **Iddings JA**, **Stern JE**, **Blanco VM**, **Croom D**, **Kirov SA**, **Filosa JA**. Astrocyte contributions to flow/pressure-evoked parenchymal arteriole vasoconstriction. *J Neurosci* 35: 8245–8257, 2015. doi: 10.1523/JNEUROSCI.4486-14.2015.

187. **Kim KJ**, **Ramiro Diaz J**, **Iddings JA**, **Filosa JA**. Vasculo-Neuronal Coupling: Retrograde Vascular Communication to Brain Neurons. *J Neurosci* 36: 12624–12639, 2016. doi: 10.1523/JNEUROSCI.1300-16.2016.

188. **Kim SK**, **McCurley AT**, **DuPont JJ**, **Aronovitz M**, **Moss ME**, **Stillman IE**, **Karumanchi SA**, **Christou DD**, **Jaffe IZ**. Smooth Muscle Cell-Mineralocorticoid Receptor as a Mediator of Cardiovascular Stiffness With Aging. *Hypertension* 71: 609–621, 2018. doi: 10.1161/HYPERTENSIONAHA.117.10437.

189. **Köhler R**, **Heyken W-T**, **Heinau P**, **Schubert R**, **Si H**, **Kacik M**, **Busch C**, **Grgic I**, **Maier T**, **Hoyer J**. Evidence for a functional role of endothelial transient receptor potential V4 in shear stress-induced vasodilatation. *Arterioscler Thromb Vasc Biol* 26: 1495–1502, 2006. doi: 10.1161/01.ATV.0000225698.36212.6a.

190. **Kolkhof P**, **Bärfacker L**. 30 YEARS OF THE MINERALOCORTICOID RECEPTOR: Mineralocorticoid receptor antagonists: 60 years of research and development. *J Endocrinol* 234: T125–T140, 2017. doi: 10.1530/JOE-16-0600.

191. **Korner P**, **Bobik A**, **Oddie C**, **Friberg P**. Sympathoadrenal system is critical for structural changes in genetic hypertension. *Hypertension* 22: 243–252, 1993. doi: 10.1161/01.hyp.22.2.243.

192. **Kraeuter A-K**, **Guest PC**, **Sarnyai Z**. The Y-Maze for Assessment of Spatial Working and Reference Memory in Mice. *Methods Mol Biol* 1916: 105–111, 2019. doi: 10.1007/978-1-4939-8994-2_10.

193. **Krug AW**, **Allenhöfer L**, **Monticone R**, **Spinetti G**, **Gekle M**, **Wang M**, **Lakatta EG**. Elevated mineralocorticoid receptor activity in aged rat vascular smooth muscle cells promotes a proinflammatory phenotype via extracellular signal-regulated kinase 1/2 mitogen-activated protein kinase and epidermal growth factor receptor-dependent pathways. *Hypertension* 55: 1476–1483, 2010. doi: 10.1161/HYPERTENSIONAHA.109.148783.

194. **Kumar S**, **Singh O**, **Singh U**, **Goswami C**, **Singru PS**. Transient receptor potential vanilloid 1-6 (Trpv1-6) gene expression in the mouse brain during estrous cycle. *Brain Res* 1701: 161–170, 2018. doi: 10.1016/j.brainres.2018.09.005.

195. **Kusche-Vihrog K**, **Callies C**, **Fels J**, **Oberleithner H**. The epithelial sodium channel (ENaC): Mediator of the aldosterone response in the vascular endothelium? *Steroids* 75: 544–549, 2010. doi: 10.1016/j.steroids.2009.09.003.

196. **Kyle BD**, **Mishra RC**, **Braun AP**. The augmentation of BK channel activity by nitric oxide signaling in rat cerebral arteries involves co-localized regulatory elements. *J Cereb Blood Flow Metab* 37: 3759–3773, 2017. doi: 10.1177/0271678X17691291.

197. **Lacombe P**, **Oligo C**, **Domenga V**, **Tournier-Lasserve E**, **Joutel A**. Impaired cerebral vasoreactivity in a transgenic mouse model of cerebral autosomal dominant arteriopathy with subcortical infarcts and leukoencephalopathy arteriopathy. *Stroke* 36: 1053–1058, 2005. doi: 10.1161/01.STR.0000163080.82766.eb.

198. **Lagrange J**, **Li Z**, **Fassot C**, **Bourhim M**, **Louis H**, **Nguyen Dinh Cat A**, **Parlakian A**, **Wahl D**, **Lacolley P**, **Jaisser F**, **Regnault V**. Endothelial mineralocorticoid receptor activation enhances endothelial protein C receptor and decreases vascular thrombosis in mice. *FASEB J* 28: 2062–2072, 2014. doi: 10.1096/fj.13-238188.

199. **Lainscak M**, **Pelliccia F**, **Rosano G**, **Vitale C**, **Schiariti M**, **Greco C**, **Speziale G**, **Gaudio C**. Safety profile of mineralocorticoid receptor antagonists: Spironolactone and eplerenone. *Int J Cardiol* 200: 25–29, 2015. doi: 10.1016/j.ijcard.2015.05.127.

200. **Lai AY**, **Bazzigaluppi P**, **Morrone CD**, **Hill ME**, **Stefanovic B**, **McLaurin J**. Compromised Cortical-Hippocampal Network Function From Transient Hypertension: Linking Mid-Life Hypertension to Late Life Dementia Risk. *Front Neurosci* 16: 897206, 2022. doi: 10.3389/fnins.2022.897206.

201. **Launer LJ**, **Ross GW**, **Petrovitch H**, **Masaki K**, **Foley D**, **White LR**, **Havlik RJ**. Midlife blood pressure and dementia: the Honolulu-Asia aging study. *Neurobiol Aging* 21: 49–55, 2000. doi: 10.1016/s0197-4580(00)00096-8.

202. **Lefferts WK**, **DeBlois JP**, **Barreira TV**, **Heffernan KS**. Neurovascular coupling during cognitive activity in adults with controlled hypertension. *J Appl Physiol* 125: 1906–1916, 2018. doi: 10.1152/japplphysiol.00100.2018.

203. **Leffler CW**, **Busija DW**, **Armstead WM**, **Mirro R**. H2O2 effects on cerebral prostanoids and pial arteriolar diameter in piglets. *Am J Physiol* 258: H1382-7, 1990. doi: 10.1152/ajpheart.1990.258.5.H1382.

204. **Lemarié CA**, **Schiffrin EL**. The angiotensin II type 2 receptor in cardiovascular disease. *J Renin Angiotensin Aldosterone Syst* 11: 19–31, 2010. doi: 10.1177/1470320309347785.

205. **Lerman LO**, **Kurtz TW**, **Touyz RM**, **Ellison DH**, **Chade AR**, **Crowley SD**, **Mattson DL**, **Mullins JJ**, **Osborn J**, **Eirin A**, **Reckelhoff JF**, **Iadecola C**, **Coffman TM**. Animal models of hypertension: A scientific statement from the american heart

association. *Hypertension* 73: e87–e120, 2019. doi: 10.1161/HYP.0000000000000090.

206. **Lindekleiv HM**, **Valen-Sendstad K**, **Morgan MK**, **Mardal K-A**, **Faulder K**, **Magnus JH**, **Waterloo K**, **Romner B**, **Ingebrigtsen T**. Sex differences in intracranial arterial bifurcations. *Gend Med* 7: 149–155, 2010. doi: 10.1016/j.genm.2010.03.003.

207. **Lindsey SH**, **Songu-Mize E**. Stretch-induced TRPC4 downregulation is accompanied by reduced capacitative Ca2+ entry in WKY but not SHR mesenteric smooth muscle cells. *Clin Exp Hypertens* 32: 288–292, 2010. doi: 10.3109/10641960903443525.

208. **Liu D**, **Yang D**, **He H**, **Chen X**, **Cao T**, **Feng X**, **Ma L**, **Luo Z**, **Wang L**, **Yan Z**, **Zhu Z**, **Tepel M**. Increased transient receptor potential canonical type 3 channels in vasculature from hypertensive rats. *Hypertension* 53: 70–76, 2009. doi: 10.1161/HYPERTENSIONAHA.108.116947.

209. **Liu M-Y**, **Hattori Y**, **Sato A**, **Ichikawa R**, **Zhang X-H**, **Sakuma I**. Ovariectomy attenuates hyperpolarization and relaxation mediated by endothelium-derived hyperpolarizing factor in female rat mesenteric artery: a concomitant decrease in connexin-43 expression. *J Cardiovasc Pharmacol* 40: 938–948, 2002. doi: 10.1097/00005344-200212000-00016.

210. **Liu MY**, **Hattori Y**, **Fukao M**, **Sato A**, **Sakuma I**, **Kanno M**. Alterations in EDHF-mediated hyperpolarization and relaxation in mesenteric arteries of female rats in long-term deficiency of oestrogen and during oestrus cycle. *Br J Pharmacol* 132: 1035–1046, 2001. doi: 10.1038/sj.bjp.0703899.

211. **Liu W**, **Lou X**, **Ma L**. Use of 3D pseudo-continuous arterial spin labeling to characterize sex and age differences in cerebral blood flow. *Neuroradiology* 58: 943–948, 2016. doi: 10.1007/s00234-016-1713-y.

212. **Li Y**, **Baylie RL**, **Tavares MJ**, **Brayden JE**. TRPM4 channels couple purinergic receptor mechanoactivation and myogenic tone development in cerebral parenchymal arterioles. *J Cereb Blood Flow Metab* 34: 1706–1714, 2014. doi: 10.1038/jcbfm.2014.139.

213. **Lloyd GW**, **Patel NR**, **McGing E**, **Cooper AF**, **Brennand-Roper D**, **Jackson G**. Does angina vary with the menstrual cycle in women with premenopausal coronary artery disease? *Heart* 84: 189–192, 2000. doi: 10.1136/heart.84.2.189.

214. **Lobo A**, **Launer LJ**, **Fratiglioni L**, **Andersen K**, **Di Carlo A**, **Breteler MM**, **Copeland JR**, **Dartigues JF**, **Jagger C**, **Martinez-Lage J**, **Soininen H**, **Hofman A**. Prevalence of dementia and major subtypes in Europe: A collaborative study of

population-based cohorts. Neurologic Diseases in the Elderly Research Group. *Neurology* 54: S4-9, 2000.

215. **Longden TA**, **Dabertrand F**, **Koide M**, **Gonzales AL**, **Tykocki NR**, **Brayden JE**, **Hill-Eubanks D**, **Nelson MT**. Capillary K+-sensing initiates retrograde hyperpolarization to increase local cerebral blood flow. *Nat Neurosci* 20: 717–726, 2017. doi: 10.1038/nn.4533.

216. **Longden TA**, **Hill-Eubanks DC**, **Nelson MT**. Ion channel networks in the control of cerebral blood flow. *J Cereb Blood Flow Metab* 36: 492–512, 2016. doi: 10.1177/0271678X15616138.

217. **Ma X**, **Cheng K-T**, **Wong C-O**, **O'Neil RG**, **Birnbaumer L**, **Ambudkar IS**, **Yao X**. Heteromeric TRPV4-C1 channels contribute to store-operated Ca(2+) entry in vascular endothelial cells. *Cell Calcium* 50: 502–509, 2011. doi: 10.1016/j.ceca.2011.08.006.

218. **MacRitchie AN**, **Jun SS**, **Chen Z**, **German Z**, **Yuhanna IS**, **Sherman TS**, **Shaul PW**. Estrogen upregulates endothelial nitric oxide synthase gene expression in fetal pulmonary artery endothelium. *Circ Res* 81: 355–362, 1997. doi: 10.1161/01.res.81.3.355.

219. **Maillard P**, **Carmichael O**, **Fletcher E**, **Reed B**, **Mungas D**, **DeCarli C**. Coevolution of white matter hyperintensities and cognition in the elderly. *Neurology* 79: 442–448, 2012. doi: 10.1212/WNL.0b013e3182617136.

220. **Marques-Lopes J**, **Lynch M-K**, **Van Kempen TA**, **Waters EM**, **Wang G**, **Iadecola C**, **Pickel VM**, **Milner TA**. Female protection from slow-pressor effects of angiotensin II involves prevention of ROS production independent of NMDA receptor trafficking in hypothalamic neurons expressing angiotensin 1A receptors. *Synapse* 69: 148–165, 2015. doi: 10.1002/syn.21800.

221. **Mathiisen TM**, **Lehre KP**, **Danbolt NC**, **Ottersen OP**. The perivascular astroglial sheath provides a complete covering of the brain microvessels: an electron microscopic 3D reconstruction. *Glia* 58: 1094–1103, 2010. doi: 10.1002/glia.20990.

222. **Matin N**, **Fisher C**, **Jackson WF**, **Diaz-Otero JM**, **Dorrance AM**. Carotid artery stenosis in hypertensive rats impairs dilatory pathways in parenchymal arterioles. *Am J Physiol Heart Circ Physiol* 314: H122–H130, 2018. doi: 10.1152/ajpheart.00638.2016.

223. **Matin N**, **Fisher C**, **Jackson WF**, **Dorrance AM**. Bilateral common carotid artery stenosis in normotensive rats impairs endothelium-dependent dilation of parenchymal arterioles. *Am J Physiol Heart Circ Physiol* 310: H1321-9, 2016. doi: 10.1152/ajpheart.00890.2015.

224. **Matin N**, **Fisher C**, **Lansdell TA**, **Hammock BD**, **Yang J**, **Jackson WF**, **Dorrance AM**. Soluble epoxide hydrolase inhibition improves cognitive function and parenchymal artery dilation in a hypertensive model of chronic cerebral hypoperfusion. *Microcirculation* 28: e12653, 2021. doi: 10.1111/micc.12653.

225. **Mayhan WG**, **Faraci FM**, **Heistad DD**. Impairment of endothelium-dependent responses of cerebral arterioles in chronic hypertension. *Am J Physiol* 253: H1435-40, 1987. doi: 10.1152/ajpheart.1987.253.6.H1435.

226. **McClain JL**, **Dorrance AM**. Temporary mineralocorticoid receptor antagonism during the development of hypertension improves cerebral artery dilation. *Exp Biol Med (Maywood)* 239: 619–627, 2014. doi: 10.1177/1535370214522586.

227. **McCurley A**, **Jaffe IZ**. Mineralocorticoid receptors in vascular function and disease. *Mol Cell Endocrinol* 350: 256–265, 2012. doi: 10.1016/j.mce.2011.06.014.

228. **McCurley A**, **Pires PW**, **Bender SB**, **Aronovitz M**, **Zhao MJ**, **Metzger D**, **Chambon P**, **Hill MA**, **Dorrance AM**, **Mendelsohn ME**, **Jaffe IZ**. Direct regulation of blood pressure by smooth muscle cell mineralocorticoid receptors. *Nat Med* 18: 1429–1433, 2012. doi: 10.1038/nm.2891.

229. **McGrath ER**, **Beiser AS**, **DeCarli C**, **Plourde KL**, **Vasan RS**, **Greenberg SM**, **Seshadri S**. Blood pressure from mid- to late life and risk of incident dementia. *Neurology* 89: 2447–2454, 2017. doi: 10.1212/WNL.0000000000004741.

230. **McIntyre M**, **Hamilton CA**, **Rees DD**, **Reid JL**, **Dominiczak AF**. Sex differences in the abundance of endothelial nitric oxide in a model of genetic hypertension. *Hypertension* 30: 1517–1524, 1997. doi: 10.1161/01.hyp.30.6.1517.

231. **McNeill AM**, **Kim N**, **Duckles SP**, **Krause DN**, **Kontos HA**. Chronic estrogen treatment increases levels of endothelial nitric oxide synthase protein in rat cerebral microvessels. *Stroke* 30: 2186–2190, 1999. doi: 10.1161/01.str.30.10.2186.

232. **McNeill AM**, **Zhang C**, **Stanczyk FZ**, **Duckles SP**, **Krause DN**. Estrogen increases endothelial nitric oxide synthase via estrogen receptors in rat cerebral blood vessels: effect preserved after concurrent treatment with medroxyprogesterone acetate or progesterone. *Stroke* 33: 1685–1691, 2002. doi: 10.1161/01.str.0000016325.54374.93.

233. **Meder JF**, **Chiras J**, **Roland J**, **Guinet P**, **Bracard S**, **Bargy F**. Venous territories of the brain. *J Neuroradiol* 21: 118–133, 1994.

234. **Medina D**, **Arnold AC**. Angiotensin-(1-7): Translational Avenues in Cardiovascular Control. *Am J Hypertens* 32: 1133–1142, 2019. doi: 10.1093/ajh/hpz146.

235. **Medina D**, **Mehay D**, **Arnold AC**. Sex differences in cardiovascular actions of the renin-angiotensin system. *Clin Auton Res* 30: 393–408, 2020. doi: 10.1007/s10286-020-00720-2.

236. **Mendoza SA**, **Fang J**, **Gutterman DD**, **Wilcox DA**, **Bubolz AH**, **Li R**, **Suzuki M**, **Zhang DX**. TRPV4-mediated endothelial Ca2+ influx and vasodilation in response to shear stress. *Am J Physiol Heart Circ Physiol* 298: H466-76, 2010. doi: 10.1152/ajpheart.00854.2009.

237. **Mercado J**, **Baylie R**, **Navedo MF**, **Yuan C**, **Scott JD**, **Nelson MT**, **Brayden JE**, **Santana LF**. Local control of TRPV4 channels by AKAP150-targeted PKC in arterial smooth muscle. *J Gen Physiol* 143: 559–575, 2014. doi: 10.1085/jgp.201311050.

238. **Mishra JS**, **More AS**, **Gopalakrishnan K**, **Kumar S**. Testosterone plays a permissive role in angiotensin II-induced hypertension and cardiac hypertrophy in male rats. *Biol Reprod* 100: 139–148, 2019. doi: 10.1093/biolre/ioy179.

239. **Miyata K**, **Rahman M**, **Shokoji T**, **Nagai Y**, **Zhang G-X**, **Sun G-P**, **Kimura S**, **Yukimura T**, **Kiyomoto H**, **Kohno M**, **Abe Y**, **Nishiyama A**. Aldosterone stimulates reactive oxygen species production through activation of NADPH oxidase in rat mesangial cells. *J Am Soc Nephrol* 16: 2906–2912, 2005. doi: 10.1681/ASN.2005040390.

240. **Moore SA**, **Spector AA**, **Hart MN**. Eicosanoid metabolism in cerebromicrovascular endothelium. *Am J Physiol* 254: C37-44, 1988. doi: 10.1152/ajpcell.1988.254.1.C37.

241. **Mueller KB**, **Bender SB**, **Hong K**, **Yang Y**, **Aronovitz M**, **Jaisser F**, **Hill MA**, **Jaffe IZ**. Endothelial mineralocorticoid receptors differentially contribute to coronary and mesenteric vascular function without modulating blood pressure. *Hypertension* 66: 988–997, 2015. doi: 10.1161/HYPERTENSIONAHA.115.06172.

242. **Mulvany MJ**, **Baumbach GL**, **Aalkjaer C**, **Heagerty AM**, **Korsgaard N**, **Schiffrin EL**, **Heistad DD**. Vascular remodeling. *Hypertension* 28: 505–506, 1996.

243. **Muoio V**, **Persson PB**, **Sendeski MM**. The neurovascular unit - concept review. *Acta Physiol (Oxf)* 210: 790–798, 2014. doi: 10.1111/apha.12250.

244. **Myers SI**, **Turnage RH**, **Bartula L**, **Kalley B**, **Meng Y**. Estrogen increases male rat aortic endothelial cell (RAEC) PGI2 release. *Prostaglandins Leukot Essent Fatty Acids* 54: 403–409, 1996. doi: 10.1016/s0952-3278(96)90023-x.

245. **Neely CLC**, **Pedemonte KA**, **Boggs KN**, **Flinn JM**. Nest building behavior as an early indicator of behavioral deficits in mice. *J Vis Exp* , 2019. doi: 10.3791/60139.

246. **Nelson MT**, **Cheng H**, **Rubart M**, **Santana LF**, **Bonev AD**, **Knot HJ**, **Lederer WJ**. Relaxation of arterial smooth muscle by calcium sparks. *Science* 270: 633–637, 1995. doi: 10.1126/science.270.5236.633.

247. **Nelson MT**, **Conway MA**, **Knot HJ**, **Brayden JE**. Chloride channel blockers inhibit myogenic tone in rat cerebral arteries. *J Physiol (Lond)* 502 (Pt 2): 259–264, 1997. doi: 10.1111/j.1469-7793.1997.259bk.x.

248. **Nemeth Z**, **Hildebrandt E**, **Ryan MJ**, **Granger JP**, **Drummond HA**. Pressure-induced constriction of the middle cerebral artery is abolished in TrpC6 knockout mice. .

249. **Nguyen Dinh Cat A**, **Griol-Charhbili V**, **Loufrani L**, **Labat C**, **Benjamin L**, **Farman N**, **Lacolley P**, **Henrion D**, **Jaisser F**. The endothelial mineralocorticoid receptor regulates vasoconstrictor tone and blood pressure. *FASEB J* 24: 2454–2463, 2010. doi: 10.1096/fj.09-147926.

250. **Nielsen MS**, **Axelsen LN**, **Sorgen PL**, **Verma V**, **Delmar M**, **Holstein-Rathlou N-H**. Gap junctions. *Compr Physiol* 2: 1981–2035, 2012. doi: 10.1002/cphy.c110051.

251. **Nikolaev YA**, **Cox CD**, **Ridone P**, **Rohde PR**, **Cordero-Morales JF**, **Vásquez V**, **Laver DR**, **Martinac B**. Mammalian TRP ion channels are insensitive to membrane stretch. *J Cell Sci* 132, 2019. doi: 10.1242/jcs.238360.

252. **Nishida M**, **Kitajima N**, **Saiki S**, **Nakaya M**, **Kurose H**. Regulation of Angiotensin II receptor signaling by cysteine modification of NF-κB. *Nitric Oxide* 25: 112–117, 2011. doi: 10.1016/j.niox.2010.10.003.

253. **Nishimura N**, **Schaffer CB**, **Friedman B**, **Lyden PD**, **Kleinfeld D**. Penetrating arterioles are a bottleneck in the perfusion of neocortex. *Proc Natl Acad Sci USA* 104: 365–370, 2007. doi: 10.1073/pnas.0609551104.

254. **Nogueira EF**, **Xing Y**, **Morris CAV**, **Rainey WE**. Role of angiotensin II-induced rapid response genes in the regulation of enzymes needed for aldosterone synthesis. *J Mol Endocrinol* 42: 319–330, 2009. doi: 10.1677/JME-08-0112.

255. **O'Connor AT**, **Haspula D**, **Alanazi AZ**, **Clark MA**. Roles of Angiotensin III in the brain and periphery. *Peptides* 153: 170802, 2022. doi: 10.1016/j.peptides.2022.170802.

256. **Osol G**, **Brekke JF**, **McElroy-Yaggy K**, **Gokina NI**. Myogenic tone, reactivity, and forced dilatation: a three-phase model of in vitro arterial myogenic behavior. *Am J Physiol Heart Circ Physiol* 283: H2260-7, 2002. doi: 10.1152/ajpheart.00634.2002.

257. **Osol G**, **Laher I**, **Kelley M**. Myogenic tone is coupled to phospholipase C and G protein activation in small cerebral arteries. *Am J Physiol* 265: H415-20, 1993. doi: 10.1152/ajpheart.1993.265.1.H415.

258. **Ospina JA**, **Krause DN**, **Duckles SP**. 17beta-estradiol increases rat cerebrovascular prostacyclin synthesis by elevating cyclooxygenase-1 and prostacyclin synthase. *Stroke* 33: 600–605, 2002. doi: 10.1161/hs0202.102732.

259. **Otte C**, **Moritz S**, **Yassouridis A**, **Koop M**, **Madrischewski AM**, **Wiedemann K**, **Kellner M**. Blockade of the mineralocorticoid receptor in healthy men: effects on experimentally induced panic symptoms, stress hormones, and cognition. *Neuropsychopharmacology* 32: 232–238, 2007. doi: 10.1038/sj.npp.1301217.

260. **Ottolini M**, **Hong K**, **Cope EL**, **Daneva Z**, **DeLalio LJ**, **Sokolowski JD**, **Marziano C**, **Nguyen NY**, **Altschmied J**, **Haendeler J**, **Johnstone SR**, **Kalani MY**, **Park MS**, **Patel RP**, **Liedtke W**, **Isakson BE**, **Sonkusare SK**. Local peroxynitrite impairs endothelial transient receptor potential vanilloid 4 channels and elevates blood pressure in obesity. *Circulation* 141: 1318–1333, 2020. doi: 10.1161/CIRCULATIONAHA.119.043385.

261. **Ou Y-N**, **Tan C-C**, **Shen X-N**, **Xu W**, **Hou X-H**, **Dong Q**, **Tan L**, **Yu J-T**. Blood Pressure and Risks of Cognitive Impairment and Dementia: A Systematic Review and Meta-Analysis of 209 Prospective Studies. *Hypertension* 76: 217–225, 2020. doi: 10.1161/HYPERTENSIONAHA.120.14993.

262. **Özkan E**, **Çetin-Taş Y**, **Şekerdağ E**, **Kızılırmak AB**, **Taş A**, **Yıldız E**, **Yapıcı-Eser H**, **Karahüseyinoğlu S**, **Zeybel M**, **Gürsoy-Özdemir Y**. Blood-brain barrier leakage and perivascular collagen accumulation precede microvessel rarefaction and memory impairment in a chronic hypertension animal model. *Metab Brain Dis* 36: 2553–2566, 2021. doi: 10.1007/s11011-021-00767-8.

263. **Pankey EA**, **Zsombok A**, **Lasker GF**, **Kadowitz PJ**. Analysis of responses to the TRPV4 agonist GSK1016790A in the pulmonary vascular bed of the intact-chest rat. *Am J Physiol Heart Circ Physiol* 306: H33-40, 2014. doi: 10.1152/ajpheart.00303.2013.

264. **Pantoni L**. Cerebral small vessel disease: from pathogenesis and clinical characteristics to therapeutic challenges. *Lancet Neurol* 9: 689–701, 2010. doi: 10.1016/S1474-4422(10)70104-6.

265. **Paravicini TM**, **Touyz RM**. Redox signaling in hypertension. *Cardiovasc Res* 71: 247–258, 2006. doi: 10.1016/j.cardiores.2006.05.001.

266. **Parkington HC**, **Coleman HA**, **Tare M**. Prostacyclin and endothelium-dependent hyperpolarization. *Pharmacol Res* 49: 509–514, 2004. doi: 10.1016/j.phrs.2003.11.012.

267. **Park KS**, **Kim Y**, **Lee Y-H**, **Earm YE**, **Ho W-K**. Mechanosensitive cation channels in arterial smooth muscle cells are activated by diacylglycerol and inhibited by phospholipase C inhibitor. *Circ Res* 93: 557–564, 2003. doi: 10.1161/01.RES.0000093204.25499.83.

268. **Pires PW**, **Girgla SS**, **McClain JL**, **Kaminski NE**, **van Rooijen N**, **Dorrance AM**. Improvement in middle cerebral artery structure and endothelial function in stroke-prone spontaneously hypertensive rats after macrophage depletion. *Microcirculation* 20: 650–661, 2013. doi: 10.1111/micc.12064.

269. **Pires PW**, **Jackson WF**, **Dorrance AM**. Regulation of myogenic tone and structure of parenchymal arterioles by hypertension and the mineralocorticoid receptor. *Am J Physiol Heart Circ Physiol* 309: H127-36, 2015. doi: 10.1152/ajpheart.00168.2015.

270. **Pires PW**, **Ko E-A**, **Pritchard HAT**, **Rudokas M**, **Yamasaki E**, **Earley S**. The angiotensin II receptor type 1b is the primary sensor of intraluminal pressure in cerebral artery smooth muscle cells. *J Physiol (Lond)* 595: 4735–4753, 2017. doi: 10.1113/JP274310.

271. **Pires PW**, **Sullivan MN**, **Pritchard HAT**, **Robinson JJ**, **Earley S**. Unitary TRPV3 channel Ca2+ influx events elicit endothelium-dependent dilation of cerebral parenchymal arterioles. *Am J Physiol Heart Circ Physiol* 309: H2031-41, 2015. doi: 10.1152/ajpheart.00140.2015.

272. **Pitts MW**. Barnes maze procedure for spatial learning and memory in mice. *Bio Protoc* 8, 2018. doi: 10.21769/bioprotoc.2744.

273. **Pitt B**, **Reichek N**, **Willenbrock R**, **Zannad F**, **Phillips RA**, **Roniker B**, **Kleiman J**, **Krause S**, **Burns D**, **Williams GH**. Effects of eplerenone, enalapril, and eplerenone/enalapril in patients with essential hypertension and left ventricular hypertrophy: the 4E-left ventricular hypertrophy study. *Circulation* 108: 1831–1838, 2003. doi: 10.1161/01.CIR.0000091405.00772.6E.

274. **Presa JL**, **Saravia F**, **Bagi Z**, **Filosa JA**. Vasculo-Neuronal Coupling and Neurovascular Coupling at the Neurovascular Unit: Impact of Hypertension. *Front Physiol* 11: 584135, 2020. doi: 10.3389/fphys.2020.584135.

275. **Primo V**, **Graham M**, **Bigger-Allen AA**, **Chick JM**, **Ospina C**, **Quiroz YT**, **Manent J**, **Gygi SP**, **Lopera F**, **D'Amore PA**, **Arboleda-Velasquez JF**. Blood biomarkers in a mouse model of CADASIL. *Brain Res* 1644: 118–126, 2016. doi: 10.1016/j.brainres.2016.05.008.

276. **Prins ND**, **Scheltens P**. White matter hyperintensities, cognitive impairment and dementia: an update. *Nat Rev Neurol* 11: 157–165, 2015. doi: 10.1038/nrneurol.2015.10.

277. **Przysinda A**, **Feng W**, **Li G**. Diversity of Organism-Wide and Organ-Specific Endothelial Cells. *Curr Cardiol Rep* 22: 19, 2020. doi: 10.1007/s11886-020-1275-9.

278. **Rajagopalan S**, **Kurz S**, **Münzel T**, **Tarpey M**, **Freeman BA**, **Griendling KK**, **Harrison DG**. Angiotensin II-mediated hypertension in the rat increases vascular superoxide production via membrane NADH/NADPH oxidase activation. Contribution to alterations of vasomotor tone. *J Clin Invest* 97: 1916–1923, 1996. doi: 10.1172/JCI118623.

279. **Ravid JD**, **Laffin LJ**. Effects of finerenone, a novel nonsteroidal mineralocorticoid receptor antagonist, on cardiovascular disease, chronic kidney disease, and blood pressure. *Curr Cardiol Rep* 24: 1251–1259, 2022. doi: 10.1007/s11886-022-01750-0.

280. **Reed JT**, **Pareek T**, **Sriramula S**, **Pabbidi MR**. Aging influences cerebrovascular myogenic reactivity and BK channel function in a sex-specific manner. *Cardiovasc Res* 116: 1372–1385, 2020. doi: 10.1093/cvr/cvz314.

281. **Rickard AJ**, **Morgan J**, **Chrissobolis S**, **Miller AA**, **Sobey CG**, **Young MJ**. Endothelial cell mineralocorticoid receptors regulate deoxycorticosterone/salt-mediated cardiac remodeling and vascular reactivity but not blood pressure. *Hypertension* 63: 1033–1040, 2014. doi: 10.1161/HYPERTENSIONAHA.113.01803.

282. **Rigsby CS**, **Burch AE**, **Ogbi S**, **Pollock DM**, **Dorrance AM**. Intact female stroke-prone hypertensive rats lack responsiveness to mineralocorticoid receptor antagonists. *Am J Physiol Regul Integr Comp Physiol* 293: R1754-63, 2007. doi: 10.1152/ajpregu.00145.2007.

283. **Rigsby CS**, **Cannady WE**, **Dorrance AM**. Aldosterone: good guy or bad guy in cerebrovascular disease? *Trends Endocrinol Metab* 16: 401–406, 2005. doi: 10.1016/j.tem.2005.09.002.

284. **Rigsby CS**, **Ergul A**, **Portik Dobos V**, **Pollock DM**, **Dorrance AM**. Effects of spironolactone on cerebral vessel structure in rats with sustained hypertension. *Am J Hypertens* 24: 708–715, 2011. doi: 10.1038/ajh.2011.20.

285. **Rigsby CS**, **Pollock DM**, **Dorrance AM**. Spironolactone improves structure and increases tone in the cerebral vasculature of male spontaneously hypertensive stroke-prone rats. *Microvasc Res* 73: 198–205, 2007. doi: 10.1016/j.mvr.2006.12.001.

286. **Ritchey MD**, **Gillespie C**, **Wozniak G**, **Shay CM**, **Thompson-Paul AM**, **Loustalot F**, **Hong Y**. Potential need for expanded pharmacologic treatment and

lifestyle modification services under the 2017 ACC/AHA Hypertension Guideline. *J Clin Hypertens (Greenwich)* 20: 1377–1391, 2018. doi: 10.1111/jch.13364.

287. **Robertson BE**, **Schubert R**, **Hescheler J**, **Nelson MT**. cGMP-dependent protein kinase activates Ca-activated K channels in cerebral artery smooth muscle cells. *Am J Physiol* 265: C299-303, 1993. doi: 10.1152/ajpcell.1993.265.1.C299.

288. **Rodriguez G**, **Warkentin S**, **Risberg J**, **Rosadini G**. Sex differences in regional cerebral blood flow. *J Cereb Blood Flow Metab* 8: 783–789, 1988. doi: 10.1038/jcbfm.1988.133.

289. **Rönnemaa E**, **Zethelius B**, **Lannfelt L**, **Kilander L**. Vascular risk factors and dementia: 40-year follow-up of a population-based cohort. *Dement Geriatr Cogn Disord* 31: 460–466, 2011. doi: 10.1159/000330020.

290. **Roos A**. Poiseuille's law and its limitations in vascular systems. *Med Thorac* 19: 224–238, 1962.

291. **Rosner J**, **Reddy V**, **Lui F**. Neuroanatomy, circle of willis. In: *StatPearls*. Treasure Island (FL): StatPearls Publishing, 2022.

292. **Royea J**, **Hamel E**. Brain angiotensin II and angiotensin IV receptors as potential Alzheimer's disease therapeutic targets. *Geroscience* 42: 1237–1256, 2020. doi: 10.1007/s11357-020-00231-y.

293. **Rude MK**, **Duhaney T-AS**, **Kuster GM**, **Judge S**, **Heo J**, **Colucci WS**, **Siwik DA**, **Sam F**. Aldosterone stimulates matrix metalloproteinases and reactive oxygen species in adult rat ventricular cardiomyocytes. *Hypertension* 46: 555–561, 2005. doi: 10.1161/01.HYP.0000176236.55322.18.

294. **Ruitenberg A**, **Ott A**, **van Swieten JC**, **Hofman A**, **Breteler MM**. Incidence of dementia: does gender make a difference? *Neurobiol Aging* 22: 575–580, 2001. doi: 10.1016/s0197-4580(01)00231-7.

295. **Sader MA**, **Celermajer DS**. Endothelial function, vascular reactivity and gender differences in the cardiovascular system. *Cardiovasc Res* 53: 597–604, 2002. doi: 10.1016/s0008-6363(01)00473-4.

296. **Salomonsson M**, **Braunstein TH**, **Holstein-Rathlou NH**, **Jensen LJ**. Na+-independent, nifedipine-resistant rat afferent arteriolar Ca2+ responses to noradrenaline: possible role of TRPC channels. *Acta Physiol (Oxf)* 200: 265–278, 2010. doi: 10.1111/j.1748-1716.2010.02141.x.

297. **Sampson AK**, **Moritz KM**, **Jones ES**, **Flower RL**, **Widdop RE**, **Denton KM**. Enhanced angiotensin II type 2 receptor mechanisms mediate decreases in arterial pressure attributable to chronic low-dose angiotensin II in female rats.

Hypertension 52: 666–671, 2008. doi: 10.1161/HYPERTENSIONAHA.108.114058.

298. **Sancho M**, **Gao Y**, **Hald BO**, **Yin H**, **Boulton M**, **Steven DA**, **MacDougall KW**, **Parrent AG**, **Pickering JG**, **Welsh DG**. An assessment of KIR channel function in human cerebral arteries. *Am J Physiol Heart Circ Physiol* 316: H794–H800, 2019. doi: 10.1152/ajpheart.00022.2019.

299. **Sandoval KE**, **Witt KA**. Blood-brain barrier tight junction permeability and ischemic stroke. *Neurobiol Dis* 32: 200–219, 2008. doi: 10.1016/j.nbd.2008.08.005.

300. **Sandow SL**, **Hill CE**. Incidence of myoendothelial gap junctions in the proximal and distal mesenteric arteries of the rat is suggestive of a role in endothelium-derived hyperpolarizing factor-mediated responses. *Circ Res* 86: 341–346, 2000. doi: 10.1161/01.res.86.3.341.

301. **Santos RAS**, **Sampaio WO**, **Alzamora AC**, **Motta-Santos D**, **Alenina N**, **Bader M**, **Campagnole-Santos MJ**. The ACE2/Angiotensin-(1-7)/MAS Axis of the Renin-Angiotensin System: Focus on Angiotensin-(1-7). *Physiol Rev* 98: 505–553, 2018. doi: 10.1152/physrev.00023.2016.

302. **Sarnyai Z**, **Sibille EL**, **Pavlides C**, **Fenster RJ**, **McEwen BS**, **Toth M**. Impaired hippocampal-dependent learning and functional abnormalities in the hippocampus in mice lacking serotonin(1A) receptors. *Proc Natl Acad Sci USA* 97: 14731–14736, 2000. doi: 10.1073/pnas.97.26.14731.

303. **Satterthwaite TD**, **Shinohara RT**, **Wolf DH**, **Hopson RD**, **Elliott MA**, **Vandekar SN**, **Ruparel K**, **Calkins ME**, **Roalf DR**, **Gennatas ED**, **Jackson C**, **Erus G**, **Prabhakaran K**, **Davatzikos C**, **Detre JA**, **Hakonarson H**, **Gur RC**, **Gur RE**. Impact of puberty on the evolution of cerebral perfusion during adolescence. *Proc Natl Acad Sci USA* 111: 8643–8648, 2014. doi: 10.1073/pnas.1400178111.

304. **Schaffer CB**, **Friedman B**, **Nishimura N**, **Schroeder LF**, **Tsai PS**, **Ebner FF**, **Lyden PD**, **Kleinfeld D**. Two-photon imaging of cortical surface microvessels reveals a robust redistribution in blood flow after vascular occlusion. *PLoS Biol* 4: e22, 2006. doi: 10.1371/journal.pbio.0040022.

305. **Schubert R**, **Kalentchuk VU**, **Krien U**. Rho kinase inhibition partly weakens myogenic reactivity in rat small arteries by changing calcium sensitivity. *Am J Physiol Heart Circ Physiol* 283: H2288-95, 2002. doi: 10.1152/ajpheart.00549.2002.

306. **Schwartz E**, **Adamany AM**, **Blumenfeld OO**. Isolation and characterization of the internal elastic lamina from calf thoracic aorta. *Exp Mol Pathol* 34: 299–306, 1981. doi: 10.1016/0014-4800(81)90047-2.

307. **Seki T**, **Goto K**, **Kiyohara K**, **Kansui Y**, **Murakami N**, **Haga Y**, **Ohtsubo T**, **Matsumura K**, **Kitazono T**. Downregulation of Endothelial Transient Receptor Potential Vanilloid Type 4 Channel and Small-Conductance of Ca2+-Activated K+ Channels Underpins Impaired Endothelium-Dependent Hyperpolarization in Hypertension. *Hypertension* 69: 143–153, 2017. doi: 10.1161/HYPERTENSIONAHA.116.07110.

308. **Shatri J**, **Bexheti D**, **Bexheti S**, **Kabashi S**, **Krasniqi S**, **Ahmetgjekaj I**, **Zhjeqi V**. Influence of gender and age on average dimensions of arteries forming the circle of willis study by magnetic resonance angiography on kosovo's population. *Open Access Maced J Med Sci* 5: 714–719, 2017. doi: 10.3889/oamjms.2017.160.

309. **Shimokawa H**, **Yasutake H**, **Fujii K**, **Owada MK**, **Nakaike R**, **Fukumoto Y**, **Takayanagi T**, **Nagao T**, **Egashira K**, **Fujishima M**, **Takeshita A**. The importance of the hyperpolarizing mechanism increases as the vessel size decreases in endothelium-dependent relaxations in rat mesenteric circulation. *J Cardiovasc Pharmacol* 28: 703–711, 1996. doi: 10.1097/00005344-199611000-00014.

310. **Silva-Antonialli MM**, **Tostes RCA**, **Fernandes L**, **Fior-Chadi DR**, **Akamine EH**, **Carvalho MHC**, **Fortes ZB**, **Nigro D**. A lower ratio of AT1/AT2 receptors of angiotensin II is found in female than in male spontaneously hypertensive rats. *Cardiovasc Res* 62: 587–593, 2004. doi: 10.1016/j.cardiores.2004.01.020.

311. **Skarsgard P**, **van Breemen C**, **Laher I**. Estrogen regulates myogenic tone in pressurized cerebral arteries by enhanced basal release of nitric oxide. *Am J Physiol* 273: H2248-56, 1997. doi: 10.1152/ajpheart.1997.273.5.H2248.

312. **Sobey CG**, **Heistad DD**, **Faraci FM**. Mechanisms of bradykinin-induced cerebral vasodilatation in rats. Evidence that reactive oxygen species activate K+ channels. *Stroke* 28: 2290–4; discussion 2295, 1997. doi: 10.1161/01.str.28.11.2290.

313. **Sobey CG**, **Weiler JM**, **Boujaoude M**, **Woodman OL**. Effect of short-term phytoestrogen treatment in male rats on nitric oxide-mediated responses of carotid and cerebral arteries: comparison with 17beta-estradiol. *J Pharmacol Exp Ther* 310: 135–140, 2004. doi: 10.1124/jpet.103.063255.

314. **Sokolova IA**, **Manukhina EB**, **Blinkov SM**, **Koshelev VB**, **Pinelis VG**, **Rodionov IM**. Rarefication of the arterioles and capillary network in the brain of rats with different forms of hypertension. *Microvasc Res* 30: 1–9, 1985. doi: 10.1016/0026-2862(85)90032-9.

315. **Sonkusare SK**, **Bonev AD**, **Ledoux J**, **Liedtke W**, **Kotlikoff MI**, **Heppner TJ**, **Hill-Eubanks DC**, **Nelson MT**. Elementary Ca2+ signals through endothelial TRPV4 channels regulate vascular function. *Science* 336: 597–601, 2012. doi: 10.1126/science.1216283.

316. **Sonkusare SK**, **Dalsgaard T**, **Bonev AD**, **Hill-Eubanks DC**, **Kotlikoff MI**, **Scott JD**, **Santana LF**, **Nelson MT**. AKAP150-dependent cooperative TRPV4 channel gating is central to endothelium-dependent vasodilation and is disrupted in hypertension. *Sci Signal* 7: ra66, 2014. doi: 10.1126/scisignal.2005052.

317. **Sonkusare SK**, **Dalsgaard T**, **Bonev AD**, **Nelson MT**. Inward rectifier potassium (Kir2.1) channels as end-stage boosters of endothelium-dependent vasodilators. *J Physiol (Lond)* 594: 3271–3285, 2016. doi: 10.1113/JP271652.

318. **Straub AC**, **Billaud M**, **Johnstone SR**, **Best AK**, **Yemen S**, **Dwyer ST**, **Looft-Wilson R**, **Lysiak JJ**, **Gaston B**, **Palmer L**, **Isakson BE**. Compartmentalized connexin 43 s-nitrosylation/denitrosylation regulates heterocellular communication in the vessel wall. *Arterioscler Thromb Vasc Biol* 31: 399–407, 2011. doi: 10.1161/ATVBAHA.110.215939.

319. **Straub AC**, **Zeigler AC**, **Isakson BE**. The myoendothelial junction: connections that deliver the message. *Physiology (Bethesda)* 29: 242–249, 2014. doi: 10.1152/physiol.00042.2013.

320. **Suboc TM**, **Dharmashankar K**, **Wang J**, **Ying R**, **Couillard A**, **Tanner MJ**, **Widlansky ME**. Moderate obesity and endothelial dysfunction in humans: influence of gender and systemic inflammation. *Physiol Rep* 1, 2013. doi: 10.1002/phy2.58.

321. **Sullivan JC**, **Rodriguez-Miguelez P**, **Zimmerman MA**, **Harris RA**. Differences in angiotensin (1-7) between men and women. *Am J Physiol Heart Circ Physiol* 308: H1171-6, 2015. doi: 10.1152/ajpheart.00897.2014.

322. **Sullivan MN**, **Gonzales AL**, **Pires PW**, **Bruhl A**, **Leo MD**, **Li W**, **Oulidi A**, **Boop FA**, **Feng Y**, **Jaggar JH**, **Welsh DG**, **Earley S**. Localized TRPA1 channel Ca2+ signals stimulated by reactive oxygen species promote cerebral artery dilation. *Sci Signal* 8: ra2, 2015. doi: 10.1126/scisignal.2005659.

323. **Sun J-Y**, **Li C**, **Shen Z-X**, **Zhang W-C**, **Ai T-J**, **Du L-J**, **Zhang Y-Y**, **Yao G-F**, **Liu Y**, **Sun S**, **Naray-Fejes-Toth A**, **Fejes-Toth G**, **Peng Y**, **Chen M**, **Liu X**, **Tao J**, **Zhou B**, **Yu Y**, **Guo F**, **Du J**, **Duan S-Z**. Mineralocorticoid Receptor Deficiency in Macrophages Inhibits Neointimal Hyperplasia and Suppresses Macrophage Inflammation Through SGK1-AP1/NF-κB Pathways. *Arterioscler Thromb Vasc Biol* 36: 874–885, 2016. doi: 10.1161/ATVBAHA.115.307031.

324. **Swonger AK**, **Rech RH**. Serotonergic and cholinergic involvement in habituation of activity and spontaneous alternation of rats in a Y maze. *J Comp Physiol Psychol* 81: 509–522, 1972. doi: 10.1037/h0033690.

325. **Takeda Y**, **Zhu A**, **Yoneda T**, **Usukura M**, **Takata H**, **Yamagishi M**. Effects of aldosterone and angiotensin II receptor blockade on cardiac angiotensinogen and

angiotensin-converting enzyme 2 expression in Dahl salt-sensitive hypertensive rats. *Am J Hypertens* 20: 1119–1124, 2007. doi: 10.1016/j.amjhyper.2007.05.008.

326. **Thakore P**, **Alvarado MG**, **Ali S**, **Mughal A**, **Pires PW**, **Yamasaki E**, **Pritchard HA**, **Isakson BE**, **Tran CHT**, **Earley S**. Brain endothelial cell TRPA1 channels initiate neurovascular coupling. *eLife* 10: e63040, 2021. doi: 10.7554/eLife.63040.

327. **Thakore P**, **Earley S**. Transient receptor potential channels and endothelial cell calcium signaling. *Compr Physiol* 9: 1249–1277, 2019. doi: 10.1002/cphy.c180034.

328. **Thijssen DHJ**, **Black MA**, **Pyke KE**, **Padilla J**, **Atkinson G**, **Harris RA**, **Parker B**, **Widlansky ME**, **Tschakovsky ME**, **Green DJ**. Assessment of flow-mediated dilation in humans: a methodological and physiological guideline. *Am J Physiol Heart Circ Physiol* 300: H2-12, 2011. doi: 10.1152/ajpheart.00471.2010.

329. **Tontisirin N**, **Muangman SL**, **Suz P**, **Pihoker C**, **Fisk D**, **Moore A**, **Lam AM**, **Vavilala MS**. Early childhood gender differences in anterior and posterior cerebral blood flow velocity and autoregulation. *Pediatrics* 119: e610-5, 2007. doi: 10.1542/peds.2006-2110.

330. **Toth P**, **Tarantini S**, **Tucsek Z**, **Ashpole NM**, **Sosnowska D**, **Gautam T**, **Ballabh P**, **Koller A**, **Sonntag WE**, **Csiszar A**, **Ungvari Z**. Resveratrol treatment rescues neurovascular coupling in aged mice: role of improved cerebromicrovascular endothelial function and downregulation of NADPH oxidase. *Am J Physiol Heart Circ Physiol* 306: H299-308, 2014. doi: 10.1152/ajpheart.00744.2013.

331. **Tsai PS**, **Kaufhold JP**, **Blinder P**, **Friedman B**, **Drew PJ**, **Karten HJ**, **Lyden PD**, **Kleinfeld D**. Correlations of neuronal and microvascular densities in murine cortex revealed by direct counting and colocalization of nuclei and vessels. *J Neurosci* 29: 14553–14570, 2009. doi: 10.1523/JNEUROSCI.3287-09.2009.

332. **Tsutsumi Y**, **Matsubara H**, **Masaki H**, **Kurihara H**, **Murasawa S**, **Takai S**, **Miyazaki M**, **Nozawa Y**, **Ozono R**, **Nakagawa K**, **Miwa T**, **Kawada N**, **Mori Y**, **Shibasaki Y**, **Tanaka Y**, **Fujiyama S**, **Koyama Y**, **Fujiyama A**, **Takahashi H**, **Iwasaka T**. Angiotensin II type 2 receptor overexpression activates the vascular kinin system and causes vasodilation. *J Clin Invest* 104: 925–935, 1999. doi: 10.1172/JCI7886.

333. **Tuo Q-Z**, **Zou J-J**, **Lei P**. Rodent models of vascular cognitive impairment. *J Mol Neurosci* 71: 1–12, 2021. doi: 10.1007/s12031-020-01733-2.

334. **van Hespen KM**, **Mackaaij C**, **Waas ISE**, **de Bree MP**, **Zwanenburg JJM**, **Kuijf HJ**, **Daemen MJAP**, **Hendrikse J**, **Hermkens DMA**. Arterial remodeling of the intracranial arteries in patients with hypertension and controls: A postmortem

study. *Hypertension* 77: 135–146, 2021. doi: 10.1161/HYPERTENSIONAHA.120.16029.

335. **Wang S**, **Zhang H**, **Liu Y**, **Li L**, **Guo Y**, **Jiao F**, **Fang X**, **Jefferson JR**, **Li M**, **Gao W**, **Gonzalez-Fernandez E**, **Maranon RO**, **Pabbidi MR**, **Liu R**, **Alexander BT**, **Roman RJ**, **Fan F**. Sex differences in the structure and function of rat middle cerebral arteries. .

336. **Watanabe H**, **Davis JB**, **Smart D**, **Jerman JC**, **Smith GD**, **Hayes P**, **Vriens J**, **Cairns W**, **Wissenbach U**, **Prenen J**, **Flockerzi V**, **Droogmans G**, **Benham CD**, **Nilius B**. Activation of TRPV4 channels (hVRL-2/mTRP12) by phorbol derivatives. *J Biol Chem* 277: 13569–13577, 2002. doi: 10.1074/jbc.M200062200.

337. **Wei EP**, **Kontos HA**. H2O2 and endothelium-dependent cerebral arteriolar dilation. Implications for the identity of endothelium-derived relaxing factor generated by acetylcholine. *Hypertension* 16: 162–169, 1990. doi: 10.1161/01.hyp.16.2.162.

338. **Welsh DG**, **Morielli AD**, **Nelson MT**, **Brayden JE**. Transient receptor potential channels regulate myogenic tone of resistance arteries. *Circ Res* 90: 248–250, 2002. doi: 10.1161/hh0302.105662.

339. **Xing C-Y**, **Tarumi T**, **Liu J**, **Zhang Y**, **Turner M**, **Riley J**, **Tinajero CD**, **Yuan L-J**, **Zhang R**. Distribution of cardiac output to the brain across the adult lifespan. *J Cereb Blood Flow Metab* 37: 2848–2856, 2017. doi: 10.1177/0271678X16676826.

340. **Xi Q**, **Adebiyi A**, **Zhao G**, **Chapman KE**, **Waters CM**, **Hassid A**, **Jaggar JH**. IP3 constricts cerebral arteries via IP3 receptor-mediated TRPC3 channel activation and independently of sarcoplasmic reticulum Ca2+ release. *Circ Res* 102: 1118–1126, 2008. doi: 10.1161/CIRCRESAHA.108.173948.

341. **Xue B**, **Johnson AK**, **Hay M**. Sex differences in angiotensin II- induced hypertension. *Braz J Med Biol Res* 40: 727–734, 2007. doi: 10.1590/S0100-879X2006005000093.

342. **Xue B**, **Pamidimukkala J**, **Hay M**. Sex differences in the development of angiotensin II-induced hypertension in conscious mice. *Am J Physiol Heart Circ Physiol* 288: H2177-84, 2005. doi: 10.1152/ajpheart.00969.2004.

343. **Xue B**, **Pamidimukkala J**, **Lubahn DB**, **Hay M**. Estrogen receptor-alpha mediates estrogen protection from angiotensin II-induced hypertension in conscious female mice. *Am J Physiol Heart Circ Physiol* 292: H1770-6, 2007. doi: 10.1152/ajpheart.01011.2005.

344. **Xu H**, **Delling M**, **Jun JC**, **Clapham DE**. Oregano, thyme and clove-derived flavors and skin sensitizers activate specific TRP channels. *Nat Neurosci* 9: 628–635, 2006. doi: 10.1038/nn1692.

345. **Xu S-Z**, **Boulay G**, **Flemming R**, **Beech DJ**. E3-targeted anti-TRPC5 antibody inhibits store-operated calcium entry in freshly isolated pial arterioles. *Am J Physiol Heart Circ Physiol* 291: H2653-9, 2006. doi: 10.1152/ajpheart.00495.2006.

346. **Yagi S**, **Akaike M**, **Aihara K**, **Iwase T**, **Yoshida S**, **Sumitomo-Ueda Y**, **Ikeda Y**, **Ishikawa K**, **Matsumoto T**, **Sata M**. High plasma aldosterone concentration is a novel risk factor of cognitive impairment in patients with hypertension. *Hypertens Res* 34: 74–78, 2011. doi: 10.1038/hr.2010.179.

347. **Yamakawa H**, **Jezova M**, **Ando H**, **Saavedra JM**. Normalization of endothelial and inducible nitric oxide synthase expression in brain microvessels of spontaneously hypertensive rats by angiotensin II AT1 receptor inhibition. *J Cereb Blood Flow Metab* 23: 371–380, 2003. doi: 10.1097/01.WCB.0000047369.05600.03.

348. **Yamasaki E**, **Thakore P**, **Krishnan V**, **Earley S**. Differential expression of angiotensin II type 1 receptor subtypes within the cerebral microvasculature. *Am J Physiol Heart Circ Physiol* 318: H461–H469, 2019. doi: 10.1152/ajpheart.00582.2019.

349. **Yan T**, **Liu B**, **Du D**, **Eisenach JC**, **Tong C**. Estrogen amplifies pain responses to uterine cervical distension in rats by altering transient receptor potential-1 function. *Anesth Analg* 104: 1246–50, tables of contents, 2007. doi: 10.1213/01.ane.0000263270.39480.a2.

350. **Yeon DS**, **Kim JS**, **Ahn DS**, **Kwon SC**, **Kang BS**, **Morgan KG**, **Lee YH**. Role of protein kinase C- or RhoA-induced Ca(2+) sensitization in stretch-induced myogenic tone. *Cardiovasc Res* 53: 431–438, 2002. doi: 10.1016/s0008-6363(01)00496-5.

351. **Zeldin DC**, **DuBois RN**, **Falck JR**, **Capdevila JH**. Molecular cloning, expression and characterization of an endogenous human cytochrome P450 arachidonic acid epoxygenase isoform. *Arch Biochem Biophys* 322: 76–86, 1995. doi: 10.1006/abbi.1995.1438.

352. **Zeldin DC**. Epoxygenase pathways of arachidonic acid metabolism. *J Biol Chem* 276: 36059–36062, 2001. doi: 10.1074/jbc.R100030200.

353. **Zhen G**, **Doré S**. Optimized protocol to reduce variable outcomes for the bilateral common carotid artery occlusion model in mice. *J Neurosci Methods* 166: 73–80, 2007. doi: 10.1016/j.jneumeth.2007.06.029.

354. **Zheng X**, **Zinkevich NS**, **Gebremedhin D**, **Gauthier KM**, **Nishijima Y**, **Fang J**, **Wilcox DA**, **Campbell WB**, **Gutterman DD**, **Zhang DX**. Arachidonic acid-induced dilation in human coronary arterioles: convergence of signaling mechanisms on endothelial TRPV4-mediated Ca2+ entry. *J Am Heart Assoc* 2: e000080, 2013. doi: 10.1161/JAHA.113.000080.

355. **Zhong XZ**, **Harhun MI**, **Olesen SP**, **Ohya S**, **Moffatt JD**, **Cole WC**, **Greenwood IA**. Participation of KCNQ (Kv7) potassium channels in myogenic control of cerebral arterial diameter. *J Physiol (Lond)* 588: 3277–3293, 2010. doi: 10.1113/jphysiol.2010.192823.

356. **Zlokovic BV**. Neurovascular mechanisms of Alzheimer's neurodegeneration. *Trends Neurosci* 28: 202–208, 2005. doi: 10.1016/j.tins.2005.02.001.

357. **Zuloaga KL**, **Davis CM**, **Zhang W**, **Alkayed NJ**. Role of aromatase in sex-specific cerebrovascular endothelial function in mice. *Am J Physiol Heart Circ Physiol* 306: H929-37, 2014. doi: 10.1152/ajpheart.00698.2013.

Chapter 2:

Mineralocorticoid Receptor Antagonism Improves Transient Receptor Potential Vanilloid 4-dependent Dilation of Cerebral Parenchymal Arterioles and Cognition in a Genetic Model of Hypertension

This chapter was adapted from: Chambers LC, Diaz-Otero JM, Fisher CL, Jackson WF, Dorrance AM. Mineralocorticoid receptor antagonism improves transient receptor potential vanilloid 4-dependent dilation of cerebral parenchymal arterioles and cognition in a genetic model of hypertension. J Hypertens. 2022 Sep 1;40(9):1722-1734. doi: 10.1097/HJH.0000000000003208. PMID: 35943101; PMCID: PMC9373385.

2.1 – Abstract

In a model of secondary hypertension, MR antagonism during the development of hypertension prevents the impairment of TRPV4 activation in PAs and cognitive impairment. However, it is unknown whether MR antagonism can improve these impairments when treatment begins after the onset of essential hypertension. We tested the hypothesis that MR activation in SHRSP leads to impaired TRPV4-mediated dilation in PAs that is associated with cognitive dysfunction and neuroinflammation. 20-22-week-old male SHRSP ± EPL (100mg/kg daily for 4 weeks) were compared to normotensive Sprague Dawley (SD) rats. Pressure myography was used to assess PA function. Cognition was tested using Y-maze. Neuroinflammation was assessed using immunofluorescence and qRT-PCR. Carbachol-mediated endothelium-dependent dilation was impaired in SHRSP, and MR antagonism improved this without affecting myogenic tone. Dilation to TRPV4 agonist GSK1016790A was impaired in SHRSP, and EPL treatment restored this. IK_{Ca}/SK_{Ca}-mediated dilation was impaired by hypertension and unaffected by EPL treatment. TRPV4 and IK_{Ca}/SK_{Ca} channel mRNA expression were reduced in PAs from hypertensive rats, and EPL did not improve this. Impairments in PA dilation in SHRSP were associated with cognitive decline, microglial activation, reactive

astrogliosis, and neuroinflammation; cognitive and inflammatory changes were improved with MR blockade. These data advance our understanding of the effects of hypertension on cerebral arterioles using a clinically relevant model and treatment paradigm. Our studies suggest TRPV4 and the MR are potential therapeutic targets to improve cerebrovascular function and cognition during hypertension.

2.2 – Introduction

MR activation has been linked to vascular damage in hypertension (48, 59, 61, 62) and stroke (21, 22) and is associated with cognitive and memory impairment in rodents (19) and humans (65). In a mouse model of AngII-hypertension, we showed that MR activation during the development of hypertension impairs endothelium-dependent dilation and causes inward remodeling of cerebral PAs; these changes were associated with cognitive decline (16, 19).

The PAs regulate blood flow from pial arterioles to the capillary bed, where gas and nutrient exchange occurs. Unlike pial arteries, PAs lack collateral connections and are considered the weak link in cerebral perfusion. Strikingly, occlusion of a single PA results in a microinfarct that is sufficient to cause cognitive decline (69, 72). The brain is a metabolically demanding organ that does not have energy stores; therefore, tightly regulated blood flow is an absolute requirement for proper function. Modifiable vascular risk factors such as hypertension disrupt cerebral hemodynamics and lead to cerebral hypoperfusion (51, 75). Chronic cerebral hypoperfusion is associated with cognitive decline because it prevents neurons from receiving the necessary nutrients (23, 34, 70, 78). In fact, appropriate vascular function is so vital for brain health that the severity of hypoperfusion can predict the rate of cognitive decline in patients with Alzheimer's

disease (5). Our studies in AngII-hypertensive mice confirm the importance of vascular function in cognition, as the impaired PA endothelium-dependent dilation observed is associated with cognitive dysfunction (19).

We have shown that PA endothelium-dependent dilation is primarily mediated by TRPV4 channels and that this dilator pathway is impaired in mice with AngII-hypertension (18, 19, 45). Ca^{2+} influx through TRPV4 triggers the activation of IK_{Ca}/SK_{Ca} in endothelial cells (10, 79). IK_{Ca}/SK_{Ca} activation produces a hyperpolarizing current that travels to vascular smooth muscle cells through myoendothelial gap junctions to cause vasodilation. The importance of TRPV4 in regulating cerebrovascular health is highlighted in our recent studies using a global TRPV4 knockout rat model. These rats exhibit cerebral hypoperfusion and impaired cognitive function (18).

Our previous studies implicating the MR and TRPV4 in hypertension-associated PA dysfunction were conducted in a model of secondary hypertension using angiotensin II, and the MR antagonists were administered as hypertension was developing (16, 19). Administration of pharmacological therapy alongside hypertension development does not reflect the timing of treatments in humans, where therapy would only be administered after hypertension is detected. This is a significant limitation of our previous studies and prevents us from knowing if hypertension-associated dementia is treatable or merely preventable. Our goal was to determine if cerebrovascular and cognitive impairments associated with hypertension can be improved with MR antagonism after the onset of hypertension. The current study utilized a rat model of polygenic multifactorial hypertension that accurately reflects human essential hypertension. We also used a clinically relevant treatment regime in which MR antagonist administration began after the

development of hypertension. We tested the hypothesis that MR activation impairs PA TRPV4-mediated dilation in SHRSP, that these impairments are associated with impaired cognitive function and neuroinflammation, and that MR antagonism improves these impairments.

2.3 – Materials and Methods

2.3.1 – Experimental Models and Treatment

All experimental protocols were approved by the Michigan State University Animal Care and Use Committee and performed according to the National Institutes of Health Guide for the Care and Use of Laboratory Animals. Male 20-22-week-old stroke-prone spontaneously hypertensive rats (SHRSP; n=15-16 total for each group) from the colony housed at Michigan State University were used. All rats were given standard rodent chow containing 0.3% sodium (Envigo, diet 8904). A group of SHRSP were treated with the MR antagonist EPL (100mg/kg/day), given orally suspended in 2g peanut butter daily for 4 weeks. This amount of peanut butter does not significantly alter the amount of dietary sodium. Treatment began when rats were 16-18 weeks of age. Age-matched male Sprague Dawley (SD) rats (n=16) purchased from Envigo (Indianapolis, IN) served as control. We used SD rats as the control for the SHRSP because previous studies found biological variability in WKY rats that results in variable blood pressures (40). WKY rats also express depressive behavior that confounds behavior analyses (41, 54). Though they do not share the same genetic background, SDs are commonly used as a normotensive control for SHRSP (68, 73, 76). All animals studied were male and housed on 12h:12h light/dark cycle with food and water ad libitum.

2.3.2 – Tail-Cuff Plethysmography

Blood pressure was measured in conscious rats by tail-cuff plethysmography using a RTBP1001 tail-cuff blood pressure system (CODA-6, Kent Scientific, Torrington, CT). Rats (n=8) were randomly selected for blood pressure analysis. All rats were acclimatized to both handling and the blood pressure measurement system ahead of the experimental measurements. Of the 25 cycles measured, the first 15 were used as acclimation, and the remaining 10 were averaged to provide the final data point for each animal.

2.3.3 – Laser Speckle Contrast Imaging

Pial cerebral blood flow was measured by laser speckle contrast imaging in n=8 rats randomly selected per group; variable numbers are due to the removal of an outlier identified by Grubb's test and the death of one SHRSP under isoflurane. Rats were anesthetized under 2% isoflurane before imaging, and a 2cm vertical incision was made through the skin and connective tissue to expose the skull. The closed skull was cleaned using a saturated ferric chloride solution followed by hydrogen peroxide. To improve the resolution of the image, clear nail polish was applied to the surface of the skull. Before beginning the measurements, isoflurane was reduced to 1%, and the rats were equilibrated for 5min. Images were then acquired for 1min at a rate of 22 images/s. Images were analyzed using PIMSoft software (PeriMed, Las Vegas, NV). Mean flux values were measured in regions of interest defined in each brain hemisphere between the bregma and lambda sutures.

2.3.4 – Pressure Myography

The endothelial function of PAs was assessed by pressure myography as described previously by our lab (16, 17, 46, 59). A 5 x 3mm section of the brain containing

the middle cerebral artery (MCA) was dissected to isolate the arterioles. The pia with the MCA was separated from the brain, and the PAs branching off the MCA were used for experiments. A total of n=15-16 rats were used to complete dilation and myogenic tone experiments; each arteriole was used for only one concentration-response curve. Isolated arterioles were cannulated using two glass micropipettes in a custom-made cannulation chamber. PAs were equilibrated in physiological salt solution (PSS) containing 140mmol/L NaCl, 5mmol/L KCl, 1.8mmol/L $CaCl_2$, 1mmol/L $MgCl_2$, 10mmol/L HEPES, and 10mmol/L glucose. A servo-null system was used to pressurize the arterioles, and a leak test was performed before each experiment. Arterioles were pressurized to 60mmHg (45, 46, 59) until the development of stable myogenic tone (% tone = [1-(active lumen diameter/passive lumen diameter)] x 100. Arterioles that generated less than 20% myogenic tone were discarded. The diameter of the arterioles was recorded using MyoView 2.0 software (Danish Myo Technology, Aarhus, Denmark).

2.3.5 **–** Parenchymal Arteriole Vasodilation

Endothelium-dependent vasodilation was assessed after myogenic tone generation by incubating the arterioles with increasing concentrations of the muscarinic receptor agonist carbachol (CCh; 10^{-9}-10^{-5} mol/L) added to the bath. To determine the role played by TRPV4 in PA dilation, arterioles were incubated with the TRPV4 antagonist GSK2193874 (10^{-7}mol/L) for 10min after the development of stable myogenic tone, then CCh-induced dilation (10^{-9}-10^{-5}mol/L) was assessed. A separate group of PAs were incubated with increasing concentrations of the TRPV4 agonist GSK1016790A (10^{-9}-10^{-5} mol/L). To evaluate the role of IK_{Ca}/SK_{Ca} channels in PA dilation, arterioles were incubated with increasing concentrations of the agonist NS309 (10^{-9}-10^{-5}mol/L) in the bath.

2.3.6 – TRPV4 Channels in Myogenic Tone

To assess the role of TRPV4 specifically in endothelial cells in the maintenance of myogenic tone, the endothelium of PAs from SHRSPs was removed by passing an air bubble through the lumen of the arteriole. The PAs were then pressurized, and after the development of stable myogenic tone, we confirmed endothelium denudation by incubating the arterioles with CCh (10^{-4}mol/L) for 10min. Successfully denuded arterioles did not dilate in response to CCh. PAs without endothelium were incubated with 10^{-7}mol/L GSK2193874 for 10min, and changes in myogenic tone maintenance were recorded. At the end of each experiment, Ca^{2+} free buffer containing ethylene glycol tetraacetic acid (EGTA; 29mmol/L) and sodium nitroprusside (SNP; 10^{-5}mol/L) were added to the bath to maximally relax the smooth muscle. Dilation was calculated using the following formula: [lumen diameter at drug concentration – baseline lumen diameter) / (passive lumen diameter – baseline lumen diameter)] x 100.

2.3.7 **–** qRT-PCR

Brain tissue from rats used in pressure myography experiments was saved for qRT-PCR. RNA was extracted from whole brain tissue anterior to the MCA, excluding the olfactory bulb, as well as from rat PAs for qRT-PCR analysis using Trizol. RNA was reverse transcribed using VILO reverse transcriptase (Invitrogen, Carlsbad, CA). TAQMAN-specific probes were used for the PCR to assess the mRNA expression of TRPV4, IK_{Ca}, and SK_{Ca} in pooled PAs (~10 PAs per rat) and tumor necrosis factor alpha (TNF-α), tumor necrosis factor receptor (TNFR1), interleukin 6 (IL-6), synaptophysin (SYP), sortilin-related receptor 1 (SORL1), and amyloid precursor protein (APP) in brain

tissue. mRNA expression is expressed as the fold change from control using the $2^{-\Delta\Delta Ct}$ method. β2-microglobulin was used for normalization.

2.3.8 – Y-Maze

Y-maze was used to assess spatial recognition memory. The Y-maze consists of three identical arms placed at a 120° angle to one another. Unique spatial cues made of colored laboratory tape were placed at the far end of the wall. Each rat received two trials. In the first trial, rats were placed in the maze with one arm of the maze blocked off and were allowed to explore for 5min. The blocked arm was rotated within the testing groups to prevent arm placement bias. After exploration, the rats were placed back in their home cages for a 60min retention time. In the second trial, all three maze arms were accessible, and rats were allowed to explore for 5min. The first 2min of this trial were used to assess spatial recognition memory, and the full 5min were used to assess any locomotor differences between groups. Spatial recognition memory was measured by the percentage of time spent exploring the novel arm and the number of visits to the novel arm. Recordings were tracked and analyzed using EthoVision XT software.

2.3.9 – Immunofluorescence

Brains from the rats used for the pressure myography experiments were also used for microglia and astrocyte analysis. Because the PA studies used arterioles branching off the MCA, brains for immunofluorescence studies were sectioned beginning about 3mm posterior to the MCA, and images were taken from the cortex. Brains were post-fixed in 4% paraformaldehyde for 48hrs, washed in 1x PBS (24hrs each), and stored in 20% sucrose-PBS until sectioned. The brains were sliced into 40μm sections for analysis of the cortex. For microglia quantification, free-floating sections were blocked and

permeabilized in 0.1% Triton X-100 with 10% normal horse serum-PBS for 30min at room temperature, then incubated in 1:200 rabbit anti-ionized Ca^{2+}-binding adapter molecule-1 (IBA-1, PA5-27436, Invitrogen, Rockford, IL) in blocking buffer overnight at 4°C. Sections were washed three times in 1x PBS and then incubated in secondary AlexaFluor 568 donkey anti-rabbit (A10042, Invitrogen, Rockford, IL). For astrocyte analysis, free-floating brain sections were blocked and permeabilized in 0.1% Triton X-100 with 10% normal horse serum-PBS for 30min at room temperature, then incubated in 1:1000 rabbit anti-glial fibrillary acidic protein (GFAP; ab7260, Abcam, Cambridge, MA) in blocking buffer overnight at 4°C. The sections were washed three times in 1x PBS and then incubated for 1hr in secondary AlexaFluor 568 donkey anti-rabbit (A10042, Invitrogen, Rockford, IL). Sections were washed 3 x 5min in 0.1% Tween-20 in 1x PBS, then mounted with Vectashield mounting medium. For each subject, two z-stack images were acquired in each hemisphere of the cortex immediately dorsal to the CA1 region of the hippocampus using a 20x objective coupled to a Zeiss LSM 880 confocal microscope. Iba-1- and GFAP-stained sections were analyzed by FIJI software (ImageJ, NIH). Representative astrocytes from GFAP-stained sections were reconstructed then analyzed using the Simple Neurite Tracer plugin described by others (74). Briefly, z-stack images were loaded into FIJI, and the Simple Neurite Tracer was used to reconstruct individual astrocytes. Morphological analyses include process length and astrocyte volume using the volume filler application. All quantifications and analyses were conducted by an investigator blinded to study groups.

2.3.10 – Plasma Aldosterone

Blood was collected by cardiac puncture prior to euthanasia in anesthetized rats. Plasma aldosterone levels were measured by ELISA (ADI-900-173, Enzo Life Sciences).

2.3.11 – Drugs and Chemicals

GSK1016790A and GSK2193874 were purchased from Cayman Chemicals (Ann Arbor, MI). All other drugs and chemicals are obtained from Sigma Aldrich unless otherwise specified.

2.3.12 – Statistical Analysis

All data are presented as means ± SEM. For analysis of artery vasodilation, two-way analysis of variance with repeated measures in one factor (concentration) was utilized followed by Bonferroni-adjusted t-tests for post-hoc comparisons. All other statistical analyses were assessed by One-Way Analysis of Variance or Kruskal-Wallis if non-parametric testing was required. The Grubb's test was used to identify outliers. All statistical analyses were performed using GraphPad Prism 7.0 software (GraphPad, San Diego, CA). In all cases, statistical significance was denoted by $p<0.05$.

2.4 – Results

2.4.1 – Mineralocorticoid receptor antagonism does not affect blood pressure or cerebral pial artery blood flow in SHRSP

SD rats were chosen as the normotensive control for SHRSP in this study. Plasma aldosterone levels were measured to confirm they fell within expected ranges (SD: 196.5 ± 28.4; SHRSP: 545.8 ± 135; SHRSP + EPL: 775.1 ± 116.5pg/mL; data not shown). These measurements reflect what has been observed by others (8, 15, 20, 38, 44, 55, 77). To confirm the SHRSP were hypertensive compared to SD rats and that EPL

treatment does not alter blood pressure, systolic blood pressure was measured using tail-cuff plethysmography. Systolic blood pressure in SHRSP was significantly higher than controls (Figure 2.1A), and MR antagonism did not lower blood pressure. Hypertension is associated with cerebral hypoperfusion, and MR antagonism rescued blood flow impairments in our previous study (16). Laser speckle contrast imaging was used to measure pial blood flow. SHRSP had a trend toward reduced pial artery perfusion compared to controls (Figure 2.1B; p=0.0633 vs. control by one-way ANOVA). Treatment with EPL did not improve pial artery perfusion.

2.4.2 – Mineralocorticoid receptor antagonism improves impaired endothelium-dependent dilation during hypertension

The role of MR activation in the generation of myogenic tone in PAs was assessed. The PAs from SHRSPs had increased myogenic tone compared to control. MR antagonism did not alter the amount of tone generated by PAs from SHRSP (Figure 2.2A); this confirms our published studies (59). We then assessed endothelium-dependent dilation in response to CCh. The CCh-mediated dilation was impaired in the PAs from SHRSP, which was improved after EPL treatment (Figure 2.2B). TRPV4 antagonism with GSK2193874 (10^{-7}mol/L) inhibited the CCh-induced dilation of PAs from all groups (Figure 2.3A-C), indicating an important role of TRPV4 activation in PA endothelium-dependent dilation in SHRSP and SD rats.

2.4.3 – Mineralocorticoid receptor antagonism improves impaired TRPV4-mediated dilation but does not impact IK_{Ca}/SK_{Ca}-mediated dilation or TRPV4, IK_{Ca}, and SK_{Ca} channel mRNA expression during hypertension

To explore the role of MR signaling in EDH-mediated dilation, we assessed TRPV4-dependent dilation in PAs. The TRPV4 agonist, GSK1016790A, caused a robust dilation in PAs from SD rats (Figure 2.4A). Hypertension impaired the TRPV4-mediated dilation, and EPL treatment improved this response. The influx of Ca^{2+} through TRPV4 triggers the activation of nearby IK_{Ca}/SK_{Ca} channels, producing a K^+ efflux that hyperpolarizes the endothelial cell, ultimately causing vasodilation. To test IK_{Ca}/SK_{Ca}-dependent dilation, PAs were incubated with increasing concentrations of the IK_{Ca}/SK_{Ca} channel agonist NS309 in the bath. At lower concentrations of NS309, SHRSP had impaired IK_{Ca}/SK_{Ca}-mediated dilation compared to SD controls, demonstrated by a greater -logEC50 value in SHRSP +/- EPL compared to controls (control: 8.148±0.54, SHRSP: 6.508±0.10, SHRSP+EPL: 6.389±0.11 logEC50; p=0.009 by one-way ANOVA). This was not improved by MR antagonism (Figure 2.4B); however, the maximum dilation produced in response to NS309 was similar in all groups. We assessed the mRNA expression of TRPV4, IK_{Ca}, and SK_{Ca} channels in isolated PAs using qRT-PCR. Our data suggest that the mRNA expression for TRPV4, IK_{Ca}, and SK_{Ca} was reduced in PAs from SHRSP compared to SD rats, and EPL treatment had no statistically significant effect (Figure 2.4C-E).

2.4.4 – Endothelial TRPV4 activity modulates parenchymal arteriole myogenic tone generation

Our previous studies in AngII-hypertensive mice showed that TRPV4 inhibition with GSK2193874 reduced myogenic tone in the PAs from AngII-treated mice but not normotensive mice (19). The same loss of myogenic tone was observed in the PAs from SHRSP and SHRSP+EPL but not in the normotensive SD rats. To explore if endothelial TRPV4 was involved in the loss of myogenic tone, we removed the endothelium from a group of PAs isolated from SHRSP. When endothelium-denuded PAs were incubated with GSK2193874, there was no loss of myogenic tone, suggesting that endothelial TRPV4 is involved in regulating myogenic tone in SHRSP (Figure 2.5).

2.4.5 – Mineralocorticoid receptor antagonism improves cognitive function in SHRSP

We used the Y-maze to assess the role of MR activation in cognition in SHRSP. SHRSP spent less time in the novel arm of the Y-maze and had fewer total novel arm visits compared to SD rats, indicating impairment of spatial memory (Figure 2.6A, B). Notably, SHRSP traveled less total distance during the testing period than controls. MR antagonism did not alter the total distance traveled by SHRSP, but it improved the total time spent in the novel arm and the number of visits to the novel arm, indicating improvement of spatial memory (Figure 2.6C).

2.4.6 – SHRSP have elevated mRNA expression of proinflammatory markers and increased activated microglia, which are reduced by MR antagonism

We assessed changes in proinflammatory markers in whole brain tissue from the frontal region of the brain. The mRNA expression of the proinflammatory markers TNF-α and its receptor, TNFR1, were significantly increased in SHRSP compared to SD rats,

and these differences were eliminated by EPL treatment (Figure 2.7A, B). IL-6 mRNA expression was also elevated in SHRSP, but this was not significantly reduced by EPL (Figure 2.7C). Next, we used immunofluorescence to quantify and assess the quantity and morphology of cortical microglia labeled with an Iba-1 antibody. SHRSP had more microglia compared to control (Figure 2.7G). The microglia in the SHRSP also had larger somas, suggesting these microglia were in their activated state (Figure 2.7H) (13). EPL treatment did not change the number of microglia but did reduce their soma size.

2.4.7 – Mineralocorticoid receptor antagonism corrects the elevated mRNA expression of markers associated with cognitive dysfunction in SHRSP

We also measured the mRNA expression of proteins involved in cognition. mRNA expression of amyloid precursor protein (APP) and sortilin-related receptor (SORL1), a protein involved in APP processing, were increased in SHRSP compared to control; these differences also were reduced by EPL treatment (Figure 2.7D, E).

2.4.8 – Reactive astrogliosis in SHRSP is reduced with MR antagonism

Astrocytes play a critical role in relaying information between the cerebral vasculature and the neurons and are therefore important in maintaining cognitive function. A GFAP antibody was used to label astrocytes in the cortex near the corpus callosum. SHRSP had more astrocytes compared to control (Figure 2.8B). Astrocytes from SHRSP also had greater soma and process thickness, referred to as astrocyte volume, than control (Figure 2.8C). A greater astrocyte volume indicates that the cells are reactive. MR antagonism reduced the overall number of astrocytes and improved their morphology.

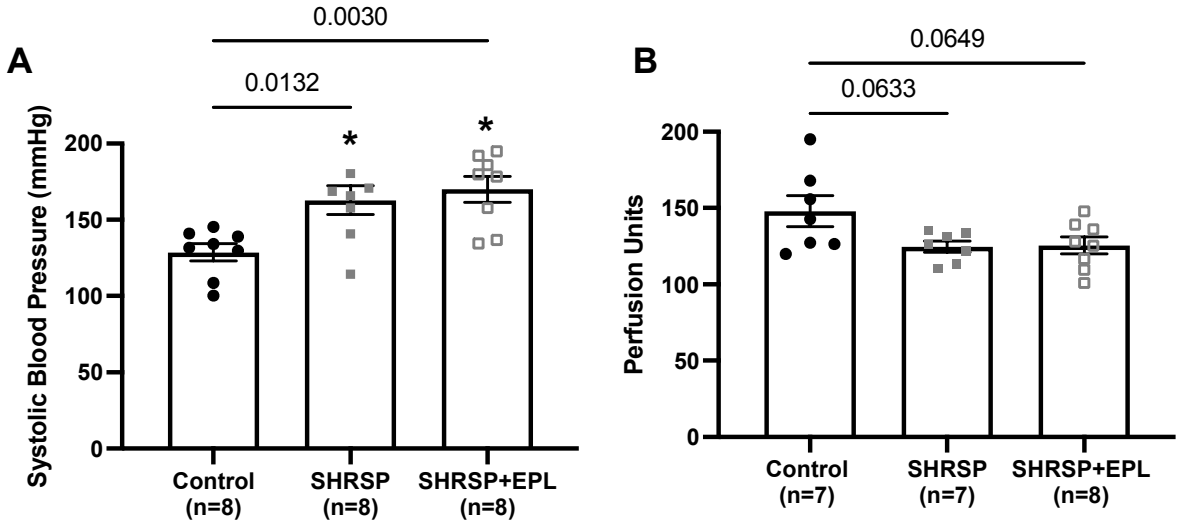

Figure 2.1: Systolic blood pressure is elevated and pial blood flow is reduced in SHRSP compared to control, and this is not changed by MR antagonism. A) Blood pressure in each group was measured by tail-cuff plethysmography. Data are presented as means ± SEM. SHRSP rats had elevated systolic blood pressure compared to SD controls. MR blockade did not affect blood pressure. B) Pial blood flow was measured by laser speckle contrast imaging. SHRSP rats had a trend toward reduced pial blood flow compared to controls (ANOVA p=0.0497). EPL treatment did not improve pial blood flow. *=different from control by one-way ANOVA with Bonferroni correction for multiple comparisons.

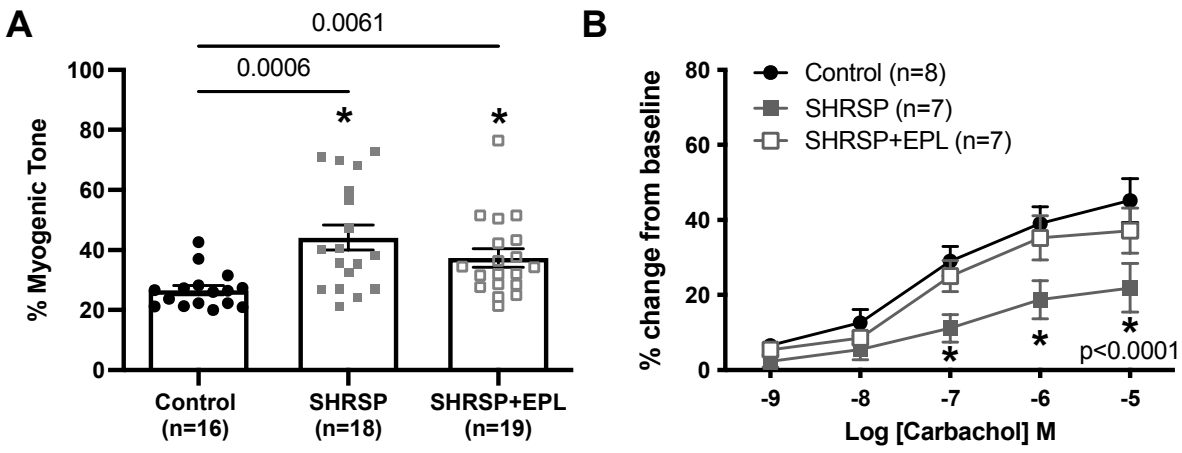

Figure 2.2: MR blockade improves PA endothelium-dependent dilation in rats with essential hypertension. Myogenic tone and endothelium-dependent dilation in isolated PAs were assessed by pressure myography. Data are presented as means ± SEM. A) The PAs from SHRSP had increased myogenic tone and this was not prevented by EPL treatment. B) The CCh-mediated dilation was impaired in SHRSP, and this was prevented by EPL treatment. In Figure 2.2A n= number of vessels from 7-8 rats. *=different from control. Comparisons for Figure 2.2A made by Kruskal-Wallis and for Figure 2.2B by two-way ANOVA.

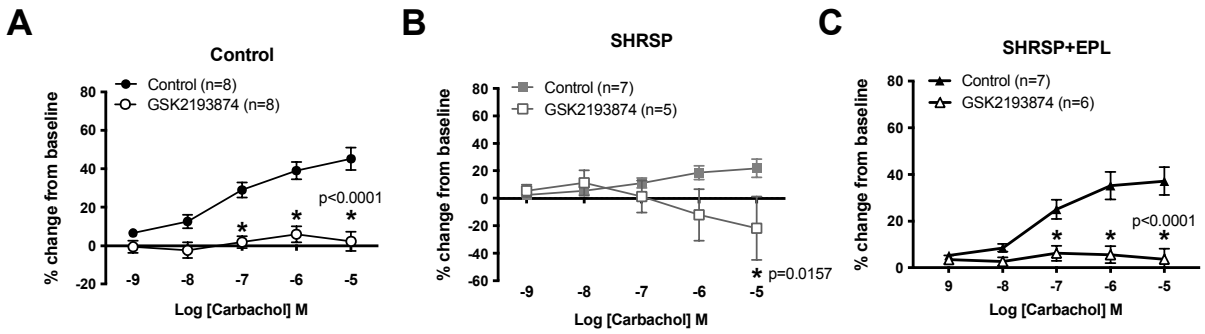

Figure 2.3: TRPV4 channels are critical regulators of PA dilation. The role of TRPV4 in PA endothelium-dependent dilation was assessed by pressure myography. PAs were incubated with the TRPV4 antagonist GSK2193874 for 10 mins after the generation of myogenic tone. Data are presented as means ± SEM. TRPV4 inhibition with GSK2193874 prevented the CCh-mediated dilation in A) Sprague Dawley, B) SHRSP, and C) SHRSP+EPL. *=different from control by two-way ANOVA.

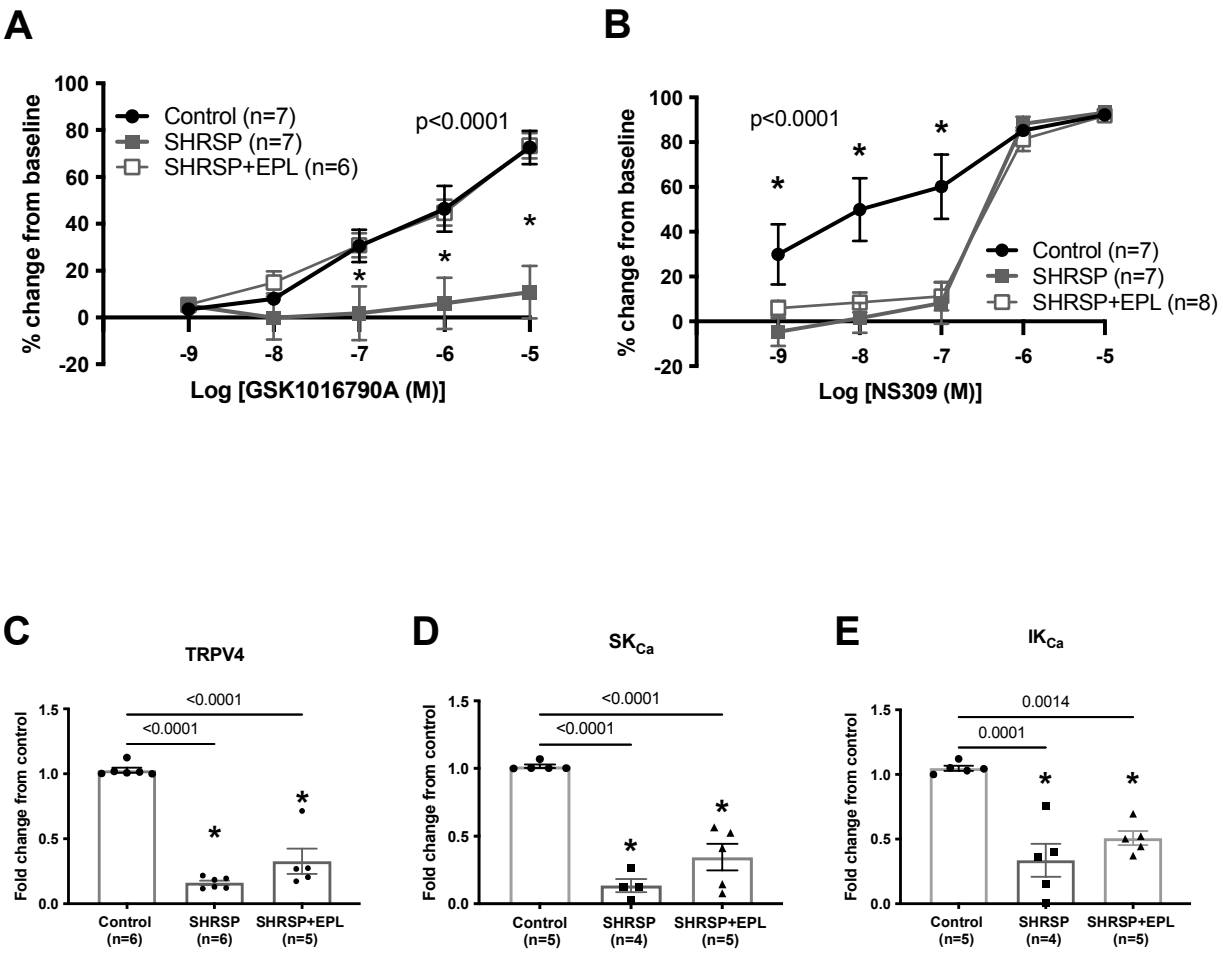

Figure 2.4: MR blockade prevents impaired TRPV4-mediated dilation of PAs, but not reduced mRNA expression of ion channels during hypertension. PA endothelium-dependent dilation mediated by TRPV4 and IK_{Ca}/SK_{Ca} channels was assessed by pressure myography. mRNA expression of these channels was assessed by qRT-PCR. Data are presented as means ± SEM. A) The TRPV4 agonist caused dilation in the PAs from control rats. This dilation was impaired in SHRSP, and impairment was prevented by MR blockade with EPL. B) PA dilation to IK_{Ca}/SK_{Ca} agonist NS309 was impaired in SHRSP compared to controls, which was not improved by MR antagonism with EPL. C-E) The mRNA expression of TRPV4, IK_{Ca} and SK_{Ca} channels was reduced in

Figure 2.4 (cont'd): the PAs from SHRSP; these changes were not prevented by EPL treatment. B2M was used as the housekeeping gene. *=different from control and SHRSP+EPL by two-way ANOVA in Figure 2.4A-B. *=different from control by one-way ANOVA in Figure 2.4C-E.

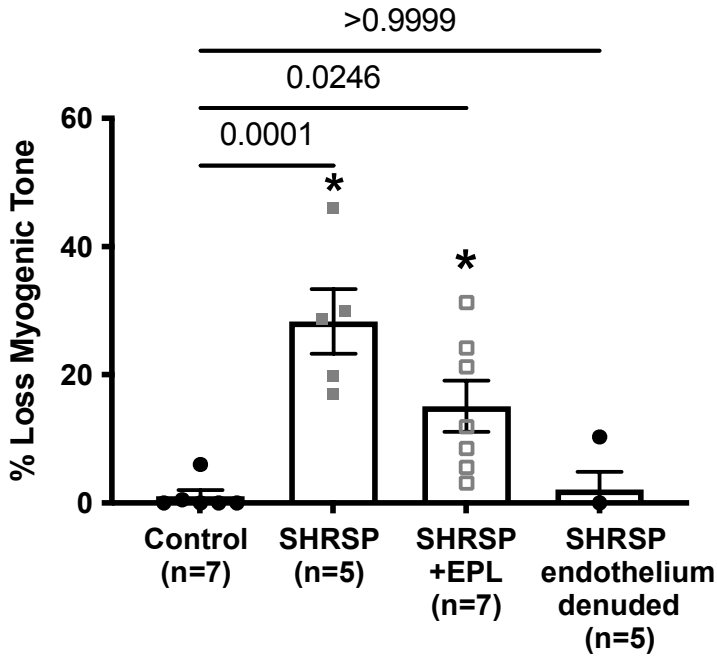

Figure 2.5: Endothelial TRPV4 channel modulate PA myogenic tone generation. The role of TRPV4 channels in myogenic tone generation was assessed by pressure myography. Data are presented as means ± SEM. TRPV4 inhibition with GSK2193874 resulted in a significant loss of myogenic tone in the PAs from SHRSP and SHRSP+EPL, but not in the normotensive controls. Denuding the endothelium of PAs from SHRSPs prevented the loss in myogenic tone after TRPV4 inhibition. *= different from control by one-way ANOVA.

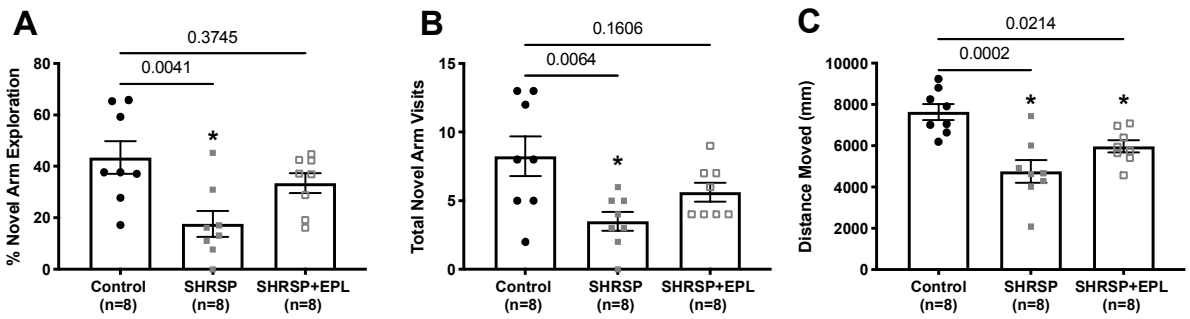

Figure 2.6: SHRSP have impaired spatial memory that is rescued by MR antagonism. The Y-maze was used to measure spatial memory. Data are presented as means ± SEM. (A) SHRSP explored the novel arm in the Y-maze significantly less than controls. EPL treatment improved novel arm exploration. (B) SHRSP had fewer total visits to the novel arm compared to control, which was improved with EPL treatment. *=different from control by one-way ANOVA.

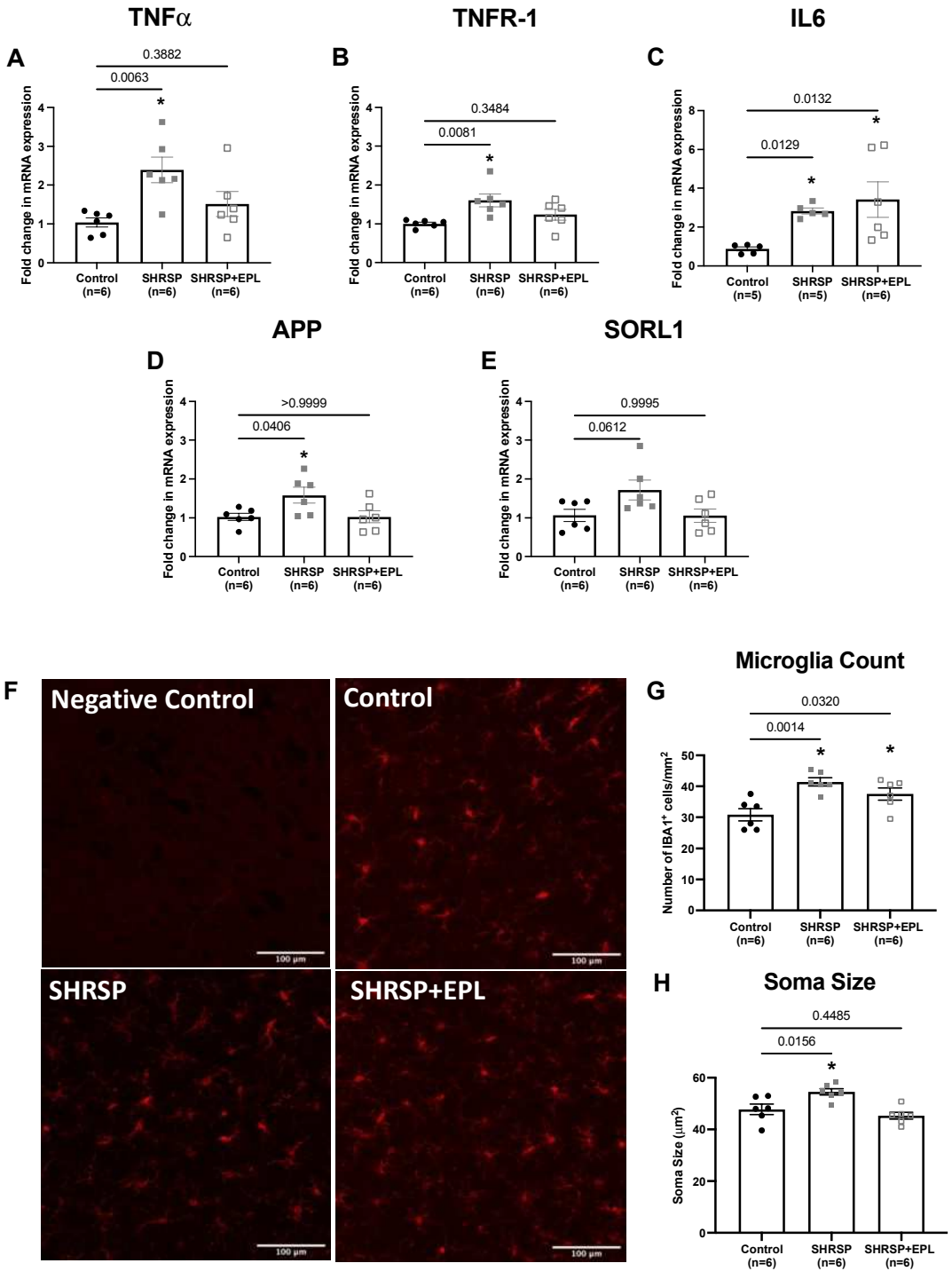

Figure 2.7: MR blockade prevents increased brain mRNA expression of genes associated with neuroinflammation and cognition in hypertension. qRT-PCR was used to measure mRNA expression of genes associated with inflammation and cognitive

Figure 2.7 (cont'd): function. Data are presented as means ± SEM. The brain mRNA expression of the inflammatory markers A) TNF-α and B) its receptor TNFR-1 were elevated in SHRSP compared to control and this was prevented by EPL treatment. C) The inflammatory marker IL-6 was also increased in SHRSP but EPL treatment did not prevent this increase. D) APP mRNA expression was elevated and E) SORL1, a protein involved in APP processing, trended toward an increase in SHRSP (p=0.0612 vs. control). These changes were prevented by MR antagonism. The number of ionized Ca^{2+}-binding adapter molecule 1 (IBA-1)-positive microglia was quantified in the cortex. F) Representative images of IBA-1 staining. G) The number of IBA-1-positive cells was elevated in SHRSP compared to SD controls; this was unchanged by MR antagonism. H) IBA-1-positive cells in the cortex of SHRSP had greater soma sizes compared to SD controls and this was prevented by MR antagonism. Scale bar=100μm *=different from control by one-way ANOVA or Kruskall-Wallis. Abbreviations: TNF-α=tumor necrosis factor α, TNFR1=tumor necrosis factor receptor 1, IL-6=interleukin-6, APP=amyloid precursor protein, SORL1=sortilin-related receptor 1

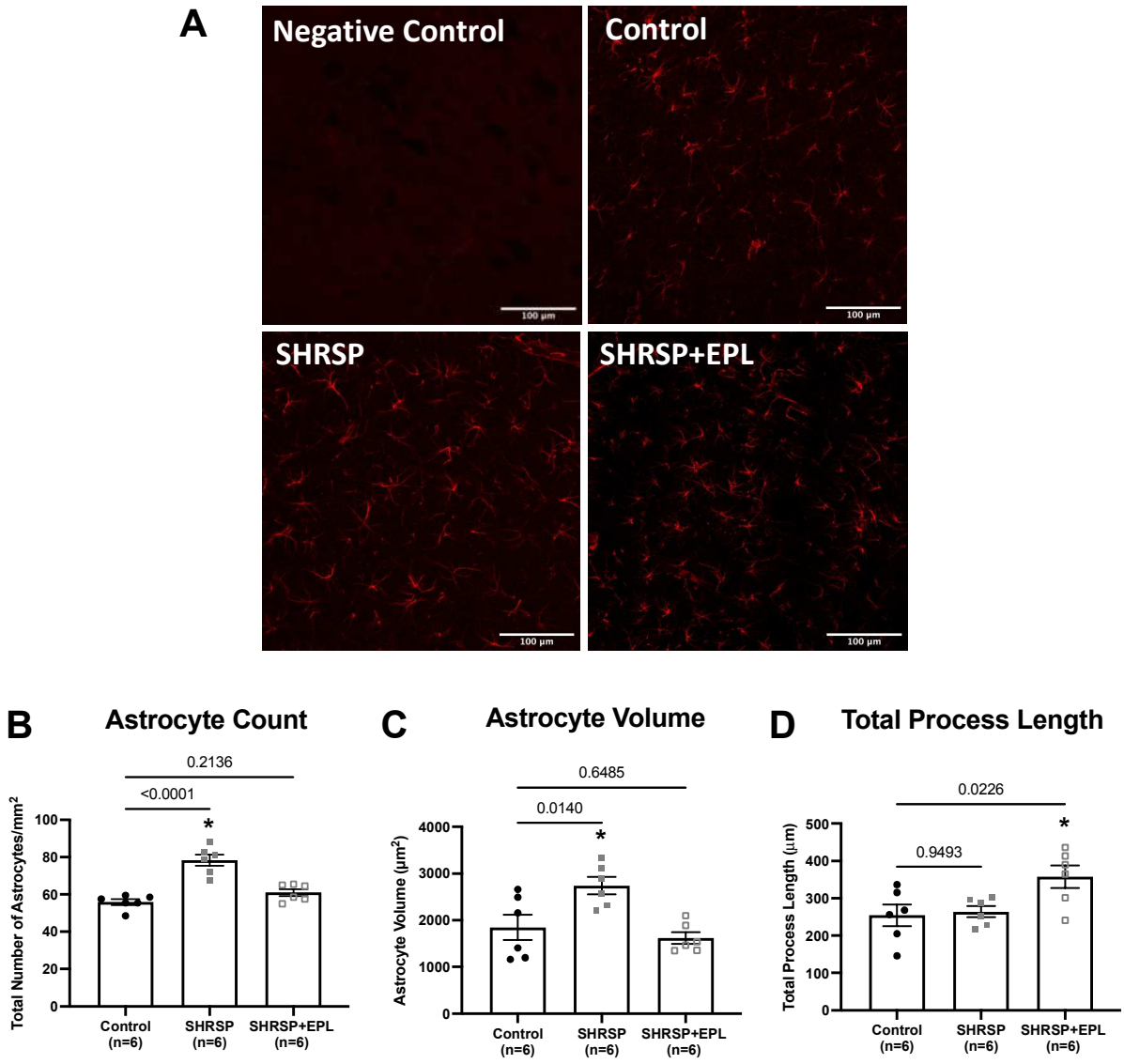

Figure 2.8: MR antagonism prevents astrogliosis observed in SHRSP. The number of glial fibrillary acidic protein (GFAP)-positive astrocytes were quantified in the cortex. Data are presented as means ± SEM A) Representative images of GFAP staining. B) The total number of astrocytes was elevated in the cortex of SHRSP compared to control; this was prevented by EPL treatment. C) Astrocytes in the cortex of SHRSP had increased volume, which was prevented by EPL treatment. D) The total process length of astrocytes

Figure 2.8 (cont'd): in the cortex of SHRSP treated with EPL was elevated compared to control. Scale bar=100μm. *=different from control by one-way ANOVA.

2.5 – Discussion

Our goal was to examine the role of MR activation in cerebral arteriolar function, cognition, and neuroinflammation in a hypertensive model using a clinically relevant treatment paradigm. We used SHRSP to show that: 1) MR activation is involved in the impairment of TRPV4-mediated PA endothelium-dependent dilation observed in hypertension; 2) Endothelial TRPV4 channels modulate myogenic tone during hypertension; 3) MR antagonists, delivered after the onset of hypertension, reduce hypertension-associated cognitive dysfunction, neuroinflammation, and reactive astrogliosis. These new data complement and expand on our previous findings in a mouse model of AngII-hypertension and improve our understanding of the role of vascular MR signaling in cerebral arteriolar and cognitive function. These studies suggest MR antagonists may be an effective pharmacological tool to mitigate the increased risk of vascular cognitive impairment and dementia development associated with hypertension. Hypertension-associated dementia is a significant public health concern. Midlife hypertension significantly increases the risk of dementia later in life, with a 20% increased dementia risk for every 10mmHg of systolic blood pressure elevation (50). The current studies were designed to reflect this temporal development of hypertension with treatment beginning just before midlife in the SHRSP given their shortened life span (42).

MR activation plays a significant role in the development of hypertension; it is estimated that up to 60% of patients with essential hypertension have hyperaldosteronism

(31). Excessive MR activation is associated with endothelial dysfunction and heart failure (7, 43). Elevated MR activation leads to increased inflammation, and oxidative stress is associated with endothelial dysfunction via impaired nitric oxide (NO)-mediated dilation in peripheral arteries (4, 49). Less is known about the molecular mechanisms related to MR-induced cerebrovascular damage, particularly in vessels like the PAs that are not dependent on NO for dilation.

MR activation has been implicated in cerebrovascular injury in two stroke models (21, 63). MR activation also regulates cerebral artery remodeling during hypertension; we have shown that MR antagonism prevents and reverses the inward remodeling of middle cerebral arteries and PAs in SHRSP (59, 61, 62). Using a mouse model of AngII-hypertension, we have shown that MR activation results in impaired cerebral PA dilation, inward hypotrophic remodeling, and reduced cerebral perfusion; these changes were associated with impaired cognitive function (16, 19). Data presented here support the hypothesis that MR antagonism protects against vascular and cognitive dysfunction during hypertension.

Using tail-cuff plethysmography, we confirmed that SHRSP have significantly elevated systolic blood pressure compared to SD rats and that EPL treatment did not affect blood pressure. This mimics our findings from previous studies showing that MR antagonism does not lower blood pressure in AngII-hypertensive mice (16, 19) or SHRSP (59, 61), including one utilizing radiotelemetry, the gold standard for blood pressure measurement (62). Therefore, the effects of MR antagonism presented here are independent of blood pressure.

Cerebral hypoperfusion increases the risk of cognitive impairment and dementia (23, 78). Studies from our lab show that hypertension reduces cerebral pial artery perfusion in AngII-hypertensive mice, and MR antagonism, administered while the hypertension is developing, prevents this (16). We used laser speckle contrast imaging to measure pial blood flow in the current study. We observed that SHRSP had a trend toward reduced pial blood flow compared to controls. The p-value for the one-way ANOVA was p=0.0497, but statistical significance was lost after application of Bonferroni correction for multiple comparisons. In contrast to our previous studies, EPL treatment did not improve pial flow. The difference in these findings could be due to the difference in species and the model of hypertension used. In our previous study using AngII hypertensive mice, the EPL and AngII administration occurred simultaneously. This contrasts with the current study, SHRSP develop hypertension by 6 weeks of age, and EPL treatment did not begin until the rats were 16-18 weeks of age (36). Technical limitations may also have contributed to the lack of an observed effects of EPL. Measurements were made through a closed skull, which significantly reduces the image resolution. The laser penetration for the PeriMed system is 1mm; thus, we were only able to measure flow in the pial arterioles. It is possible that the changes we observed in PA function caused reduced flow in the deeper brain structures; MRI would be required to make these measurements, which is outside the scope of these studies.

PAs play a critical role in regulating cerebrovascular resistance through their ability to generate significant myogenic tone. The myogenic tone in PAs from SHRSP was increased relative to SD rats, and this was not reversed with EPL treatment. We produced similar results in previous studies that utilized WKY rats as controls for SHRSP (59). We

acknowledge these data are at odds with an earlier study showing spironolactone treatment increased myogenic tone in SHRSP (62). That study was conducted in middle cerebral arteries from twelve-week-old rats treated as hypertension developed. The differences in arteries, ages of rats, and treatment regime used are likely behind the observed differences.

Impaired endothelium-dependent dilation in cerebral arteries and arterioles from SHRSP has been reported by others (47, 58, 80). In keeping with our hypothesis, PAs from SHRSP exhibited impaired endothelium-dependent CCh-mediated dilation, which was improved with EPL treatment. In all three experimental groups, PA dilation to CCh was prevented when TRPV4 was blocked with GSK2193874, supporting our previous findings that endothelium-dependent dilation in PAs is TRPV4 dependent (18, 19, 45). It is important to note that other groups have proposed that NO also contributes to dilation in PAs (14). While we cannot explain the differences in our findings, we acknowledge the possibility that EPL treatment improved dilation through a NO-mediated mechanism. Thus, we used a specific TRPV4 agonist (GSK1016790A) to further examine the impact of MR activation in TRPV4-mediated dilation. PAs from SHRSP had markedly impaired TRPV4-mediated dilation, which was reversed by EPL treatment.

TRPV4 activation in endothelial cells produces a Ca^{2+} influx that activates IK_{Ca}/SK_{Ca} channels, producing K^+ efflux and hyperpolarization (24, 25, 29). This EDH crosses to smooth muscle cells via myoendothelial gap junctions to hyperpolarize the smooth muscle cells and produce vasodilation. We used the IK_{Ca}/SK_{Ca} agonist NS309 to assess dilation via EDH, which is downstream of TRPV4 activation. While NS309 is an agonist for both IK_{Ca} and SK_{Ca} channels, IK_{Ca} channels are the predominate channels influencing

dilation in PAs (10). The EC50 values suggest the PAs from SHRSP were less sensitive to the effects of NS309. However, the maximum dilation in response to high concentrations of NS309 was similar across the groups. This finding is reflected in our qRT-PCR data from PAs showing that SHRSP +/- EPL had similarly reduced mRNA expression of these Ca^{2+}-activated K^+ channels compared to controls, suggesting the difference in IK_{Ca}/SK_{Ca}-mediated dilation is due to hypertension and is not an MR-mediated event.

We also found that TRPV4 mRNA expression is reduced in SHRSP +/- EPL compared to control, despite improvement in TRPV4-mediated dilation. While we did not measure protein expression in the present study, studies using mesenteric arteries from SHRSP have shown reduced protein levels of TRPV4 (67). Taken together, these data present the possibility that in untreated SHRSP, TRPV4-mediated dilation is impaired at the level of functionality rather than protein expression. Endothelial TRPV4 channels are localized to myoendothelial projections by A-kinase anchoring protein 150 (AKAP150), ensuring their proximity to IK_{Ca}/SK_{Ca} channels. A previous study found that the interaction between TRPV4 and AKAP150 is dysregulated during hypertension (71). EPL treatment may improve the cooperative gating between TRPV4 and AKAP150 to maintain channel function. The lack of an effect of EPL on TRPV4 mRNA expression is at odds with our previous studies in AngII-hypertensive mice that showed that EPL treatment prevented changes in TRPV4 mRNA expression. This could be explained by differences in the rodent and hypertension models used. However, it is also possible that the differences in treatment paradigms, as described previously, are also significant. It is also worth mentioning that a previous study from our group did not identify a role for the MR in the

dilation of PAs from SHRSP (59). However, we used nifedipine, an L-type calcium channel blocker, in that study to measure the dilatory response. L-type calcium channels are the primary source of calcium influx during myogenic tone generation (1). Directly blocking these channels produces a robust dilation that is not endothelium dependent.

We previously showed that TRPV4 activation modulates myogenic tone generation in hypertensive mice, and this effect is not modulated by MR activation (19). The same was true in the current studies. TRPV4 inhibition resulted in a loss of myogenic tone in the PAs from SHRSP. The loss of tone was not observed when the endothelium of the arterioles was removed, suggesting endothelial TRPV4 channels are responsible for the effect. This presents the possibility that under pathological conditions, TRPV4 activates other signaling pathways such as cytosolic phospholipase A_2 ($cPLA_2$) to modulate vascular tone (81). However, the mechanisms for the actions of endothelial TRPV4 in myogenic tone maintenance remain to be explored.

Cerebrovascular dysfunction in hypertension is associated with vascular cognitive impairment and dementia development (2, 56, 66). Our previous studies in AngII-hypertensive mice demonstrated that hypertension is associated with cognitive decline that was prevented by MR antagonism (19). In this study, we used the novel arm Y-maze to identify impairments in spatial recognition memory. This test uses the innate characteristic of rats to preferentially explore novel areas (39). During the probe trial, SHRSP explored the novel arm significantly less than the control group, and this was improved with EPL treatment. Further, SHRSP had fewer total visits to the novel arm, which was enhanced with EPL. Notably, there was a difference in the total distance traveled between SD controls and SHRSP +/- EPL treatment, with SDs traveling more

than SHRSP groups. While EPL treatment improved the exploration time and visitation frequency of SHRSP in the novel arm, it did not impact the total distance traveled. Therefore, it is unlikely that differences in distance traveled played a role in the cognitive improvement in the EPL group. These data indicate that MR antagonism improves PA function during hypertension and prevents the cognitive impairment that occurs alongside vascular dysfunction.

MR activation has been linked to increased inflammation, which, in turn, contributes to hypertension-associated cognitive decline and cerebral small vessel disease (27, 28, 32). In the current study, we showed that the mRNA expression of TNF-α and its receptor, TNFR-1, were significantly increased in the brain from SHRSP, and these differences were reduced with EPL treatment. Others have shown that MR antagonism decreases plasma TNF-α in SDs with heart failure (26, 35), but to the best of our knowledge, we are the first to show a role for the MR in regulating the expression of TNF-α and its receptor in brain tissue from SHRSP. IL-6 expression was also elevated in SHRSP; however, this was not improved with EPL treatment. Using immunofluorescence, we showed that SHRSP had more microglia in the cerebral cortex than control. Others have identified a role for the MR in regulating microglia polarity; microglia from mice with myeloid cell-specific MR deletion favored M2 polarity compared to control, indicating MR activation is associated with the inflammatory properties of microglia (52). It should be noted that these studies were conducted in animals undergoing an experimental model of multiple sclerosis. Thus, the microglia were activated by inflammation associated with autoimmunity. Our data suggest increased inflammation in hypertension has a similar effect on cortical microglia. Microglia from SHRSP had an increased average soma size,

indicating a preference for the inflammatory M1 polarity. EPL treatment reduced microglial activation, indicating less neuroinflammation in the EPL-treated group; however, EPL treatment did not impact microglia proliferation in SHRSP.

The presence of extracellular β-amyloid plaque deposits is a requirement for diagnosing Alzheimer's disease (53). Hypertension has been found to exacerbate cognitive dysfunction associated with β-amyloid plaque deposition in humans (11) and rodents (9, 12, 30) and is also associated with greater plaque accumulation (33). β-amyloid is a product of its precursor protein, APP, which is processed by both amyloidogenic and non-amyloidogenic pathways. While deposition of β-amyloid plaques is uncommon in rats, especially those within the age range studied here (6), we observed an increase in the expression of the mRNA for APP, which was reversed by EPL treatment. Increased expression of SORL1, a protein involved in several pathways of APP proteolytic processing, was also observed in SHRSP; this also was corrected by EPL treatment. Mutation or dysfunction of SORL1 is a possible contributor to β-amyloid plaque deposition (3, 64). At present, it is unclear if the elevated mRNA expression of APP in SHRSP is directly associated with cognitive impairment in this group. Our data suggest that APP expression is modulated by MR activity, but additional experiments are necessary to determine which pathways of APP processing are active in SHRSP and if this plays a role in cognitive function.

Astrocyte numbers and morphology were assessed by GFAP staining in the cortex. Astrocytes have classically been considered to relay information from neurons to arterioles. However, a novel role for these cells has recently been established, showing bi-directional communication extending from arterioles to neurons (37). Reactive

astrogliosis is observed during increased neuroinflammation and hypertension (57, 60). SHRSP had more cortical astrocytes than control and had astrocytes with increased soma and process volume, which is indicative of astrogliosis. These differences were prevented by MR blockade. SHRSP did not have an elevated summed process length in these astrocytes, but EPL treatment in SHRSP did increase the process length of the astrocytes compared to control. Increased total process length of the astrocytes could enhance connections between PAs and neurons, potentially improving cognitive function during hypertension.

Some limitations in our study must be acknowledged. First, all our studies were conducted in male rats to expand our previous findings to a new model; thus, exploring possible sex differences is outside the scope of the current study, but we will consider this in future studies. In the future, we should also identify the cell-specific actions of MR signaling in PA myogenic tone and vasodilation. It is important to acknowledge the disagreement in the data presented in this paper; EPL treatment improves endothelium-dependent dilation yet does not improve cerebral pial blood flow in SHRSP. The conflict observed here is due to the difference in the areas of the vasculature examined. While PAs dive deeply into the brain, the laser speckle contrast imager can only measure blood flow through the surface arteries and arterioles. In the future, it would be beneficial to analyze blood flow alterations in the hippocampal region to accompany our PA studies; however, this is not possible at present.

In summary, our data confirm the key findings from a previous study in a model of human essential hypertension. PAs are important for the development of cerebral small vessel disease, and we show that MR activation impairs the TRPV4-mediated

dilation of PAs during hypertension. TRPV4 may be a critical determinant of the hypertension-associated changes in cerebral arteriolar function. Endothelial TRPV4 channels are modulators of myogenic tone generation and maintenance in the PAs during hypertension. Impairment of vasodilation and alterations in myogenic tone may reduce cerebral blood flow during hypertension and increase the risk of cognitive decline and neuroinflammation in cerebrovascular disease.

REFERENCES

1. **Abd El-Rahman RR**, **Harraz OF**, **Brett SE**, **Anfinogenova Y**, **Mufti RE**, **Goldman D**, **Welsh DG**. Identification of L- and T-type Ca2+ channels in rat cerebral arteries: role in myogenic tone development. *Am J Physiol Heart Circ Physiol* 304: H58-71, 2013. doi: 10.1152/ajpheart.00476.2012.

2. **Azarpazhooh MR**, **Hachinski V**. Vascular cognitive impairment: A preventable component of dementia. *Handb Clin Neurol* 167: 377–391, 2019. doi: 10.1016/B978-0-12-804766-8.00020-0.

3. **Barthelson K**, **Newman M**, **Lardelli M**. Sorting Out the Role of the Sortilin-Related Receptor 1 in Alzheimer's Disease. *J Alzheimers Dis Rep* 4: 123–140, 2020. doi: 10.3233/ADR-200177.

4. **Bauersachs J**, **Jaisser F**, **Toto R**. Mineralocorticoid receptor activation and mineralocorticoid receptor antagonist treatment in cardiac and renal diseases. *Hypertension* 65: 257–263, 2015. doi: 10.1161/HYPERTENSIONAHA.114.04488.

5. **Benedictus MR**, **Leeuwis AE**, **Binnewijzend MAA**, **Kuijer JPA**, **Scheltens P**, **Barkhof F**, **van der Flier WM**, **Prins ND**. Lower cerebral blood flow is associated with faster cognitive decline in Alzheimer's disease. *Eur Radiol* 27: 1169–1175, 2017. doi: 10.1007/s00330-016-4450-z.

6. **Bueche CZ**, **Hawkes C**, **Garz C**, **Vielhaber S**, **Attems J**, **Knight RT**, **Reymann K**, **Heinze H-J**, **Carare RO**, **Schreiber S**. Hypertension drives parenchymal β-amyloid accumulation in the brain parenchyma. *Ann Clin Transl Neurol* 1: 124–129, 2014. doi: 10.1002/acn3.27.

7. **Cachofeiro V**, **Miana M**, **de Las Heras N**, **Martín-Fernández B**, **Ballesteros S**, **Fernández-Tresguerres J**, **Lahera V**. Aldosterone and the vascular system. *J Steroid Biochem Mol Biol* 109: 331–335, 2008. doi: 10.1016/j.jsbmb.2008.03.005.

8. **Chander PN**, **Rocha R**, **Ranaudo J**, **Singh G**, **Zuckerman A**, **Stier CT**. Aldosterone plays a pivotal role in the pathogenesis of thrombotic microangiopathy in SHRSP. *J Am Soc Nephrol* 14: 1990–1997, 2003. doi: 10.1097/01.asn.0000078960.15147.05.

9. **Cifuentes D**, **Poittevin M**, **Dere E**, **Broquères-You D**, **Bonnin P**, **Benessiano J**, **Pocard M**, **Mariani J**, **Kubis N**, **Merkulova-Rainon T**, **Lévy BI**. Hypertension accelerates the progression of Alzheimer-like pathology in a mouse model of the disease. *Hypertension* 65: 218–224, 2015. doi: 10.1161/HYPERTENSIONAHA.114.04139.

10. **Cipolla MJ**, **Smith J**, **Kohlmeyer MM**, **Godfrey JA**. SKCa and IKCa Channels, myogenic tone, and vasodilator responses in middle cerebral arteries and

parenchymal arterioles: effect of ischemia and reperfusion. *Stroke* 40: 1451–1457, 2009. doi: 10.1161/STROKEAHA.108.535435.

11. **Clark LR**, **Koscik RL**, **Allison SL**, **Berman SE**, **Norton D**, **Carlsson CM**, **Betthauser TJ**, **Bendlin BB**, **Christian BT**, **Chin NA**, **Asthana S**, **Johnson SC**. Hypertension and obesity moderate the relationship between β-amyloid and cognitive decline in midlife. *Alzheimers Dement* 15: 418–428, 2019. doi: 10.1016/j.jalz.2018.09.008.

12. **Csiszar A**, **Tucsek Z**, **Toth P**, **Sosnowska D**, **Gautam T**, **Koller A**, **Deak F**, **Sonntag WE**, **Ungvari Z**. Synergistic effects of hypertension and aging on cognitive function and hippocampal expression of genes involved in β-amyloid generation and Alzheimer's disease. *Am J Physiol Heart Circ Physiol* 305: H1120-30, 2013. doi: 10.1152/ajpheart.00288.2013.

13. **Davis BM**, **Salinas-Navarro M**, **Cordeiro MF**, **Moons L**, **De Groef L**. Characterizing microglia activation: a spatial statistics approach to maximize information extraction. *Sci Rep* 7: 1576, 2017. doi: 10.1038/s41598-017-01747-8.

14. **De Silva TM**, **Modrick ML**, **Dabertrand F**, **Faraci FM**. Changes in cerebral arteries and parenchymal arterioles with aging: role of rho kinase 2 and impact of genetic background. *Hypertension* 71: 921–927, 2018. doi: 10.1161/HYPERTENSIONAHA.118.10865.

15. **Dhar I**, **Dhar A**, **Wu L**, **Desai KM**. Methylglyoxal, a reactive glucose metabolite, increases renin angiotensin aldosterone and blood pressure in male Sprague-Dawley rats. *Am J Hypertens* 27: 308–316, 2014. doi: 10.1093/ajh/hpt281.

16. **Diaz-Otero JM**, **Fisher C**, **Downs K**, **Moss EM**, **Jaffe IZ**, **Jackson WF**, **Dorrance AM**. Endothelial Mineralocorticoid Receptor Mediates Parenchymal Arteriole and Posterior Cerebral Artery Remodeling During Angiotensin II–Induced Hypertension. .

17. **Diaz-Otero JM**, **Garver H**, **Fink GD**, **Jackson WF**, **Dorrance AM**. Aging is associated with changes to the biomechanical properties of the posterior cerebral artery and parenchymal arterioles. *Am J Physiol Heart Circ Physiol* 310: H365-75, 2016. doi: 10.1152/ajpheart.00562.2015.

18. **Diaz-Otero JM**, **Yen T-C**, **Ahmad A**, **Laimon-Thomson E**, **Abolibdeh B**, **Kelly K**, **Lewis MT**, **Wiseman RW**, **Jackson WF**, **Dorrance AM**. Transient receptor potential vanilloid 4 channels are important regulators of parenchymal arteriole dilation and cognitive function. *Microcirculation* 26: e12535, 2019. doi: 10.1111/micc.12535.

19. **Diaz-Otero JM**, **Yen T-C**, **Fisher C**, **Bota D**, **Jackson WF**, **Dorrance AM**. Mineralocorticoid receptor antagonism improves parenchymal arteriole dilation via

a TRPV4-dependent mechanism and prevents cognitive dysfunction in hypertension. *Am J Physiol Heart Circ Physiol* 315: H1304–H1315, 2018. doi: 10.1152/ajpheart.00207.2018.

20. **Dizaye K**, **Mustafa ZA**. The effect of eplerenone on the renin-angiotensin-aldosterone system of rats with thyroid dysfunction. *J Pharm Pharmacol* 71: 1800–1808, 2019. doi: 10.1111/jphp.13168.

21. **Dorrance AM**, **Osborn HL**, **Grekin R**, **Webb RC**. Spironolactone reduces cerebral infarct size and EGF-receptor mRNA in stroke-prone rats. *Am J Physiol Regul Integr Comp Physiol* 281: R944-50, 2001. doi: 10.1152/ajpregu.2001.281.3.R944.

22. **Dorrance AM**, **Rupp NC**, **Nogueira EF**. Mineralocorticoid receptor activation causes cerebral vessel remodeling and exacerbates the damage caused by cerebral ischemia. *Hypertension* 47: 590–595, 2006. doi: 10.1161/01.HYP.0000196945.73586.0d.

23. **Duncombe J**, **Kitamura A**, **Hase Y**, **Ihara M**, **Kalaria RN**, **Horsburgh K**. Chronic cerebral hypoperfusion: a key mechanism leading to vascular cognitive impairment and dementia. Closing the translational gap between rodent models and human vascular cognitive impairment and dementia. *Clin Sci* 131: 2451–2468, 2017. doi: 10.1042/CS20160727.

24. **Ellinsworth DC**, **Earley S**, **Murphy TV**, **Sandow SL**. Endothelial control of vasodilation: integration of myoendothelial microdomain signalling and modulation by epoxyeicosatrienoic acids. *Pflugers Arch* 466: 389–405, 2014. doi: 10.1007/s00424-013-1303-3.

25. **Félétou M**. Endothelium-Dependent Hyperpolarization and Endothelial Dysfunction. *J Cardiovasc Pharmacol* 67: 373–387, 2016. doi: 10.1097/FJC.0000000000000346.

26. **Francis J**, **Weiss RM**, **Johnson AK**, **Felder RB**. Central mineralocorticoid receptor blockade decreases plasma TNF-alpha after coronary artery ligation in rats. *Am J Physiol Regul Integr Comp Physiol* 284: R328-35, 2003. doi: 10.1152/ajpregu.00376.2002.

27. **Funder JW**. Aldosterone and Mineralocorticoid Receptors-Physiology and Pathophysiology. *Int J Mol Sci* 18, 2017. doi: 10.3390/ijms18051032.

28. **Fu Y**, **Yan Y**. Emerging role of immunity in cerebral small vessel disease. *Front Immunol* 9: 67, 2018. doi: 10.3389/fimmu.2018.00067.

29. **Garland CJ**, **Dora KA**. EDH: endothelium-dependent hyperpolarization and microvascular signalling. *Acta Physiol (Oxf)* 219: 152–161, 2017. doi: 10.1111/apha.12649.

30. **Gentile MT**, **Poulet R**, **Di Pardo A**, **Cifelli G**, **Maffei A**, **Vecchione C**, **Passarelli F**, **Landolfi A**, **Carullo P**, **Lembo G**. Beta-amyloid deposition in brain is enhanced in mouse models of arterial hypertension. *Neurobiol Aging* 30: 222–228, 2009. doi: 10.1016/j.neurobiolaging.2007.06.005.

31. **Hundemer GL**, **Kline GA**, **Leung AA**. How common is primary aldosteronism? *Curr Opin Nephrol Hypertens* 30: 353–360, 2021. doi: 10.1097/MNH.0000000000000702.

32. **Iadecola C**, **Gottesman RF**. Neurovascular and cognitive dysfunction in hypertension. *Circ Res* 124: 1025–1044, 2019. doi: 10.1161/CIRCRESAHA.118.313260.

33. **Jeon SY**, **Byun MS**, **Yi D**, **Lee JH**, **Choe YM**, **Ko K**, **Sohn BK**, **Choi HJ**, **Lee J-Y**, **Lee DY**, **KBASE Research Group**. Influence of hypertension on brain amyloid deposition and Alzheimer's disease signature neurodegeneration. *Neurobiol Aging* 75: 62–70, 2019. doi: 10.1016/j.neurobiolaging.2018.11.001.

34. **Johnson AC**, **Miller JE**, **Cipolla MJ**. Memory impairment in spontaneously hypertensive rats is associated with hippocampal hypoperfusion and hippocampal vascular dysfunction. .

35. **Kang Y-M**, **Zhang Z-H**, **Johnson RF**, **Yu Y**, **Beltz T**, **Johnson AK**, **Weiss RM**, **Felder RB**. Novel effect of mineralocorticoid receptor antagonism to reduce proinflammatory cytokines and hypothalamic activation in rats with ischemia-induced heart failure. *Circ Res* 99: 758–766, 2006. doi: 10.1161/01.RES.0000244092.95152.86.

36. **Kato N**, **Nabika T**, **Liang Y-Q**, **Mashimo T**, **Inomata H**, **Watanabe T**, **Yanai K**, **Yamori Y**, **Yazaki Y**, **Sasazuki T**. Isolation of a chromosome 1 region affecting blood pressure and vascular disease traits in the stroke-prone rat model. *Hypertension* 42: 1191–1197, 2003. doi: 10.1161/01.HYP.0000103161.27190.67.

37. **Kim KJ**, **Ramiro Diaz J**, **Iddings JA**, **Filosa JA**. Vasculo-Neuronal Coupling: Retrograde Vascular Communication to Brain Neurons. *J Neurosci* 36: 12624–12639, 2016. doi: 10.1523/JNEUROSCI.1300-16.2016.

38. **Kim S**, **Tokuyama M**, **Hosoi M**, **Yamamoto K**. Adrenal and circulating renin-angiotensin system in stroke-prone hypertensive rats. *Hypertension* 20: 280–291, 1992. doi: 10.1161/01.hyp.20.3.280.

39. **Kraeuter A-K**, **Guest PC**, **Sarnyai Z**. The Y-Maze for Assessment of Spatial Working and Reference Memory in Mice. *Methods Mol Biol* 1916: 105–111, 2019. doi: 10.1007/978-1-4939-8994-2_10.

40. **Kurtz TW**, **Morris RC**. Biological variability in Wistar-Kyoto rats. Implications for research with the spontaneously hypertensive rat. *Hypertension* 10: 127–131, 1987. doi: 10.1161/01.hyp.10.1.127.

41. **Lemos JC**, **Zhang G**, **Walsh T**, **Kirby LG**, **Akanwa A**, **Brooks-Kayal A**, **Beck SG**. Stress-hyperresponsive WKY rats demonstrate depressed dorsal raphe neuronal excitability and dysregulated CRF-mediated responses. *Neuropsychopharmacology* 36: 721–734, 2011. doi: 10.1038/npp.2010.200.

42. **Linz W**, **Jessen T**, **Becker RH**, **Schölkens BA**, **Wiemer G**. Long-term ACE inhibition doubles lifespan of hypertensive rats. *Circulation* 96: 3164–3172, 1997. doi: 10.1161/01.cir.96.9.3164.

43. **Marney AM**, **Brown NJ**. Aldosterone and end-organ damage. *Clin Sci* 113: 267–278, 2007. doi: 10.1042/CS20070123.

44. **Masineni SN**, **Chander PN**, **Singh GD**, **Powers CA**, **Stier CT**. Male gender and not the severity of hypertension is associated with end-organ damage in aged stroke-prone spontaneously hypertensive rats. *Am J Hypertens* 18: 878–884, 2005. doi: 10.1016/j.amjhyper.2004.12.014.

45. **Matin N**, **Fisher C**, **Jackson WF**, **Diaz-Otero JM**, **Dorrance AM**. Carotid artery stenosis in hypertensive rats impairs dilatory pathways in parenchymal arterioles. *Am J Physiol Heart Circ Physiol* 314: H122–H130, 2018. doi: 10.1152/ajpheart.00638.2016.

46. **Matin N**, **Fisher C**, **Jackson WF**, **Dorrance AM**. Bilateral common carotid artery stenosis in normotensive rats impairs endothelium-dependent dilation of parenchymal arterioles. *Am J Physiol Heart Circ Physiol* 310: H1321-9, 2016. doi: 10.1152/ajpheart.00890.2015.

47. **Mayhan WG**, **Faraci FM**, **Heistad DD**. Impairment of endothelium-dependent responses of cerebral arterioles in chronic hypertension. *Am J Physiol* 253: H1435-40, 1987. doi: 10.1152/ajpheart.1987.253.6.H1435.

48. **McClain JL**, **Dorrance AM**. Temporary mineralocorticoid receptor antagonism during the development of hypertension improves cerebral artery dilation. *Exp Biol Med (Maywood)* 239: 619–627, 2014. doi: 10.1177/1535370214522586.

49. **McCurley A**, **Jaffe IZ**. Mineralocorticoid receptors in vascular function and disease. *Mol Cell Endocrinol* 350: 256–265, 2012. doi: 10.1016/j.mce.2011.06.014.

50. **McGrath ER**, **Beiser AS**, **DeCarli C**, **Plourde KL**, **Vasan RS**, **Greenberg SM**, **Seshadri S**. Blood pressure from mid- to late life and risk of incident dementia. *Neurology* 89: 2447–2454, 2017. doi: 10.1212/WNL.0000000000004741.

51. **Meyer JS**, **Rauch G**, **Rauch RA**, **Haque A**. Risk factors for cerebral hypoperfusion, mild cognitive impairment, and dementia. *Neurobiol Aging* 21: 161–169, 2000. doi: 10.1016/s0197-4580(00)00136-6.

52. **Montes-Cobos E**, **Schweingruber N**, **Li X**, **Fischer HJ**, **Reichardt HM**, **Lühder F**. Deletion of the mineralocorticoid receptor in myeloid cells attenuates central nervous system autoimmunity. *Front Immunol* 8: 1319, 2017. doi: 10.3389/fimmu.2017.01319.

53. **Murphy MP**, **LeVine H**. Alzheimer's disease and the amyloid-beta peptide. *J Alzheimers Dis* 19: 311–323, 2010. doi: 10.3233/JAD-2010-1221.

54. **Nam H**, **Clinton SM**, **Jackson NL**, **Kerman IA**. Learned helplessness and social avoidance in the Wistar-Kyoto rat. *Front Behav Neurosci* 8: 109, 2014. doi: 10.3389/fnbeh.2014.00109.

55. **Northcott CA**, **Fink GD**, **Garver H**, **Haywood JR**, **Laimon-Thomson EL**, **McClain JL**, **Pires PW**, **Rainey WE**, **Rigsby CS**, **Dorrance AM**. The development of hypertension and hyperaldosteronism in a rodent model of life-long obesity. *Endocrinology* 153: 1764–1773, 2012. doi: 10.1210/en.2011-1176.

56. **Paglieri C**, **Bisbocci D**, **Caserta M**, **Rabbia F**, **Bertello C**, **Canadè A**, **Veglio F**. Hypertension and cognitive function. *Clin Exp Hypertens* 30: 701–710, 2008. doi: 10.1080/10641960802563584.

57. **Pekny M**, **Pekna M**. Astrocyte reactivity and reactive astrogliosis: costs and benefits. *Physiol Rev* 94: 1077–1098, 2014. doi: 10.1152/physrev.00041.2013.

58. **Pires PW**, **Girgla SS**, **McClain JL**, **Kaminski NE**, **van Rooijen N**, **Dorrance AM**. Improvement in middle cerebral artery structure and endothelial function in stroke-prone spontaneously hypertensive rats after macrophage depletion. *Microcirculation* 20: 650–661, 2013. doi: 10.1111/micc.12064.

59. **Pires PW**, **Jackson WF**, **Dorrance AM**. Regulation of myogenic tone and structure of parenchymal arterioles by hypertension and the mineralocorticoid receptor. *Am J Physiol Heart Circ Physiol* 309: H127-36, 2015. doi: 10.1152/ajpheart.00168.2015.

60. **Price BR**, **Norris CM**, **Sompol P**, **Wilcock DM**. An emerging role of astrocytes in vascular contributions to cognitive impairment and dementia. *J Neurochem* 144: 644–650, 2018. doi: 10.1111/jnc.14273.

61. **Rigsby CS**, **Ergul A**, **Portik Dobos V**, **Pollock DM**, **Dorrance AM**. Effects of spironolactone on cerebral vessel structure in rats with sustained hypertension. *Am J Hypertens* 24: 708–715, 2011. doi: 10.1038/ajh.2011.20.

62. **Rigsby CS**, **Pollock DM**, **Dorrance AM**. Spironolactone improves structure and increases tone in the cerebral vasculature of male spontaneously hypertensive stroke-prone rats. *Microvasc Res* 73: 198–205, 2007. doi: 10.1016/j.mvr.2006.12.001.

63. **Rocha R**, **Chander PN**, **Khanna K**, **Zuckerman A**, **Stier CT**. Mineralocorticoid blockade reduces vascular injury in stroke-prone hypertensive rats. *Hypertension* 31: 451–458, 1998. doi: 10.1161/01.hyp.31.1.451.

64. **Rogaeva E**, **Meng Y**, **Lee JH**, **Gu Y**, **Kawarai T**, **Zou F**, **Katayama T**, **Baldwin CT**, **Cheng R**, **Hasegawa H**, **Chen F**, **Shibata N**, **Lunetta KL**, **Pardossi-Piquard R**, **Bohm C**, **Wakutani Y**, **Cupples LA**, **Cuenco KT**, **Green RC**, **Pinessi L**, **Rainero I**, **Sorbi S**, **Bruni A**, **Duara R**, **Friedland RP**, **Inzelberg R**, **Hampe W**, **Bujo H**, **Song Y-Q**, **Andersen OM**, **Willnow TE**, **Graff-Radford N**, **Petersen RC**, **Dickson D**, **Der SD**, **Fraser PE**, **Schmitt-Ulms G**, **Younkin S**, **Mayeux R**, **Farrer LA**, **St George-Hyslop P**. The neuronal sortilin-related receptor SORL1 is genetically associated with Alzheimer disease. *Nat Genet* 39: 168–177, 2007. doi: 10.1038/ng1943.

65. **Rotenstein LS**, **Sheridan M**, **Garg R**, **Adler GK**. Effect of mineralocorticoid receptor blockade on hippocampal-dependent memory in adults with obesity. *Obesity (Silver Spring)* 23: 1136–1142, 2015. doi: 10.1002/oby.21104.

66. **Santisteban MM**, **Iadecola C**. Hypertension, dietary salt and cognitive impairment. *J Cereb Blood Flow Metab* 38: 2112–2128, 2018. doi: 10.1177/0271678X18803374.

67. **Seki T**, **Goto K**, **Kiyohara K**, **Kansui Y**, **Murakami N**, **Haga Y**, **Ohtsubo T**, **Matsumura K**, **Kitazono T**. Downregulation of Endothelial Transient Receptor Potential Vanilloid Type 4 Channel and Small-Conductance of Ca2+-Activated K+ Channels Underpins Impaired Endothelium-Dependent Hyperpolarization in Hypertension. *Hypertension* 69: 143–153, 2017. doi: 10.1161/HYPERTENSIONAHA.116.07110.

68. **Senanayake GVK**, **Banigesh A**, **Wu L**, **Lee P**, **Juurlink BHJ**. The dietary phase 2 protein inducer sulforaphane can normalize the kidney epigenome and improve blood pressure in hypertensive rats. *Am J Hypertens* 25: 229–235, 2012. doi: 10.1038/ajh.2011.200.

69. **Shih AY**, **Blinder P**, **Tsai PS**, **Friedman B**, **Stanley G**, **Lyden PD**, **Kleinfeld D**. The smallest stroke: occlusion of one penetrating vessel leads to infarction and a cognitive deficit. *Nat Neurosci* 16: 55–63, 2013. doi: 10.1038/nn.3278.

70. **Shi X**, **Ohta Y**, **Liu X**, **Shang J**, **Morihara R**, **Nakano Y**, **Feng T**, **Huang Y**, **Sato K**, **Takemoto M**, **Hishikawa N**, **Yamashita T**, **Abe K**. Chronic cerebral hypoperfusion activates the coagulation and complement cascades in alzheimer's disease mice. *Neuroscience* 416: 126–136, 2019. doi: 10.1016/j.neuroscience.2019.07.050.

71. **Sonkusare SK**, **Dalsgaard T**, **Bonev AD**, **Hill-Eubanks DC**, **Kotlikoff MI**, **Scott JD**, **Santana LF**, **Nelson MT**. AKAP150-dependent cooperative TRPV4 channel gating is central to endothelium-dependent vasodilation and is disrupted in hypertension. *Sci Signal* 7: ra66, 2014. doi: 10.1126/scisignal.2005052.

72. **Stanimirovic DB**, **Friedman A**. Pathophysiology of the neurovascular unit: disease cause or consequence? *J Cereb Blood Flow Metab* 32: 1207–1221, 2012. doi: 10.1038/jcbfm.2012.25.

73. **Tang J**, **Xiao W**, **Li Q**, **Deng Q**, **Chu X**, **Chen Y**, **Pan D**, **Fu J**. A Cyclooxygenase-2 Inhibitor Reduces Vascular Wall Thickness and Ameliorates Cognitive Impairment in a Cerebral Small Vessel Diseases Rat Model. *Curr Alzheimer Res* 12: 704–710, 2015. doi: 10.2174/1567205012666150710104924.

74. **Tavares G**, **Martins M**, **Correia JS**, **Sardinha VM**, **Guerra-Gomes S**, **das Neves SP**, **Marques F**, **Sousa N**, **Oliveira JF**. Employing an open-source tool to assess astrocyte tridimensional structure. *Brain Struct Funct* 222: 1989–1999, 2017. doi: 10.1007/s00429-016-1316-8.

75. **Waldstein SR**, **Lefkowitz DM**, **Siegel EL**, **Rosenberger WF**, **Spencer RJ**, **Tankard CF**, **Manukyan Z**, **Gerber EJ**, **Katzel L**. Reduced cerebral blood flow in older men with higher levels of blood pressure. *J Hypertens* 28: 993–998, 2010. doi: 10.1097/hjh.0b013e328335c34f.

76. **Wang X**, **Desai K**, **Juurlink BHJ**, **de Champlain J**, **Wu L**. Gender-related differences in advanced glycation endproducts, oxidative stress markers and nitric oxide synthases in rats. *Kidney Int* 69: 281–287, 2006. doi: 10.1038/sj.ki.5000043.

77. **Weinberger MH**, **Roniker B**, **Krause SL**, **Weiss RJ**. Eplerenone, a selective aldosterone blocker, in mild-to-moderate hypertension. *Am J Hypertens* 15: 709–716, 2002. doi: 10.1016/S0895-7061(02)02957-6.

78. **Wolters FJ**, **Zonneveld HI**, **Hofman A**, **van der Lugt A**, **Koudstaal PJ**, **Vernooij MW**, **Ikram MA**, **Heart-Brain Connection Collaborative Research Group**. Cerebral Perfusion and the Risk of Dementia: A Population-Based Study. *Circulation* 136: 719–728, 2017. doi: 10.1161/CIRCULATIONAHA.117.027448.

79. **Xia XM**, **Fakler B**, **Rivard A**, **Wayman G**, **Johnson-Pais T**, **Keen JE**, **Ishii T**, **Hirschberg B**, **Bond CT**, **Lutsenko S**, **Maylie J**, **Adelman JP**. Mechanism of

calcium gating in small-conductance calcium-activated potassium channels. *Nature* 395: 503–507, 1998. doi: 10.1038/26758.

80. **Yang ST**, **Mayhan WG**, **Faraci FM**, **Heistad DD**. Endothelium-dependent responses of cerebral blood vessels during chronic hypertension. *Hypertension* 17: 612–618, 1991. doi: 10.1161/01.hyp.17.5.612.

81. **Zhang P**, **Sun C**, **Li H**, **Tang C**, **Kan H**, **Yang Z**, **Mao A**, **Ma X**. TRPV4 (Transient Receptor Potential Vanilloid 4) Mediates Endothelium-Dependent Contractions in the Aortas of Hypertensive Mice. *Hypertension* 71: 134–142, 2018. doi: 10.1161/HYPERTENSIONAHA.117.09767.

Chapter 3:

Female Mice are Protected from Impaired Parenchymal Arteriolar TRPV4 Function and Impaired Cognition in Hypertension

3.1 – Abstract

Hypertension is a leading risk factor for cerebral small vessel disease. Our lab has shown that endothelium-dependent dilation in PAs is dependent on TRPV4 activation, and that this pathway is impaired in hypertension. This PA dilation impairment is associated with cognitive deficits and increased neuroinflammation. Epidemiological evidence suggests women with midlife hypertension have an increase in dementia risk that does not exist in age-matched men, though the mechanisms behind this are unclear. This study aimed to determine the sex differences in vascular injury and cognitive impairment in young, hypertensive mice to serve as a foundation for future determination of sex differences at midlife. We tested the hypothesis that young hypertensive female mice would be protected from the impaired TRPV4-mediated PA dilation and cognitive dysfunction observed in male mice. AngII-filled osmotic minipumps (800ng/kg/min, 4 weeks) were implanted in 16-19-week-old male C57BL/6 mice. Age-matched female mice received either 800ng/kg/min or 1200ng/kg/min AngII. Sham mice served as control. Systolic blood pressure was elevated in AngII-treated male mice and in 1200ng AngII-treated female mice vs sex-matched sham. PA dilation in response to the TRPV4 agonist GSK1016790A (10^{-9}-10^{-5}M) was impaired in hypertensive male mice and was associated with cognitive dysfunction and increased neuroinflammation. Hypertensive female mice exhibited normal TRPV4-medated PA dilation and were cognitively normal. Female mice also exhibited fewer signs of neuroinflammation than male mice. Determining the sex differences in cerebrovascular health in hypertension is critical for the development of effective therapeutic strategies for women.

3.2 – Introduction

Hypertension is a leading risk factor for vascular contributions to cognitive impairment and dementia (VCID). Hypertension results in arterial remodeling and impaired endothelium-dependent dilation in both peripheral and cerebral arteries and arterioles, contributing to vascular insufficiency. Inadequate cerebral blood flow can lead to cerebral hypoperfusion and, ultimately, cognitive decline. VCID encompasses a wide range of cognitive disorders that result from cerebrovascular pathology. VCID can progress to vascular dementia, which is the second leading cause of dementia following Alzheimer's disease. Importantly, VCID often presents as "mixed dementia," as nearly half of patients with Alzheimer's disease are found to have vascular damage at autopsy (30, 103). The additional vascular insult exacerbates existing dementia and worsens clinical outcome.

Epidemiological evidence suggests an important sex difference in the contribution of hypertension in eventual VCID development. While data is mixed concerning sex differences in overall VCID prevalence, multiple studies have demonstrated that hypertension increases VCID risk in women more so than in men (36, 43). Hypertension in midlife is particularly detrimental, with a 65% increased dementia risk in women, but not in men (36). The reasons behind this sex difference are not well understood. Female subjects have historically been excluded from studies investigating cerebrovascular mechanisms, which has prevented the field from advancing. Understanding the sex differences that exist in basic cerebrovascular physiology is essential in identifying better targeted therapies for women.

The present study focuses on cerebral PAs, which are important contributors to cerebrovascular resistance. These small arterioles direct blood flow from the pial arteries and arterioles to capillaries, which are the critical site of gas and nutrient exchange. PAs lack collateral connections and are therefore considered the weak link in cerebral perfusion. Appropriate PA perfusion is so crucial that occlusion of a single PA is sufficient to cause cognitive decline (82, 86). PAs are highly dependent on endothelium-derived hyperpolarization (EDH) for dilation, which occurs through the activation of transient receptor potential vanilloid 4 (TRPV4) channels. Endothelial TRPV4 activation triggers a robust calcium influx that subsequently activates intermediate and small conductance calcium-activated potassium channels (IK_{Ca}/SK_{Ca}), causing a hyperpolarization that ultimately leads to vasodilation. TRPV4-mediated-dilation of PAs is impaired in male mice with angiotensin II (AngII)-induced hypertension (23, 25). Even in the absence of hypertension, impaired TRPV4 function in PAs is associated with cognitive decline (24, 25, 55). It is well established that female sex hormones offer protection against endothelial dysfunction by maintaining nitric oxide (NO) production, (4, 26, 33, 56, 58). We know much less about the effects of sex on EDH-mediated dilation, particularly in the cerebral circulation where impaired vascular function can precipitate dementia. Therefore, using a model of AngII-hypertension in young male and female mice, we tested the hypothesis that female mice will be protected from impaired TRPV4-mediated dilation and impaired cognition observed in male mice in hypertension.

3.3 – Materials and Methods

3.3.1 – Experimental Models and Treatment

All experimental protocols were approved by the Michigan State University Animal Care and Use Committee and were performed in accordance with the National Institutes of Health Guide for the Care and Use of Laboratory Animals. Male and female C57Bl/6 mice (n=142 total; n=54 males and 88 females) were purchased from Charles River Laboratory. All animals studied were singly housed on 12h:12h light/dark cycle with food and water ad libitum. Hypertension was induced in 16-19-week-old male and female C57Bl/6 mice. Treatment lasted for 4 weeks, and mice were euthanized at 20-23 weeks of age. Mice were randomized into treatment groups.

3.3.2 – AngII Infusion

To induce hypertension, AngII was infused subcutaneously in both male and female mice using osmotic minipumps (Alzet model 1004, Durect Corp, Cupertino CA). Male mice received an AngII dose of 800ng/kg/min; this dose has been used previously by our group and others to induce hypertension (12, 23, 25, 98). Because young female mice are resistant to AngII-hypertension (98), we conducted pilot studies to determine an AngII dose that produces hypertension in female mice. Accordingly, one group of female mice received 800ng/kg/min to match the dose in the male mice, and a separate group received a dose of 1200ng/kg/min to produce hypertension. To insert the minipumps, mice were anesthetized with 3% isoflurane in oxygen and body temperature was maintained at 37°C. A single dose of the analgesic Rimadyl (5mg/kg, subcutaneous) and the antibiotic Baytril (5mg/kg, intramuscular) were administered immediately prior to surgery. A subcutaneous pocket was made and minipumps were inserted. Control mice

received sham operations. These mice were anesthetized, and a subcutaneous pocket was made but minipumps were not inserted. Mice were allowed to recover for one week after the surgical implantation of the osmotic minipump.

3.3.3 – Blood Pressure

Blood pressure was measured in conscious mice via tail-cuff plethysmography once weekly during the 4 weeks of treatment, using a RTBP1001 tail-cuff blood pressure system (Kent Scientific, Torrington, CT). Reported blood pressures were collected in the 4^{th} week of treatment.

3.3.4 – Laser Speckle Contrast Imaging

Pial blood flow was measured just before euthanasia using laser speckle contrast imaging. Mice were anesthetized with 3% isoflurane in oxygen. The scalp was removed, and the skull was cleared of connective tissue. A thin coat of clear nail polish was applied to the skull to improve image resolution. To minimize the vasodilatory effects of isoflurane (81), the concentration was reduced to 1% and the mice equilibrated at this concentration for 5min. Pial blood flow was then measured at 21 images/s for 1min. Regions of interest were defined as the parietal, frontal, and temporal regions in the left and right hemispheres (72). Mean blood flow in each of these regions was compared among treatment groups. Images were analyzed using PIMSoft software (PeriMed, Las Vegas, NV).

3.3.5 – Pressure Myography

Pressure myography was used to assess the endothelial function and passive structure of PAs as described previously (23, 25, 54, 71). The brain was collected at euthanasia and was placed in a cooled (4°C) dissection chamber in Ca^{2+}-free PSS

containing (in mM): 140.00 NaCl, 5.00 KCl, 1.00 $MgCl_2$ * $7H_2O$, 10.00 HEPES, 10.00 dextrose; the pH was adjusted to 7.4. To isolate PAs, a 5 x 3mm section of the brain containing the MCA was dissected. The pia with the MCA were separated from the brain and the PAs branching off the MCA were used for experiments. Isolated arterioles were cannulated with two glass micropipettes in a custom-made cannulation chamber. Arterioles were equilibrated at 37°C in artificial cerebral spinal fluid containing (in mM): 124.00 NaCl, 3.00 KCl, 2.00 $CaCl_2$, 2.00 $MgCl_2$, 1.25 NaH_2PO_4, 26.00 $NaHCO_3$, and 4.00 dextrose. A servo-controlled system was used to pressurize the arterioles (Living Systems, St Albans City, VT). A leak test was performed prior to each experiment and any arteriole that could not maintain its intralumenal pressure was discarded. Arterioles were pressurized to 40mmHg until the development of stable myogenic tone {percent tone = [1 – (active lumen diameter/passive lumen diameter)] x 100}. Arterioles that generated at least 20% myogenic tone were used for experiments. Arterioles that did not develop myogenic tone were discarded. The diameter of the arterioles was tracked using MyoView 2.0 software (Danish Myo Technology, Aarhus, Denmark).

3.3.6 – Endothelial Function

After generation of myogenic tone, endothelium-dependent dilation was assessed. To measure TRPV4-mediated dilation, increasing concentrations of the specific TRPV4 agonist GSK1016790A (10^{-9}–10^{-5}M) was added to the bath. To assess IK_{Ca}/SK_{Ca}-mediated dilation, PAs were incubated with increasing concentrations of the agonist NS309 (10^{-9}–10^{-5}M). A subset of arterioles was incubated with NS309 as well as either the IK_{Ca} antagonist TRAM34 (1μM) or the SK_{Ca} antagonist apamin (300nM) to determine the role of IK_{Ca} and SK_{Ca} channels individually. TRAM34 or apamin were added after the

generation of myogenic tone and circulated through the system for 10min before dilation to NS309 was assessed. Neither antagonist altered the amount of tone generated. Each PA was used for only one dilation experiment.

3.3.7 – Passive PA Structure

After completion of endothelial function experiments, arterioles were incubated with Ca^{2+}-free PSS containing EGTA (29mM) and SNP (10^{-5}M). To assess the structure of the arterioles, a pressure-diameter curve was constructed by increasing the intralumenal pressure from 3 to 120mmHg at 20mmHg increments. The arterioles were equilibrated at each pressure for 5min and the lumen and outer diameters were measured. These values were used to calculate wall thickness (outer diameter – lumen diameter), wall stress, strain, and stiffness, as described (8). Wall stiffness was quantified using the β-coefficient calculated from the individual stress-strain curves using the model $y = ae^{\beta x}$, where y is wall stress, x is wall strain, a is the intercept and β is the slope of the exponential fit; a higher β-coefficient represents a stiffer vessel.

3.3.8 – Spontaneous Alternation

Spatial working memory was assessed using a Y-maze spontaneous alternation task. A custom Y-maze was constructed by Dr. Nathan Tykocki (Michigan State University). The maze consists of three arms placed at a 120° angle from one another. Each arm is 35cm long, 5cm wide, and 20cm high. Mice were each placed in a random arm of the maze and were allowed to explore freely for 3min. A mouse with intact memory will preferentially visit the arm it has visited the least recently, and a correct alternation is defined as consecutive entries into all three arms (52). Percent alternation was calculated as:

$$\%\ alternation = \frac{(number\ of\ alternations)}{[(Total\ number\ of\ arm\ entries) - 2]} \times 100$$

3.3.9 – Barnes Maze

Barnes maze was used to assess spatial memory (7, 25). Mice were trained over the course of 4 days (three, 3min trials) to locate the escape hole. Visual cues were placed on each of the walls to aid in spatial orientation. A 4,000Hz sound acted as an aversive stimulus, which was removed when the mice climbed into the escape hole. Mice were left in the escape box for 1min before being returned to their home cages. On the fifth day, the escape hole was covered but left in the same location, and the movement of the mice was tracked for 90s using EthoVision XT (6). The amount of time mice spent exploring the holes of the quadrant of the maze containing the escape hole was measured.

3.3.10 – Immunofluorescence

Brains were post-fixed in 4% paraformaldehyde and stored in sucrose. To assess microglia quantity and morphology, free-floating 40μm sections were blocked and permeabilized in 0.1% Triton X-100 with 10% donkey serum-PBS for 1h at room temperature, then incubated with 1:200 rabbit anti-ionized Ca^{2+}-binding adapter molecule 1 (Iba-1; no. 019-19741, Wako, Richmond, VA) primary antibody overnight at 4°C. After being washed in PBS, sections were incubated in AlexaFluor 564 donkey anti-rabbit secondary antibody (ab150073, Abcam, Cambridge, UK) for 1h. Images were obtained from the cortex and hippocampus in each hemisphere.

To assess quantity and morphology of astrocytes, brain sections were blocked and permeabilized in 0.5% Triton X-100 with 10% horse serum-PBS for 30min at room temperature, then incubated in 1:1000 rabbit anti-glial fibrillary acidic protein (GFAP;

ab7260, Abcam, Waltham, MA) primary antibody overnight at 4°C. Sections were washed in PBS, then incubated AlexaFluor 564 donkey anti-rabbit secondary antibody. Images were obtained from the corpus collosum in both hemispheres of each sample. A Sholl analysis was used to assess astrocyte structure as described by others (89). In brief, the Simple Neurite Tracer plugin in ImageJ was used to trace five random astrocytes for each mouse. The tracings were skeletonized and the automated Sholl analysis was used to draw concentric circles away from the soma around the astrocyte. The number of intersections of the astrocytic processes at these circles was plotted against the distance of the circle from the soma.

All images were acquired using a 20x objective coupled to a Zeiss LSM880 confocal microscope. Z-stacks were taken through the entire thickness of each 40μm section and then compressed. Sections without primary antibody served as negative controls. All quantifications were done manually by a blinded investigator using ImageJ.

3.3.11 – Drugs and Chemicals

GSK1016790A and NS309 were purchased from Cayman Chemical (Ann Arbor, MI). All other reagents were purchased from Sigma-Aldrich unless otherwise specified. Agonists and antagonists for endothelial function experiments were diluted in DMSO and then added to the circulating artificial cerebral spinal fluid.

3.3.12 – Statistical Analysis

All data are presented as means ± SEM. For analysis of arteriole structure and vasodilation and the Sholl analysis for astrocytes, two-way ANOVA with repeated measures in one factor (pressure, concentration, or distance from soma) was utilized, followed by Bonferroni-adjusted t-tests for post-hoc comparisons. All other statistical

analyses were assessed by Student's t-test, one-way ANOVA, or their non-parametric counterparts if necessary (Mann-Whitney or Kruskal-Wallis). The Grubb's test was used to identify outliers. All statistical analyses were performed using GraphPad Prism 7.0 software (GraphPad, San Diego, CA). In all cases, statistical significance was denoted by $p<0.05$.

3.4 – Results

3.4.1 – Female mice require a higher dose of AngII to develop hypertension

AngII was delivered to male and female mice via subcutaneous implantation of osmotic minipumps. Male mice given 800ng/kg/min AngII for 4 weeks had elevated systolic blood pressure compared to sham (Figure 3.1A). Female mice given 800ng/kg/min AngII did not have elevated systolic blood pressure compared to sham (Figure 3.1B). This resistance to AngII hypertension in cycling female mice has previously been demonstrated by others (98). Systolic blood pressure was increased in female mice given 1200ng/kg/min AngII (Figure 3.1B).

3.4.2 – AngII infusion reduces pial blood flow in both male and female mice

Cerebral pial blood flow was measured using laser speckle contrast imaging. Regions of interest were specified in the frontal, temporal, and parietal regions of the brain, as described by others (72, 77). These regions were chosen because they are perfused by the anterior, middle, and posterior cerebral arteries, respectively. As expected, control female mice had greater pial blood flow than control male mice (1, 2, 39, 53, 74). Hypertensive male mice had reduced pial blood flow in the parietal region, while blood flow in the frontal and temporal regions were unchanged (Figure 3.2B, D, F). AngII-infused female mice, however, had reduced pial blood flow in all measured regions

(Figure 3.2C, E, G). Notably, the female mice given the 800ng/kg/min dose AngII had the same degree of blood flow reduction as the mice given 1200ng/kg/min AngII, despite not being hypertensive.

3.4.3 – Hypertension results in increased PA myogenic tone generation in male mice

Myogenic tone generation was measured in PAs using pressure myography. PAs were pressurized to 40mmHg until the generation of spontaneous myogenic tone. Myogenic tone increases in hypertension; we have previously shown this using various models of hypertension, including AngII infusion (25, 71). In the present study, myogenic tone generation was elevated in PAs from hypertensive male mice (Figure 3.3A). Hypertensive female mice did not have altered tone generation compared to control (Figure 3.3B).

3.4.4 – Female mice are protected against impaired TRPV4-mediated dilation in hypertension

After spontaneous generation of myogenic tone, we used the TRPV4 agonist GSK1016790A to measure TRPV4-mediated dilation in PAs. We have demonstrated previously that PAs from AngII-hypertensive male mice have impaired TRPV4-mediated dilation (25). These findings were reproduced in the present study, with PAs from hypertensive male mice having significantly blunted dilation after TRPV4 activation (Figure 3.4A). PAs from AngII-infused female mice, however, did not exhibit impaired TRPV4-mediated dilation in either treatment group (Figure 3.4B). The overall ANOVA p-value did reach significance in this test ($p=0.0239$), indicating AngII treatment did influence dilation. However, maximum dilation to TRPV4 activation was unchanged after AngII infusion compared to sham, and dilation comparisons at individual concentrations

were not statistically significant. These data demonstrate that hypertension-induced impairment of TRPV4-mediated dilation in PAs is sex dependent.

3.4.5 – IK_{Ca}/SK_{Ca}-mediated dilation in PAs is unaltered in hypertensive mice

TRPV4 activation produces a calcium influx that activates nearby IK_{Ca}/SK_{Ca} channels that ultimately produce EDH and subsequent vasodilation (84). To determine whether dilatory impairment was at the level of TRPV4 or at downstream IK_{Ca}/SK_{Ca} channels, PA dilation to agonist NS309 was evaluated. Our data in this study disagree with our previous finding that hypertensive male mice have impaired IK_{Ca}/SK_{Ca}-mediated dilation. AngII-infused male and female mice had intact dilation to NS309 (Figure 3.4C, D). In fact, female mice given 800ng/kg/min AngII had slightly improved dilation to NS309 compared to control.

NS309 is a non-specific agonist that activates both IK_{Ca} and SK_{Ca} channels. To determine if hypertension alters the dilatory contribution of either of these channels, we used IK_{Ca} antagonist TRAM34 and SK_{Ca} antagonist apamin to separate dilatory contribution through these two channels. Antagonists were added to the bath after the generation of myogenic tone and did not alter the amount of tone generated. After the addition of apamin, neither male nor female mice (Figure 3.5A, B) had significant alterations in dilation to NS309, indicating SK_{Ca} channels are not major contributors of EDH in murine PAs. This was not changed after AngII infusion. Comparisons to a typical NS309 dilation from a control mouse of each sex are noted by the dotted line across the y-axis. In keeping with reports from other groups, addition of TRAM34 nearly abolished the NS309-mediated dilation (Figure 3.5C, D) (41). This was not altered by sex or AngII infusion.

3.4.6 – AngII-hypertension results in inward hypotrophic remodeling in PAs of both male and female mice

Pressure myography was used to assess passive PA structure under zero-flow and calcium-free conditions. Reproducing previous findings from our lab, PAs from AngII-hypertensive male mice underwent inward hypotrophic remodeling compared to PAs from control mice (Figure 3.6A-C) (23). This was characterized by reduction of outer and lumen diameters, accompanied by reduction in wall thickness. PAs from AngII-infused female mice underwent a dose-dependent reduction in outer and lumen diameters, with statistical significance being reached in the outer diameters of the 1200ng/kg/min AngII group vs. sham (Figure 3.6D-E). The hypertensive group of female mice also had PAs with reduced wall thickness, mimicking what is observed in hypertensive male mice (Figure 3.6F). Biomechanical properties of PAs in both male and female mice were unchanged in response to hypertension, with the exception of hypertensive female mice having increased wall stress at an intralumenal pressure of 120mmHg. (Figure 3.7).

3.4.7 – Hypertension impairs cognitive function in male mice only

Impaired TRPV4 function is associated with cognitive impairment, even in the absence of hypertension (16, 24, 25). To determine if the observed sex differences in TRPV4 function were associated with sex differences in cognition, we used two different memory tasks. First, we measured spatial working memory using the spontaneous alternation task in a Y-maze. Hypertensive male mice made fewer correct alternations compared to control mice, indicating impairments in spatial working memory (Figure 3.8B). AngII-infused female mice did not exhibit differences in spontaneous alternation

behavior compared to control (Figure 3.8C). AngII-infused male and female mice had comparable total arm entries to their respective controls (Figure 3.8D, E).

We then used Barnes maze to assess spatial memory. In the analysis, the maze was divided into quadrants, with the escape hole being in the target quadrant. Replicating previous findings from our group, hypertensive male mice spent significantly less time exploring holes in the target quadrant of the maze compared to sham, indicating deficits in spatial memory (Figure 3.8G). Female mice, however, did not have alterations in the amount of time exploring holes in the target quadrant, indicating intact spatial memory (Figure 3.8H). These data demonstrate an important sexual dimorphism in hypertension: impaired TRPV4 function in PAs is associated with impaired cognitive function in hypertensive male mice, while maintenance of TRPV4 function is associated with intact cognition in female mice.

3.4.8 – AngII-hypertension produces neuroinflammation in both male and female mice

The quantity and morphology of cortical and hippocampal microglia was assessed using an Iba-1 antibody. AngII-hypertensive male mice had more microglia in the cortex and hippocampus compared to sham (Figure 3.9B, C). Hippocampal microglia from hypertensive male mice had increased soma size, indicating these microglia were in their pro-inflammatory phenotype (Figure 3.9G). AngII infusion did not affect microglia quantity in the cortex of female mice (Figure 3.9D) but resulted in fewer microglia in the hippocampus at both AngII doses (Figure 3.9E). It is important to note that control female mice started with more microglia than control male mice. Female mice also had microglia with greater soma sizes in both the cortex and the hippocampus after AngII-infusion (Figure 3.9H, I). While there appear to be sex differences in how microglia respond to

AngII infusion, both male and female mice have evidence of increased neuroinflammation.

3.4.9 – Hypertensive male mice exhibit characteristics of reactive astrogliosis, while female mice do not

We used a GFAP antibody to assess astrocytic quantity and structure. Hypertensive male mice had more astrocytes compared to control. The morphology of astrocytes was assessed using a Sholl analysis. Hypertensive male mice had astrocytes with more arborization at points further away from the soma compared to control (Figure 3.10B, D). The observed astrocytic proliferation and increased process complexity are indicators of reactive astrogliosis (68, 96). AngII-infused female mice had a reduction in astrocyte quantity, regardless of hypertensive status, compared to sham (Figure 3.10C). Similar to what is observed with microglia, control female mice had more astrocytes at baseline compared to control male mice. Astrocytes in the group receiving 1200ng/kg/min AngII had reduced process arborization compared to sham (Figure 3.10E). These data suggest that both sexes undergo increased inflammation during hypertension, but only male mice exhibit indicators of reactive astrogliosis.

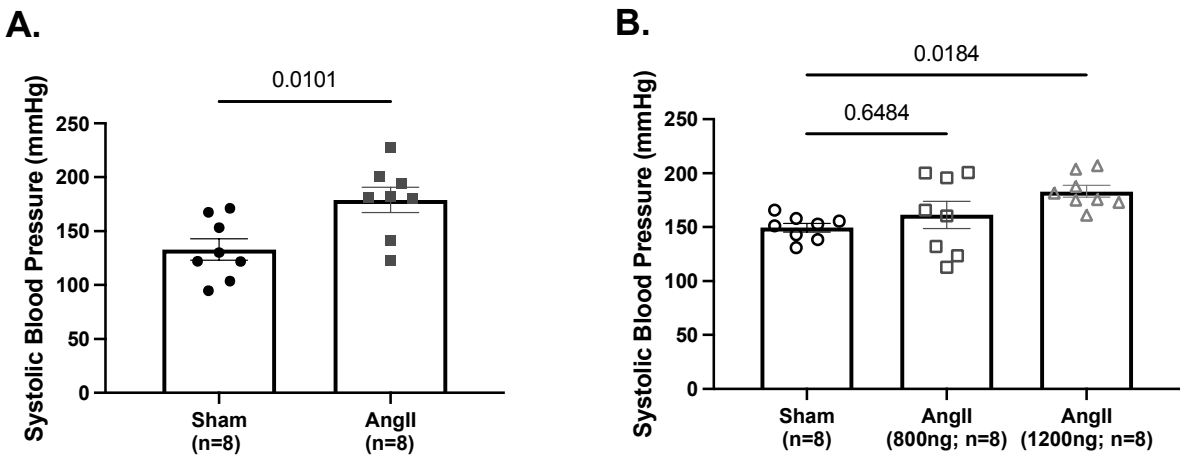

Figure 3.1: Female mice require a higher dose than male mice to become hypertensive. Blood pressure was measured in conscious mice using tail-cuff plethysmography. Data are presented as means ± SEM. A) Systolic blood pressure was elevated in male mice infused with 800ng/kg/min AngII, compared to sham. B) 800ng/kg/min AngII was not sufficient to elevate systolic blood pressure in female mice; however, female mice given 1200ng/kg/min AngII had increased systolic blood pressure compared to controls. $p<0.05$ indicates statistical significance vs. sham by Student's t-test (A) or one-way ANOVA (B). Legend: Angiotensin II (AngII).

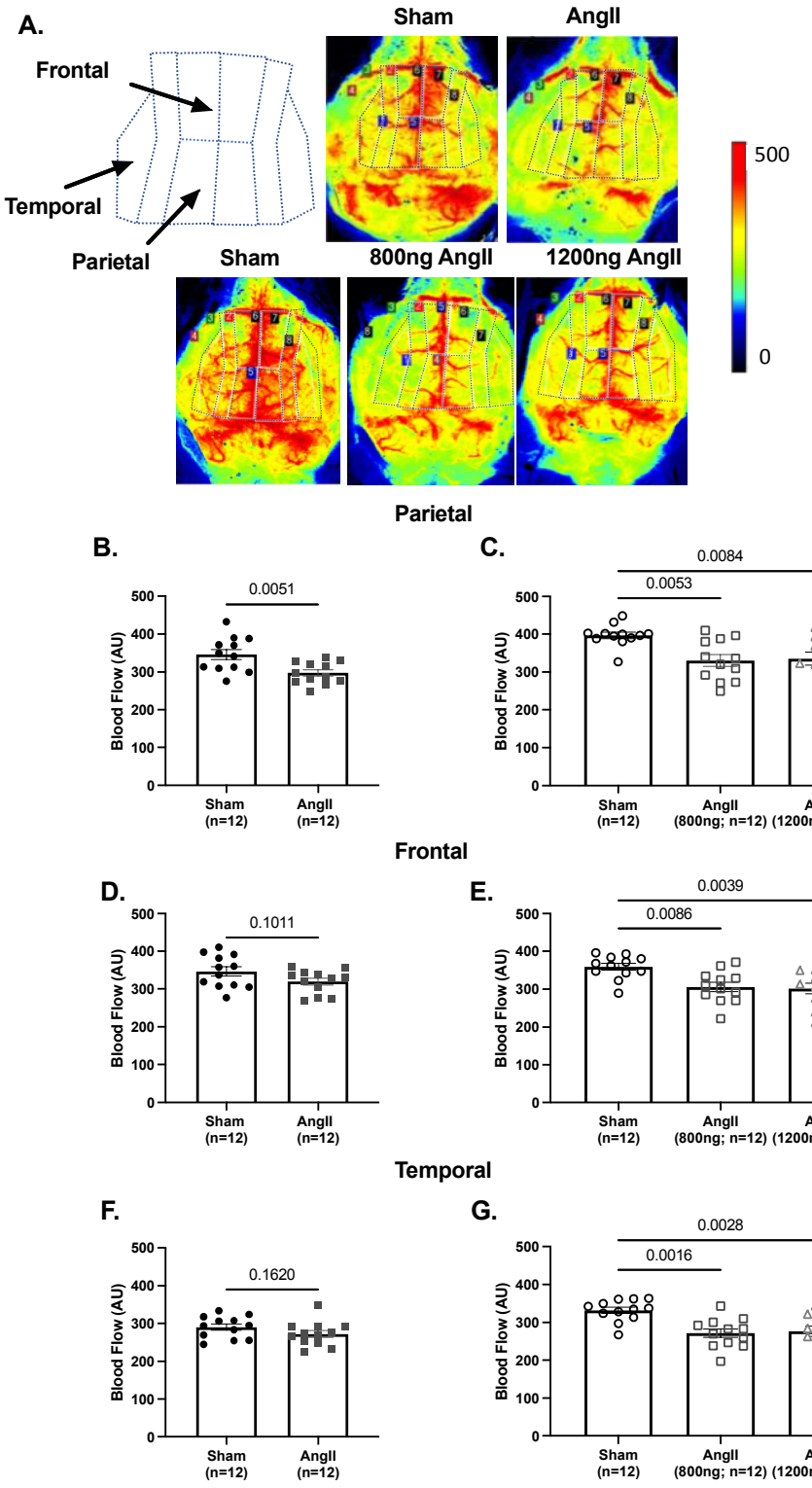

Figure 3.2: AngII-hypertension reduces pial perfusion in both male and female mice. Pial perfusion was measured in anesthetized mice using laser speckle contrast

Figure 3.2 (cont'd): imaging. Data are presented as means ± SEM. A) Representative images of regions of interest (top left), pial perfusion in male mice (top) and female mice (bottom). The perfusion scale bar ranges from 0 to 500 arbitrary perfusion units. B) AngII infusion reduces pial perfusion in the parietal region of both male and C) female mice. D) Pial perfusion is unchanged in the frontal region in AngII-hypertensive male, E) but is reduced in female mice in both AngII groups. F) Temporal perfusion is unchanged in hypertensive male mice, G) but is reduced in both female AngII groups compared to sham. $p<0.05$ indicates statistical significance compared to sham, measured by Student's t-test (B, D, F) or one-way ANOVA (C, E, G). Legend: Angiotensin II (AngII).

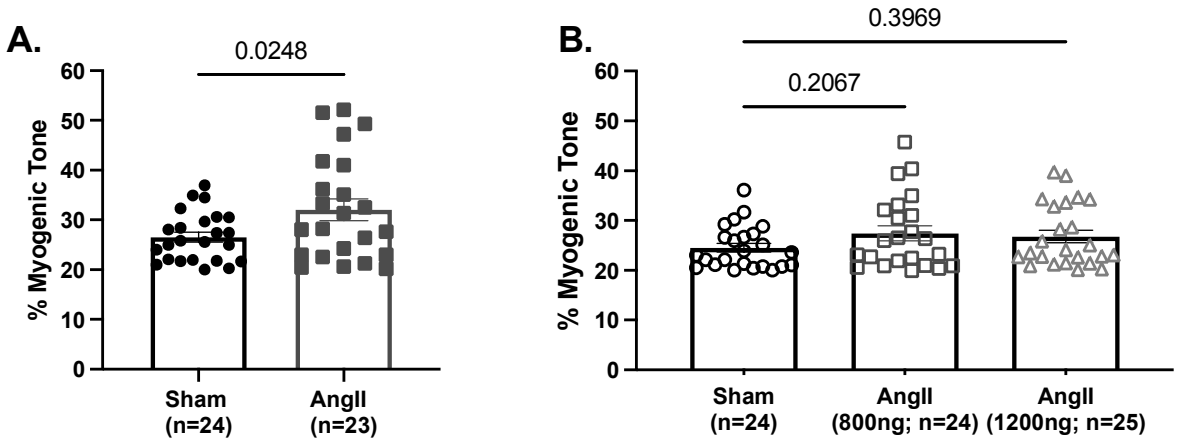

Figure 3.3: AngII hypertension increases myogenic tone generation in PAs of male mice. Myogenic tone generation in PAs was measured using pressure myography. Data are presented as means ± SEM. A) PAs from AngII-hypertensive male mice generated more myogenic tone compared to sham. B) In female mice, PA myogenic tone generation was not significantly altered after AngII infusion. n=number of PAs used. Myogenic tone values were collected before the start of each dilation experiment. Some mice are represented more than once. $p<0.05$ indicates statistical significance vs. sham, measured by Student's t-test (A) or one-way ANOVA (B). Legend: Angiotensin II (AngII).

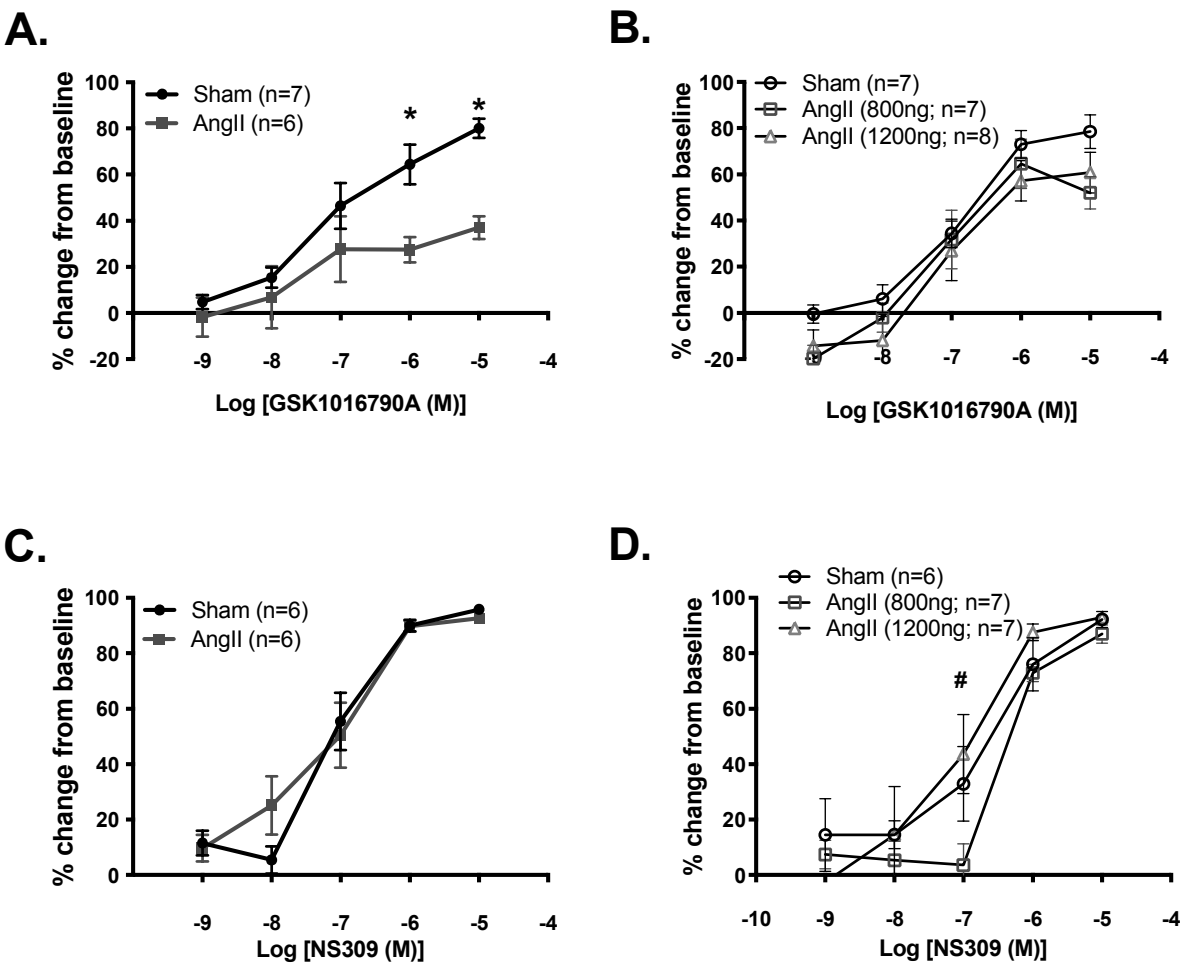

Figure 3.4: Female hypertensive mice are protected against impaired PA TRPV4-mediated dilation. Pressure myography was used to assess TRPV4- and IK_{Ca}/SK_{Ca}-mediated dilation in PAs. Data are presented as means ± SEM. A) AngII-hypertensive male mice had impaired PA TRPV4-mediated dilation. B) Female mice, however, were protected against impaired PA TRPV4-mediated dilation, though there was a significant effect of treatment on dilation to GSK10167090A. C) AngII-hypertensive male D) and female mice did not have impaired IK_{Ca}/SK_{Ca}-mediated dilation, assessed by dilation to agonist NS309. Female mice treated with 1200ng/kg/min AngII had significantly greater dilation to NS309 at 10^{-7}M compared to female mice treated with 800ng/kg/min AngII.

Figure 3.4 (cont'd): n=number of mice used. One PA was used per mouse per dilation experiment. #=$p<0.05$ by two-way ANOVA followed by Bonferroni correction for post-hoc comparisons. Legend: Angiotensin II (AngII).

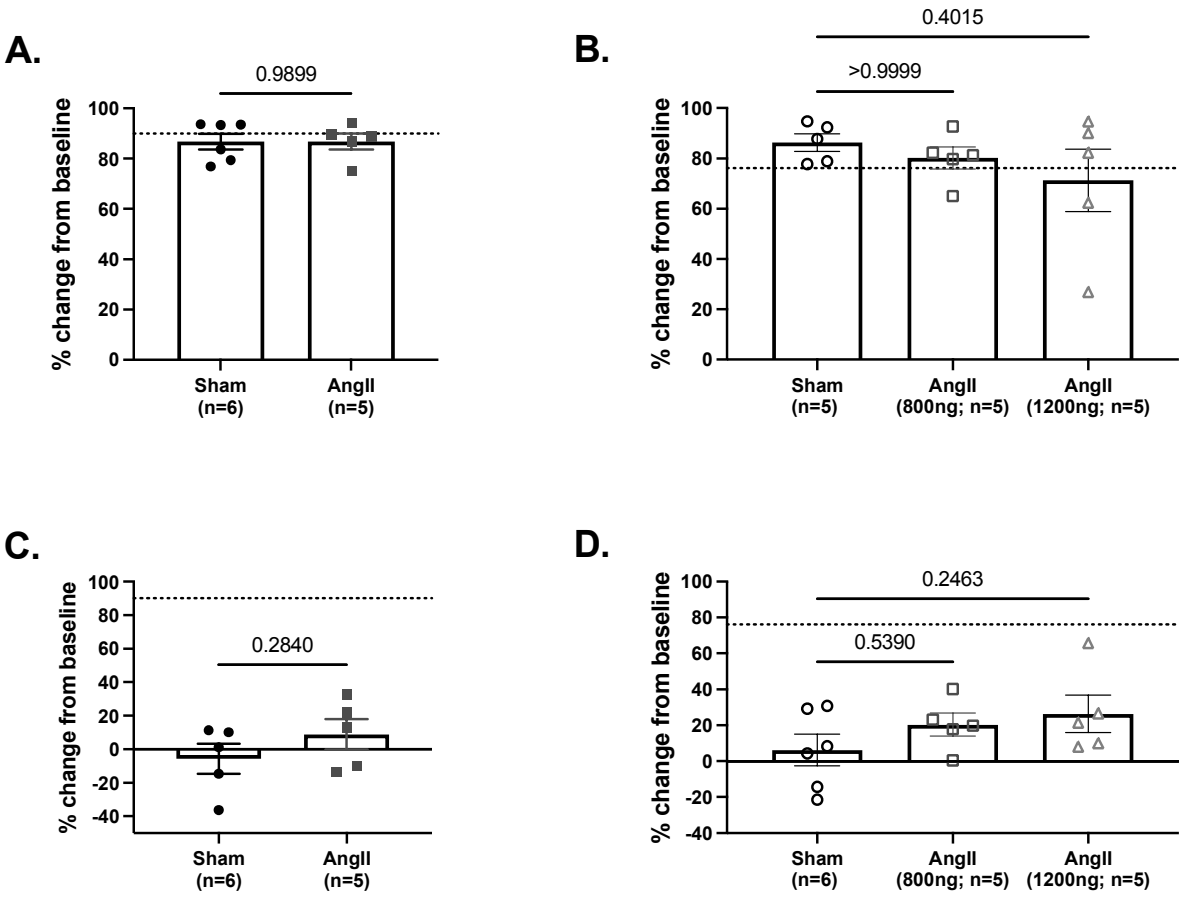

Figure 3.5: Hypertension does not alter IK_{Ca}/SK_{Ca} channel contribution in PAs. Pressure myography was used to assess IK_{Ca} and SK_{Ca} dilatory contribution in PAs using TRAM34 and apamin, respectively. Data are presented as means ± SEM. The dotted lines on the graphs represent the average dilation of the sham group of each sex to 1μm NS309. Statistical comparisons were made between sham and treated mice of each sex. A) AngII-infused male and B) female mice did not have altered dilation to 1μM NS309 compared to their controls after apamin was added to the bath. C) AngII-infused male and D) female mice have severely blunted PA dilation to 1μM NS309 after addition of TRAM34. n=number of mice used. One PA was used per mouse per dilation experiment.

Figure 3.5 (cont'd): $p<0.05$ indicates statistical significance vs. sham, measured by Student's t-test (A, C) or one-way ANOVA (B, D). Legend: Angiotensin II (AngII).

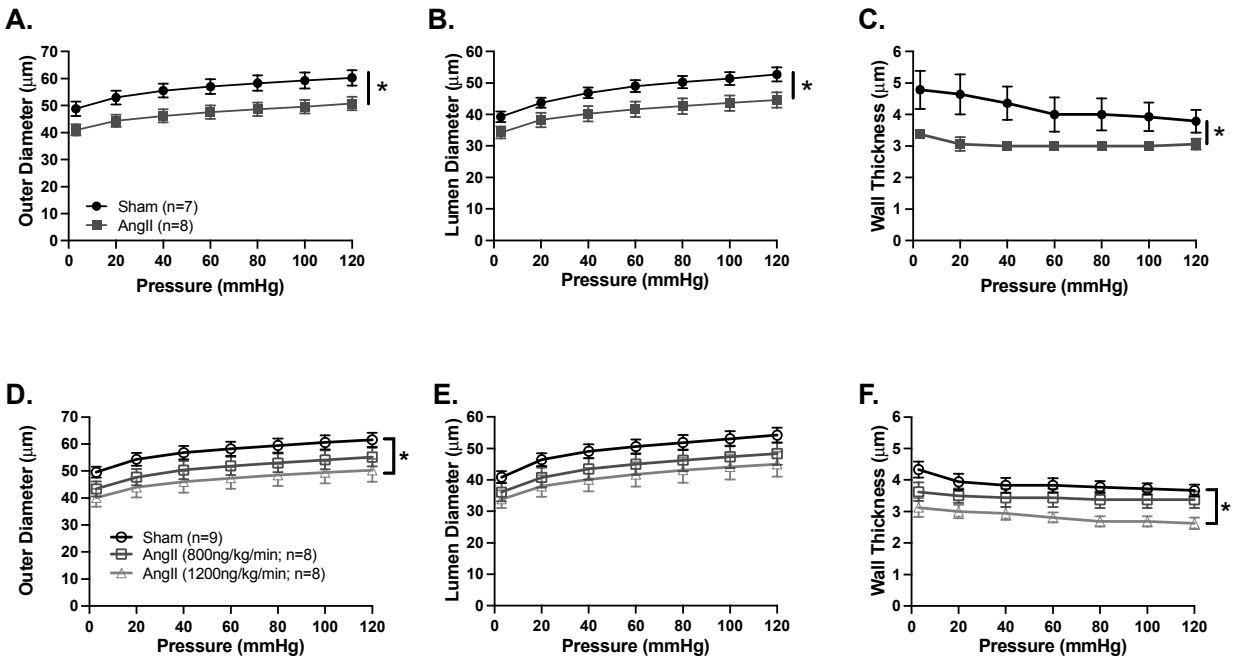

Figure 3.6: AngII-hypertension results in inward hypotrophic remodeling in PAs of male and female mice. The structure of PAs from male and female mice was assessed by pressure myography. Data are presented as means ± SEM. In male mice, AngII-hypertension resulted in PAs with A) reduced outer diameter, B) lumen diameter, and C) wall thickness. PAs of female mice underwent a dose-dependent reduction in D) outer diameter, E) lumen diameter, and F) wall thickness, Structural changes reached significance in the 1200ng/kg/min AngII group vs. sham for the outer diameter and wall thickness measurements. n=number of mice used. One PA was used per mouse per dilation experiment. *$p<0.05$ indicates statistical significance vs. sham, measured by two-way ANOVA followed by Bonferroni correction for post-hoc comparisons. Legend: Angiotensin II (AngII).

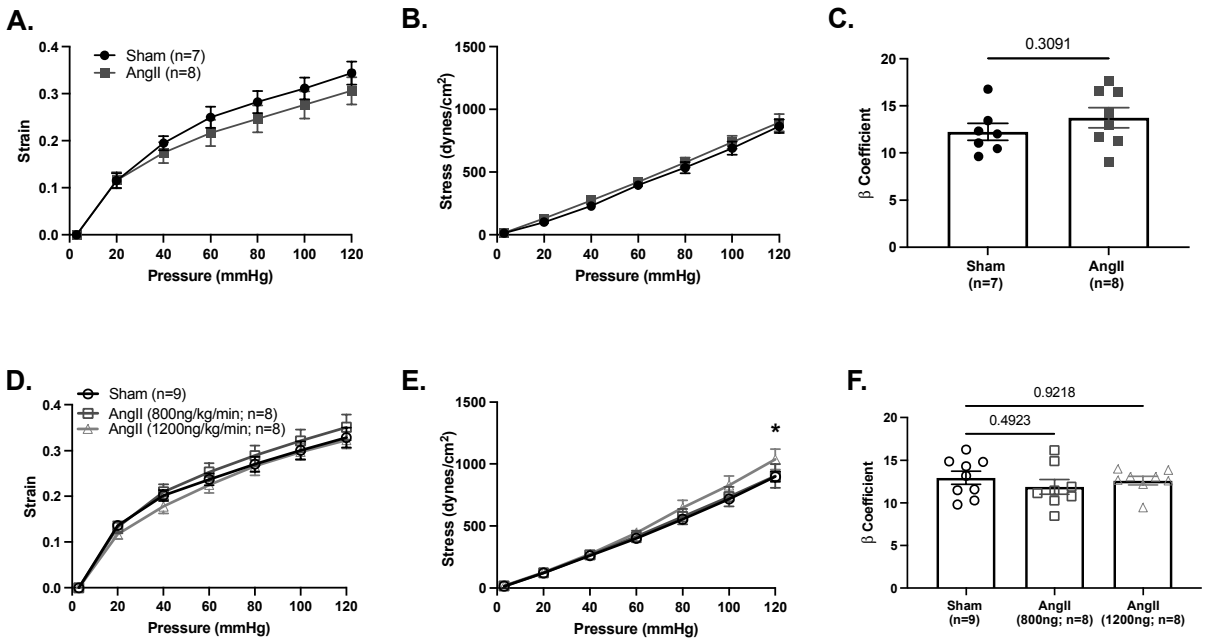

Figure 3.7: AngII-hypertension does not alter biomechanical properties of PAs in male or female mice. Pressure myography was used to assess the biomechanical properties of PAs from male and female mice. AngII infusion did not significantly alter PA wall strain (A, D) or β-coefficient (C, F) in male or female mice. While wall stress was largely unchanged in both sexes in response to AngII infusion (B, E), female mice given 1200ng/kg/min AngII had greater stress compared to sham at 120mmHg. n=number of mice used. One PA was used per mouse per dilation experiment. *$p<0.05$ indicates statistical significance vs sham by two-way ANOVA followed by Bonferroni correction for post-hoc comparisons. Legend: Angiotensin II (AngII).

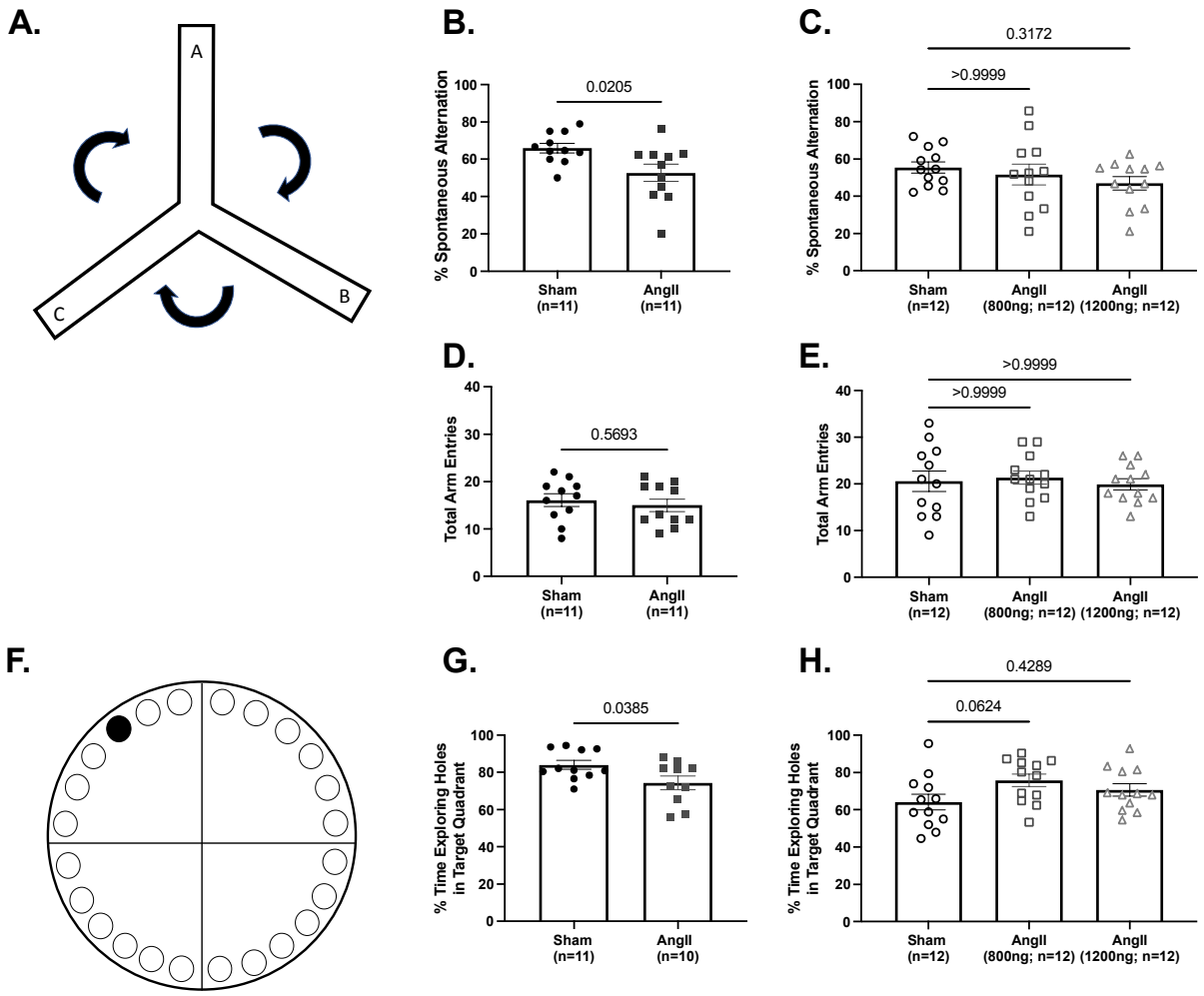

Figure 3.8: Female mice are protected against cognitive impairment observed in male mice during hypertension. Data are presented as means ± SEM. Spatial working memory was assessed using the spontaneous alternation task. A) Schematic of the Y-maze with a representation of a correct alternation. B) Male AngII-hypertensive mice had impaired alternation behavior compared to sham, while C) female AngII-infused mice had no difference in spontaneous alternation compared to sham. The total number of arm entries was not changed after AngII infusion in D) male or E) female mice. Spatial memory was assessed using Barnes maze. F) Schematic of a Barnes maze. G) Hypertensive

Figure 3.8 (cont'd): male mice spent less time exploring the quadrant of the maze containing the escape hole compared to sham. H) Female AngII-infused mice had no differences in time spent exploring the target quadrant of the maze. $p<0.05$ indicates statistical significance vs. sham, measured by Student's t-test (B, D, G) or one-way ANOVA (C, E, H). Legend: Angiotensin II (AngII).

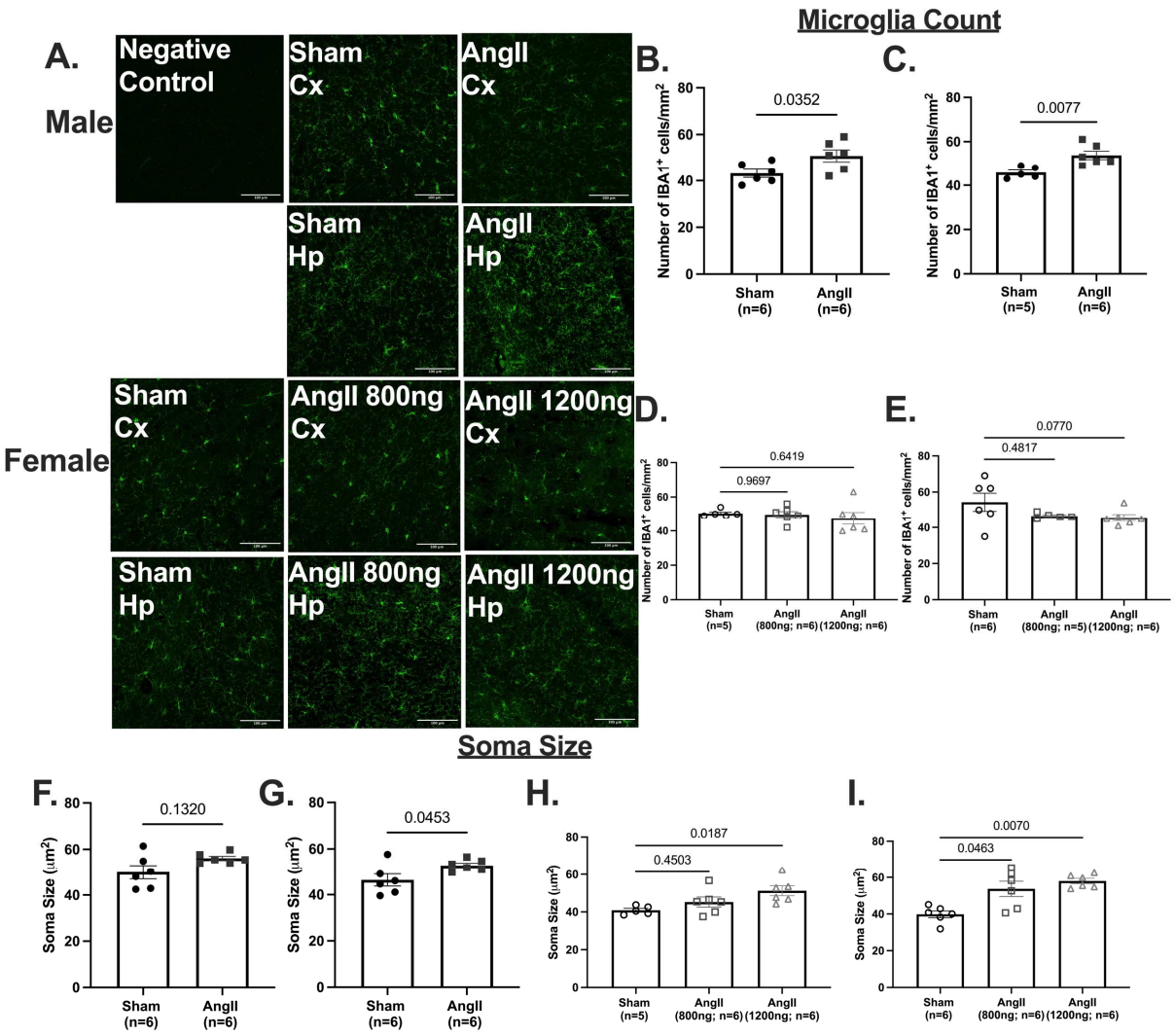

Figure 3.9: The microglial inflammation response to AngII infusion differs between male and female mice. Quantity and morphology of microglia in the cortex and hippocampus were assessed using Iba-1 staining. Data are presented as means ± SEM. A) Representative images of Iba-1 staining in the cortex and hippocampus of male and female mice. B) The number of Iba-1-positive cells was elevated in the cortex and C) hippocampus of AngII-hypertensive male mice compared to control. D) AngII-infused female mice had no change in microglia quantity in the cortex but had fewer microglia in

Figure 3.9 (cont'd): E) the hippocampus compared to control. F) In male mice, there was no significant increase in soma size of cortical microglia, but G) hippocampal microglia had increased soma size compared to sham. H) Female mice given the 1200ng dose of AngII had increased microglial soma size in the cortex, I) and both AngII doses resulted in increased soma size in the hippocampus compared to sham. Scale bar=100μm. $P<0.05$ indicates statistical significance compared to sham by Student's t-test (B, C, G), one-way ANOVA (D, H), Mann-Whitney (F), or Kruskal-Wallis (E, I). Legend: Angiotensin II (AngII); ionized calcium-binding adaptor molecule 1 (Iba-1).

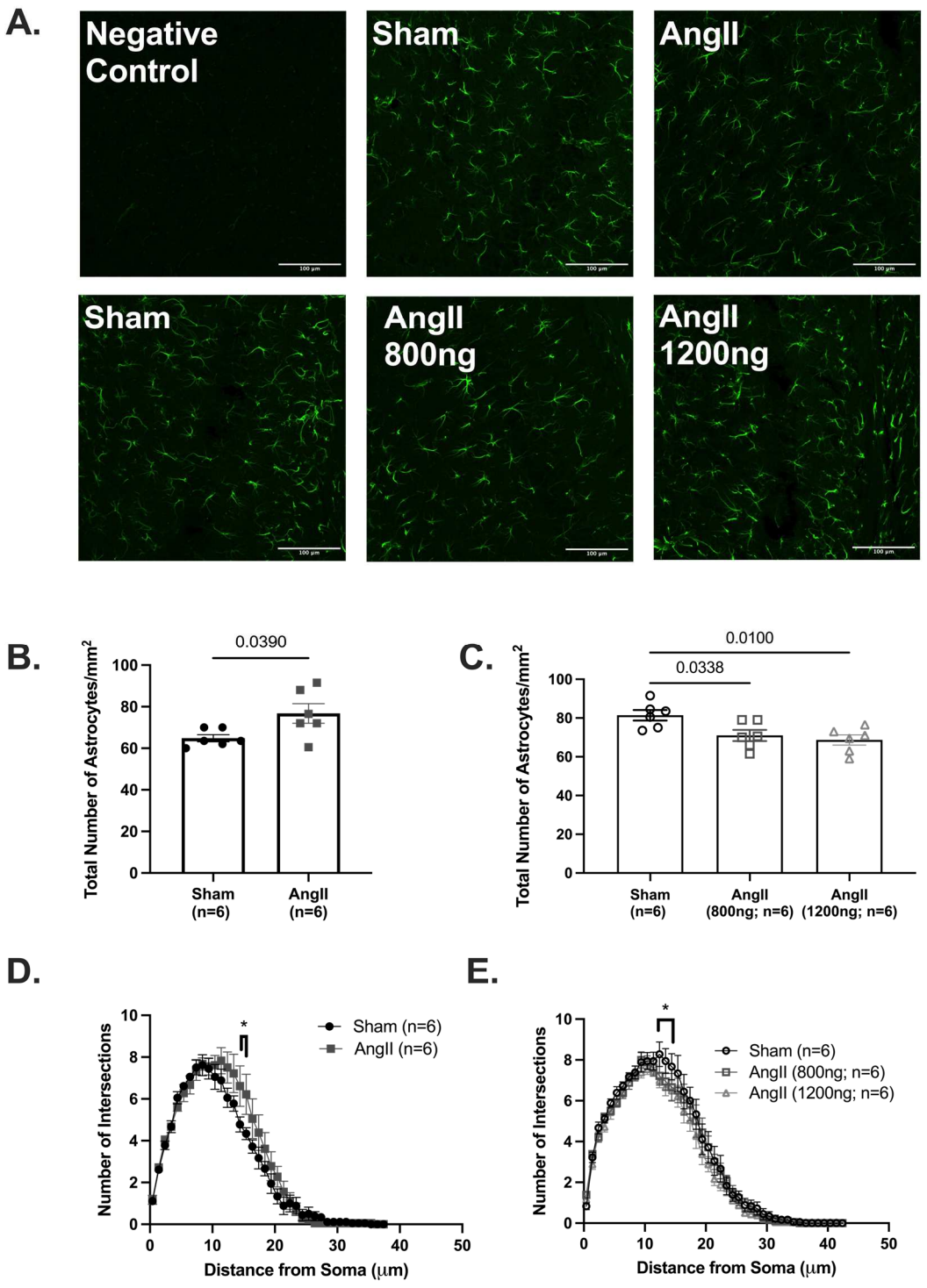

Figure 3.10: AngII infusion results in reactive astrogliosis in male, but not female mice. The number of GFAP-positive astrocytes and their morphology were assessed in

Figure 3.10 (cont'd): the corpus collosum. Data are presented as means ± SEM. A) Representative images of GFAP staining in male (top) and female mice (bottom). B) AngII-hypertensive male mice had increased astrocytes compared to sham. C) AngII-infused female mice had fewer astrocytes compared to sham, regardless of AngII dose. D) Astrocytes from AngII-hypertensive male mice had more arborization away from the soma compared to sham, assessed by Sholl analysis. E) Astrocytes from 1200ng AngII-infused female mice had reduced arborization compared to sham. Scale bar=100μm. $P<0.05$ (marked by *) indicates statistical difference from control by Student's t-test (B), one-way ANOVA (C), or two-way ANOVA (D, E). Legend: Angiotensin II (AngII); glial fibrillary acidic protein (GFAP).

3.5 – Discussion

The goal of this study was to determine how biological sex influences the impact of hypertension on cerebrovascular health. This study provides novel evidence that cycling female mice are protected from impaired PA TRPV4-mediated dilation and associated cognitive decline during hypertension. Further, the data suggest a sex dependent difference in inflammation that may mediate vascular and cognitive changes. These data improve our knowledge of sex differences in cerebrovascular physiology, a subject that has received very little study. Further, our observations expand on our previous findings that hypertension-associated cognitive impairment is associated with dysfunctional arteriolar TRPV4 signaling.

Before discussing the specific findings of our study, it is important to acknowledge the sex differences in RAAS activation that may contribute to our observations. AngII exerts its effects on the vasculature by activating both type 1 angiotensin II receptors (AT1R) and type 2 angiotensin II receptors (AT2R). AT1R activation in vascular smooth muscle cells leads to vasoconstriction, cell proliferation, migration, and extracellular matrix deposition (88, 90, 94). AT1R activation also increases inflammation and oxidative stress through NADPH oxidase activity (22, 64). AT2R activation plays a counterregulatory role to the effects of AT1R, promoting vasodilation, NO production, angiogenesis, and reducing neuroinflammation (42). Importantly, female rats have a higher ratio of AT2R to AT1R compared to males, shifting the balance of RAAS system activation toward cardiovascular protection (79, 83). Compared to male rats, females also express more angiotensin-converting enzyme 2 (ACE2), an enzyme responsible for converting AngII to angiotensin-(1-7) (79). Angiotensin-(1-7) activates the Mas receptor, which promotes vasodilation, and combats inflammation, vascular oxidative stress, and endothelial dysfunction (29, 32, 78). The sex differences in RAAS activation are hormone dependent, with testosterone stimulating the AngII-AT1R pathway (18, 34, 60) and estrogen stimulating the AngII-AT2R / angiotensin-(1-7)-Mas receptor pathway (13, 14, 59, 87). Given that this study was conducted in young adult mice, it is highly likely that sex differences in RAAS contribute to the observations in the present study, including differences in blood pressure elevation, vascular remodeling, and neuroinflammation. It is also important to note that estrogen also exerts neuroprotective effects via pathways beyond RAAS (92).

Our data agree with studies by other groups demonstrating that female mice require a higher dose of AngII to become hypertensive (98). Follow-up studies by Xue *et al* showed the observed resistance to hypertension is estrogen-dependent (99). We identified a dose of AngII that overcomes the estrogen-mediated protection against hypertension. Female mice given 1200ng/kg/min AngII developed hypertension, although the magnitude of the blood pressure increase (22%) was less than what was observed in male mice treated with 800ng/kg/min (34%). This difference in the magnitude of the blood pressure elevation may be explained by control female mice having a higher baseline systolic blood pressure than control male mice. Blood pressures were measured using tail-cuff plethysmography and both sexes were acclimated to the procedure in the same way. Because females have a greater physiological response to acute stressors (66), the higher baseline blood pressure in female mice is not surprising. Future studies will use radiotelemetry for blood pressure measurement to mitigate stress-induced pressor effects.

In our vasodilation studies, we focused on the effects of TRPV4 because this cation channel is the primary contributor to endothelium-dependent dilation in PAs (16, 24, 25). We observed that the hypertension-induced impairment of TRPV4-mediated dilation in PAs is sex dependent and occurs in males only. TRPV4 channels are expressed in both endothelial and vascular smooth muscle cells. In endothelial cells, TRPV4 channels that are localized to myoendothelial projections (MEPs) produce a calcium influx upon activation that ultimately produces EDH via subsequent IK_{Ca}/SK_{Ca} channel activation. TRPV4 activity is enhanced AKAP150, which anchors PKA and PKC to MEPs to facilitate TRPV4 phosphorylation (15, 28, 85). Studies from our group show

that endothelium-dependent dilation in PAs in primarily dependent on TRPV4 signaling (16, 24, 25). In mesenteric arteries and cerebral PAs, TRPV4 channels are dysfunctional in hypertensive male rodents (16, 25, 85). This study is the first to show that hypertensive female mice are resistant to this impairment in TRPV4 activity. It is well-established, however, that female sex conserves endothelial function in pathological conditions through increased NO production and maintained endothelial nitric oxide synthase activity (57, 70). Our novel data suggest female sex protects against endothelial dysfunction via mechanisms that extend beyond NO-mediated pathways.

In response to the calcium influx through endothelial TRPV4 channels, activation of IK_{Ca}/SK_{Ca} channels produces a potassium ion efflux out of endothelial cells. This loss of positive ions hyperpolarizes the endothelial cells. Redistribution of ions through myoendothelial gap junctions ultimately passes this hyperpolarization to smooth muscle cells, causing vasodilation. NS309 activates both IK_{Ca} and SK_{Ca} channels. AngII-hypertensive male mice have increased IK_{Ca} and reduced SK_{Ca} mRNA expression in cerebral arteries, suggesting RAAS activation influences transcription of these ion channels (25). To determine if hypertension alters ion channel contribution to EDH, we used the antagonists TRAM34 and apamin to block IK_{Ca} and SK_{Ca} channels, respectively. Consistent with findings by Cipolla *et al* (19), we observed that in both males and females, IK_{Ca} channels are the primary contributor to EDH in PAs. Our data suggests AngII-infusion does not result in altered ion channel contribution to EDH. Notably, we previously reported that hypertensive male mice had impaired IK_{Ca}/SK_{Ca}-mediated dilation in PAs, which contradicts our present findings that this dilation remained intact in both male and female hypertensive mice (25). This disagreement was unexpected. Mice from our previous

study were provided to us by a collaborator, while mice from the present study were purchased from Charles River. It is possible that differences in environmental background of the mice may contribute to our observations, though further study will be necessary to determine reasons behind these disparate findings.

Myogenic reactivity plays a critical role in cerebral blood flow regulation, especially in PAs, which generate high levels of myogenic tone relative to larger arteries. There is limited data comparing myogenic tone generation in PAs between the sexes. However, it has been reported that MCAs of female rats generate more myogenic tone than MCAs of male rats, potentially due to smaller artery size (47, 73). Conversely, our data suggest sex does not significantly impact myogenic tone generation in PAs of control mice. Because of the small size of these arterioles, it is possible that any sex associated changes in myogenic tone are too minute to be detected. Notably, hypertension resulted in more myogenic tone generation in PAs of male mice only, indicating female sex prevents this elevated tone generation.

There is ample evidence that RAAS activity is directly linked to structural changes observed in the vasculature in hypertension. AT1R activation leads to rearrangement of vascular smooth muscle cells and extracellular matrix proteins that ultimately produce changes in arterial structure (17, 31, 67). In both peripheral arteries and large cerebral arteries, hypertension induces inward hypertrophic remodeling, characterized by a smaller lumen diameter and thickening of the artery wall (45, 50, 75). PAs of hypertensive rodents, however, undergo inward hypotrophic remodeling, characterized instead by a reduction in wall thickness (23, 71). In the present study, both male and female hypertensive mice exhibited inward hypotrophic remodeling, though changes in female

mice were of a smaller magnitude. AngII-infused female mice had a dose-dependent reduction in PA diameter and wall thickness that reached significance in the hypertensive group only. Increased preference of female mice for the AT2R/Mas receptor arms of RAAS activation may contribute to this apparent resistance. Additionally, our group found that in AngII-hypertensive male mice, PA remodeling is mediated by endothelial mineralocorticoid receptor activation (23). Though there are apparent sex differences in mineralocorticoid receptor activation in cardiovascular disease (62), the mechanisms involved in cerebral microvessels are thus far unknown.

Hypertension reduces cerebral blood flow (49, 63, 93) and inadequate cerebral perfusion increases risk of dementia development (27, 97). Using scanning laser Doppler flowmetry, we showed that male AngII-hypertensive mice have reduced cerebral pial artery perfusion (23). Here, we used laser speckle contrast imaging to determine sex differences in cerebral pial perfusion in response to hypertension. As expected, sham female mice had greater cerebral blood flow compared to sham male mice. There was an unexpected finding, however, that AngII-infused female mice exhibited global reductions in cerebral blood flow while hypertensive male mice had reductions only in the parietal region. Blood flow reduction in female mice was comparable between the 800ng/kg/min and the 1200ng/kg/min groups, indicating it was a blood pressure-independent effect. Differences in cerebral blood flow may be attributable to sex dependent variances in myogenic reactivity in pial arteries. Others have demonstrated that while MCAs of 3 month old female rats have greater basal myogenic tone compared to males, they are also more susceptible to force-mediated dilation at high intralumenal pressures (95). This concept contradicts our observations, though the differences in species, subject age, and

vessel type complicate direct comparisons. Another possibility is a difference in the direct constrictor effects of AngII. Pial arteries are particularly susceptible to AngII-induced constriction (100). AT1R are quickly internalized after activation (20, 21, 44), and greater blood flow reduction in female mice presents the possibility of a lessened tachyphylactic response of AT1R after activation. A recent study by Zaccor *et al.* presented an interesting concept that TRPV4 activation prevents AT1R internalization, which could explain the globally reduced pial blood flow in female mice (101). Additional studies will be required to test directly test this hypothesis.

Our group has reliably found across various models that impaired TRPV4 channel activity is associated with cognitive dysfunction (16, 24, 25, 55). Here, we present novel data that the maintenance of TRPV4-mediated signaling in PAs of female mice is associated with protection against cognitive impairment in hypertension. Hypertensive male mice demonstrated impairments in both spatial working memory and spatial memory, while female mice did not exhibit memory impairments in either task. Interestingly, female mice given 800ng/kg/min AngII spent more time in the target quadrant of Barnes maze compared to sham, though this did not reach statistical significance. In both behavioral tests, control male mice outperformed control female mice. This is expected, as studies reliably report better performance in spatial tasks in male compared to female rodents (9, 11, 76, 80). The maintenance of cognitive function in AngII-infused female mice is interesting considering their global reduction in pial blood flow. Together, these observations present the possibility that neurons from female mice are protected from the negative effects of reduced cerebral blood flow. In primary neuron cultures and *in vivo* stroke studies, neurons from female rats have better survival

compared to neurons from male rats, suggesting greater resilience to low oxygen environments (3, 40, 102). Furthermore, AngII-hypertensive female mice have conserved neurovascular coupling, which describes the ability of the cerebrovasculature to adjust blood flow to meet neuronal metabolic demands (37, 46). These previous reports combined with data presented here suggest that sex dependent protection against PA and neuronal impairments may mediate maintained cognitive function in hypertensive female mice.

Increased inflammation is a hallmark of various hypertension-associated neurovascular alterations including vascular remodeling (48), endothelial dysfunction (61), and cognitive impairment. The anti-inflammatory effects of estrogen have been well documented (35, 92), and this reduction of inflammatory factors helps maintain neurovascular health in pathological states. At baseline, male mice have more pro-inflammatory microglia than female mice, and male mice that have undergone cerebral ischemia have a more favorable outcome after transplantation of microglia isolated and purified from female mice (91). Furthermore, female mice have more GFAP-positive astrocytes than male mice and female sex protects against reactive astrogliosis after injury (5, 69). Our data are consistent with these reports, and suggest male mice have a greater inflammatory response to AngII-hypertension than female mice. AngII infusion directly increases inflammation and oxidative stress via increased NADPH oxidase activity (10, 38, 51). Importantly, others have demonstrated that oxidative stress impairs AKAP150-TRPV4 interaction at MEPs in mesenteric arteries (65), which likely mediates disrupted TRPV4 signaling in hypertension (85). It is therefore possible that reduced inflammation and oxidative stress observed in the female mice facilitate their protection

against impaired TRPV4-mediated dilation and cognitive dysfunction. Future studies will be necessary to directly investigate the influence of sex hormones on neuroinflammation and TRPV4 signaling in PAs.

There are some limitations in our study we must address. Laser speckle contrast imaging allows for assessment of blood flow alterations on the surface of the brain but does not allow for measurements at the level of the PAs. This prevents us from determining hypertension-induced sex differences in blood flow alterations in the microcirculation. Additionally, this study did not include experiments to directly assess the influence of sex hormones on the vascular and cognitive changes observed. Our goal was to determine sex differences in the response to hypertension in young mice. Future studies will be focused on assessing the specific role sex hormones play in this paradigm.

This study is the first to directly compare sex differences in PA and cognitive function in hypertension. To make these comparisons, we used a novel method of matching both the dose of AngII and the blood pressure elevation between sexes. To summarize our findings, hypertensive female mice were protected from impaired TRPV4-mediated PA dilation and associated cognitive decline observed in hypertensive male mice. This was accompanied by a dampened response to neuroinflammation in female mice. Our findings indicate that some, but not all, of the negative effects of AngII are mitigated by female sex hormones. Further, we demonstrate that at least in females, it is possible to have cerebral hypoperfusion yet be cognitively intact. Understanding sex differences in cerebrovascular physiology and the influence of hypertension in young mice is an essential first step in defining underlying sex dependent mechanisms in vascular dementia development.

REFERENCES

1. **Aanerud J**, **Borghammer P**, **Rodell A**, **Jónsdottir KY**, **Gjedde A**. Sex differences of human cortical blood flow and energy metabolism. *J Cereb Blood Flow Metab* 37: 2433–2440, 2017. doi: 10.1177/0271678X16668536.

2. **Alisch JSR**, **Khattar N**, **Kim RW**, **Cortina LE**, **Rejimon AC**, **Qian W**, **Ferrucci L**, **Resnick SM**, **Spencer RG**, **Bouhrara M**. Sex and age-related differences in cerebral blood flow investigated using pseudo-continuous arterial spin labeling magnetic resonance imaging. *Aging (Albany NY)* 13: 4911–4925, 2021. doi: 10.18632/aging.202673.

3. **Alkayed NJ**, **Harukuni I**, **Kimes AS**, **London ED**, **Traystman RJ**, **Hurn PD**. Gender-linked brain injury in experimental stroke. *Stroke* 29: 159–65; discussion 166, 1998. doi: 10.1161/01.str.29.1.159.

4. **Arias-Loza P-A**, **Muehlfelder M**, **Pelzer T**. Estrogen and estrogen receptors in cardiovascular oxidative stress. *Pflugers Arch* 465: 739–746, 2013. doi: 10.1007/s00424-013-1247-7.

5. **Arias C**, **Zepeda A**, **Hernández-Ortega K**, **Leal-Galicia P**, **Lojero C**, **Camacho-Arroyo I**. Sex and estrous cycle-dependent differences in glial fibrillary acidic protein immunoreactivity in the adult rat hippocampus. *Horm Behav* 55: 257–263, 2009. doi: 10.1016/j.yhbeh.2008.10.016.

6. **Attar A**, **Liu T**, **Chan W-TC**, **Hayes J**, **Nejad M**, **Lei K**, **Bitan G**. A shortened Barnes maze protocol reveals memory deficits at 4-months of age in the triple-transgenic mouse model of Alzheimer's disease. *PLoS ONE* 8: e80355, 2013. doi: 10.1371/journal.pone.0080355.

7. **Barnes CA**. Memory deficits associated with senescence: a neurophysiological and behavioral study in the rat. *J Comp Physiol Psychol* 93: 74–104, 1979. doi: 10.1037/h0077579.

8. **Baumbach GL**, **Hajdu MA**. Mechanics and composition of cerebral arterioles in renal and spontaneously hypertensive rats. *Hypertension* 21: 816–826, 1993. doi: 10.1161/01.hyp.21.6.816.

9. **Berger-Sweeney J**, **Arnold A**, **Gabeau D**, **Mills J**. Sex differences in learning and memory in mice: effects of sequence of testing and cholinergic blockade. *Behav Neurosci* 109: 859–873, 1995. doi: 10.1037//0735-7044.109.5.859.

10. **Bloch S**, **Obari D**, **Girouard H**. Angiotensin and neurovascular coupling: beyond hypertension. *Microcirculation* 22: 159–167, 2015. doi: 10.1111/micc.12193.

11. **Blokland A**, **Rutten K**, **Prickaerts J**. Analysis of spatial orientation strategies of male and female Wistar rats in a Morris water escape task. *Behav Brain Res* 171: 216–224, 2006. doi: 10.1016/j.bbr.2006.03.033.

12. **Brands MW**, **Banes-Berceli AKL**, **Inscho EW**, **Al-Azawi H**, **Allen AJ**, **Labazi H**. Interleukin 6 knockout prevents angiotensin II hypertension: role of renal vasoconstriction and janus kinase 2/signal transducer and activator of transcription 3 activation. *Hypertension* 56: 879–884, 2010. doi: 10.1161/HYPERTENSIONAHA.110.158071.

13. **Brosnihan KB**, **Li P**, **Ganten D**, **Ferrario CM**. Estrogen protects transgenic hypertensive rats by shifting the vasoconstrictor-vasodilator balance of RAS. *Am J Physiol* 273: R1908-15, 1997. doi: 10.1152/ajpregu.1997.273.6.R1908.

14. **Bukowska A**, **Spiller L**, **Wolke C**, **Lendeckel U**, **Weinert S**, **Hoffmann J**, **Bornfleth P**, **Kutschka I**, **Gardemann A**, **Isermann B**, **Goette A**. Protective regulation of the ACE2/ACE gene expression by estrogen in human atrial tissue from elderly men. *Exp Biol Med (Maywood)* 242: 1412–1423, 2017. doi: 10.1177/1535370217718808.

15. **Cao S**, **Anishkin A**, **Zinkevich NS**, **Nishijima Y**, **Korishettar A**, **Wang Z**, **Fang J**, **Wilcox DA**, **Zhang DX**. Transient receptor potential vanilloid 4 (TRPV4) activation by arachidonic acid requires protein kinase A-mediated phosphorylation. .

16. **Chambers LC**, **Diaz-Otero JM**, **Fisher CL**, **Jackson WF**, **Dorrance AM**. Mineralocorticoid receptor antagonism improves transient receptor potential vanilloid 4-dependent dilation of cerebral parenchymal arterioles and cognition in a genetic model of hypertension. *J Hypertens* 40: 1722–1734, 2022. doi: 10.1097/HJH.0000000000003208.

17. **Chen D-R**, **Jiang H**, **Chen J**, **Ruan C-C**, **Han W-Q**, **Gao P-J**. Involvement of Angiotensin II Type 1 Receptor and Calcium Channel in Vascular Remodeling and Endothelial Dysfunction in Rats with Pressure Overload. *CURR MED SCI* 40: 320–326, 2020. doi: 10.1007/s11596-020-2171-7.

18. **Chinnathambi V**, **More AS**, **Hankins GD**, **Yallampalli C**, **Sathishkumar K**. Gestational exposure to elevated testosterone levels induces hypertension via heightened vascular angiotensin II type 1 receptor signaling in rats. *Biol Reprod* 91: 6, 2014. doi: 10.1095/biolreprod.114.118968.

19. **Cipolla MJ**, **Smith J**, **Kohlmeyer MM**, **Godfrey JA**. SKCa and IKCa Channels, myogenic tone, and vasodilator responses in middle cerebral arteries and parenchymal arterioles: effect of ischemia and reperfusion. *Stroke* 40: 1451–1457, 2009. doi: 10.1161/STROKEAHA.108.535435.

20. **de Godoy MAF**, **de Oliveira AM**, **Rattan S**. Angiotensin II-induced relaxation of anococcygeus smooth muscle via desensitization of AT1 receptor, and activation of AT2 receptor associated with nitric-oxide synthase pathway. *J Pharmacol Exp Ther* 311: 394–401, 2004. doi: 10.1124/jpet.104.069856.

21. **De Mey C**, **Vanhoutte PM**. Effect of age and spontaneous hypertension on the tachyphylaxis to 5-hydroxytryptamine and angiotensin II in the isolated rat kidney. *Hypertension* 3: 718–724, 1981. doi: 10.1161/01.hyp.3.6.718.

22. **De Silva TM**, **Faraci FM**. Effects of angiotensin II on the cerebral circulation: role of oxidative stress. *Front Physiol* 3: 484, 2012. doi: 10.3389/fphys.2012.00484.

23. **Diaz-Otero JM**, **Fisher C**, **Downs K**, **Moss EM**, **Jaffe IZ**, **Jackson WF**, **Dorrance AM**. Endothelial Mineralocorticoid Receptor Mediates Parenchymal Arteriole and Posterior Cerebral Artery Remodeling During Angiotensin II–Induced Hypertension. .

24. **Diaz-Otero JM**, **Yen T-C**, **Ahmad A**, **Laimon-Thomson E**, **Abolibdeh B**, **Kelly K**, **Lewis MT**, **Wiseman RW**, **Jackson WF**, **Dorrance AM**. Transient receptor potential vanilloid 4 channels are important regulators of parenchymal arteriole dilation and cognitive function. *Microcirculation* 26: e12535, 2019. doi: 10.1111/micc.12535.

25. **Diaz-Otero JM**, **Yen T-C**, **Fisher C**, **Bota D**, **Jackson WF**, **Dorrance AM**. Mineralocorticoid receptor antagonism improves parenchymal arteriole dilation via a TRPV4-dependent mechanism and prevents cognitive dysfunction in hypertension. *Am J Physiol Heart Circ Physiol* 315: H1304–H1315, 2018. doi: 10.1152/ajpheart.00207.2018.

26. **Duckles SP**, **Krause DN**. Cerebrovascular effects of oestrogen: multiplicity of action. *Clin Exp Pharmacol Physiol* 34: 801–808, 2007. doi: 10.1111/j.1440-1681.2007.04683.x.

27. **Duncombe J**, **Kitamura A**, **Hase Y**, **Ihara M**, **Kalaria RN**, **Horsburgh K**. Chronic cerebral hypoperfusion: a key mechanism leading to vascular cognitive impairment and dementia. Closing the translational gap between rodent models and human vascular cognitive impairment and dementia. *Clin Sci* 131: 2451–2468, 2017. doi: 10.1042/CS20160727.

28. **Fan H-C**, **Zhang X**, **McNaughton PA**. Activation of the TRPV4 ion channel is enhanced by phosphorylation. *J Biol Chem* 284: 27884–27891, 2009. doi: 10.1074/jbc.M109.028803.

29. **Fernandes L**, **Fortes ZB**, **Nigro D**, **Tostes RC**, **Santos RA**, **Catelli De Carvalho MH**. Potentiation of bradykinin by angiotensin-(1-7) on arterioles of spontaneously

hypertensive rats studied in vivo. *Hypertension* 37: 703–709, 2001. doi: 10.1161/01.hyp.37.2.703.

30. **Fernando MS**, **Ince PG**, **MRC Cognitive Function and Ageing Neuropathology Study Group**. Vascular pathologies and cognition in a population-based cohort of elderly people. *J Neurol Sci* 226: 13–17, 2004. doi: 10.1016/j.jns.2004.09.004.

31. **Forrester SJ**, **Booz GW**, **Sigmund CD**, **Coffman TM**, **Kawai T**, **Rizzo V**, **Scalia R**, **Eguchi S**. Angiotensin II signal transduction: an update on mechanisms of physiology and pathophysiology. *Physiol Rev* 98: 1627–1738, 2018. doi: 10.1152/physrev.00038.2017.

32. **Fraga-Silva RA**, **Costa-Fraga FP**, **Murça TM**, **Moraes PL**, **Martins Lima A**, **Lautner RQ**, **Castro CH**, **Soares CMA**, **Borges CL**, **Nadu AP**, **Oliveira ML**, **Shenoy V**, **Katovich MJ**, **Santos RAS**, **Raizada MK**, **Ferreira AJ**. Angiotensin-converting enzyme 2 activation improves endothelial function. *Hypertension* 61: 1233–1238, 2013. doi: 10.1161/HYPERTENSIONAHA.111.00627.

33. **Fredette NC**, **Meyer MR**, **Prossnitz ER**. Role of GPER in estrogen-dependent nitric oxide formation and vasodilation. *J Steroid Biochem Mol Biol* 176: 65–72, 2018. doi: 10.1016/j.jsbmb.2017.05.006.

34. **Freshour JR**, **Chase SE**, **Vikstrom KL**. Gender differences in cardiac ACE expression are normalized in androgen-deprived male mice. *Am J Physiol Heart Circ Physiol* 283: H1997-2003, 2002. doi: 10.1152/ajpheart.01054.2001.

35. **Ghisletti S**, **Meda C**, **Maggi A**, **Vegeto E**. 17beta-estradiol inhibits inflammatory gene expression by controlling NF-kappaB intracellular localization. *Mol Cell Biol* 25: 2957–2968, 2005. doi: 10.1128/MCB.25.8.2957-2968.2005.

36. **Gilsanz P**, **Mayeda ER**, **Glymour MM**, **Quesenberry CP**, **Mungas DM**, **DeCarli C**, **Dean A**, **Whitmer RA**. Female sex, early-onset hypertension, and risk of dementia. *Neurology* 89: 1886–1893, 2017. doi: 10.1212/WNL.0000000000004602.

37. **Girouard H**, **Lessard A**, **Capone C**, **Milner TA**, **Iadecola C**. The neurovascular dysfunction induced by angiotensin II in the mouse neocortex is sexually dimorphic. *Am J Physiol Heart Circ Physiol* 294: H156-63, 2008. doi: 10.1152/ajpheart.01137.2007.

38. **Girouard H**, **Park L**, **Anrather J**, **Zhou P**, **Iadecola C**. Angiotensin II attenuates endothelium-dependent responses in the cerebral microcirculation through nox-2-derived radicals. *Arterioscler Thromb Vasc Biol* 26: 826–832, 2006. doi: 10.1161/01.ATV.0000205849.22807.6e.

39. **Gur RC**, **Gur RE**, **Obrist WD**, **Hungerbuhler JP**, **Younkin D**, **Rosen AD**, **Skolnick BE**, **Reivich M**. Sex and handedness differences in cerebral blood flow during rest and cognitive activity. *Science* 217: 659–661, 1982. doi: 10.1126/science.7089587.

40. **Hall ED**, **Pazara KE**, **Linseman KL**. Sex differences in postischemic neuronal necrosis in gerbils. *J Cereb Blood Flow Metab* 11: 292–298, 1991. doi: 10.1038/jcbfm.1991.61.

41. **Hannah RM**, **Dunn KM**, **Bonev AD**, **Nelson MT**. Endothelial SK(Ca) and IK(Ca) channels regulate brain parenchymal arteriolar diameter and cortical cerebral blood flow. *J Cereb Blood Flow Metab* 31: 1175–1186, 2011. doi: 10.1038/jcbfm.2010.214.

42. **Hannan RE**, **Davis EA**, **Widdop RE**. Functional role of angiotensin II AT2 receptor in modulation of AT1 receptor-mediated contraction in rat uterine artery: involvement of bradykinin and nitric oxide. *Br J Pharmacol* 140: 987–995, 2003. doi: 10.1038/sj.bjp.0705484.

43. **Hébert R**, **Lindsay J**, **Verreault R**, **Rockwood K**, **Hill G**, **Dubois MF**. Vascular dementia : incidence and risk factors in the Canadian study of health and aging. *Stroke* 31: 1487–1493, 2000. doi: 10.1161/01.str.31.7.1487.

44. **Holloway AC**, **Qian H**, **Pipolo L**, **Ziogas J**, **Miura S**, **Karnik S**, **Southwell BR**, **Lew MJ**, **Thomas WG**. Side-chain substitutions within angiotensin II reveal different requirements for signaling, internalization, and phosphorylation of type 1A angiotensin receptors. *Mol Pharmacol* 61: 768–777, 2002. doi: 10.1124/mol.61.4.768.

45. **Husarek KE**, **Katz PS**, **Trask AJ**, **Galantowicz ML**, **Cismowski MJ**, **Lucchesi PA**. The angiotensin receptor blocker losartan reduces coronary arteriole remodeling in type 2 diabetic mice. *Vascul Pharmacol* 76: 28–36, 2016. doi: 10.1016/j.vph.2015.06.013.

46. **Iadecola C**. The Neurovascular Unit Coming of Age: A Journey through Neurovascular Coupling in Health and Disease. *Neuron* 96: 17–42, 2017. doi: 10.1016/j.neuron.2017.07.030.

47. **Ibrahim J**, **McGee A**, **Graham D**, **McGrath JC**, **Dominiczak AF**. Sex-specific differences in cerebral arterial myogenic tone in hypertensive and normotensive rats. *Am J Physiol Heart Circ Physiol* 290: H1081-9, 2006. doi: 10.1152/ajpheart.00752.2005.

48. **Intengan HD**, **Schiffrin EL**. Vascular Remodeling in Hypertension. *Hypertension* 38: 581–587, 2001. doi: 10.1161/hy09t1.096249.

49. **Jennings JR**, **Muldoon MF**, **Ryan C**, **Price JC**, **Greer P**, **Sutton-Tyrrell K**, **van der Veen FM**, **Meltzer CC**. Reduced cerebral blood flow response and compensation among patients with untreated hypertension. *Neurology* 64: 1358–1365, 2005. doi: 10.1212/01.WNL.0000158283.28251.3C.

50. **Jiménez-Altayó F**, **Martín A**, **Rojas S**, **Justicia C**, **Briones AM**, **Giraldo J**, **Planas AM**, **Vila E**. Transient middle cerebral artery occlusion causes different structural, mechanical, and myogenic alterations in normotensive and hypertensive rats. *Am J Physiol Heart Circ Physiol* 293: H628-35, 2007. doi: 10.1152/ajpheart.00165.2007.

51. **Kazama K**, **Anrather J**, **Zhou P**, **Girouard H**, **Frys K**, **Milner TA**, **Iadecola C**. Angiotensin II impairs neurovascular coupling in neocortex through NADPH oxidase-derived radicals. *Circ Res* 95: 1019–1026, 2004. doi: 10.1161/01.RES.0000148637.85595.c5.

52. **Kraeuter A-K**, **Guest PC**, **Sarnyai Z**. The Y-Maze for Assessment of Spatial Working and Reference Memory in Mice. *Methods Mol Biol* 1916: 105–111, 2019. doi: 10.1007/978-1-4939-8994-2_10.

53. **Liu W**, **Lou X**, **Ma L**. Use of 3D pseudo-continuous arterial spin labeling to characterize sex and age differences in cerebral blood flow. *Neuroradiology* 58: 943–948, 2016. doi: 10.1007/s00234-016-1713-y.

54. **Matin N**, **Fisher C**, **Jackson WF**, **Dorrance AM**. Bilateral common carotid artery stenosis in normotensive rats impairs endothelium-dependent dilation of parenchymal arterioles. *Am J Physiol Heart Circ Physiol* 310: H1321-9, 2016. doi: 10.1152/ajpheart.00890.2015.

55. **Matin N**, **Fisher C**, **Lansdell TA**, **Hammock BD**, **Yang J**, **Jackson WF**, **Dorrance AM**. Soluble epoxide hydrolase inhibition improves cognitive function and parenchymal artery dilation in a hypertensive model of chronic cerebral hypoperfusion. *Microcirculation* 28: e12653, 2021. doi: 10.1111/micc.12653.

56. **McIntyre M**, **Hamilton CA**, **Rees DD**, **Reid JL**, **Dominiczak AF**. Sex differences in the abundance of endothelial nitric oxide in a model of genetic hypertension. *Hypertension* 30: 1517–1524, 1997. doi: 10.1161/01.hyp.30.6.1517.

57. **McNeill AM**, **Kim N**, **Duckles SP**, **Krause DN**, **Kontos HA**. Chronic estrogen treatment increases levels of endothelial nitric oxide synthase protein in rat cerebral microvessels. *Stroke* 30: 2186–2190, 1999. doi: 10.1161/01.str.30.10.2186.

58. **McNeill AM**, **Zhang C**, **Stanczyk FZ**, **Duckles SP**, **Krause DN**. Estrogen increases endothelial nitric oxide synthase via estrogen receptors in rat cerebral blood vessels: effect preserved after concurrent treatment with

medroxyprogesterone acetate or progesterone. *Stroke* 33: 1685–1691, 2002. doi: 10.1161/01.str.0000016325.54374.93.

59. **Medina D**, **Mehay D**, **Arnold AC**. Sex differences in cardiovascular actions of the renin-angiotensin system. *Clin Auton Res* 30: 393–408, 2020. doi: 10.1007/s10286-020-00720-2.

60. **Mishra JS**, **More AS**, **Gopalakrishnan K**, **Kumar S**. Testosterone plays a permissive role in angiotensin II-induced hypertension and cardiac hypertrophy in male rats. *Biol Reprod* 100: 139–148, 2019. doi: 10.1093/biolre/ioy179.

61. **Montezano AC**, **Nguyen Dinh Cat A**, **Rios FJ**, **Touyz RM**. Angiotensin II and vascular injury. *Curr Hypertens Rep* 16: 431, 2014. doi: 10.1007/s11906-014-0431-2.

62. **Moss ME**, **Carvajal B**, **Jaffe IZ**. The endothelial mineralocorticoid receptor: Contributions to sex differences in cardiovascular disease. *Pharmacol Ther* 203: 107387, 2019. doi: 10.1016/j.pharmthera.2019.06.009.

63. **Muller M**, **van der Graaf Y**, **Visseren FL**, **Mali WPTM**, **Geerlings MI**, **SMART Study Group**. Hypertension and longitudinal changes in cerebral blood flow: the SMART-MR study. *Ann Neurol* 71: 825–833, 2012. doi: 10.1002/ana.23554.

64. **Nakashima T**, **Umemoto S**, **Yoshimura K**, **Matsuda S**, **Itoh S**, **Murata T**, **Fukai T**, **Matsuzaki M**. TLR4 is a critical regulator of angiotensin II-induced vascular remodeling: the roles of extracellular SOD and NADPH oxidase. *Hypertens Res* 38: 649–655, 2015. doi: 10.1038/hr.2015.55.

65. **Ottolini M**, **Hong K**, **Cope EL**, **Daneva Z**, **DeLalio LJ**, **Sokolowski JD**, **Marziano C**, **Nguyen NY**, **Altschmied J**, **Haendeler J**, **Johnstone SR**, **Kalani MY**, **Park MS**, **Patel RP**, **Liedtke W**, **Isakson BE**, **Sonkusare SK**. Local peroxynitrite impairs endothelial transient receptor potential vanilloid 4 channels and elevates blood pressure in obesity. *Circulation* 141: 1318–1333, 2020. doi: 10.1161/CIRCULATIONAHA.119.043385.

66. **Oyola MG**, **Handa RJ**. Hypothalamic-pituitary-adrenal and hypothalamic-pituitary-gonadal axes: sex differences in regulation of stress responsivity. *Stress* 20: 476–494, 2017. doi: 10.1080/10253890.2017.1369523.

67. **Pacurari M**, **Kafoury R**, **Tchounwou PB**, **Ndebele K**. The Renin-Angiotensin-aldosterone system in vascular inflammation and remodeling. *Int J Inflam* 2014: 689360, 2014. doi: 10.1155/2014/689360.

68. **Pekny M**, **Pekna M**. Astrocyte reactivity and reactive astrogliosis: costs and benefits. *Physiol Rev* 94: 1077–1098, 2014. doi: 10.1152/physrev.00041.2013.

69. **Pérez-Álvarez MJ**, **Maza MDC**, **Anton M**, **Ordoñez L**, **Wandosell F**. Post-ischemic estradiol treatment reduced glial response and triggers distinct cortical and hippocampal signaling in a rat model of cerebral ischemia. *J Neuroinflammation* 9: 157, 2012. doi: 10.1186/1742-2094-9-157.

70. **Pessôa BS**, **Slump DE**, **Ibrahimi K**, **Grefhorst A**, **van Veghel R**, **Garrelds IM**, **Roks AJM**, **Kushner SA**, **Danser AHJ**, **van Esch JHM**. Angiotensin II type 2 receptor- and acetylcholine-mediated relaxation: essential contribution of female sex hormones and chromosomes. *Hypertension* 66: 396–402, 2015. doi: 10.1161/HYPERTENSIONAHA.115.05303.

71. **Pires PW**, **Jackson WF**, **Dorrance AM**. Regulation of myogenic tone and structure of parenchymal arterioles by hypertension and the mineralocorticoid receptor. *Am J Physiol Heart Circ Physiol* 309: H127-36, 2015. doi: 10.1152/ajpheart.00168.2015.

72. **Polycarpou A**, **Hricisák L**, **Iring A**, **Safar D**, **Ruisanchez É**, **Horváth B**, **Sándor P**, **Benyó Z**. Adaptation of the cerebrocortical circulation to carotid artery occlusion involves blood flow redistribution between cortical regions and is independent of eNOS. *Am J Physiol Heart Circ Physiol* 311: H972–H980, 2016. doi: 10.1152/ajpheart.00197.2016.

73. **Reed JT**, **Pareek T**, **Sriramula S**, **Pabbidi MR**. Aging influences cerebrovascular myogenic reactivity and BK channel function in a sex-specific manner. *Cardiovasc Res* 116: 1372–1385, 2020. doi: 10.1093/cvr/cvz314.

74. **Rodriguez G**, **Warkentin S**, **Risberg J**, **Rosadini G**. Sex differences in regional cerebral blood flow. *J Cereb Blood Flow Metab* 8: 783–789, 1988. doi: 10.1038/jcbfm.1988.133.

75. **Roman MJ**, **Saba PS**, **Pini R**, **Spitzer M**, **Pickering TG**, **Rosen S**, **Alderman MH**, **Devereux RB**. Parallel cardiac and vascular adaptation in hypertension. *Circulation* 86: 1909–1918, 1992. doi: 10.1161/01.cir.86.6.1909.

76. **Safari S**, **Ahmadi N**, **Mohammadkhani R**, **Ghahremani R**, **Khajvand-Abedeni M**, **Shahidi S**, **Komaki A**, **Salehi I**, **Karimi SA**. Sex differences in spatial learning and memory and hippocampal long-term potentiation at perforant pathway-dentate gyrus (PP-DG) synapses in Wistar rats. *Behav Brain Funct* 17: 9, 2021. doi: 10.1186/s12993-021-00184-y.

77. **Salinero AE**, **Robison LS**, **Gannon OJ**, **Riccio D**, **Mansour F**, **Abi-Ghanem C**, **Zuloaga KL**. Sex-specific effects of high-fat diet on cognitive impairment in a mouse model of VCID. *FASEB J* 34: 15108–15122, 2020. doi: 10.1096/fj.202000085R.

78. **Sampaio WO**, **Souza dos Santos RA**, **Faria-Silva R**, **da Mata Machado LT**, **Schiffrin EL**, **Touyz RM**. Angiotensin-(1-7) through receptor Mas mediates endothelial nitric oxide synthase activation via Akt-dependent pathways. *Hypertension* 49: 185–192, 2007. doi: 10.1161/01.HYP.0000251865.35728.2f.

79. **Sampson AK**, **Moritz KM**, **Jones ES**, **Flower RL**, **Widdop RE**, **Denton KM**. Enhanced angiotensin II type 2 receptor mechanisms mediate decreases in arterial pressure attributable to chronic low-dose angiotensin II in female rats. *Hypertension* 52: 666–671, 2008. doi: 10.1161/HYPERTENSIONAHA.108.114058.

80. **Saucier DM**, **Shultz SR**, **Keller AJ**, **Cook CM**, **Binsted G**. Sex differences in object location memory and spatial navigation in Long-Evans rats. *Anim Cogn* 11: 129–137, 2008. doi: 10.1007/s10071-007-0096-1.

81. **Schwinn DA**, **McIntyre RW**, **Reves JG**. Isoflurane-induced vasodilation: role of the alpha-adrenergic nervous system. *Anesth Analg* 71: 451–459, 1990.

82. **Shih AY**, **Blinder P**, **Tsai PS**, **Friedman B**, **Stanley G**, **Lyden PD**, **Kleinfeld D**. The smallest stroke: occlusion of one penetrating vessel leads to infarction and a cognitive deficit. *Nat Neurosci* 16: 55–63, 2013. doi: 10.1038/nn.3278.

83. **Silva-Antonialli MM**, **Tostes RCA**, **Fernandes L**, **Fior-Chadi DR**, **Akamine EH**, **Carvalho MHC**, **Fortes ZB**, **Nigro D**. A lower ratio of AT1/AT2 receptors of angiotensin II is found in female than in male spontaneously hypertensive rats. *Cardiovasc Res* 62: 587–593, 2004. doi: 10.1016/j.cardiores.2004.01.020.

84. **Sonkusare SK**, **Bonev AD**, **Ledoux J**, **Liedtke W**, **Kotlikoff MI**, **Heppner TJ**, **Hill-Eubanks DC**, **Nelson MT**. Elementary Ca2+ signals through endothelial TRPV4 channels regulate vascular function. *Science* 336: 597–601, 2012. doi: 10.1126/science.1216283.

85. **Sonkusare SK**, **Dalsgaard T**, **Bonev AD**, **Hill-Eubanks DC**, **Kotlikoff MI**, **Scott JD**, **Santana LF**, **Nelson MT**. AKAP150-dependent cooperative TRPV4 channel gating is central to endothelium-dependent vasodilation and is disrupted in hypertension. *Sci Signal* 7: ra66, 2014. doi: 10.1126/scisignal.2005052.

86. **Stanimirovic DB**, **Friedman A**. Pathophysiology of the neurovascular unit: disease cause or consequence? *J Cereb Blood Flow Metab* 32: 1207–1221, 2012. doi: 10.1038/jcbfm.2012.25.

87. **Sullivan JC**, **Rodriguez-Miguelez P**, **Zimmerman MA**, **Harris RA**. Differences in angiotensin (1-7) between men and women. *Am J Physiol Heart Circ Physiol* 308: H1171-6, 2015. doi: 10.1152/ajpheart.00897.2014.

88. **Tamura K**, **Kanaoka T**, **Kobayashi R**, **Ohki K**, **Ohsawa M**. TLR4 as a possible key regulator of pathological vascular remodeling by Ang II receptor activation. *Hypertens Res* 38: 642–643, 2015. doi: 10.1038/hr.2015.65.

89. **Tavares G**, **Martins M**, **Correia JS**, **Sardinha VM**, **Guerra-Gomes S**, **das Neves SP**, **Marques F**, **Sousa N**, **Oliveira JF**. Employing an open-source tool to assess astrocyte tridimensional structure. *Brain Struct Funct* 222: 1989–1999, 2017. doi: 10.1007/s00429-016-1316-8.

90. **Touyz RM**. Intracellular mechanisms involved in vascular remodelling of resistance arteries in hypertension: role of angiotensin II. *Exp Physiol* 90: 449–455, 2005. doi: 10.1113/expphysiol.2005.030080.

91. **Villa A**, **Gelosa P**, **Castiglioni L**, **Cimino M**, **Rizzi N**, **Pepe G**, **Lolli F**, **Marcello E**, **Sironi L**, **Vegeto E**, **Maggi A**. Sex-Specific Features of Microglia from Adult Mice. *Cell Rep* 23: 3501–3511, 2018. doi: 10.1016/j.celrep.2018.05.048.

92. **Villa A**, **Vegeto E**, **Poletti A**, **Maggi A**. Estrogens, neuroinflammation, and neurodegeneration. *Endocr Rev* 37: 372–402, 2016. doi: 10.1210/er.2016-1007.

93. **Waldstein SR**, **Lefkowitz DM**, **Siegel EL**, **Rosenberger WF**, **Spencer RJ**, **Tankard CF**, **Manukyan Z**, **Gerber EJ**, **Katzel L**. Reduced cerebral blood flow in older men with higher levels of blood pressure. *J Hypertens* 28: 993–998, 2010. doi: 10.1097/hjh.0b013e328335c34f.

94. **Wang C**, **Qian X**, **Sun X**, **Chang Q**. Angiotensin II increases matrix metalloproteinase 2 expression in human aortic smooth muscle cells via AT1R and ERK1/2. *Exp Biol Med (Maywood)* 240: 1564–1571, 2015. doi: 10.1177/1535370215576312.

95. **Wang S**, **Zhang H**, **Liu Y**, **Li L**, **Guo Y**, **Jiao F**, **Fang X**, **Jefferson JR**, **Li M**, **Gao W**, **Gonzalez-Fernandez E**, **Maranon RO**, **Pabbidi MR**, **Liu R**, **Alexander BT**, **Roman RJ**, **Fan F**. Sex differences in the structure and function of rat middle cerebral arteries. .

96. **Wilhelmsson U**, **Bushong EA**, **Price DL**, **Smarr BL**, **Phung V**, **Terada M**, **Ellisman MH**, **Pekny M**. Redefining the concept of reactive astrocytes as cells that remain within their unique domains upon reaction to injury. *Proc Natl Acad Sci USA* 103: 17513–17518, 2006. doi: 10.1073/pnas.0602841103.

97. **Wolters FJ**, **Zonneveld HI**, **Hofman A**, **van der Lugt A**, **Koudstaal PJ**, **Vernooij MW**, **Ikram MA**, **Heart-Brain Connection Collaborative Research Group**. Cerebral Perfusion and the Risk of Dementia: A Population-Based Study. *Circulation* 136: 719–728, 2017. doi: 10.1161/CIRCULATIONAHA.117.027448.

98. **Xue B**, **Pamidimukkala J**, **Hay M**. Sex differences in the development of angiotensin II-induced hypertension in conscious mice. *Am J Physiol Heart Circ Physiol* 288: H2177-84, 2005. doi: 10.1152/ajpheart.00969.2004.

99. **Xue B**, **Pamidimukkala J**, **Lubahn DB**, **Hay M**. Estrogen receptor-alpha mediates estrogen protection from angiotensin II-induced hypertension in conscious female mice. *Am J Physiol Heart Circ Physiol* 292: H1770-6, 2007. doi: 10.1152/ajpheart.01011.2005.

100. **Yamasaki E**, **Thakore P**, **Krishnan V**, **Earley S**. Differential expression of angiotensin II type 1 receptor subtypes within the cerebral microvasculature. *Am J Physiol Heart Circ Physiol* 318: H461–H469, 2019. doi: 10.1152/ajpheart.00582.2019.

101. **Zaccor NW**, **Sumner CJ**, **Snyder SH**. The nonselective cation channel TRPV4 inhibits angiotensin II receptors. *J Biol Chem* 295: 9986–9997, 2020. doi: 10.1074/jbc.RA120.014325.

102. **Zhang L**, **Li P-P**, **Feng X**, **Barker JL**, **Smith SV**, **Rubinow DR**. Sex-related differences in neuronal cell survival and signaling in rats. *Neurosci Lett* 337: 65–68, 2003. doi: 10.1016/s0304-3940(02)01179-5.

103. 2022 Alzheimer's disease facts and figures. *Alzheimers Dement* 18: 700–789, 2022. doi: 10.1002/alz.12638.

Chapter 4:

Endothelial TRPV4 Deletion Impairs Parenchymal Arteriolar Dilation and Cognitive Function

4.1 – Abstract

In models of hypertension and cerebral hypoperfusion, TRPV4 channel impairment is associated with cognitive decline. PA and cognitive function are severely impaired in rats with global TRPV4 deletion. However, this channel is ubiquitously expressed throughout the brain and due to lack of appropriate animal models, its cell type specific contribution has been difficult to elucidate. I tested the hypothesis that endothelial TRPV4 channels are critical for both PA and cognitive function. To this end, I used male and female 30-35-week-old endothelial TRPV4 knockout mice ($TRPV4_{EC^{-/-}}$) and littermate controls. Cerebral pial perfusion was measured by laser speckle contrast imaging. Pressure myography was used to assess PA dilatory function and structure. Cognitive function was tested using the spontaneous alternation task and novel arm recognition task in the Y-maze, as well as a nesting test. qRT-PCR and immunohistochemistry was used to assess markers of neuroinflammation and neuronal support. $TRPV4_{EC^{-/-}}$ did not have altered pial perfusion but had decreased sensitivity to IK_{Ca}/SK_{Ca}-mediated dilation in PAs with no changes to PA structure. Spatial working memory, spatial reference memory, and nesting behavior was impaired in $TRPV4_{EC^{-/-}}$ mice. This was associated with increased quantity and complexity of GFAP-positive astrocytes, suggesting an increase in neuroinflammation. This study demonstrates the importance of endothelial TRPV4 channels in cerebrovascular and cognitive health and suggest TRPV4 impairment may increase dementia risk.

4.2 – Introduction

CSVD describes a group of disorders characterized by structural and functional impairment of small arteries, arterioles, capillaries, and venules in the brain (20). Because the brain lacks its own energy stores, it is highly dependent on constant perfusion to bring oxygen and glucose to neurons. Failure of the microcirculation to direct blood flow appropriately starves neurons of required nutrients and can result in cognitive decline. The leading risk factor for CSVD is old age; CSVD affects nearly everyone over 90 years of age (8). However, CSVD can also be instigated and worsened by common modifiable risk factors like hypertension and diabetes mellitus (17, 21, 24). The increasing life expectancy and the increase in patients diagnosed with relevant risk factors mean CSVD prevalence is expected to grow (2). Importantly, CSVD contributes to nearly half of all dementia cases and currently has no cure (15).

PAs direct blood flow from pial arteries and arterioles to downstream capillaries. PAs are vital regulators of cerebral blood flow and contribute to 30-40% of cerebrovascular resistance (3–5). Unlike the pial arterioles on the brain's surface, PAs lack collateral connections and thus lack the ability to divert blood flow to circumvent a blockage. Therefore, the occlusion of a PA creates a discrete column of ischemic tissue that is sufficient to produce cognitive impairment (29). PAs primarily depend on TRPV4 channels for endothelium-dependent dilation, and our group showed that hypertension impairs TRPV4-mediated dilation and cognition. To examine this concept further, we employed a rat with global TRPV4 channel knockout and found that TRPV4$^{-/-}$ rats had obliterated endothelium-dependent dilation in PAs accompanied by severely blunted cognitive function (10). TRPV4 channels are ubiquitously expressed and are present in

several cell types involved in cognition, including endothelial cells, VSMCs, astrocytes, and neurons. Because of this, it has been impossible to directly link the importance of endothelial TRPV4 channels in PAs to cognitive function. To this end, we employed an endothelial cell-specific TRPV4 knockout mouse to test the hypothesis that endothelial TRPV4 channels are critical contributors to both PA and cognitive function.

4.3 – Materials and Methods

4.3.1 – Experimental Models

All experimental protocols were approved by the Michigan State University Animal Care and Use Committee and were performed in accordance with the National Institutes of Health Guide for the Care and Use of Laboratory Animals. $TRPV4_{EC}^{-/-}$ mice were generated by Dr. Swapnil Sonkusare at the University of Virginia by crossing $TRPV4^{fl/fl}$ mice with VE-Cadherin Cre mice, as described previously (6). Endothelium-specific knockout of TRPV4 was induced by injecting 6-week-old $TRPV4^{fl/fl}$ Cre^{+} mice with tamoxifen (40mg/kg/day for 10 days, i.p.). Tamoxifen-injected $TRPV4^{fl/fl}$ Cre^{-} mice were used as controls. Male and female mice were combined in experimental groups as this study was not powered to assess sex differences. Experiments were conducted at 30-35 weeks of age. All mice were housed on a 12:12h light/dark cycle with food and water *ad libitum*.

4.3.2 – Laser speckle contrast imaging

Just before euthanasia, cerebral pial blood flow was measured using laser speckle contrast imaging. Anesthesia was induced using 3% isoflurane in oxygen. The scalp was removed, and the skull was cleared of blood or connective tissue. A very thin coat of ultrasound gel was applied to the surface of the skull to improve image resolution. The

isoflurane concentration was reduced to 1%, and the mice equilibrated at this concentration for 5 min. Pial blood flow was measured at 21 images/s for 1 min. Regions of interest were defined as the parietal, frontal, and temporal regions in each hemisphere, as described by others (26). Mean blood flow in each region was compared between groups. Images were analyzed using PIMSoft software (PeriMed, Las Vegas, NV).

4.3.3 – Assessment of PA endothelial function

Pressure myography was used to assess PA structure, as described previously (9, 11, 22, 25). The brain was collected after euthanasia and kept in a cooled (4°C) dissection chamber in calcium-free PSS containing (in mM): 140.00 NaCl, 5.00 KCl, 1.00 $MgCl_2 * 7H_2O$, 10.00 HEPES, 10.00 dextrose. To isolate PAs, a 5mm x 3 mm section of the brain containing the MCA was dissected. The pia with the MCA were separated from the brain and the PAs branching off the MCA were used for experiments. Isolated arterioles were cannulated with two glass micropipettes in a custom-made cannulation chamber. Arterioles were equilibrated at 37°C in aCSF containing (in mM): 124.00 NaCl, 3.00 KCl, 2.00 $CaCl_2$, 2.00 $MgCl_2$, 1.25 NaH_2PO_4, 26.00 $NaHCO_3$, and 4.00 dextrose. A servo-controlled system was used to pressurize the arterioles (Living Systems, St Albans City, VT). A leak test was performed before each experiment, and any arteriole that could not maintain its intralumenal pressure was discarded. Arterioles were pressurized to 40mmHg until the development of stable myogenic tone {percent tone = [1 – (active lumen diameter/passive lumen diameter)] x 100}. Arterioles that generated at least 20% myogenic tone were used for experiments. Arterioles that did not develop sufficient myogenic tone were used for structural assessment only. The lumen and outer diameters of PAs were measured using a Nikon Eclipse TS100 microscope and a 40x objective

(Nikon Plan Fluor objective; numerical aperture 0.75). The averages of the lumen and outer diameters were recorded using MyoView 2.0 software (Danish Myo Technology, Aarhus, Denmark). After the generation of myogenic tone, endothelium-dependent dilation was assessed. To measure TRPV4-mediated dilation, increasing concentrations of the specific TRPV4 agonist GSK1016790A (10^{-9} – 10^{-5}M) were added to the bath. To assess downstream IK_{Ca}/SK_{Ca}-mediated dilation, PAs were incubated with increasing concentrations of the agonist NS309 (10^{-9} – 10^{-5}M). Each PA was used for only one dilation experiment.

4.3.4 – Assessment of passive PA structure

The passive structure was assessed after the completion of dilation experiments or if PAs failed to generate sufficient myogenic tone. aCSF was washed away and replaced with Ca^{2+}-free PSS containing EGTA (29mM) and SNP (10^{-5}M). To assess the structure of the arterioles, a pressure-diameter response curve was constructed by increasing the intralumenal pressure from 3 to 120mmHg at 20mmHg increments. The arterioles were equilibrated at each pressure for 5min, and the lumen and outer diameters were measured. These values were used to calculate wall thickness (outer diameter – lumen diameter), wall cross-sectional area (arteriole area – lumen area), wall-to-lumen ratio, wall stress, strain, and distensibility, as described (1). Wall stiffness was quantified using the β -coefficient calculated from the individual stress-strain curves using the model $y = ae^{\beta x}$, where y is wall stress, x is wall strain, a is the intercept and β is the slope of the exponential fit; a higher β-coefficient represents a stiffer vessel.

4.3.5 – Open field

One week before cognitive tests were conducted, mice were assessed for locomotor differences using an open-field test. Mice were placed in an acrylic open field arena (16in x 16in, Omnitech Electronics, Inc) equipped with infrared photosensors to monitor activity. Mice were in the arena for 30min total. The first 10min were considered acclimation time and were not included in the analysis. The final 20min were analyzed to measure the distance moved, average velocity, time spent in the edges of the arena, and time spent in the center of the arena. Data were analyzed using Fusion software (Omnitech Electronics, Columbus, OH).

4.3.6 – Spontaneous alternation test

Spatial working memory was tested using a spontaneous alternation task in a Y-maze. A custom Y-maze was constructed by Dr. Nathan Tykocki (Michigan State University). The maze consists of three arms placed at a 120° angle from one another. Each arm is 35cm long, 5cm wide, and 20cm high. Mice were placed in a random arm of the maze and were allowed to explore freely for 3min. A camera was placed above the maze to record each trial. A mouse with intact memory will preferentially visit the arm it has visited the least recently, and a correct alternation is defined as consecutive entries into all three arms (18). Percent alternation was calculated as:

$$\%\ alternation = \frac{(number\ of\ alternations)}{[(Total\ number\ of\ arm\ entries) - 2]} \times 100$$

4.3.7 – Novel arm test

Spatial reference memory was assessed using the novel arm Y-maze test. This test took place one week after the spontaneous alternation task. Mice were placed in the

maze with one of the arms blocked off and allowed to explore for 5min. They then return to their home cages for a retention time of 1hr. The mice were then placed back in the maze and allowed to explore all three arms freely for 2min. The percentage of time spent in the novel arm compared to the total time spent in any of the three arms was calculated. A mouse with intact spatial reference memory will preferentially explore the novel arm, and a mouse with impaired memory will spend equal time in all three arms. Videos were recorded on a webcam and uploaded to Ethovision XT tracking software (Noldus, Leesburg, VA).

4.3.8 – Nesting behavior

Qualitative and quantitative nesting tests were used to assess nesting behavior. Mice were given a clean cage with fresh nesting material and were left under standard housing conditions to build a nest for 24hr. A blinded investigator then rated the nests on a scale of 0-5, with 0 being the worst and 5 being the best. A quality nest was considered to be one that was thoroughly shredded, domelike, and successfully covered the mouse (7). For the second phase of the nesting test, mice were given a pre-weighed cotton nestlet and were allowed 1hr to shred the nestlet to be incorporated into their existing nests. The remaining nestlet was then cleared of debris and reweighed to allow for the calculation of the percentage of nestlet shredded.

4.3.9 – Immunofluorescence

Brains were post-fixed in 4% paraformaldehyde, washed in PBS, then stored in sucrose. To assess quantity and morphology of astrocytes, brain sections were blocked and permeabilized in 0.5% Triton X-100 with 10% horse serum-PBS for 30min at room temperature. Sections were then incubated in 1:1000 anti-rabbit GFAP (ab7260, Abcam,

Waltham, MA) overnight at 4°C. They were then washed in PBS, then incubated in secondary AlexaFluor 564 donkey anti-rabbit antibody. Images were obtained from the corpus callosum in both hemispheres of each sample. Sholl analysis was used to assess astrocyte structure as described by others (31). In brief, the Simple Neurite Tracer plugin in ImageJ was used to trace five random astrocytes from each mouse. The tracings were skeletonized, and the automated Sholl analysis was used to draw concentric circles away from the soma around the astrocyte. The number of intersections of astrocytic processes with the circles was plotted against the distance of the circle from the soma.

Images were acquired using a 20x objective coupled to a Zeiss LSM 880 confocal microscope. *Z*-stacks of each image were obtained through the entire thickness of the 40µm section. Sections without primary antibodies served as negative controls. The color was changed to green in post-processing for better visualization of the images. All quantifications were done manually by a blinded investigator using ImageJ.

4.3.10 – qRT-PCR

Brain tissue was collected in 2mm slices immediately anterior to the MCA for qRT-PCR. RNA was extracted using Trizol and was reverse transcribed using VILO reverse transcriptase (Invitrogen, Carlsbad, CA). TAQMAN-specific probes were used for the PCR to assess the mRNA expression of synaptophysin, doublecortin, GFAP, NADPH oxidase 2 (*Nox2*), tumor necrosis factor α (*Tnf-α*), interleukin-6 (*Il-6*) and monocyte chemoattractant protein 1 (*Mcp1*). mRNA expression is expressed as the fold change from control using the $2^{-\Delta\Delta Ct}$ method. β2-microglobulin (*B2m*) was used for normalization.

4.3.11 – Drugs and chemicals

GSK1016790A and NS309 were purchased from Cayman Chemicals (Ann Arbor, MI). All other chemicals were purchased from Sigma-Aldrich unless otherwise noted.

4.3.12 – Statistical analysis

All data are presented as means ± SEM. Pial perfusion, mRNA expression, and behavioral and immunofluorescence data were analyzed by Student's t-test. In the case of significant differences in group variance, the non-parametric Mann Whitney U-test was used. For analysis of PA vasodilation and structure, two-way analysis of variance with repeated measures in one factor (concentration or pressure) was utilized followed by Bonferroni-adjusted t-tests for post-hoc comparisons. All statistical analyses were performed using GraphPad Prism version 9.4.0 (GraphPad, San Diego, CA). In all cases, statistical significance was denoted by $p<0.05$.

4.4 – Results

4.4.1 – Endothelial TRPV4 knockout does not alter pial blood flow

The effect of endothelial TRPV4 channel deletion in pial blood flow was measured using laser speckle contrast imaging. Endothelial TRPV4 channel knockout did not alter pial perfusion in the parietal ($p=0.9273$), temporal ($p=0.8121$), or frontal regions (0.2710) compared to controls (Figure 4.1 A-C).

4.4.2 – IK_{Ca}/SK_{Ca}-mediated PA dilation is mildly impaired in $TRPV4_{EC}^{-/-}$ mice

The importance of endothelial TRPV4 channels in the generation of myogenic tone and in PA dilation was assessed using pressure myography. There were no significant differences detected in the amount of myogenic tone generated in PAs from $TRPV4_{EC}^{-/-}$ mice and their controls (Figure 4.2A; $p=0.7544$). As expected, TRPV4-mediated dilation

in mice deficient in endothelial TRPV4 was completely abolished (Figure 4.2B; p=0.0004). Additionally, $TRPV4_{EC^{-/-}}$ mice had a rightward shift in the dilation to IK_{Ca}/SK_{Ca} activation by agonist NS309 (Figure 4.2C; p=0.0266 at 10^{-7}M), indicating a reduction in sensitivity to IK_{Ca}/SK_{Ca} activation. The EC50 in NS309-mediated dilation in the control group is less than that of the $TRPV4_{EC^{-/-}}$ group, though this did not reach statistical significance (control -logEC50: 7.71 ± 0.75, $TRPV4_{EC^{-/-}}$ -logEC50: 6.57 ± 0.18; p=0.0823 by Mann Whitney U-test). The maximum dilation to NS309 is comparable between the two groups.

4.4.3 – Endothelial TRPV4 knockout does not change PA structure

Pressure myography was used to assess PA structure and biomechanical properties under calcium-free conditions. There were no changes observed in outer diameter (Figure 4.3A; p=0.8644), lumen diameter (Figure 4.3B; p=0.8119), or wall thickness (Figure 4.3C; p=0.6033) in PAs from $TRPV4_{EC^{-/-}}$ mice compared to control. There were also no statistically significant changes to wall strain (Figure 4.3D; p=0.2512), wall stress (Figure 4.3E; p=0.5432), or wall stiffness (Figure 4.3F; p=0.2512). Together, these data suggest endothelial TRPV4 deletion does not alter PA structure or biomechanical properties.

4.4.4 – Endothelial TRPV4 deletion reduces anxiety-like behavior but does not change locomotion

Anxiety-like behavior and locomotion were assessed using the open-field test. Mice deficient in endothelial TRPV4 spent more time in the center of the arena (Figure 4.4A; p=0.400) and a trend toward less time in the corners than control mice (Figure 4.4B; p=0.0834), indicating a reduction in anxiety-like behavior. The overall distance traveled (Figure 4.4C; p=0.8061), and the velocity of travel (Figure 4.4D; p=0.7373) did not differ

between groups, suggesting endothelial TRPV4 channel deletion does not affect movement.

4.4.5 – Endothelial TRPV4 deletion impairs cognitive function

The Y-maze was used to assess spatial working and spatial reference memory. These studies rely on the inherent preference of mice for novel locations. Spatial working memory was tested using the spontaneous alternation task. $TRPV4_{EC}^{-/-}$ mice exhibited impaired spatial reference memory by having fewer correct alternation triads compared to control mice (Figure 4.5A; p=0.0436). The two groups had similar total arm entries (Figure 4.5B; p=0.6894).

A week following the spontaneous alternation task, the novel arm Y-maze test was used to assess short-term spatial reference memory. $TRPV4_{EC}^{-/-}$ mice spent significantly less time in the novel arm of the maze (Figure 4.6A; p=0.0083), indicating spatial reference memory impairment. No differences were detected in the frequency of visits to the novel arm (Figure 4.6B; p=0.7056).

Nest building in mice is an important behavior that is altered with cognitive decline. Mice deficient in endothelial TRPV4 build lower quality nests than control mice (Figure 4.7A; p=0.0231), which is indicated by a lower nest score. However, the amount of nesting material shredded did not differ between the two groups (Figure 4.7B; p=0.7049).

4.4.6 – Endothelial TRPV4 knockout does not alter mRNA expression of neuronal support or inflammatory markers

qRT-PCR was used to assess mRNA expression of markers of neuronal support and inflammation. Previous studies indicated TRPV4 knockout increases expression of neuroinflammatory markers such as *Tnf-α*, and results in a potentially compensatory

increase in markers of neuronal support, such as doublecortin (10). $TRPV4_{EC^{-/-}}$ mice did not have detectable alterations in mRNA expression of synaptophysin (Figure 4.8A; p=0.5301), doublecortin (Figure 4.8B; p=0.7385), *Tnf-α* (Figure 4.8C; p=0.5262), *Mcp-1* (Figure 4.8D; p=0.4273), *Il-6* (Figure 4.8E; p=0.8413), or *Nox2* (Figure 4.8F; p=0.4380) compared to control.

4.4.7 – $TRPV4_{EC^{-/-}}$ mice have greater quantity and complexity of GFAP-positive astrocytes

The quantity and morphology of astrocytes were assessed as an indicator of neuroinflammation. $TRPV4_{EC^{-/-}}$ mice had more GFAP-positive astrocytes compared to control (Figure 4.9A; p=0.0262). These astrocytes had more process complexity further away from the soma, measured by a Sholl analysis (Figure 4.9B; ANOVA p=0.0182).

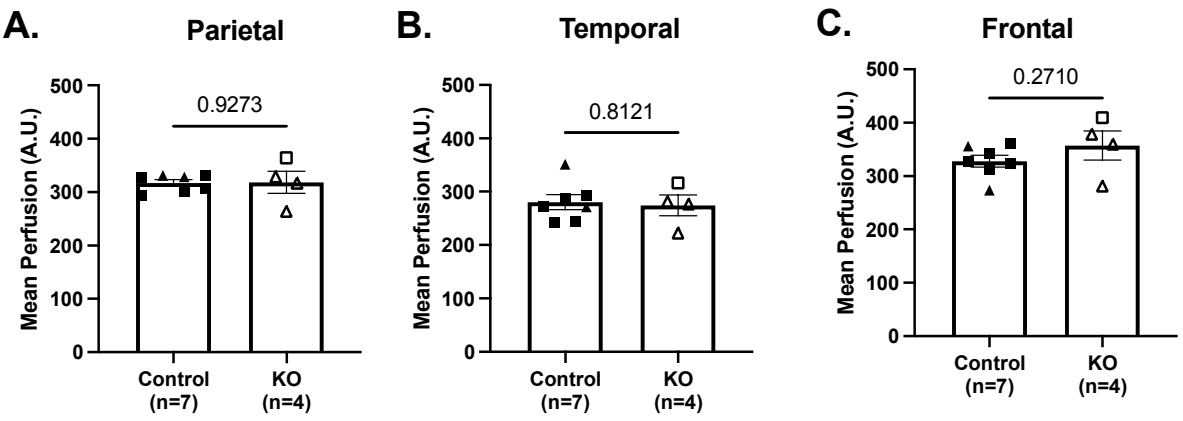

Figure 4.1: Endothelial TRPV4 knockout does not alter cerebral pial perfusion. Cerebral pial perfusion was measured using laser speckle contrast imaging. There were no detectable differences in cerebral pial perfusion in the A) parietal, B) temporal, or C) frontal regions between endothelial TRPV4 knockout mice and their endothelial TRPV4 intact controls. Closed squares = control males, closed triangles = control females, open squares = $TRPV4_{EC^{-/-}}$ males, open triangles = $TRPV4_{EC^{-/-}}$ females. $p<0.05$ indicates statistical significance by Student's t-test. Data are presented as mean ± SEM.

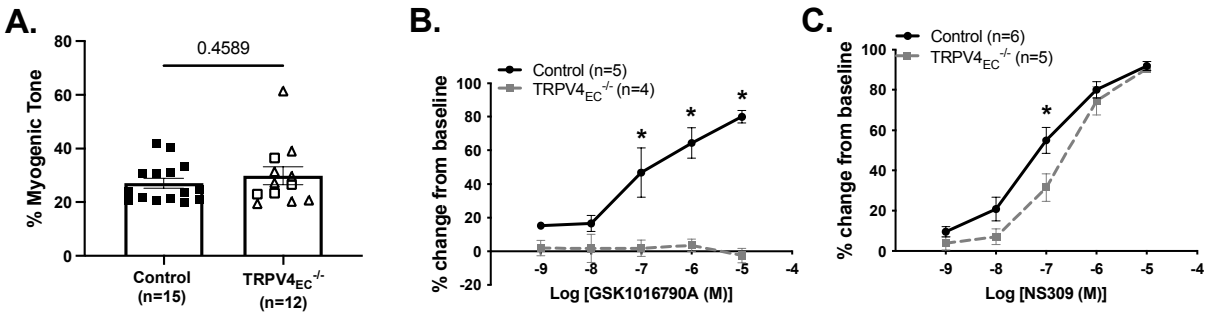

Figure 4.2: Mice deficient in endothelial TRPV4 channels have mildly impaired IK_{Ca}/SK_{Ca}-mediated dilation. Pressure myography was used to assess myogenic tone generation and dilatory properties in PAs of mice with and without endothelial TRPV4 channels. A) There was no detectable difference in amount of myogenic tone generation in PAs in mice with and without endothelial TRPV4 channels. B) Mice with endothelial TRPV4 knockout had completely abolished PA dilation to TRPV4 agonist GSK1016790A. C) IK_{Ca}/SK_{Ca}-mediated dilation was mildly impaired in $TRPV4_{EC}^{-/-}$ mice. Myogenic tone data represents 15 PAs from 7 control mice and 12 PAs from 7 $TRPV4_{EC}^{-/-}$ mice. Closed squares = control males, closed triangles = control females, open squares = $TRPV4_{EC}^{-/-}$ males, open triangles = $TRPV4_{EC}^{-/-}$ females. Data are presented as mean ± SEM. *$p<0.05$ indicates statistical significance by Student's t-test (A) or two-way ANOVA with Bonferroni correction.

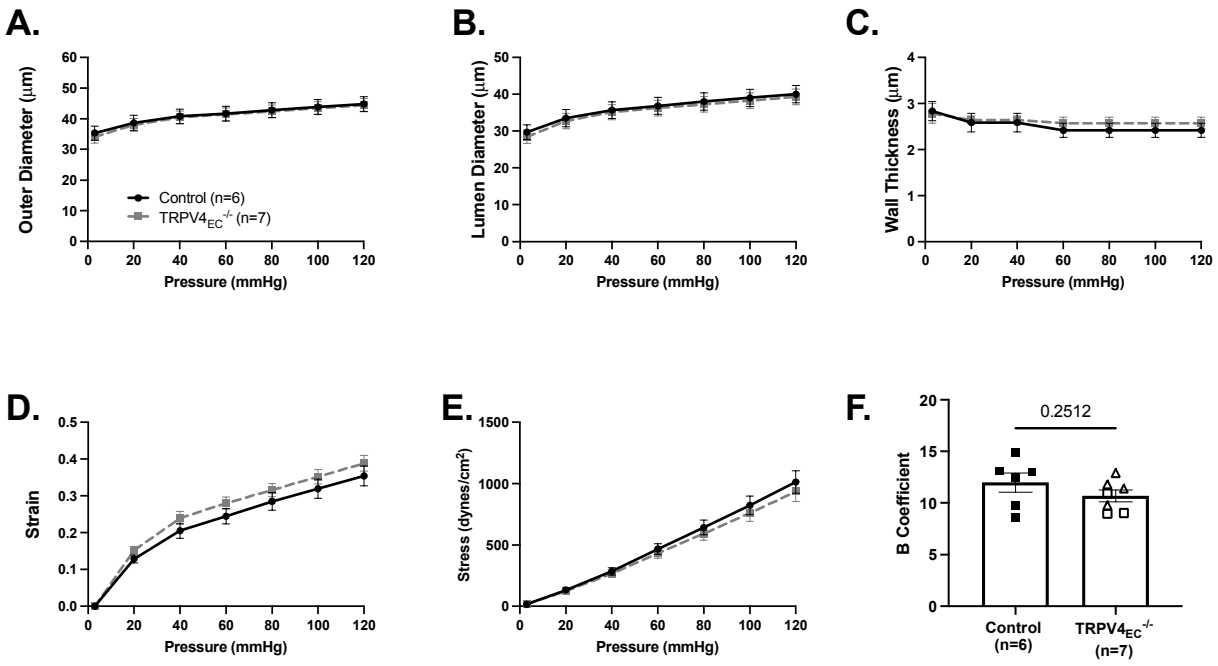

Figure 4.3: Endothelial TRPV4 knockout does not alter PA structure or biomechanical properties. Pressure myography was used to assess PA structure and biomechanical properties. There were no detectable differences in PA A) outer diameter, B) lumen diameter, C) wall thickness, D) wall strain, E) wall stress, or F) wall stiffness measured by the β-coefficient. Data are presented as mean ± SEM. $p<0.05$ indicates statistical significance by two-way ANOVA with Bonferroni correction.

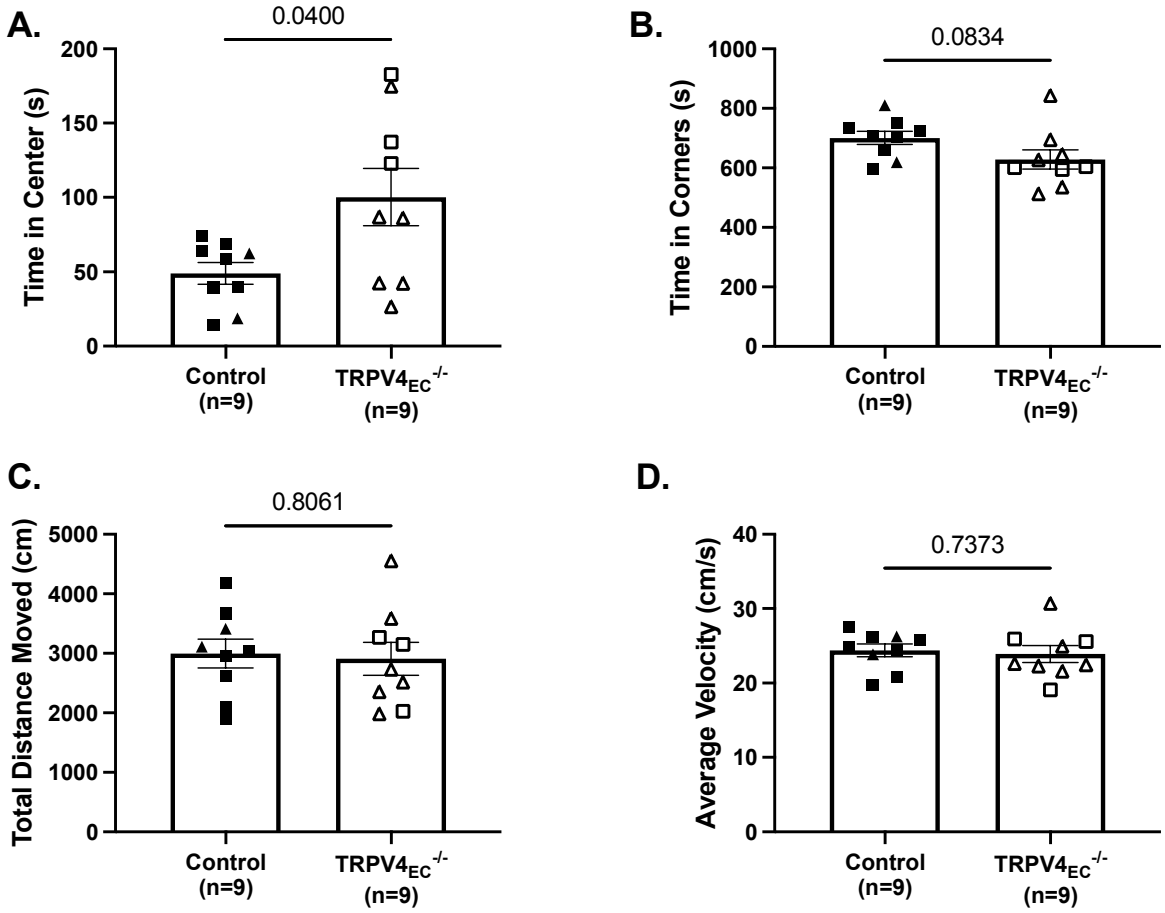

Figure 4.4: Endothelial TRPV4 deletion reduces anxiety-like behavior. The open field test was used to assess anxiety-like behavior and locomotion. $TRPV4_{EC}^{-/-}$ mice spent more time in the center and less time in the corners of the arena compared to control mice. There were no differences between $TRPV4_{EC}^{-/-}$ and control mice in the distance traveled or traveling velocity. Closed squares = control males, closed triangles = control females, open squares = $TRPV4_{EC}^{-/-}$ males, open triangles = $TRPV4_{EC}^{-/-}$ females. Data are presented as mean ± SEM. $p<0.05$ indicates statistical significance by Mann Whitney (A) or Student's t-test (B-D).

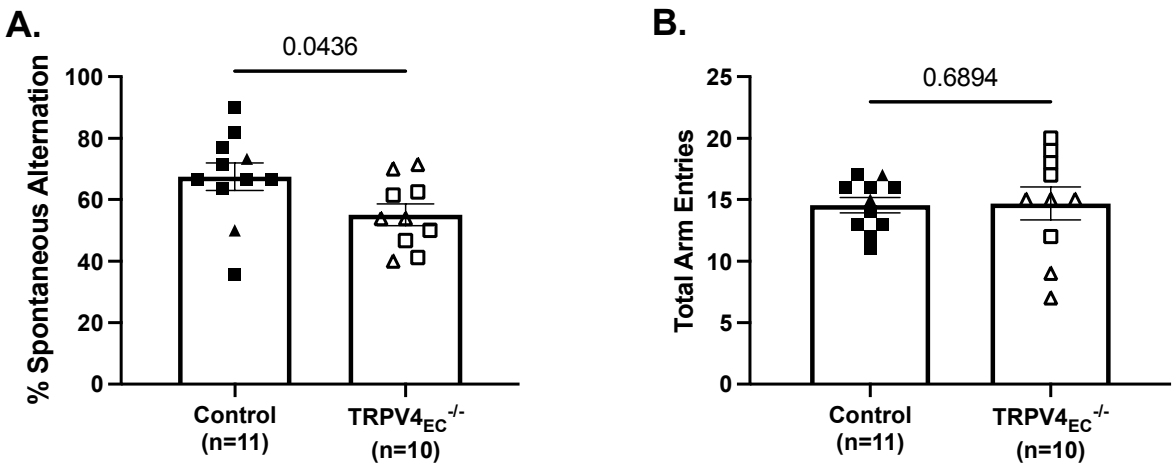

Figure 4.5: Endothelial TRPV4-deficient mice have impaired spatial working memory. Spontaneous alternation behavior in the Y-maze was used to assess spatial working memory. A) $TRPV4_{EC}^{-/-}$ mice made fewer correct alternations with B) no differences in total number of arm entries in the maze. Closed squares = control males, closed triangles = control females, open squares = $TRPV4_{EC}^{-/-}$ males, open triangles = $TRPV4_{EC}^{-/-}$ females. Data are presented as mean ± SEM. $p<0.05$ indicates statistical significance by Student's t-test.

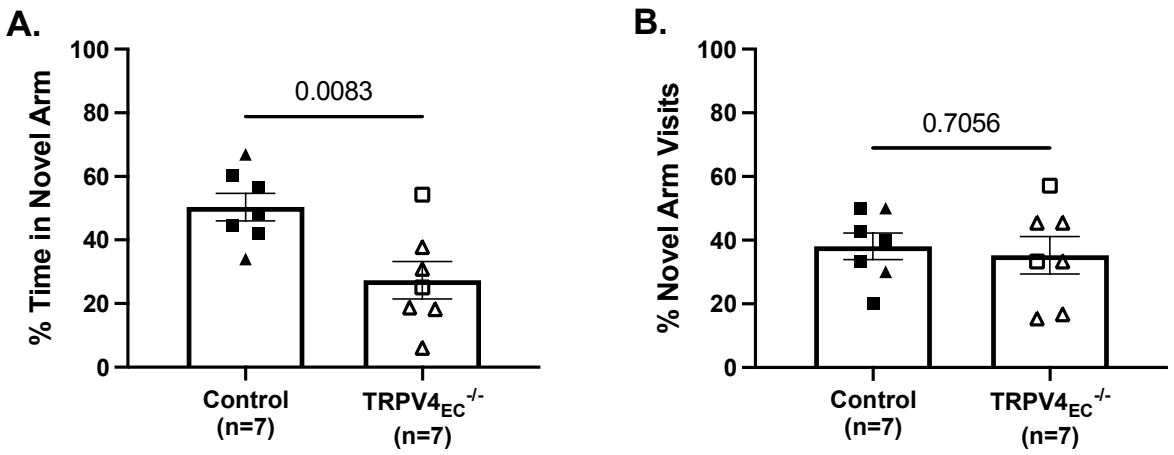

Figure 4.6: Endothelial TRPV4 deficient mice have impaired short-term spatial reference memory. The Y-maze was used to test short-term spatial reference memory. A) $TRPV4_{EC}^{-/-}$ mice spent significantly less time in the novel arm of the Y-maze compared to control. B) Frequency of novel arm visits did not differ between $TRPV4_{EC}^{-/-}$ mice and control. Closed squares = control males, closed triangles = control females, open squares = $TRPV4_{EC}^{-/-}$ males, open triangles = $TRPV4_{EC}^{-/-}$ females. Data are presented as mean ± SEM. *$p<0.05$ indicates statistical significance by Student's t-test.

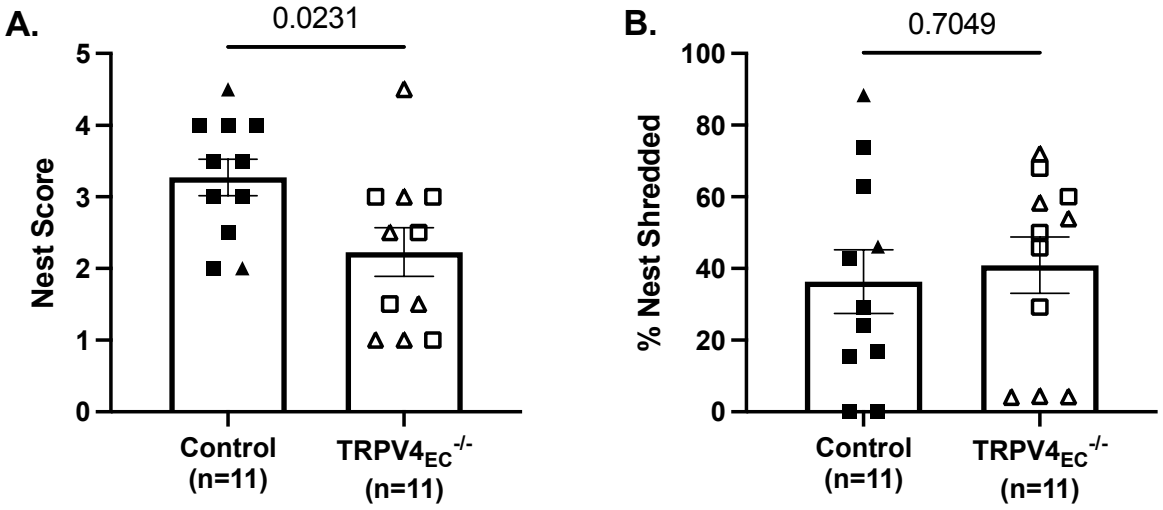

Figure 4.7: Endothelial TRPV4 deletion impairs nesting ability. Nesting ability was assessed using qualitative and quantitative nesting tests. A) $TRPV4_{EC}^{-/-}$ mice built lower quality nests compared to control, but B) the amount of cotton nestlet shredded did not differ between the two groups. Closed squares = control males, closed triangles = control females, open squares = $TRPV4_{EC}^{-/-}$ males, open triangles = $TRPV4_{EC}^{-/-}$ females. Data are presented as mean ± SEM. *$p<0.05$ indicates statistical significance by Student's t-test.

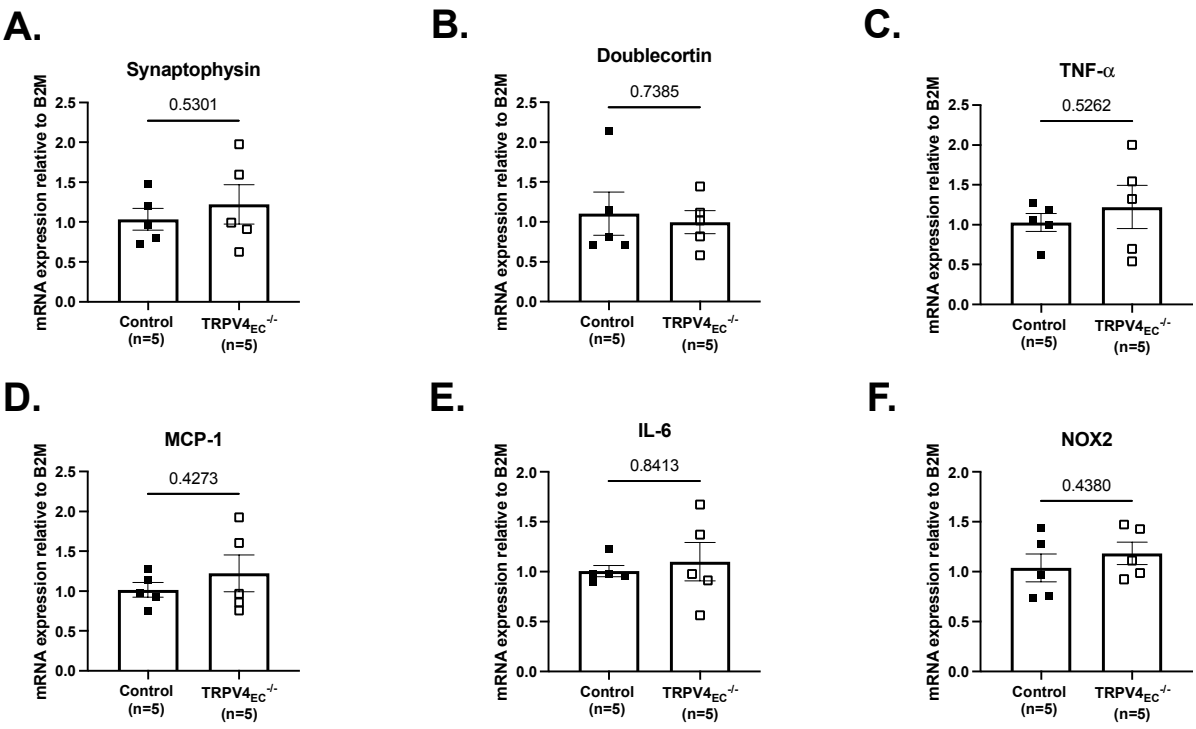

Figure 4.8: Endothelial TRPV4 knockout does not alter mRNA expression of neuronal health or inflammation markers. The mRNA expression of markers for neuronal support and neuroinflammation were assessed using qRT-PCR. $TRPV4_{EC}^{-/-}$ mice did not have detectable differences in mRNA expression of A) synaptophysin, B) doublecortin, C) TNF-α, D) MCP-1, E) IL-6, or F) NOX2. All data presented are from male mice. Data are presented as mean ± SEM. $p<0.05$ indicates statistical significance by Student's t-test.

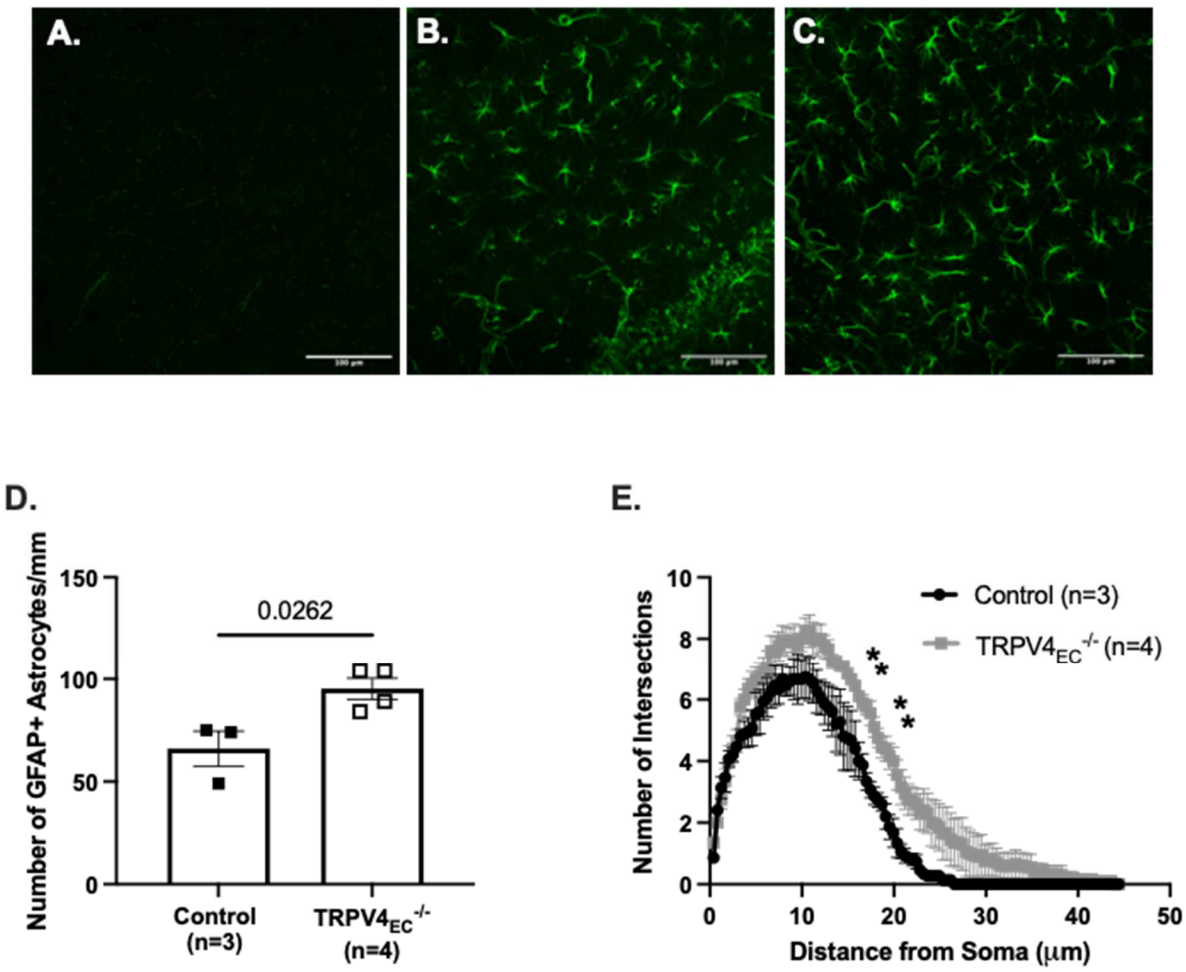

Figure 4.9: TRPV4$_{EC}^{-/-}$ mice have more GFAP-positive astrocytes with greater process complexity compared to control. The quantity and morphology of GFAP-positive astrocytes was assessed using a GFAP antibody. A-C) Representative images of negative control, control male, and TRPV4$_{EC}^{-/-}$, respectively. D) TRPV4$_{EC}^{-/-}$ mice have more GFAP-positive astrocytes compared to TRPV4$_{EC}$-intact controls. E) Astrocytes from TRPV4$_{EC}^{-/-}$ mice have more process complexity further from the soma compared to control. All data presented are from male mice. Data are presented as mean ± SEM. $p<0.05$ indicates statistical significance by A) Student's t-test or B) two-way ANOVA with Bonferroni correction.

4.5 – Discussion

The novel findings of this study are that endothelial cell specific TRPV4 deletion 1) does not alter cerebral pial perfusion, 2) reduces sensitivity to downstream IK_{Ca}/SK_{Ca} channels in PAs, 3) does not affect PA structure, 4) reduces anxiety-like behavior, 5) impairs cognitive function, and 6) increases neuroinflammation. These studies improve our understanding of the importance of endothelial TRPV4 channels in PA and cognitive function, which has thus far been precluded by the channel's ubiquitous expression. By elucidating the role of endothelial TRPV4 channels under baseline conditions, we can better understand the influence of TRPV4 channel dysfunction in pathological states, such as hypertension.

In addition to their expression in the endothelium, TRPV4 channels are expressed in vascular smooth muscle cells, neurons, microglia, astrocytes, and neurons (12, 32). Because of their ubiquitous expression, these channels are critical regulators of intercellular communication in the brain and have an important role in the regulation of blood flow throughout the cerebral and peripheral vasculature (14). While blood pressure was not measured in the current study, Ottolini *et al* reported a mild increase in mean arterial pressure in $TRPV4_{EC^{-/-}}$ mice using radiotelemetry, the gold standard in blood pressure measurement. This increase in blood pressure was not enough to consider the mice hypertensive (23). This contrasts with studies from our lab (10) and others (13) that show global TRPV4 deletion does not alter blood pressure. Because of the lack of suitable animal models, the role of endothelial TRPV4 channels in blood pressure regulation has been difficult to define. These studies suggest that at least in the peripheral vasculature, endothelial TRPV4 signaling is important for blood pressure regulation, and its deletion

results in vasoconstriction. The present study suggests the same is not true for the cerebral circulation. PAs of $TRPV4_{EC}^{-/-}$ mice had similar myogenic tone generation compared to control mice. Similarly, PAs from $TRPV4^{-/-}$ rats had comparable myogenic tone generation compared to TRPV4-intact control rats (10). Previous studies from our lab show that myogenic tone is reduced after TRPV4 inhibition in PAs of hypertensive mice (11). This suggests that, at least in the cerebral circulation, TRPV4 activity increases myogenic tone in pathological conditions, without playing much of a role in normal conditions. Additionally, these data provide evidence that TRPV4 channels have differing roles in the peripheral versus the cerebral vasculature.

Because endothelial TRPV4 deletion did not affect myogenic tone in PAs, we expected it would also not impact cerebral pial perfusion. Indeed, $TRPV4_{EC}^{-/-}$ mice do not have altered cerebral pial perfusion compared to control mice. This contrasts with observations from our previous study in $TRPV4^{-/-}$ rats. In that study, arterial spin labeling MRI revealed reduced cerebral perfusion in TRPV4-deficient rats compared to TRPV4-intact controls (10). Laser speckle contrast imaging has a penetration depth of about 1mm and can therefore only assess pial perfusion, as opposed to the more comprehensive assessment made by MRI. Differences in the type of arterioles assessed may explain the dissimilarities observed. The importance of EDH in arterial dilation decreases with increasing lumen diameter. In the pial arteries, it is possible the NO contribution in these arteries dampens the effect of TRPV4 deletion, and changes are only observed in deeper brain regions. Additionally, perfusion was assessed under resting conditions and it is possible endothelial TRPV4 channels do not play a role in basal blood flow. Differences

in age of the animals used could also contribute to these differences. The mice in the present study were 30-35 weeks of age, while TRPV4$^{-/-}$ rats were a year old.

Unlike in pial arteries and arterioles, endothelium-dependent dilation in PAs is dependent on TRPV4 channel signaling. Our group has demonstrated that when pressurized PAs are incubated with a TRPV4 antagonist, Cch-mediated dilation is nearly abolished (11). Similarly, the Cch mediated dilation is completely obliterated in PAs from TRPV4$^{-/-}$ rats (10). In the current study, PA dilation to the TRPV4 agonist GSK1016790A was eliminated. This confirms the absence of TRPV4 in the endothelium and shows that VSMC TRPV4 channels do not affect dilation to this agonist. Interestingly, PAs from TRPV4$_{EC}^{-/-}$ mice had reduced sensitivity to IK_{Ca}/SK_{Ca} activation compared to control mice. In AngII-hypertensive mice, as well as the studies in SHRSP discussed in Chapter 2, hypertension resulted in impaired IK_{Ca}/SK_{Ca}-mediated dilation that was accompanied by reduced mRNA expression of these channels in cerebral arteries (11). In these studies, it was unclear if the impaired mRNA expression and PA dilation was a direct effect of hypertension, or secondary to the observed TRPV4 impairment. The data presented here suggest endothelial TRPV4 channel deletion impairs either the function or the expression of downstream IK_{Ca}/SK_{Ca} channels. This was an unexpected observation; we expected a potential compensatory increase of channel function. Future studies should measure mRNA expression of these channels in cerebral arteries to determine whether this is an effect of altered expression.

Because of their importance in PA function, it is likely that endothelial TRPV4 channels are essential for neurovascular communication. We have shown both in hypertensive models and in TRPV4$^{-/-}$ rats that impaired TRPV4 mediated dilation is

associated with cognitive decline. In addition to severe cognitive impairment, TRPV4$^{-/-}$ rats exhibited depressive-like behavior and impaired locomotion. While TRPV4$_{EC}^{-/-}$ did not exhibit depressive-like behavior, they did have reduced anxiety-like behavior, indicated by spending more time in the center of an open field arena without changes in speed of travel or total distance moved. The differences observed in the TRPV4-deficient rats versus mice may be a function of age. Clinical data reveal a strong link between depression and dementia (27). Depression acts as both a risk factor for, and a result of, dementia. It is possible that as the mice age, TRPV4$_{EC}^{-/-}$ mice could progress to exhibit symptoms of depression. The results of the open field test influenced which behavioral assays we used. Because TRPV4$_{EC}^{-/-}$ mice are comfortable spending more time in the center of an arena, behavioral assays were chosen that did not require the use of arenas. Endothelial TRPV4 deletion resulted in impairments in spatial reference and spatial working memory, as well as nesting behavior compared to control mice, demonstrating an importance of endothelial TRPV4 channels in cognitive function. Notably, studies using global TRPV4$^{-/-}$ mice did not identify any behavioral changes compared to control (28). As mentioned, TRPV4$^{-/-}$ rats had severe cognitive impairment. Age of the animals used may contribute to these differences. Shibasaki *et al* used mice at 17-24-week-old mice while we used 30-35-week-old mice. TRPV4$^{-/-}$ rats were the oldest model used, at 1 year of age.

Cognitive decline is associated with reduced expression of neuronal health markers, such as synaptophysin, which is a marker of neuronal function and synaptic plasticity, and doublecortin, which is a marker of immature neurons (11, 33). AngII-hypertensive mice that had both TRPV4 impairment and cognitive decline had no

changes to synaptophysin mRNA but had reduced doublecortin mRNA (11). Interestingly, TRPV4$^{-/-}$ rats had a slight increase in synaptophysin mRNA and a significant increase in doublecortin mRNA compared to controls (10). These studies suggest a pattern in which impaired TRPV4 channel function triggers a potentially compensatory increase in doublecortin mRNA expression. In the present study, however, no changes were observed in either of these markers in TRPV4$_{EC}^{-/-}$ mice compared to control. The reason behind these differences is unclear. It is important to consider that mRNA expression does not directly translate to protein expression. It is therefore difficult to know how these data influence neuronal health *in vivo*.

Neurovascular dysfunction is associated with inflammation. Astroglia are a cell type widely expressed throughout the central nervous system that, under baseline conditions, play an important role in blood flow regulation and bringing nutrients to neurons. Astrocytes also respond to insults like inflammation and neurodegeneration. While the range of responses astrocytes can have to these triggers is quite broad, common indicators of central nervous system insult include astrocytic proliferation and increased branching and complexity in the processes (19, 30). While TRPV4$_{EC}^{-/-}$ mice did not exhibit altered mRNA expression of proinflammatory cytokines in brain tissue, there was an increase in the number of GFAP-positive astrocytes. These astrocytes also had greater process arborization. This complements data from TRPV4$^{-/-}$ rats that had elevated mRNA expression of GFAP compared to TRPV4-intact controls (10). Astrogliosis is involved in CSVD pathogenesis (16); it is therefore possible increased inflammation is mediating cognitive decline.

It is important to address limitations in this study. Firstly, while both male and female mice were used in both groups, there was a disproportionate weight of males in the control group and females in the knockout group in some experiments. Given the sex differences in cerebral blood flow, cognitive function, and inflammation outlined in Chapter 3, it is important that there is an equal weight of each sex. Notably, the data presented here do not suggest sex differences exist in this model, despite the cerebrovascular and cognitive protection usually observed in female mice. Further, gene expression and astrocyte data were provided for male mice only due to a lack of female control mice. More female mice will be added to this study as they become available. Lastly, these data strongly suggest that endothelial TRPV4 channels are critical for NVC, though this was not measured here. Future studies will employ functional hyperemia experiments to directly test the role of endothelial TRPV4 channels in NVC.

In summary, endothelial TRPV4 channels are essential for both cerebrovascular and cognitive function. These studies provide strong evidence that TRPV4 channel impairment may increase risk of dementia development.

REFERENCES

1. **Baumbach GL**, **Hajdu MA**. Mechanics and composition of cerebral arterioles in renal and spontaneously hypertensive rats. *Hypertension* 21: 816–826, 1993. doi: 10.1161/01.hyp.21.6.816.

2. **Cannistraro RJ**, **Badi M**, **Eidelman BH**, **Dickson DW**, **Middlebrooks EH**, **Meschia JF**. CNS small vessel disease: A clinical review. *Neurology* 92: 1146–1156, 2019. doi: 10.1212/WNL.0000000000007654.

3. **Cipolla MJ**, **Li R**, **Vitullo L**. Perivascular innervation of penetrating brain parenchymal arterioles. *J Cardiovasc Pharmacol* 44: 1–8, 2004. doi: 10.1097/00005344-200407000-00001.

4. **Cipolla MJ**, **Sweet J**, **Chan S-L**, **Tavares MJ**, **Gokina N**, **Brayden JE**. Increased pressure-induced tone in rat parenchymal arterioles vs. middle cerebral arteries: role of ion channels and calcium sensitivity. *J Appl Physiol* 117: 53–59, 2014. doi: 10.1152/japplphysiol.00253.2014.

5. **Cipolla MJ**. *The Cerebral Circulation*. San Rafael (CA): Morgan & Claypool Life Sciences, 2009.

6. **Daneva Z**, **Marziano C**, **Ottolini M**, **Chen Y-L**, **Baker TM**, **Kuppusamy M**, **Zhang A**, **Ta HQ**, **Reagan CE**, **Mihalek AD**, **Kasetti RB**, **Shen Y**, **Isakson BE**, **Minshall RD**, **Zode GS**, **Goncharova EA**, **Laubach VE**, **Sonkusare SK**. Caveolar peroxynitrite formation impairs endothelial TRPV4 channels and elevates pulmonary arterial pressure in pulmonary hypertension. *Proc Natl Acad Sci USA* 118, 2021. doi: 10.1073/pnas.2023130118.

7. **Deacon RMJ**. Assessing nest building in mice. *Nat Protoc* 1: 1117–1119, 2006. doi: 10.1038/nprot.2006.170.

8. **De Silva TM**, **Faraci FM**. Contributions of aging to cerebral small vessel disease. *Annu Rev Physiol* 82: 275–295, 2020. doi: 10.1146/annurev-physiol-021119-034338.

9. **Diaz-Otero JM**, **Fisher C**, **Downs K**, **Moss EM**, **Jaffe IZ**, **Jackson WF**, **Dorrance AM**. Endothelial Mineralocorticoid Receptor Mediates Parenchymal Arteriole and Posterior Cerebral Artery Remodeling During Angiotensin II–Induced Hypertension. .

10. **Diaz-Otero JM**, **Yen T-C**, **Ahmad A**, **Laimon-Thomson E**, **Abolibdeh B**, **Kelly K**, **Lewis MT**, **Wiseman RW**, **Jackson WF**, **Dorrance AM**. Transient receptor potential vanilloid 4 channels are important regulators of parenchymal arteriole dilation and cognitive function. *Microcirculation* 26: e12535, 2019. doi: 10.1111/micc.12535.

11. **Diaz-Otero JM**, **Yen T-C**, **Fisher C**, **Bota D**, **Jackson WF**, **Dorrance AM**. Mineralocorticoid receptor antagonism improves parenchymal arteriole dilation via a TRPV4-dependent mechanism and prevents cognitive dysfunction in hypertension. *Am J Physiol Heart Circ Physiol* 315: H1304–H1315, 2018. doi: 10.1152/ajpheart.00207.2018.

12. **Earley S**, **Brayden JE**. Transient receptor potential channels in the vasculature. *Physiol Rev* 95: 645–690, 2015. doi: 10.1152/physrev.00026.2014.

13. **Earley S**, **Pauyo T**, **Drapp R**, **Tavares MJ**, **Liedtke W**, **Brayden JE**. TRPV4-dependent dilation of peripheral resistance arteries influences arterial pressure. *Am J Physiol Heart Circ Physiol* 297: H1096-102, 2009. doi: 10.1152/ajpheart.00241.2009.

14. **Filosa JA**, **Yao X**, **Rath G**. TRPV4 and the regulation of vascular tone. *J Cardiovasc Pharmacol* 61: 113–119, 2013. doi: 10.1097/FJC.0b013e318279ba42.

15. **Gorelick PB**, **Scuteri A**, **Black SE**, **DeCarli C**, **Greenberg SM**, **Iadecola C**, **Launer LJ**, **Laurent S**, **Lopez OL**, **Nyenhuis D**, **Petersen RC**, **Schneider JA**, **Tzourio C**, **Arnett DK**, **Bennett DA**, **Chui HC**, **Higashida RT**, **Lindquist R**, **Nilsson PM**, **Roman GC**, **Sellke FW**, **Seshadri S**. Vascular contributions to cognitive impairment and dementia. *Stroke* 42: 2672–2713, 2011. doi: 10.1161/STR.0b013e3182299496.

16. **Ihara M**, **Yamamoto Y**. Emerging evidence for pathogenesis of sporadic cerebral small vessel disease. *Stroke* 47: 554–560, 2016. doi: 10.1161/STROKEAHA.115.009627.

17. **Jiménez-Balado J**, **Riba-Llena I**, **Abril O**, **Garde E**, **Penalba A**, **Ostos E**, **Maisterra O**, **Montaner J**, **Noviembre M**, **Mundet X**, **Ventura O**, **Pizarro J**, **Delgado P**. Cognitive impact of cerebral small vessel disease changes in patients with hypertension. *Hypertension* 73: 342–349, 2019. doi: 10.1161/HYPERTENSIONAHA.118.12090.

18. **Kraeuter A-K**, **Guest PC**, **Sarnyai Z**. The Y-Maze for Assessment of Spatial Working and Reference Memory in Mice. *Methods Mol Biol* 1916: 105–111, 2019. doi: 10.1007/978-1-4939-8994-2_10.

19. **Kwon HS**, **Koh S-H**. Neuroinflammation in neurodegenerative disorders: the roles of microglia and astrocytes. *Transl Neurodegener* 9: 1–12, 2020. doi: 10.1186/s40035-020-00221-2.

20. **Litak J**, **Mazurek M**, **Kulesza B**, **Szmygin P**, **Litak J**, **Kamieniak P**, **Grochowski C**. Cerebral small vessel disease. *Int J Mol Sci* 21, 2020. doi: 10.3390/ijms21249729.

21. **Liu Y**, **Dong Y-H**, **Lyu P-Y**, **Chen W-H**, **Li R**. Hypertension-Induced Cerebral Small Vessel Disease Leading to Cognitive Impairment. *Chin Med J* 131: 615–619, 2018. doi: 10.4103/0366-6999.226069.

22. **Matin N**, **Fisher C**, **Jackson WF**, **Dorrance AM**. Bilateral common carotid artery stenosis in normotensive rats impairs endothelium-dependent dilation of parenchymal arterioles. *Am J Physiol Heart Circ Physiol* 310: H1321-9, 2016. doi: 10.1152/ajpheart.00890.2015.

23. **Ottolini M**, **Hong K**, **Cope EL**, **Daneva Z**, **DeLalio LJ**, **Sokolowski JD**, **Marziano C**, **Nguyen NY**, **Altschmied J**, **Haendeler J**, **Johnstone SR**, **Kalani MY**, **Park MS**, **Patel RP**, **Liedtke W**, **Isakson BE**, **Sonkusare SK**. Local peroxynitrite impairs endothelial transient receptor potential vanilloid 4 channels and elevates blood pressure in obesity. *Circulation* 141: 1318–1333, 2020. doi: 10.1161/CIRCULATIONAHA.119.043385.

24. **Petrea RE**, **O'Donnell A**, **Beiser AS**, **Habes M**, **Aparicio H**, **DeCarli C**, **Seshadri S**, **Romero JR**. Mid to late life hypertension trends and cerebral small vessel disease in the framingham heart study. *Hypertension* 76: 707–714, 2020. doi: 10.1161/HYPERTENSIONAHA.120.15073.

25. **Pires PW**, **Jackson WF**, **Dorrance AM**. Regulation of myogenic tone and structure of parenchymal arterioles by hypertension and the mineralocorticoid receptor. *Am J Physiol Heart Circ Physiol* 309: H127-36, 2015. doi: 10.1152/ajpheart.00168.2015.

26. **Polycarpou A**, **Hricisák L**, **Iring A**, **Safar D**, **Ruisanchez É**, **Horváth B**, **Sándor P**, **Benyó Z**. Adaptation of the cerebrocortical circulation to carotid artery occlusion involves blood flow redistribution between cortical regions and is independent of eNOS. *Am J Physiol Heart Circ Physiol* 311: H972–H980, 2016. doi: 10.1152/ajpheart.00197.2016.

27. **Rubin R**. Exploring the relationship between depression and dementia. *JAMA* 320: 961–962, 2018. doi: 10.1001/jama.2018.11154.

28. **Shibasaki K**, **Sugio S**, **Takao K**, **Yamanaka A**, **Miyakawa T**, **Tominaga M**, **Ishizaki Y**. TRPV4 activation at the physiological temperature is a critical determinant of neuronal excitability and behavior. *Pflugers Arch* 467: 2495–2507, 2015. doi: 10.1007/s00424-015-1726-0.

29. **Shih AY**, **Blinder P**, **Tsai PS**, **Friedman B**, **Stanley G**, **Lyden PD**, **Kleinfeld D**. The smallest stroke: occlusion of one penetrating vessel leads to infarction and a cognitive deficit. *Nat Neurosci* 16: 55–63, 2013. doi: 10.1038/nn.3278.

30. **Sofroniew MV**. Molecular dissection of reactive astrogliosis and glial scar formation. *Trends Neurosci* 32: 638–647, 2009. doi: 10.1016/j.tins.2009.08.002.

31. **Tavares G**, **Martins M**, **Correia JS**, **Sardinha VM**, **Guerra-Gomes S**, **das Neves SP**, **Marques F**, **Sousa N**, **Oliveira JF**. Employing an open-source tool to assess astrocyte tridimensional structure. *Brain Struct Funct* 222: 1989–1999, 2017. doi: 10.1007/s00429-016-1316-8.

32. **Zhang E**, **Liao P**. Brain transient receptor potential channels and stroke. *J Neurosci Res* 93: 1165–1183, 2015. doi: 10.1002/jnr.23529.

33. **Zhan SS**, **Beyreuther K**, **Schmitt HP**. Synaptophysin immunoreactivity of the cortical neuropil in vascular dementia of Binswanger type compared with the dementia of Alzheimer type and nondemented controls. *Dementia* 5: 79–87, 1994. doi: 10.1159/000106701.

Chapter 5:

Conclusions and Perspectives

5.1 – General conclusions

The data presented in this dissertation shed light on the link between hypertension and dementia development. These data provide evidence for the therapeutic potential of MR antagonism as a therapeutic intervention and provide novel evidence that the influence of hypertension on cognitive decline is sex dependent in young mice. Further evidence supports the overarching hypothesis that TRPV4 channels, particularly in the endothelium, are important regulators of cerebrovascular and cognitive function. This hypothesis was tested with three aims.

My first aim used middle-aged SHRSP to determine whether MR antagonism can reverse cerebrovascular and cognitive decline in hypertension that has already occurred or whether it merely prevents these impairments. Previous studies examining the therapeutical potential of MR antagonism during AngII-hypertension revealed that impaired PA function, reduced cerebral blood flow, and impaired cognition were all improved with EPL treatment (4, 6). However, in these studies, EPL treatment began alongside the development of hypertension. This presents a considerable limitation because pharmacological intervention would only begin after hypertension is detected in humans. To combat this limitation, EPL treatment began in 20-22-week-old SHRSP that already have established hypertension. Our lab has shown that these rats develop significant cerebrovascular injury by 12 weeks, so using these older rats truly tests the ability of MR antagonism to reverse the damage, not just prevent it. Importantly, EPL treatment did not reduce blood pressure in SHRSP. I assessed cerebrovascular function, cerebral pial blood flow, memory function, and measured markers of neuroinflammation. As expected, untreated SHRSP had reduced pial perfusion and impaired TRPV4-

mediated dilation compared to SD controls; these changes were associated with cognitive decline and increased neuroinflammation. Four weeks of treatment with the MR antagonist EPL did not improve resting pial perfusion but improved TRPV4-mediated dilation, spatial reference memory and neuroinflammation. Notably, this is the first time our lab has observed an improvement in cognitive function without an improvement in cerebral blood flow.

Previous studies from our lab showed that PAs primarily depend on EDH through TRPV4 channels for endothelium-dependent dilation (5, 6, 12). My first aim confirmed this when the incubation of PAs with the TRPV4 antagonist GSK2193874 blocked Cch-mediated dilation in all three groups. EPL treatment corrected the impaired PA dilation in SHRSP to the specific TRPV4 agonist GSK1016790A but did not correct the reduced TRPV4 mRNA expression compared to the control rats. EPL treatment corrected neither the impaired IK_{Ca}/SK_{Ca}-mediated dilation nor the reduced mRNA expression of these channels relative to control. Together, this suggests EPL improves PA endothelium-dependent dilation in SHRSP at the level of TRPV4 functionality, not its expression. This disagrees with the study from our lab using AngII-hypertensive mice, which showed MR antagonism corrected the mRNA expression of these channels in hypertensive mice (6). These studies have very different treatment paradigms that could explain the disparities. In AngII-hypertensive mice, treatment with EPL began as hypertension developed. In SHRSP, however, EPL treatment began after the rats had been hypertensive for several months, which may make these impairments more difficult to correct.

Increases in inflammation and oxidative stress uncouple TRPV4 from AKAP150, which places the channel in close proximity to kinases that enhance its activity (14, 22).

To better understand how MR antagonism influences inflammation in SHRSP, my studies assessed various indicators of inflammation, including mRNA expression of TNF-α and its receptor, and the quantity and morphology of microglia and astrocytes. Increased neuroinflammation was observed in SHRSP using several markers, which was generally corrected by EPL. The reductions in inflammation and corrected TRPV4-mediated PA dilation were associated with improved cognitive function in EPL-treated SHRSP. Significantly, MR antagonism did not reduce blood pressure; therefore, this study agrees with previous data indicating the benefits of MR antagonism occur independently of blood pressure correction. This study provided further evidence that MR antagonists are a promising therapeutic approach during hypertension and that there is a strong link between TRPV4 function in PAs and cognitive health.

There were several limitations to my first aim. Because of the limited penetration depth of laser speckle contrast imaging and the skull thickness of the rats, cerebral perfusion was only able to be measured at the very surface of the brain. It is possible that perfusion was improved deeper in the brain as a result of improved PA function. Assessing cerebral perfusion by MRI would yield more relevant data. The gene expression data was collected using whole brain tissue. This was done to limit the total number of rats required for the study because the tissue could be collected from the same rats used in pressure myography experiments. This study would have benefited from using a separate group of rats and specifically isolating the hippocampus. Because of the link between oxidative stress and TRPV4 dysfunction, future studies should treat SHRSP with tempol, a superoxide dismutase mimetic. Our lab has shown that tempol prevents MCA remodeling in young SHRSP (16), but the effect of this treatment in older SHRSP

is unclear. Future studies should also treat SHRSP with ω-3 fatty acid supplementation. A recent study revealed ω-3 fatty acid supplementation in mice improved arterial TRPV4-mediated dilation by reducing channel desensitization (1).

My second aim was designed to assess sex differences in the cerebrovascular response to hypertension and how it relates to cognitive function. While the link between hypertension and cognitive decline has been consistently observed, the studies investigating this relationship were conducted in male rodents only, revealing a massive knowledge gap. Given that epidemiological evidence suggests risk factors for VaD affect the sexes differently, determining mechanisms behind these sex differences is paramount. Previous studies revealed that AngII-hypertension in male mice impairs PA endothelium-dependent dilation through a TRPV4-mediated mechanism. This impaired dilation was associated with cognitive decline. In my second aim, I studied male and female mice alongside one another to determine sex differences in hypertension. Female mice are resistant to AngII-hypertension (27–29). Therefore, female mice in my study were given two doses of AngII, one that matched the dose given to the males and one to produce an elevation in systolic blood pressure. This is a novel approach and a major strength of my study. By giving the female mice two different doses, I can separate effects from AngII dosage from the effects of a blood pressure increase. I found that regardless of AngII dose, female mice are protected against the impaired TRPV4-mediated dilation in PAs observed in AngII-hypertensive male mice. Both male and female mice exhibited inward hypotrophic remodeling in PAs after AngII infusion, though this was observed to a lesser degree in females. Importantly, AngII-infused female mice were protected against the memory impairments observed in hypertensive male mice, further indicating that

TRPV4 function in PAs is intertwined with cognition. These data demonstrate that PA remodeling does not impair blood flow enough to alter cognitive function. Rather, PA function is critical for neurovascular health.

The inflammatory response to AngII infusion was also sex dependent. Hypertensive male mice exhibited morphological changes in microglia and astrocytes indicative of increased inflammation and oxidative stress. Female mice did not exhibit these morphological changes, suggesting resistance to AngII-induced inflammation. Together, these data suggest female sex is associated with maintained cerebrovascular and cognitive function in hypertension, potentially through the preservation of TRPV4 channel function. These observations coincide with sex differences in the RAAS (see section 1.3.1.2) and suggest that the anti-inflammatory benefits of female sex hormones may aid in the maintenance of TRPV4 channel function in PAs, which is associated with maintained cognitive function. The role of female sex hormones was not addressed here, and future studies will define their importance regarding TRPV4 function in hypertension.

One limitation of my second aim is that control female mice had elevated systolic blood pressure, which made it difficult to choose a dose of AngII that increased blood pressure similarly to that in male mice. Blood pressure was measured by tail-cuff plethysmography, and despite being acclimated to the procedure in the same way as the male mice, female mice showed signs of anxiety that likely contributed to their blood pressure elevation. Using radiotelemetry likely would have mitigated this issue. Another limitation is that I was unable to successfully use the novel object recognition test to assess episodic memory. Despite acclimating mice to handling and to the testing arena, control male and female mice did not preferentially explore the novel object, and the assay

was not usable. This study would have benefited from a behavior test that did not rely on spatial memory, which would have diversified the data. To better understand the sex differences observed in this aim, future studies should employ the VCD model of menopause. As opposed to ovariectomy, which results in a sudden loss of sex hormones, the VCD model results in gradual ovarian failure that more closely mimics what is observed in women. This model has a perimenopause phase that would be particularly useful to accompany my studies. Epidemiological evidence suggests hypertension in women of perimenopausal age is particularly detrimental in regard to future dementia development. Because the VCD model requires a series of injections and a waiting period, BPH/BPN mice would be a better choice than AngII-hypertensive mice; the osmotic minipumps that fit in mice have a maximum duration of 4 weeks.

Previous studies from our lab and my first two aims show the importance of TRPV4 channel function in cognition. Because of the ubiquitous expression of TRPV4 channels in the NVU, it has thus far been impossible to discern the importance of TRPV4 specifically in the vascular endothelium and how they relate to cognitive function. To this end, my third aim was focused on determining the role of endothelial TRPV4 channels in cerebrovascular and cognitive function. I employed a mouse model with endothelial cell-specific TRPV4 channel knockout to achieve this. My data suggest that functional endothelial TRPV4 channels are essential for cognitive function, as their deletion results in memory impairment. The observed memory impairment was associated with reduced anxiety-like behavior and impaired nesting ability. These changes were observed without having a detectable effect of endothelial TRPV4 deletion on pial perfusion. Though endothelial TRPV4 channels are very important in PAs, they play less of a role in larger

pial arteries (7, 21). Pial arteries have a greater dependence on NO in the myogenic response, which may explain why endothelial TRPV4 deletion did not have an effect on pial perfusion. Interestingly, mice deficient in endothelial TRPV4 also had slightly impaired IK_{Ca}/SK_{Ca}-mediated dilation in PAs, evidenced by a rightward shift in the concentration-response curve to NS309. This change may be in response to the lack of TRPV4-mediated dilation in these arterioles. IK_{Ca}/SK_{Ca} expression and function may have been reduced because of a lack of upstream activation. This theory was not tested here; future studies should measure IK_{Ca}/SK_{Ca} channel mRNA expression or protein expression to determine if it is influenced by endothelial TRPV4 channel expression.

The observed cognitive impairment may indicate a stress on neurons that could result in increased neuroinflammation. Though mRNA expression of inflammatory markers was not significantly altered, $TRPV4_{EC^{-/-}}$ mice had more astrocytes with more process arborization, indicating increased inflammation. To expand on these findings, future studies should include quantification and morphological assessment of microglia. Importantly, future studies should include NVC experiments to directly test the importance of endothelial TRPV4 channels in functional hyperemia. A major limitation in this study is the unequal weight of male mice in the control group and female mice in the knockout group. Though no sex differences in response to endothelial TRPV4 deletion are expected, it is important that more mice be included to equalize the sex distribution.

Taken together, the studies presented in this dissertation demonstrate the importance of endothelial TRPV4 function in cognitive function. Further, these studies show for the first time that female sex protects against hypertension-associated impaired TRPV4-mediated dilation and the cognitive decline typically associated with this. My

studies suggest treatment with an MR antagonist is sufficient to reverse the damage done by hypertension and has the potential to restore cognitive function. Because EPL treatment was not associated with improvement of TRPV4 channel mRNA expression, it suggests that improvement of endothelium-dependent dilation is at the level of functionality rather than mRNA or protein expression. Therefore, the results suggest that dampening hypertension's inflammatory and oxidative stress response is paramount in restoring TRPV4 channel function.

5.2 – Considerations of the model and treatment regimens used

I used multiple animal models to complete my studies. In my first aim I used SHRSP to determine the impact of EPL treatment on rats that have established hypertension. I chose SHRSP for these experiments because they are a polygenic and multifactorial model that mimics essential hypertension in humans. Further, the age of rats was essential to the model. Because SHRSP have a shortened lifespan of about 9-12 months, EPL treatment began shortly before midlife (11). Using older rodents is advantageous over younger animals, as many studies do, because it is more translationally relevant. Importantly, these rats had been hypertensive for several months at this point and had established cerebrovascular and cognitive damage, which was important for the study question. The dose of EPL used in these studies was higher than that used therapeutically in humans. Our group and others have used this higher dose of EPL in previous studies (17); we also used high doses of other MR antagonists, like spironolactone (18, 19), without observing adverse effects. Rodents require a higher dose of ELP than humans because they metabolize and excrete EPL faster than humans and therefore require more drug to reach a therapeutic effect (3, 30). Toxicity studies using

similar dosages in mice did not harm the mice or produce carcinogenicity (2, 3, 30). EPL was given to the rats daily in peanut butter. This vehicle was chosen because EPL is not readily soluble in water and administering it in peanut butter provides accurate dosing. The amount of peanut butter given daily (2g) was insufficient to significantly alter dietary sodium and therefore did not affect RAAS. It is important to acknowledge that I used a nonstandard control for SHRSP in these studies. SHRSP were derived from WKY rats, which are typically used as the control. WKY rats exhibit depressive behavior, which would confound behavior analysis (10, 13). I, therefore, opted to use SD rats as my normotensive control, which has also been done by others (20, 24, 25).

In my second aim, I chose the AngII-dependent model of hypertension to complete my sex differences studies. While most humans do not have high AngII levels, ACE inhibitors are effective therapeutic options for hypertension, making AngII infusion in mice a clinically relevant model (15, 23, 26). Further, these studies expand upon previous studies in our lab using the AngII model of hypertension in male mice. Continuing this model to the current studies made for more appropriate comparisons.

My third aim was completed using $TRPV4_{EC}^{-/-}$ mice provided by Dr. Swapnil Sonkusare. These mice were generated by crossing $TRPV4^{fl/fl}$ mice with VE-Cadherin Cre mice and the knockout was induced with tamoxifen. Inducing the knockout under the VE-Cadherin promoter allows for the specific targeting of endothelial cells without also targeting the hematopoietic lineage, which happens under the Tie2 promoter (9). I conducted experiments in these mice at 30-35 weeks to reflect an adult population.

5.3 – Novel findings

My studies are the first to show that PA and cognitive dysfunction observed in hypertension can be reversed by MR antagonism using a model that reflects an adult human with hypertension. Further, I demonstrate for the first time that female sex protects against impairments in PA TRPV4-mediated dilation and cognitive dysfunction in hypertension. Lastly, I was the first to show that endothelial TRPV4 channels are required for appropriate cognition in the absence of hypertension.

5.3.1 – The effect of MR antagonism after hypertension development

- This study shows, for the first time, that treatment with the MR antagonist EPL can reverse impaired TRPV4-mediated dilation in PAs
- Improved TRPV4-mediated dilation is associated with improved cognitive function
- Improvement in TRPV4-mediated dilation was not associated with improved mRNA expression of the channel, indicating dilation was improved at the level of channel functionality
- Endothelial TRPV4 channels contribute to myogenic tone in hypertension
- MR antagonism reduces neuroinflammation during hypertension
- These findings expand our knowledge of the impact of MR antagonists during hypertension

5.3.2 – Sex differences in AngII-hypertension

- Female mice require a higher dose of AngII to become hypertensive
- AngII infusion reduces pial perfusion in both sexes, regardless of AngII dose
- Hypertensive female mice do not have impaired TRPV4-mediated dilation in PAs, while hypertensive male mice do

- Impaired TRPV4-mediated dilation in hypertensive male mice is associated with impaired spatial and spatial working memory; female mice are protected from this as well
- AngII-hypertension results in inward hypotrophic remodeling in both male and female mice, but has no effect on biomechanical properties
- AngII-hypertension in male mice produces neuroinflammation in male but not female mice
- These studies show for the first time that female mice are resistant to impaired TRPV4 function in PAs during hypertension, and this is associated with preserved cognition

5.3.3 – The role of endothelial TRPV4 channels in PA function and cognition

- Endothelial TRPV4 channels are essential for appropriate cognitive function
- Endothelial TRPV4 knockout mildly impairs IK_{Ca}/SK_{Ca}-mediated dilation in PAs
- Cerebral pial perfusion is not impaired after endothelial TRPV4 deletion
- Endothelial TRPV4 channels are not important for PA structure
- These studies improve our understanding of the role of endothelial TRPV4 channels in PA function, PA structure, and cognition

5.4 – Limitations

- Pressure myography is a widely used *ex vivo* technique to assess arteriolar structure and function. Pressurized arterioles are flushed with and bathed in aCSF, thus the effects of blood viscosity are lost. The effects of flow through PAs are also lost because the small lumen diameter make the resistance too great

- Laser speckle contrast imaging has a penetration depth of ~1mm, which only allows for the assessment of pial arteries. We therefore are unable to discern how blood flow was affected in the brain parenchyma throughout my studies. Future studies should use arterial spin labeling MRI

5.5 – Perspectives

VaD is a devastating condition that greatly affects quality of life and currently has no cure. Hypertension is the leading modifiable risk factor for VaD, partly because of its detrimental effect on the structure and function of cerebral arterioles. Epidemiological evidence suggests hypertension increases the risk of dementia in women to a greater degree than in does in men (8). As of yet, we do not fully understand the mechanisms involved in hypertension associated VaD, and we know even less about sex differences that exist in this pathway. Therefore, we must identify treatments that can mitigate the negative vascular and inflammatory consequences of hypertension. The MR is a potential therapeutic target because MR antagonism prevents cerebrovascular and cognitive damage induced by hypertension. My studies proposed that MR antagonism would reverse PA dysfunction and cognitive decline in hypertension. The data presented herein support previous studies showing that the MR is an important regulator of TRPV4 channel function in cerebral arteries, and that maintenance of TRPV4 function is associated with appropriate cognitive function. Further, my studies show that the negative consequences of hypertension in cerebrovascular health are sex dependent. Female mice given the same dose of AngII as male mice, and those given a greater dose to induce hypertension, were protected against impaired PA dilation and memory dysfunction observed in males. This was associated with a dampened inflammatory response in female mice relative to

males, which may play a key role in mediating the observed sex differences. Lastly, my studies provided evidence that in the absence of hypertension, endothelial TRPV4 channel deletion is sufficient to cause cognitive decline, without detectable reductions in pial perfusion. In conclusion, MR blockade, or other approaches that reduce hypertension associated inflammation, may be beneficial therapeutic approaches to improve cerebrovascular function in hypertensive patients.

REFERENCES

1. **Caires R**, **Garrud TAC**, **Romero LO**, **Fernández-Peña C**, **Vásquez V**, **Jaggar JH**, **Cordero-Morales JF**. Genetic- and diet-induced ω-3 fatty acid enrichment enhances TRPV4-mediated vasodilation in mice. *Cell Rep* 40: 111306, 2022. doi: 10.1016/j.celrep.2022.111306.

2. **Cook CS**, **Berry LM**, **Bible RH**, **Hribar JD**, **Hajdu E**, **Liu NW**. Pharmacokinetics and metabolism of [14C]eplerenone after oral administration to humans. *Drug Metab Dispos* 31: 1448–1455, 2003. doi: 10.1124/dmd.31.11.1448.

3. **Delyani JA**, **Rocha R**, **Cook CS**, **Tobert DS**, **Levin S**, **Roniker B**, **Workman DL**, **Sing YL**, **Whelihan B**. Eplerenone: a selective aldosterone receptor antagonist (SARA). *Cardiovasc Drug Rev* 19: 185–200, 2001.

4. **Diaz-Otero JM**, **Fisher C**, **Downs K**, **Moss EM**, **Jaffe IZ**, **Jackson WF**, **Dorrance AM**. Endothelial Mineralocorticoid Receptor Mediates Parenchymal Arteriole and Posterior Cerebral Artery Remodeling During Angiotensin II–Induced Hypertension. .

5. **Diaz-Otero JM**, **Yen T-C**, **Ahmad A**, **Laimon-Thomson E**, **Abolibdeh B**, **Kelly K**, **Lewis MT**, **Wiseman RW**, **Jackson WF**, **Dorrance AM**. Transient receptor potential vanilloid 4 channels are important regulators of parenchymal arteriole dilation and cognitive function. *Microcirculation* 26: e12535, 2019. doi: 10.1111/micc.12535.

6. **Diaz-Otero JM**, **Yen T-C**, **Fisher C**, **Bota D**, **Jackson WF**, **Dorrance AM**. Mineralocorticoid receptor antagonism improves parenchymal arteriole dilation via a TRPV4-dependent mechanism and prevents cognitive dysfunction in hypertension. *Am J Physiol Heart Circ Physiol* 315: H1304–H1315, 2018. doi: 10.1152/ajpheart.00207.2018.

7. **Garland CJ**, **Dora KA**. EDH: endothelium-dependent hyperpolarization and microvascular signalling. *Acta Physiol (Oxf)* 219: 152–161, 2017. doi: 10.1111/apha.12649.

8. **Gilsanz P**, **Mayeda ER**, **Glymour MM**, **Quesenberry CP**, **Mungas DM**, **DeCarli C**, **Dean A**, **Whitmer RA**. Female sex, early-onset hypertension, and risk of dementia. *Neurology* 89: 1886–1893, 2017. doi: 10.1212/WNL.0000000000004602.

9. **Kilani B**, **Gourdou-Latyszenok V**, **Guy A**, **Bats M-L**, **Peghaire C**, **Parrens M**, **Renault M-A**, **Duplàa C**, **Villeval J-L**, **Rautou P-E**, **Couffinhal T**, **James C**. Comparison of endothelial promoter efficiency and specificity in mice reveals a subset of Pdgfb-positive hematopoietic cells. *J Thromb Haemost* 17: 827–840, 2019. doi: 10.1111/jth.14417.

10. **Lemos JC**, **Zhang G**, **Walsh T**, **Kirby LG**, **Akanwa A**, **Brooks-Kayal A**, **Beck SG**. Stress-hyperresponsive WKY rats demonstrate depressed dorsal raphe neuronal excitability and dysregulated CRF-mediated responses. *Neuropsychopharmacology* 36: 721–734, 2011. doi: 10.1038/npp.2010.200.

11. **Linz W**, **Jessen T**, **Becker RH**, **Schölkens BA**, **Wiemer G**. Long-term ACE inhibition doubles lifespan of hypertensive rats. *Circulation* 96: 3164–3172, 1997. doi: 10.1161/01.cir.96.9.3164.

12. **Matin N**, **Fisher C**, **Jackson WF**, **Diaz-Otero JM**, **Dorrance AM**. Carotid artery stenosis in hypertensive rats impairs dilatory pathways in parenchymal arterioles. *Am J Physiol Heart Circ Physiol* 314: H122–H130, 2018. doi: 10.1152/ajpheart.00638.2016.

13. **Nam H**, **Clinton SM**, **Jackson NL**, **Kerman IA**. Learned helplessness and social avoidance in the Wistar-Kyoto rat. *Front Behav Neurosci* 8: 109, 2014. doi: 10.3389/fnbeh.2014.00109.

14. **Ottolini M**, **Hong K**, **Cope EL**, **Daneva Z**, **DeLalio LJ**, **Sokolowski JD**, **Marziano C**, **Nguyen NY**, **Altschmied J**, **Haendeler J**, **Johnstone SR**, **Kalani MY**, **Park MS**, **Patel RP**, **Liedtke W**, **Isakson BE**, **Sonkusare SK**. Local peroxynitrite impairs endothelial transient receptor potential vanilloid 4 channels and elevates blood pressure in obesity. *Circulation* 141: 1318–1333, 2020. doi: 10.1161/CIRCULATIONAHA.119.043385.

15. **Patel VB**, **Zhong J-C**, **Fan D**, **Basu R**, **Morton JS**, **Parajuli N**, **McMurtry MS**, **Davidge ST**, **Kassiri Z**, **Oudit GY**. Angiotensin-converting enzyme 2 is a critical determinant of angiotensin II-induced loss of vascular smooth muscle cells and adverse vascular remodeling. *Hypertension* 64: 157–164, 2014. doi: 10.1161/HYPERTENSIONAHA.114.03388.

16. **Pires PW**, **Deutsch C**, **McClain JL**, **Rogers CT**, **Dorrance AM**. Tempol, a superoxide dismutase mimetic, prevents cerebral vessel remodeling in hypertensive rats. *Microvasc Res* 80: 445–452, 2010. doi: 10.1016/j.mvr.2010.06.004.

17. **Pires PW**, **Jackson WF**, **Dorrance AM**. Regulation of myogenic tone and structure of parenchymal arterioles by hypertension and the mineralocorticoid receptor. *Am J Physiol Heart Circ Physiol* 309: H127-36, 2015. doi: 10.1152/ajpheart.00168.2015.

18. **Rigsby CS**, **Ergul A**, **Portik Dobos V**, **Pollock DM**, **Dorrance AM**. Effects of spironolactone on cerebral vessel structure in rats with sustained hypertension. *Am J Hypertens* 24: 708–715, 2011. doi: 10.1038/ajh.2011.20.

19. **Rigsby CS**, **Pollock DM**, **Dorrance AM**. Spironolactone improves structure and increases tone in the cerebral vasculature of male spontaneously hypertensive stroke-prone rats. *Microvasc Res* 73: 198–205, 2007. doi: 10.1016/j.mvr.2006.12.001.

20. **Senanayake GVK**, **Banigesh A**, **Wu L**, **Lee P**, **Juurlink BHJ**. The dietary phase 2 protein inducer sulforaphane can normalize the kidney epigenome and improve blood pressure in hypertensive rats. *Am J Hypertens* 25: 229–235, 2012. doi: 10.1038/ajh.2011.200.

21. **Shimokawa H**, **Yasutake H**, **Fujii K**, **Owada MK**, **Nakaike R**, **Fukumoto Y**, **Takayanagi T**, **Nagao T**, **Egashira K**, **Fujishima M**, **Takeshita A**. The importance of the hyperpolarizing mechanism increases as the vessel size decreases in endothelium-dependent relaxations in rat mesenteric circulation. *J Cardiovasc Pharmacol* 28: 703–711, 1996. doi: 10.1097/00005344-199611000-00014.

22. **Sonkusare SK**, **Dalsgaard T**, **Bonev AD**, **Hill-Eubanks DC**, **Kotlikoff MI**, **Scott JD**, **Santana LF**, **Nelson MT**. AKAP150-dependent cooperative TRPV4 channel gating is central to endothelium-dependent vasodilation and is disrupted in hypertension. *Sci Signal* 7: ra66, 2014. doi: 10.1126/scisignal.2005052.

23. **Sörös P**, **Whitehead S**, **Spence JD**, **Hachinski V**. Antihypertensive treatment can prevent stroke and cognitive decline. *Nat Rev Neurol* 9: 174–178, 2013. doi: 10.1038/nrneurol.2012.255.

24. **Tang J**, **Xiao W**, **Li Q**, **Deng Q**, **Chu X**, **Chen Y**, **Pan D**, **Fu J**. A Cyclooxygenase-2 Inhibitor Reduces Vascular Wall Thickness and Ameliorates Cognitive Impairment in a Cerebral Small Vessel Diseases Rat Model. *Curr Alzheimer Res* 12: 704–710, 2015. doi: 10.2174/1567205012666150710104924.

25. **Wang X**, **Desai K**, **Juurlink BHJ**, **de Champlain J**, **Wu L**. Gender-related differences in advanced glycation endproducts, oxidative stress markers and nitric oxide synthases in rats. *Kidney Int* 69: 281–287, 2006. doi: 10.1038/sj.ki.5000043.

26. **Wincewicz D**, **Braszko JJ**. Angiotensin II AT1 receptor blockade by telmisartan reduces impairment of spatial maze performance induced by both acute and chronic stress. *J Renin Angiotensin Aldosterone Syst* 16: 495–505, 2015. doi: 10.1177/1470320314526269.

27. **Xue B**, **Johnson AK**, **Hay M**. Sex differences in angiotensin II- and aldosterone-induced hypertension: the central protective effects of estrogen. *Am J Physiol Regul Integr Comp Physiol* 305: R459-63, 2013. doi: 10.1152/ajpregu.00222.2013.

28. **Xue B**, **Pamidimukkala J**, **Hay M**. Sex differences in the development of angiotensin II-induced hypertension in conscious mice. *Am J Physiol Heart Circ Physiol* 288: H2177-84, 2005. doi: 10.1152/ajpheart.00969.2004.

29. **Xue B**, **Pamidimukkala J**, **Lubahn DB**, **Hay M**. Estrogen receptor-alpha mediates estrogen protection from angiotensin II-induced hypertension in conscious female mice. *Am J Physiol Heart Circ Physiol* 292: H1770-6, 2007. doi: 10.1152/ajpheart.01011.2005.

30. **Zou L**, **Jia K**, **Li R**, **Wang P**, **Lin J-Z**, **Chen H-J**, **Zhao G**, **Peng L-X**. Pharmacokinetic study of eplerenone in rats after long-term coadministration with buckwheat tea. *Kaohsiung J Med Sci* 32: 177–184, 2016. doi: 10.1016/j.kjms.2016.03.004.